1983-06

Effect of shroud geometry on the effectiveness of a short mixing stack gas eductor model.

Kavalis, Anastasios Emmanouil

Monterey, California. Naval Postgraduate School

NAVAL POSTGRADUATE SCHOOL
Monterey, California

THESIS

EFFECT OF SHROUD GEOMETRY ON THE EFFECTIVENESS
OF A SHORT MIXING STACK GAS EDUCTOR MODEL

by

Anastasios Emmanouil Kavalis

June 1983

Thesis Advisor: Paul F. Pucci

SECURITY CLASSIFICATION OF THIS PAGE (When Data Entered)

REPORT DOCUMENTATION PAGE		READ INSTRUCTIONS BEFORE COMPLETING FORM
1. REPORT NUMBER	2. GOVT ACCESSION NO.	3. RECIPIENT'S CATALOG NUMBER
4. TITLE (and Subtitle) Effect of Shroud Geometry on the Effectiveness of a Short Mixing Stack Gas Eductor Model		5. TYPE OF REPORT & PERIOD COVERED Master's Thesis June 1983 6. PERFORMING ORG. REPORT NUMBER
7. AUTHOR(s) Anastasios Emmanouil Kavalis		8. CONTRACT OR GRANT NUMBER(s)
9. PERFORMING ORGANIZATION NAME AND ADDRESS Naval Postgraduate School Monterey, California 93940		10. PROGRAM ELEMENT, PROJECT, TASK AREA & WORK UNIT NUMBERS
11. CONTROLLING OFFICE NAME AND ADDRESS Naval Postgraduate School Monterey, California 93940		12. REPORT DATE June 1983 13. NUMBER OF PAGES 195
14. MONITORING AGENCY NAME & ADDRESS(if different from Controlling Office)		15. SECURITY CLASS. (of this report) 15a. DECLASSIFICATION/DOWNGRADING SCHEDULE

16. DISTRIBUTION STATEMENT (of this Report)

Approved for public release; distribution unlimited

17. DISTRIBUTION STATEMENT (of the abstract entered in Block 20, if different from Report)

18. SUPPLEMENTARY NOTES

19. KEY WORDS (Continue on reverse side if necessary and identify by block number)

Gas Eductor, Multiple Nozzle, Mixing Stack, Shroud, Diffuser Rings, Primary Flow, Secondary Flow, Tertiary Flow, Exhaust, Cooling

20. ABSTRACT (Continue on reverse side if necessary and identify by block number)

An existing apparatus for testing models of gas eductor systems using high temperature primary flow was modified to provide improved control and performance over a wide range of gas temperature and flow rates. Secondary flow pumping, temperature and pressure data were recorded for two gas eductor system models. The first, previously tested under hot flow conditions, consists of a primary plate with four tilted-angled nozzles and a slotted, shrouded mixing stack with two diffuser rings (overall L/D = 1.5).

A portable pyrometer with a surface probe was used for the second model in order to identify any hot spots at the external surface of the mixing stack, shroud and diffuser rings. The second model is shown to have almost the same mixing and pumping performance with the first one but to exhibit much lower shroud and diffuser surface temperatures.

Approved for public release, distribution unlimited

Effect of Shroud Geometry on the Effectiveness of a Short Mixing Stack Gas Eductor Model

by

Anastasios Emmanouil Kavalis
Lieutenant, Hellenic Navy
B.S., Naval Postgraduate School, 1982

Submitted in partial fulfillment of the requirements for the degree of

MASTER OF SCIENCE IN MECHANICAL ENGINEERING

from the

NAVAL POSTGRADUATE SCHOOL
June 1983

ABSTRACT

An existing apparatus for testing models of gas eductor systems using high temperature primary flow was modified to provide improved control and performance over a wide range of gas temperature and flow rates. Secondary flow pumping, temperature and pressure data were recorded for two gas eductor system models. The first, previously tested under hot flow conditions, consists of a primary plate with four tilted-angled nozzles and a slotted, shrouded mixing stack with two diffuser rings (overall L/D = 1.5). The second consisted of the same nozzles and mixing stack, with a modified shroud and three diffuser rings (overall L/D = 1.5).

A portable pyrometer with a surface probe was used for the second model in order to identify any hot spots at the external surface of the mixing stack, shroud and diffuser rings. The second model is shown to have almost the same mixing and pumping performance with the first one but to exhibit much lower shroud and diffuser surface temperatures.

TABLE OF CONTENTS

LIST OF TABLES

LIST OF FIGURES

TABLE OF SYMBOLS

ENGLISH LETTER SYMBOLS

A - Area, in^2, ft^2

B - Atmospheric pressure, inches H_{ga}

c - Sonic velocity, ft/sec

C - Coefficient of discharge

D - Diameter, inches (as a reference quantity, refers to the inside diameter of the mixing stack)

DELPN - Pressure drop across the entrance reducing section, inches H_2O

DELPU - Pressure drop across the burner U-tube, in H_2O

f - Friction factor

F_{fr} - Wall skin-friction force, lbf

g_c - Proportionality factor in Newton's Second Law g_c = 32.174 lbm-ft/lbf-sec^2

h - Enthalpy, Btu/lbm

l - Arbitrary length, inches

L - Length of the mixing stack assembly, inches

p - Pressure, inches H_2O

PMS - Static pressure in the mixing stack, referenced to atmospheric, inches H_2O

PNH - Inlet air gauge pressure upstream of the reducing section, inches Hg

PPLN - Pressure differential across the measurement plenum secondary flow nozzles, inches H_2O

PUPT - Pressure in the uptake, inches H_2O

r - Radial distance from the axis of the mixing stack, inches

R - Gas Constant, for air = 53.34 ft-lbf/lbm-^{o}R

ROTA - Fuel mass flow rotameter reading

Rms - Interior radius of the mixing stack, inches

s - Entropy, Btu/lbm-^{o}R

S - Standoff, distance between the discharge plane of the primary nozzles and the entrance plane of the mixing stack, in

T - Temperature, ^{o}F, ^{o}R

TAMB - Ambient temperature, ^{o}F

TAMBR - Ambient temperature, ^{o}R

TBURN - Burner temperature, ^{o}F

TEP - Exit plane temperature, ^{o}F

TMS - Mixing stack wall temperature, ^{o}F

TNH - Inlet air temperature, ^{o}F

TNHR - Inlet air temperature, ^{o}R

TSURF - Surface temperature of shroud and diffusers, ^{o}F

TUPT - Uptake temperature, ^{o}F

TUPTR - Uptake temperature, ^{o}R

u - Internal Energy (Btu/lbm)

U - Velocity, ft/sec

UM - Average velocity in the mixing stack, ft/sec

UP - Primary flow velocity at nozzle exit, ft/sec

UU - Primary flow velocity in uptake, ft/sec

v - Specific volume (ft^3/lbm)

W - Mass flow rate, lbm/sec

WF - Mass flow rate of fuel, lbm/sec

WP - Primary mass flow rate, lbm/sec

WS - Secondary mass flow rate, lbm/sec

WPA - Mass flow rate of primary air, lbm/sec

X - Axial distance from mixing stack entrance, inches

DIMENSIONLESS GROUPINGS

A* - Secondary flow area to primary flow area ratio

A_t^* - Tertiary flow area to primary flow area ratio

K_e - Kinetic energy correction factor

Km - Momentum correction factor at mixing stack exit

K_p - Momentum correction factor at primary nozzle exit

M,UMACH - Mach number

P* - Pressure Coefficient for secondary flow

P_t^* - Pressure coefficient for tertiary flow

PMS* - Pressure coefficient for mixing stack pressures

Re - Reynolds number

T* - Secondary flow absolute temperature to primary flow absolute temperature ratio

T_t^* - Tertiary flow absolute temperature to primary flow absolute temperature ratio

W^* - Secondary mass flow rate to primary mass flow rate ratio

W_t^* - Tertiary mass flow rate to primary mass flow rate ratio

ρs^* - Secondary flow density to primary flow density ratio

ρt^* - Tertiary flow density to primary flow density ratio

GREEK LETTER SYMBOLS

β - $K + (f/2) * (A_w/Am)$

β - Ratio of ASME long radius metering nozzle throat diameter to inlet diameter

γ - Ratio of specific heats for air

μ - Absolute viscosity, lbf-sec/ft^2

ρ - Density, lbm/ft^3

Φ - "Function of"

SUBSCRIPTS

0 - Section within the measurement plenum

1 - Section at primary nozzle exit

2 - Section at mixing stack exit

a - Atmospheric

b - Burner

m - Mixed flow

ms - Mixing stack

or - Orifice

p - Primary

s - Secondary

t - Tertiary

u - Uptake

w - Mixing stack wall

ACKNOWLEDGMENT

Sincere thanks go to the author's advisor, Professor Paul F. Pucci, whose expertise and inspiration provided the foundation and catalyst for this work. The assistance and ingenuity provided by the personnel of the Department of Mechanical Engineering Machine Shop, especially Mr. John Mouton and Mr. Ron Lauqueria, is also sincerely appreciated.

Special thanks and grateful appreciation are due to my wife, Despina, for the never ending encouragement and understanding she provided during the long days and late nights devoted to this study.

I. INTRODUCTION

Energy and momentum diffusion in a low Mach number gas eductor system is an interesting problem which has been under study at the Naval Postgraduate School for some time. This research has been motivated by the U.S. Navy's introduction of marine gas turbine propulsion system in significant numbers of modern combatant ships. The marine gas turbine engine differs from conventional steam boiler systems in air breathing characteristics. The gas turbine processes four to five times the volume of combustion air and has exhaust temperatures 300 to 400 degrees Fahrenheit higher than the steam system. Such characteristics create problems in the shipboard employment of these engines.

The high temperature gas heats uptake and stack surfaces, increasing the vessel's susceptibility to detection and targeting by infrared sensing equipment. The exhaust plume itself is also a detection problem but of less significance than the heated surface of shipboard structure. Various types of electronic equipment and sensors carried by a combatant vessel must be mounted as far above the water surface as possible to obtain greatest area of coverage and to maximize effectiveness. Materials used in construction of these equipments and their associated cabling are subject to

accelerated deterioration as well as the effectiveness of the electronic components is much lower in the presence of the heated exhaust plume. It is, therefore, desirable to reduce as far as possible the plume temperatures in the vicinity of such equipment. Finally, for combatants carrying aircraft it is dangerous for these aircraft to descend through the ship's low density and highly turbulent hot exhaust plume.

Due to the inherent design of a gas turbine engine, reduction of the volume of the exhaust plume is not feasible, consequently, reduction of the gas temperatures within the plume becomes highly desirable. The most attractive way to accomplish this goal would be to employ some sort of energy recovery system within the uptakes, thereby simultaneously reducing the plume temperatures and increasing overall plant efficiency. Such energy recovery systems are, of course, entirely feasible for certain engine applications. This is demonstrated by the waste heat boilers used to provide steam for auxiliary purposes in the DD963 and CG47 class ships. These boilers, however, are installed in conjunction with the gas turbine generator sets used to provide shipboard electrical power and not with the marine propulsion engines.

An energy recovery design for use with propulsion engines which is currently receiving serious consideration is RACER (Rankine Cycle Energy Recovery). In this concept, steam from a waste heat boiler drives a steam turbine which is paired

with the gas turbine power turbine through a combining gearbox. In many proposals, it will be in operation only for cruise speed. Thus, it is fairly certain that, although desirable, energy recovery is not the solution to many aspects of the plume temperature problem.

A second means of reducing plume temperature is water suppression. In these systems, which are currently installed in some ships, salt water is sprayed into the exhaust near the stack exit. Such a method has many drawbacks. Use of the suppression spray could intensify problems with most mounted electronics equipment due to the deposition of salts. In general, this system produces increased corrosion and maintenance problems for all exposed weather deck areas. Water suppression is an intermittent system and does not meet the requirement for a system which can operate continuously to reduce the exhaust plume temperature and to cool stack surfaces.

Another method of cooling the exhaust plume, also in current use, is to dilute the exhaust gas flow with ambient air. The result is a larger volume of flow, but at significantly lower temperatures and velocities. This dilution is achieved by employing the exhaust discharge as the primary jet in a gas eductor system. The eductor action causes ambient air to become entrained in the flow and to be

drawn into the mixing section of eductor where it mixes with the primary flow.

The operation of gas eductors can be divided into three regimes: at the high Mach numbers, greater than one, with applications on aircraft and rocket engines; in the mid-region with Mach number range from 0.4 to 0.5, with applications on Vertical Takeoff and Landing (VTOL) aircraft engines; and in the low-region with Mach number less than 0.2. The latter case is the region of interest of this investigation which is an extension of work reported by Lt. C. R. Ellin [Ref. 1], Lt. C. P. Staehli and Lt. R. J. Lemke [Ref. 2], Lt. C. P. Ross [Ref. 3], Lt. D. R. Welch [Ref. 4], Lt. C. M. Moss [Ref. 5], Lt. J. A. Hill [Ref. 6], Lt. C. I. J. Eick [Ref. 7]. The scope of the work reported here includes verification of the results reported by Eick [Ref. 7], and the hot flow testing of a new eductor system similar to the one tested by Eick but with an additional diffuser ring and a different arrangement of the shroud and rings. Moss [Ref. 4] provides an extensive literature review dealing with gas eductor systems. Eick [Ref. 6] provides in complete details the work that has been done so far on both cold and hot test facilities.

The exhaust gas eductor system, Figure 1, is a device in which the exhaust gases are discharged through nozzles into a mixing stack. The purpose of this system is to induce a

secondary flow of cool ambient air, which is mixed with the hot exhaust gases in order to produce a uniform flow at an intermediate temperature.

The major requirements for a gas eductor are three: they must pump large amounts of secondary flow into the mixing stack; they must adequately mix the primary and secondary flow; and they must not decrease significantly the gas turbine's performance.

The overall performance of an eductor system of a single nozzle was analyzed in order to determine the non-dimensional parameters which govern the flow phenomenon. An experimental correlation of these parameters has been used to evaluate the eductor performance.

The geometric parameters which influence the gas eductor's performance are the number, the size and the type of primary nozzles, the distance from the primary nozzles to the mixing stack (stand-off distance), and the length and diameter of the mixing stack. Many combinations of the above parameters have been studied and reported in References 1 through 7.

The specific goal of this investigation was to verify the high temperature performance of the particular eductor configuration which was developed by Davis [Ref. 8] and Drucker [Ref. 9] and tested by Eick, and to determine the performance of that eductor modified by increasing the number

of diffuser rings from two to three and the shroud and diffuser rings arranged in a different way. Tests were made with the primary exhaust gas temperature over the range of 180 degrees Fahrenheit to 950 degrees Fahrenheit.

II. THEORY AND MODELING

An eductor is a device which can pump a fluid (called secondary fluid) by the direction of another fluid (called primary fluid) through nozzles and a mixing chamber. In this case the primary fluid is the exhaust gases of a gas turbine and the secondary fluid is the ambient air.

An eductor is composed of a primary nozzle plate with one or more nozzles, and a mixing chamber. The jet discharged from the nozzles is directed into the coaxial mixing chamber in which the primary fluid mixes with the pumped secondary fluid.

Models used in this investigation are similar to those used in previous investigations. The analysis, data reduction and error analysis are, therefore, similar to those conducted by Ellin [Ref. 1] and by Eick [Ref. 7].

One dimensional analysis of a simple eductor system was used to determine the dimensionless parameters which govern the flow. Based on this analysis, an experimental correlation of the non-dimensional parameters was developed and used in presenting and evaluating experimental results. Dynamic similarity between model and a full scale prototype was accomplished by maintaining Mach number similarity in the primary flow.

Tertiary flows, that is, flows induced by the diffuser rings, though present, were not measured in this work.

A. MODELING TECHNIQUE

The primary flow of the prototype was determined to be turbulent ($Re \approx 10^5$). Consequently, turbulent momentum exchange is the predominant mechanism characterizing primary flow, and kinetic and internal energy consideration dominate viscous effects. Since it can be shown that the Mach number represents the ratio of kinetic energy of a flow to its internal energy, it is a more significant parameter than Reynold's number in describing the primary flow through the uptake. Similarity of Mach number was therefore used to model the primary flow.

B. ONE-DIMENSIONAL ANALYSIS OF A SIMPLE EDUCTOR

The theoretical analysis of an eductor can be developed in two ways. The first method attempts to analyze the details of the mixing process of the primary and secondary flows as it takes place inside the mixing stack and so determines the parameters that describe the flow. This requires an interpretation of the mixing phenomenon which, when applied to multiple nozzle systems becomes extremely complex. The second method, which is employed here, analyzes the overall performance of the eductor system as a unit. Since details of the mixing process are not considered in this method, an

analysis of the simple single nozzle eductor system shown in Figure 1 leads to a determination of the dimensionless groupings governing the flow. The dimensional analysis which follows is from Ellin [Ref. 1] and Pucci [Ref. 10].

The one-dimensional flow analysis of the simple eductor system described depends on the simultaneous solution of the equations of continuity, momentum and energy coupled with the equation of state and specified boundary conditions.

To simplify the analysis, the following assumptions are made:

1. Both gas flows behave as perfect gases with constant specific heats.

2. The flow is steady and incompressible.

3. The flow throughout the eductor is adiabatic, the flow of the secondary stream from the plenum (at section 0) to the entrance of the mixing stack (at section 1) is isentropic. Irreversible adiabatic mixing of the primary and secondary flows occurs in the mixing stack (between sections 1 and 2).

4. At the mixing stack entrance (section 1) the temperature T_p and the primary flow velocity U_p are uniform across the primary stream, and temperature T_s and secondary velocity V_s are uniform across the secondary stream, but U_p does not equal U_s, and T_p does not equal T_s.

5. The static pressure distributions across the flow at the entrance and exit plumes of the mixing stack (at section 1 and 2) are uniform.

6. Incomplete mixing of the primary and secondary flows in the mixing stack is accounted for by the use of a non-dimensional momentum correction factor, K_m, which relates the actual momentum rate to the rate based on the bulk-average velocity and density and by the use of a non-dimensional kinetic energy correction factor, K_e, which relates the actual kinetic energy rate to the rate based on the bulk-average velocity and density.

7. Flow potential energy differences due to elevation are negligible.

8. Pressure changes P_o to $P1$ and $P1$ to P_a are small relative to the static pressure so that the gas density is principally dependent upon temperature and atmospheric pressure.

9. Wall friction in the mixing stack is accounted for with the conventional pipe friction factor term based on the bulk-average flow velocity U_m and the mixing stack wall area A_w.

The conservation of mass principle for steady state flow yields

$$W_m = W_p + W_s + W_t \tag{2.1}$$

where:

$$W_p = \rho_p U_p A_p$$

$$W_s = \rho_s U_s A_s$$

$$W_t = \rho_t U_t A_t$$

$$W_m = \rho_m U_m A_m \tag{2.2}$$

Substituting for W_m, the bulk-average velocity at the exist plane of the mixing stack becomes

$$U_m = (W_s + W_t + W_p)/\rho_m A_m \tag{2.3}$$

From the assumption 1

$$\rho_m = P_a/R\, T_m \tag{2.4}$$

where T_m is calculated as the bulk average temperature from the mixed flow. Using assumptions 5 and 6, the momentum equation for the flow in the mixing stack can be written

$$K_p(W_pU_p/g_c) + (W_sU_s/g_c) + (W_tU_t/g_c) + P1A1 = K_m(W_mU_m/g_c) + P2A2 + F_{fr} \tag{2.5}$$

K_p is a correction momentum factor which accounts for a possible non-uniform velocity profile across the primary nozzle exit. The way that K_p is defined is similar to that of K_m, using the assumption 4 it is set equal to unity, but it is included here for completeness. The momentum correction factor for the mixing stack exit is defined by the relation

$$K_m = (1/W_m U_m) \int_0^{A_m} U_2^2 \rho_2 dA \qquad (2.6)$$

where U_m is evaluated from equation (2.3) and is the bulk-average velocity. The actual variable velocity and a weighted average density at section 2 are used in the integrand. The wall skin-friction force F_{fr} can be related to the flow stream velocity by

$$F_{fr} = f \; A_w \; (U_m^2 \rho_m / 2gc) \qquad (2.7)$$

using assumption (9). For turbulent flow, the friction factor can be calculated from the Reynold's number as

$$f = 0.046 \; (Re_m)^{-0.2} \qquad (2.8)$$

where

$$Re_m = \rho_m \; U_m \; D_m / \mu_m$$

Applying the conservation of energy principle to the steady flow in the mixing stack (between sections 1 and 2) with assumption (7)

$$W_p(h_p+U_p^2/2g_c) + W_s(h_s+U_s^2/2g_c) + W_t(h_t+U_t^2/2g_c$$
$$= W_m(h_m+k_eU_m^2/2g_c) \qquad (2.9)$$

where k_e is the kinetic energy correction factor defined by the relation

$$k_e = (1/W_m\ U_m^2) \int_0^{A_m} U_2^3\ \rho_2 dA \qquad (2.10)$$

It may be demonstrated that for the purpose of evaluating the mixed mean flow temperature, T_m, the kinetic energy terms may be neglected to yield

$$h_m = (W_p\ h_p/W_m) + (W_s\ h_s/W_m) + (W_t\ h_t/W_m) \qquad (2.11)$$

where $T_m = \phi(h_m)$ only, from assumption 1.

The energy equation for the isentropic flow of the secondary air from the plenum (section 0) to the entrance of the mixing stack (section 1) may be shown to reduce to

$$(P_{os} - P_s)/\rho_s = U_s^2/2g_c \qquad (2.12)$$

This comes from the steady, adiabatic flow, energy equation

$$dh = -d\ (U_s^2/2g_c)$$

recognizing that

$$Tds = dh - (1/\rho)dP = 0$$

for the postulated isentropic conditions. Thus

$$dp/\rho_s = -d(U_s^2/2g_c) \tag{2.12a}$$

But the pressure changes from the plenum to the mixing stack are small (assumption 8), and the temperature and density are essentially constant, and thus, equation (2.12) is readily obtained. Similarly, the energy equation for the tertiary air flow is

$$(P_{ot} - Pt)/\rho_t = U_t^2/2g_c \tag{2.13}$$

The foregoing equations may be combined to yield the pressure depression created by the eductor action in the secondary and tertiary air plenums. For the secondary air plenum, the vacuum produced is

$$P_a - P_{os} = (1/g_c A_m)\ ((K_p W_p^2/A_p \rho_p) + (W_s^2/A_s \rho_s)(1 - A_m/2A_s)$$
$$- (W_m^2/A_m \rho_m)\ (K_m + fA_m/2A_m)) \tag{2.14}$$

where again the symbols are referring to Figure 1. A_w is the area of the inside wall of the mixing stack. Similarly for the tertiary air plenum, we have

$$Pa - Pot = (1/g_c A_m)\ (Kp(Wp+Ws)^2/(Ap\rho p + As\rho s)$$
$$+ (W_t^2/A_t \rho_t)\ (1 - Am/2At) - (W_m^2/A_m \rho_m)(K_m + f A_w/2A_m)) \tag{2.15}$$

We consider here as primary flow the sum of primary and secondary flows.

C. NON-DIMENSIONAL FORM OF THE SIMPLE EDUCTOR EQUATION

In order to provide the criteria of similarity of flows with geometric auxiliarity, the non-dimensional parameters which govern the flow must be determined. In order to determine these parameters, we have to normalize equations (2.14) and (2.15) which leads to the following terms:

$P^* = (P_a - P_{os})/(\rho_s/(U_p^2/2g_c))$	A pressure coefficient which compares the pumped head ($P_a - P_{os}$) for the secondary flow to the driving head ($U_p^2/2g_c$) of the primary flow.
$P_t^* = (P_a - P_{ot})/(\rho_t/(U_p^2/2g_c))$	A pressure coefficient which compares the pumped head ($P_a - P_{ot}$) for the tertiary flow to the driving head ($U_p^2/2g_c$) of the primary flow.
$W^* = W_s/W_p$	A flow rate ratio, secondary to primary mass flow rate.
$W_t^* = W_t/W_p$	A flow rate ratio, tertiary to primary mass flow rate.
$T^* = T_s/T_p$	An absolute temperature ratio secondary to primary.
$T_t^* = T_t/T_p$	An absolute temperature ratio, tertiary to primary.
$\rho_s^* = \rho_s/\rho_p$	A flow density ratio of the secondary to primary flow. Note that since the fluids are considered perfect gases, $\rho_s^* = T_p/T_s = 1/T^*$
$\rho_t^* = \rho_t/\rho_p$	A flow density ratio of the tertiary, or film cooling to the primary flow. Note that since the fluids are considered perfect gases, $\rho_t^* = T_p/T_t = 1/T_t^*$

$A_s^* = A_s/A_p$	A ratio of secondary flow area to primary flow area.
$A_t^* = A_t/A_p$	A ratio of tertiary flow area to primary flow area.
A_p/A_m	Area ratio of primary flow area to mixing stack cross sectional area.
A_w/A_m	Area ratio of wall friction area to mixing stack cross sectional area.
K_p	Momentum correction factor for primary flow.
K_m	Momentum correction factor for mixed flow.
f	Wall friction factor

With these non-dimensional groupings, equation (2.14) may be written as

$$P^*/T^* = 2A_p/A_m((K_p-A_p\beta/A_m)-W^*(K_p+T^*)A_p\beta/A_m$$
$$+W^{*2}T^*(1/A^*)(K_p-A_m/2A^*A_p)-A_p\beta/A_m)) \qquad (2.16)$$

where $\beta = K_m + (f/2)\ (A_w/A_m)$ (2.17)

Equation (2.16) can be written as

$$P^*/T^* = C_1 + C_2\ W^*(1+T^*) + C_3W^{*2}T^* \qquad (2.18)$$

where

$$C_1 = 2\ A_p/A_m\ (K_p - A_p\ \beta/A_m) \qquad (2.19)$$

$$C_2 = -\ (A_p/A_m)^2\beta \qquad (2.20)$$

$$C_3 = 2\ A_p/A_m\ (1/A^* - A_m\ /2A^*A_p - A_p\beta/A_m) \qquad (2.21)$$

Equation (2.18) may be expressed as simple functional relationship.

$$P^* = \phi(W^*, T^*) \qquad (2.22)$$

The same format is followed by equation (2.15) for the tertiary flow so it can be expressed with the equation (2.22).

Two more dimensionless quantities have been used to correlate the static pressure distribution across the length of the mixing stack.

$PMS^* = (PMS/\rho_s)/(U_p{}^2/2g_c)$	A pressure coefficient which compares the pumping head (PMS/ρ_s) for the secondary flow with the driving head $(U_p{}^2/2g_c)$ of the primary flow.
X/D	Ratio of the axial distance from the mixing stack entrance to the diameter of the mixing stack.

D. EXPERIMENTAL CORRELATION

A satisfactory correlation of P*, T* and W* takes the form

$$P^*/T^* = \phi\,(W^*\, T^{*n}) \qquad (2.23)$$

where the exponent "n" was determined to be equal to 0.44. The details of the determination of the equation (2.23) as well as of n = 0.44 are given by Ellin [Ref. 1]. The experimental data is correlated and analyzed using equation (2.23), that is P*/T* is plotted as a function of $W^*\, T^{*0.44}$

to yield an eductor's pumping characteristic curve. Variation in geometry will change the appearance of the pumping characteristic curve. The value of parameter W* T*0.44 when P*/T* = 0 will henceforth be referred to as the pumping coefficient.

III. EXPERIMENTAL APPARATUS

The experimental facility used was constructed by Ross [Ref. 3] and modified by Welch [Ref. 4] and Hill [Ref. 6]. Eick [Ref. 7] brought the facility to the present condition after extensive and significant modifications. The hot primary gas is supplied to the nozzles and mixing stack system by the combustion gas generator and associated ducting (Figures 2 through 4). The eductor system is mounted in a secondary air plenum (Figures 5 and 6). Ten ASME long radius flow nozzles mounted in the plenum walls allow measurements of the secondary flow. Combustion air is provided by a three stage carrier centrifugal air compressor. Appendix A gives complete instructions for the operation of the test facility and the procedures of taking data.

A. COMBUSTION AIR PATH

The input air to the combustion gas generator is supplied by a Carrier model 18P35 compressor (Figures 7 and 8) located in Building 230 adjacent to the test facility, Building 249. The input air is piped underground to a vertical stand pipe which contains an eight inch butterfly valve and a globe bypass valve (Figure 3). All air demands for this testing can be met with the bypass valve. At the top of the stand pipe is a tee connection. In one leg of the tee, an eight

inch butterfly valve isolates the eductor facility from other requirements. The other leg of the tee directs the air to the combustion gas generator through an eight inch to four inch reducing section. The pressure drop across this section is used to measure the primary air flow rate. Eick fitted a linear curve to Welch's calibration data for use in a data reduction program. The correlation is presented in Figure 40. Air flows next to a splitter section (Figure 2) through a four inch isolation butterfly valve.

Under control of two motor operated valves, a portion of the air flow is directed through the U-tube to the combustor section. The flow characteristics of this section, as determined by Ross are presented in Figure 38. Combustion was performed in a combustor taken from a Boeing model 502-6A gas turbine engine. The hot combustion gas was fed into the annular space of the nozzle box from the same engine. This section contains the nozzle vanes of the gas generator turbine of the engine. The by-passed cooling air was mixed with the hot gas by a mixing section designed by Ross [Ref. 3]. This section provided a swirl to the cooling air which was counter to the swirl given to the hot gas in the nozzle box vanes, thus improving the mixing of the cooling air with the hot gas. The procedure for system light-off and operation is included in Appendix A.

The hot gas passes through a flow straightening section and an uptake section which delivers the gas flow to the primary nozzles.

B. FUEL SYSTEM

Service fuel is stored in a 55 gallon drum mounted on an elevated stand adjacent to the building (Figure 10). A tank isolation valve is followed by a sediment collector outside the building (Figure 11). Another isolating two position valve is located inside the building. The temperature of the fuel is measured by a thermocouple installed adjacent to the interior bulkhead valve. Fuel then passes the Fisher Porter Model 10A3565A flow measuring rotameter installed by Eick to a fuel filter (Figure 11). The flow characteristics of the rotameter was determined by Eick and are presented in Figure 39. The linear curve fit to the data results in the expression

$$WF = -3.0716 + 0.4048 * ROTA \tag{3.1}$$

Taking suction on the filter is a 24 VDC motor driven fuel supply pump (Figure 12). This positive displacement pump contains an internal bypass and pressure regulating feature. The normal operating pressure is 14-16 psig.

The supply pump provides positive suction head for the high pressure pump (Figure 13). This is a 115 VAC motor driven fuel pump and is provided with an external bypass with valve called trimmer valve (Figure 13). The setting of this

valve controls the range of discharge of the high pressure pump. The procedure of setting of the valve is included in Appendix A. Another bypass valve controls the discharge pressure at the pump and is located at the control station (Figure 14) to allow easy adjustment of the exhaust gas temperature. The fuel system contains also a drain valve, a manually operated discharge valve (Figure 13) and an electrically operated solenoid valve, located at the entrance of the combustor. The necessary automization is produced by a Monarch type 60° and 5 GPH burner nozzle, installed and calibrated by Eick. Eick's calibration chart is presented in Figure 41. Eick's modifications to the fuel system led to a very easy and clean combustion, with 10 - 12 seconds depending on the temperature of the fuel.

C. THE MEASUREMENT PLENUM

Secondary air flow is measured with a large metering box which encloses the uptake and the inlet of the mixing stack and acts as an air plenum. Ten ASME long radius nozzles, of varying cross-sectional areas, are mounted in the sides and roof of the plenum allowing the nozzle flow area to be varied accurately. Measurement of the pressure difference between the ambient and the plenum interior, and knowledge of the ambient temperature permit calculation of the flow rate. Appendix B presents a computer program written by Hill and Eick to determine the flow rates. In order to improve the

sealing of the plenum, and to minimize the heat loss in the uptake, Eick modified the forward and rear sealing, and insulated the uptake. These improvements are shown in Figures 15 and 16. An adjustable support stand was used by Eick to support the mixing stack assembly independently of the seal plates. This stand facilitates model installation and alignment. Alignment is accomplished by mounting the model on the stand, installing centering plates, in each end of the mixing stack, and in the open uptake pipe, and adjusting the stand until the alignment ban passes freely through holes in the centering plates. The alignment apparatus can be seen in Figures 16 and 17. Standoff distance is then set by installing the primary nozzles on the uptake, and measuring the required distance from the nozzle exit plane to the mixing stack entrance plane. Both tests were made at a standoff ratio S/D equal 0.5. In order to compensate for the expansion effects of the uptake, the distance S was increased from 3.561 to 3.6875, so the actual standoff ratio is higher than 0.5 in this cold position.

D. INSTRUMENTATION

1. Temperature Measurements

Two types of thermocouples are installed. Type K thermocouples provide high temperature data, such as combustion temperatures, uptake temperatures, mixing stack wall temperature and exit plane temperatures. Table I gives

the current channel assignments. Type T thermocouples provide low temperature data. They measure inlet air, ambient air, fuel, and shroud and diffuser surface temperatures. Table II gives the current thermocouple channel assignments. The display of the thermocouple measurement and the schematic diagram of the temperature measurement system are shown in Figures 14 and 18. A portable pyrometer was used to provide data on the external surface of the eductor assembly. The portable pyrometer has the advantage that using a surface probe, it can measure temperatures at any point of the surface. Another method that has the same advantages with the portable pyrometer, but smaller accuracy, is thermal imagery. This method was used by Eick and is described in detail in his work.

2. Pressure Measurements

Five manometers are installed for gas generator operation and data collection. The installation is shown in Figure 19. They include a 20 inch upright water manometer for measurement of differential pressure across the eight to four inches inlet reducing section (DELPN), 17 inch upright oil manometer (it measures in inches of water) for measuring uptake pressure (PUPT), a 20 inch upright mercury manometer for measuring inlet air pressure (PNH), a 2 inch inclined water manometer for measuring the differential pressure across the burner U-tube (DELPU), and a 6 inch inclined water

manometer connected to a distribution manifold. Ten individual manifolds located in the main control panel (Figure 14) are interconnected to permit measurements of plenum and mixing stack static pressure with respect to atmospheric pressure. A schematic diagram of pressure measurement system is shown in Figure 20. Also installed is a laboratory mercury barometer. Another mercury barometer is installed in Building 230.

E. THE MODELS

Two eductor models were tested. Each model consists of a primary four nozzle plate mounted at the end of the uptake and a mixing stack assembly. The mixing stack assemblies include the mixing stack, a film cooling shroud, and an exit diffuser. Characteristic eductor dimensions are given in Figure 9. In both models tested, the mixing stack and the nozzles are the same. The internal diameter of the mixing stack, D, was 7.122 inches. This dimension was the same as used in previous hot flow testing and is 0.6078 scale of the cold-flow models. Both models tested employed a standoff ratio, S/D, of 0.5. Table III provides a comparison of key model characteristics.

1. Model A

Model A, which was previously tested by Eick, is shown installed in Figure 21. This configuration includes a primary nozzle plate with four tilted and angled nozzles

(Figures 22 and 23). The configuration, 15/20, of the nozzle refers to the characteristic angles. In this case the tilt of the nozzle is 15° from the vertical and it is rotated or angled in 20° from the tangential direction (Figure 24). The mixing stack cross-sectional area to primary nozzle exit flow area ratio is 2.50.

The mixing stack L/D is 1.0 and contains four rows of film cooling ports. The dimensional diagram of the film cooling ports is shown in Figure 25; the total port area to mixing stack cross-sectional area was 0.141. Eight pressure taps are installed in the wall of the mixing stack. They are arranged into two rows, 45° apart (Figure 25). Twelve type K thermocouples are located in an array 180° from the pressure taps. The locations were chosen to determine the cooling effects of the stack ports. Unfortunately, a failed thermocouple at one of the two port locations chosen, seriously reduced the information which could be obtained regarding port effects. The shroud and diffuser rings were made from 25 gauge cold rolled sheet steel. The arrangement is shown in Figure 26. The separation between shroud and mixing stack was .076 inches, and the separation between shroud and diffuser rings as well as between the diffuser rings was also .076 inches. A single row of type T thermocouples was installed along the length of the shroud and diffuser.

2. Model B

The second model tested, pictured in Figures 27 and 28, was a modification of the Model A, the nozzles and the mixing stack are the same as those of Model A. The shroud was extended towards the inlet of the mixing stack, the number of diffuser rings were increased from two to three, the first ring was extended towards the inlet of the eductor. These changes were made in order to cover the high temperature regions detected on the Model A. The cooling flow passage clearance was increased from 0.076 inches to 0.139 inches between mixing stack and shroud, and from 0.076 to 0.096 inches between shroud and diffuser rings. The concept of increasing the cooling clearance was to allow greater mass flow to pass through the diffuser, in order to achieve better cooling. The overall L/D remained the same with Model A (i.e., overall L/D = 1.5). The result of increasing the cooling clearance was an increase in the diameter and an increase in the half angle of the diffuser, the half angle is shown in Figure 30. The arrangement is shown in Figures 29 and 30. A single row of 11 type T thermocouples was installed along the length of the shroud and diffuser. A portable pyrometer was used to verify that the thermocouples installed provided data representative of the entire shroud/diffuser surface, and to detect any high temperature spots on the external surface.

IV. EXPERIMENTAL RESULTS

Modifications to the experimental apparatus having been completed, data was taken on the performance of the two eductor models described above. The purpose of retesting Model A was to validate data acquisition procedures and to ensure continuity with the results of previous researchers. Model B was the model of interest.

A. MODEL A RESULTS

1. Pumping Performance

Figures 42 through 44 display the results of pumping coefficient measurements for Model A, Tables IV through VI. In each case the data is compared with that taken by Eick [Ref. 7] on the same model. Here, the strong correlation in pumping coefficient data that was obtained in all tests throughout the current research is seen.

The pumping coefficient results for all data runs in this series are presented in Figure 45 for comparison. The dependence of pumping coefficient on temperature observed in Welch's and Hill's data is apparent here, but exactly in the opposite sense. In Model A, a substantial increase in secondary pumping capability with the higher primary temperature is observed. Although tertiary pumping was not measured here, data on shroud and diffuser temperatures

presented later indicate that strong tertiary pumping is also present in this model.

2. Mixing Stack Temperatures

Figures 46 through 48 display the results of mixing stack temperatures for Model A, Table VIII. In each case the data is compared with that taken by Eick [Ref. 7] The comparison of results is quite favorable throughout. If the differences in ambient temperature and TUPT are taken into account, it is seen that the results are almost identical. Due to a recording error, data for the two internal thermocouples located at the entrance at the mixing stack is not available.

The mixing stack temperatures for all data runs in this series are presented in Figure 49 for comparison. The data is consistent with maximum temperatures of about 320o F for the 950o F uptake temperature run.

3. Mixing Stack Pressure

The data obtained for mixing stack pressures is presented in Figures 50 through 52 and in Table VII. The comparison in results is quite favorable throughout. If the small fluctuations of the pressure are taken into account the results are almost identical. The comparison of the data for all runs in this series is presented in Figures 53 and 54. The temperature dependence at the pressure is apparent. This was expected since there was a temperature dependence of the

primary flow pumping coefficient. The pressure depression for a certain point of the mixing stack increases with the temperature.

4. <u>Shroud and Diffuser Temperatures</u>

Figures 55 through 57 display the shroud and diffuser temperature data found in Table IX. The comparison reveals highly acceptable correlation with the data obtained by Eick. If the differences in uptake temperature resulted in different pumping coefficient are taken into account, it is noticeable that the results are almost identical. The areas of highest temperature lie on the shroud before the start of the diffuser and at the termination of the second diffuser ring. Maximum temperatures of 205oF, or about 135o F above the ambient. were recorded at an uptake temperature of 950o F. External surface temperatures of this model were much higher than those appeared at Hill's model. The shroud and diffuser temperature results for all data runs in this series are presented in Figure 58 for comparison.

5. <u>Exit Plane Temperatures</u>

As with the other measures of performance presented, the exit plane temperature profile data obtained corresponds well with that of Eick. Figures 59 through 61 present the raw data obtained. This data is tabulated in Table X. There is a slight assymmetry in the profile which is probably due to a misalignment of the mixing stack. It is also possible

that a small positional error has been introduced by the traversing mechanism. This mechanism which supports and moves the thermocouple is shown in Figure 32.

A comparison of the data runs in this series is presented in Figure 62.

The non-dimensional exit plane temperature coefficients are presented in Figures 63 through 65. The data is considered to be very consistent and having the same profile with the exit plane temperature data. A comparison of those coefficients for all three nominal uptake temperatures is given in Figure 66.

B. MODEL B RESULTS

The uptake temperatures of data runs on the second model were the same with the Model A in order to allow direct comparison between the two models.

1. <u>Pumping Performance</u>

The pumping coefficient performance of Model B is shown in Figures 67 through 69. Pumping coefficient data is tabulated in Tables XI through XIII. The comparison of results is quite favorable throughout. This was expected since the primary nozzles and the mixing stack are the same on both models and the pumping coefficient measurements are based o the secondary flow. Although tertiary pumping was not measured here, data on shroud and diffuser temperatures and mixing stack pressures presented later, indicate that the

tertiary pumping is stronger in this model. A comparison of the pumping coefficient performance of Model B at all temperatures tested is found in Figure 70.

2. Mixing Stack Temperatures

The thermocouples located at the entrance of the mixing stack were welded at the same way with the remaining 10 thermocouples in order to have the same performance. The thermocouple immediately upstream of the second cooling port was replaced with a new one. The arrangement of the thermocouples remained the same as with Model A, Figure 25.

The data obtained for mixing stack temperatures is presented in Figures 71 through 73 and in Table XV. The comparison between the data in Model A reveals a highly acceptable correlation across most of the length of the mixing stack. The last portion of the mixing stack is highly influenced by the cooling effect of the shroud. Therefore, as a result, the external wall temperature immediately downstream of the last cooling port is only 40° F above the ambient temperature in the 950° F uptake temperature run. The pure effect of the cooling port is obtained by the data of the port in the first row. The cooling air entering the mixing stack through the cooling ports reduces the external wall temperature immediately downstream of the port by approximately 50° F. Points at the same L/D and 45° apart exhibit different temperature. It is suspected that due to

the tilted angle of the nozzles, the flow is not uniform across the mixing stack and the sector between consecutive nozzles exhibit lower temperatures.

Figure 74 is a comparison of the mixing stack temperature data of Model B at all temperatures tested. The maximum temperature of about 280o F being obtained in the 950o F uptake temperature run is 20o lower than the temperature of the Model A, for the same uptake temperature run.

3. Mixing Stack Pressures

The data obtained for mixing stack pressures is presented in Figures 75 through 77 and Table XIV. In addition to PMS, Table XV contains mixing stack pressure data in a non-dimensional form, PMS*, which is a ratio of the pumping head available for tertiary flow to the driving head available from primary flow. The comparison between this data and the data from Model A reveal a decrease in pressure depression throughout the mixing stack. This happens because the cooling clearance between the mixing stack and diffuser ring was greater for Model B. The data from the position "A" tap at the 0.5 L/D is higher than all other data and is suspected that this sensing line has a small leak although a search was made for such leak and none was found.

The comparison of mixing stack pressure data of Model B at all temperatures tested is found in Figures 78 and 79.

4. Shroud and Diffuser Temperatures

The data obtained on shroud and diffuser temperatures may be found in Table XVI and is presented in Figures 80 through 82. The film cooling effect can clearly be seen at the last data point on the shroud. The temperatures achieved throughout the diffuser were substantially lower than the values obtained for Model A. This is felt to be the result of the bigger cooling clearances and the better shielding of the shroud. The maximum exposed surface temperature in Model B was 122.4° F which occurred at the end of the third diffuser ring being more than 80° F lower than in Model A.

A comparison of the shroud and diffuser temperatures performance of Model B at all temperatures tested shown in Figure 85 reveals that the temperature remains constant at the entrances of the mixing stack and first and second diffuser ring. The temperature remains constant across the first ring; it increases rapidly at the last portion of the third diffuser ring. It is suspected that there is not sufficient film cooling at the last portion of the third diffuser ring to reduce the temperature to the same level as the other rings and shroud. Unlike the other rings, the last portion of the third diffuser ring is not supplied with induced film cooling on both sides, but only on the inner side. Shortening of the third diffuser ring back to a point

near the end of the second diffuser ring, might improve the performance of this assembly.

5. Eductor External Surface Temperatures

The data obtained by the portable surface probe for eductor external surface temperatures is presented in Figures 84 through 86 and in Table XVII. There are no data available from previous works for comparison. In each figure, the film cooling effect can clearly be seen in the reduction of temperature at the first data point of the first diffuser ring. The temperature remains lower than 110° F throughout the external temperature of the eductor assembly. This is consistent with the mixing stack temperature data, where the thermocouples, located at the entrance of the mixing stack, were always around 100° F shown in Figure 74 and the data obtained on shroud and diffuser temperatures (Figure 82).

The comparison of eductor external surface temperature for the range of temperatures tested shown in Figure 87 reveal a sufficient cooling of the shroud and the first two diffuser rings but an abrupt increase in temperature of the third diffuser ring. It is suspected that the velocity of the exhaust gases is relatively low at the region of the third ring and so is the pumping capability.

6. Exit Plane Temperatures

The data obtained on the exit plume temperatures may be found in Table XVIII and is presented in Figures 88

through 93. Here again both raw data and temperature coefficients are presented.

The comparison in results is quite favorable throughout. The temperature profile for Model B data is evenly arranged in contrast with Model A. It is suspected that this happens due to the adequate film cooling induced by the shroud and the diffuser rings. The comparison of exit plane temperatures and coefficients for the range of temperatures tested are shown in Figures 94 and 95. In the 850° F and 950° F runs, it is seen that the temperature coefficients are almost the same and that the percentage of cooling is independent of the uptake temperature. From this observation we can predict the maximum plume temperature for higher uptake temperatures.

V. CONCLUSIONS

This investigation studied the effects on the eductor temperature performance of a slotted, shrouded mixing stack with two and three diffuser rings. Based on the data presented, the following conclusions are drawn:

1. The data obtained from the model previously tested, Model A, is found to be consistent with previous results.

2. The short, slotted mixing stack, with L/D = 1 combined with the 15/20 tilted-angled primary nozzles, provide sufficient pumping performance and a relatively uniform mixed exit flow.

3. The reduction in mixing stack wall temperature downstream from the cooling slots is approximately 50^{o} F.

4. The shroud and diffuser combination employed in Model B permit the induction of substantial amounts of film cooling flow. The surface temperatures for this assembly are substantially lower than those found in Model A.

5. The maximum shroud temperature was reduced by increasing the annular gap between the shroud and the mixing stack.

VI. RECOMMENDATION

In addition to providing insight into the effects that geometric parameters have on eductor system parameters, this reserch has also generated an awareness of the investigation's shortcomings. Presented here are recommendations for future research and improvements to the test facility.

1. Test the effect on eductor system parameters of an air stream moving perpendicular to the external surface of the eductor. High air stream velocities may produce stagnation areas on the surface resulting in local high temperatures.

2. Install a pressure tap at the exit of the nozzles and record the pressure depression at this region and relate this pressure to the uptake pressure.

3. Take additional temperature data on Model B with the third diffuser ring cut back to the end of the second diffuser ring. Eliminating the last portion of the third diffuser ring which is cooled by film cooling only from the internal side (the other diffuser rings are cooled by induced flow on both sides); might eliminate the relatively high temperature areas existing at the end of the third diffuser ring.

FIGURES

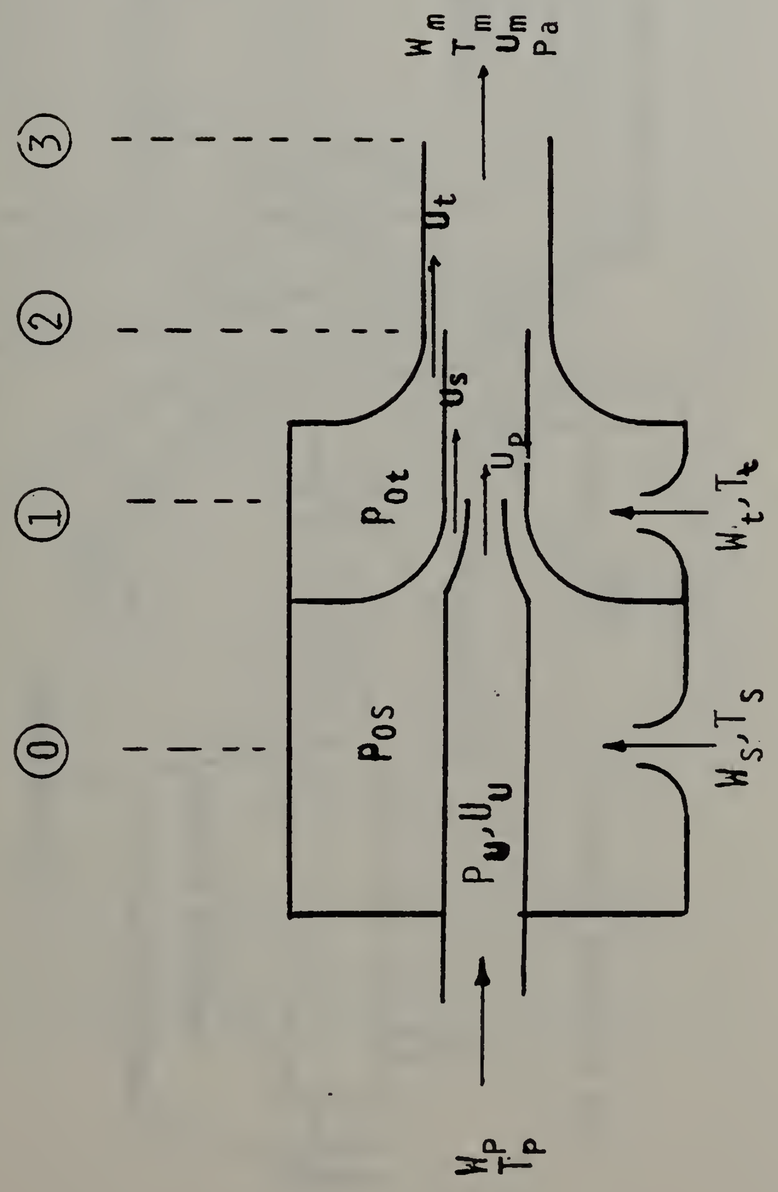

Figure 1. One Dimensional Eductor Model

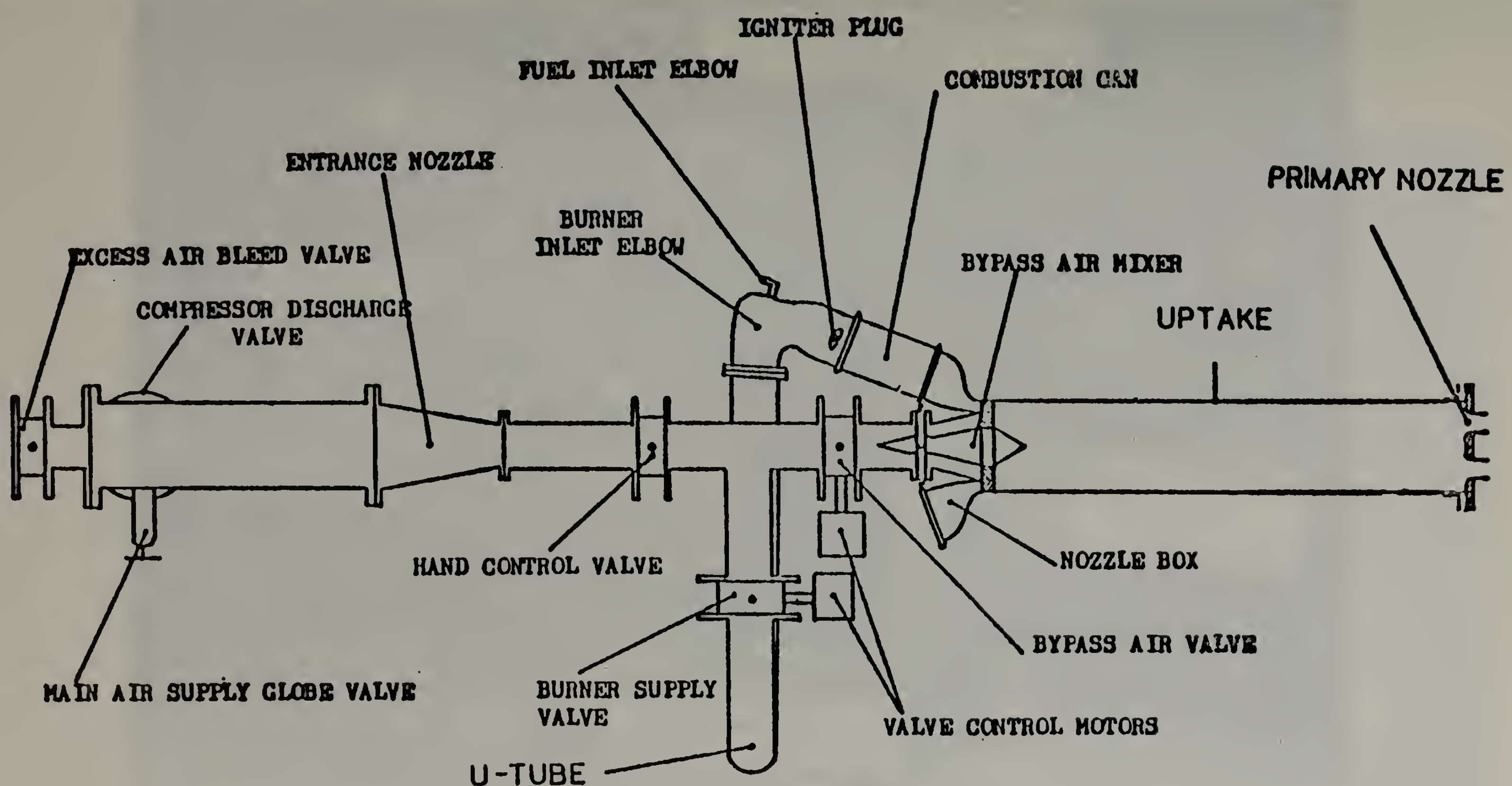

Figure 2, Gas Generator Arrangement

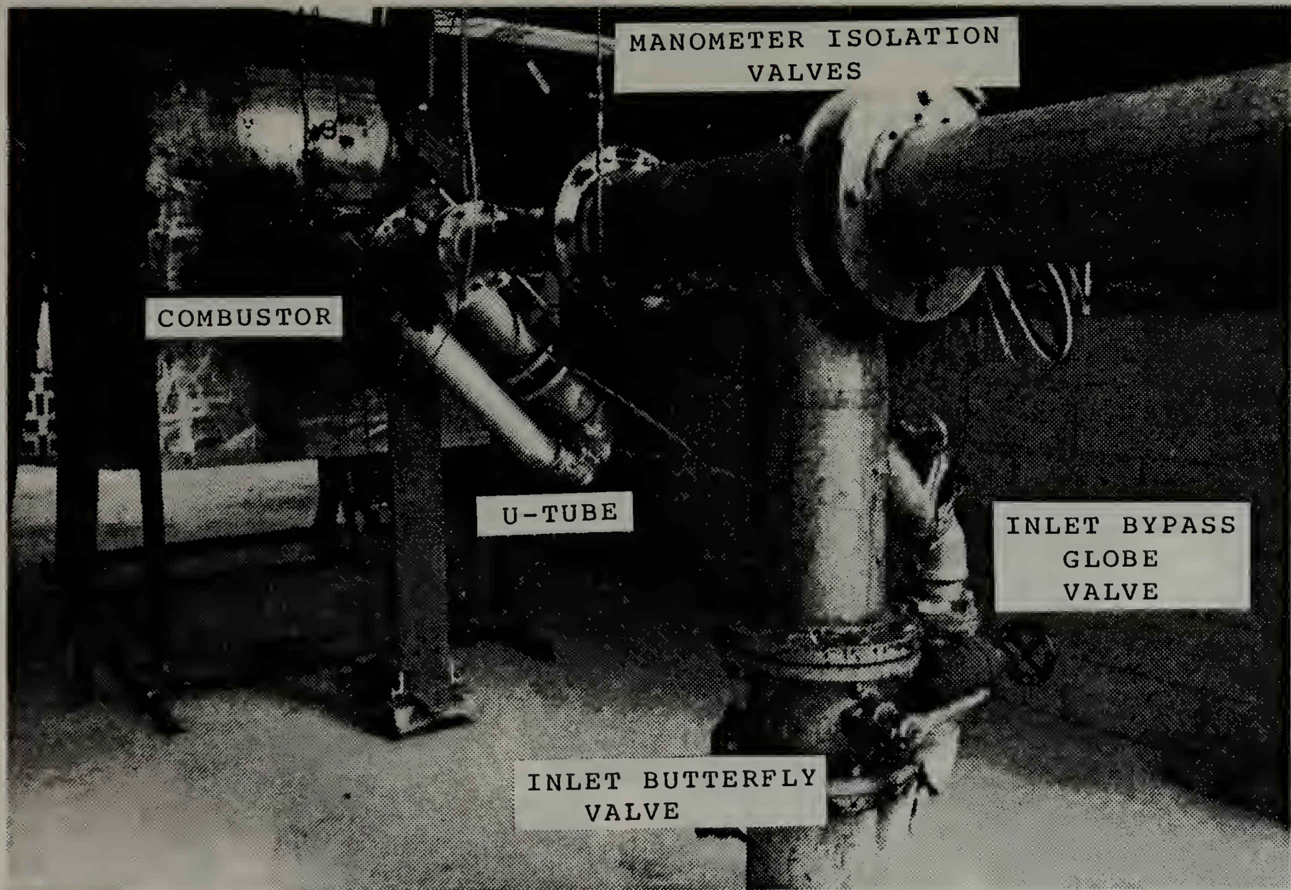

Figure 3. Air Supply Standpipe and Valving

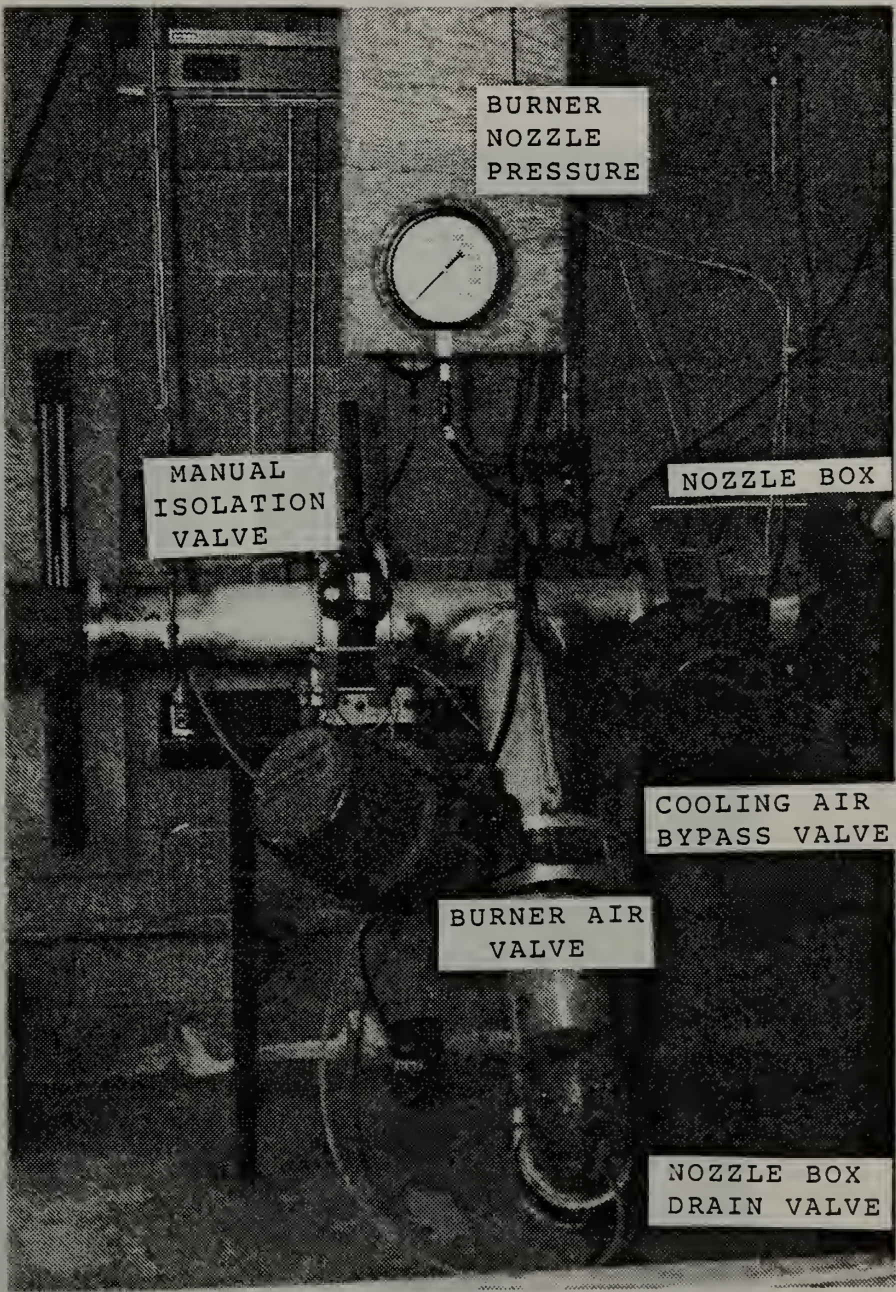

Figure 4. Combustion Air Piping

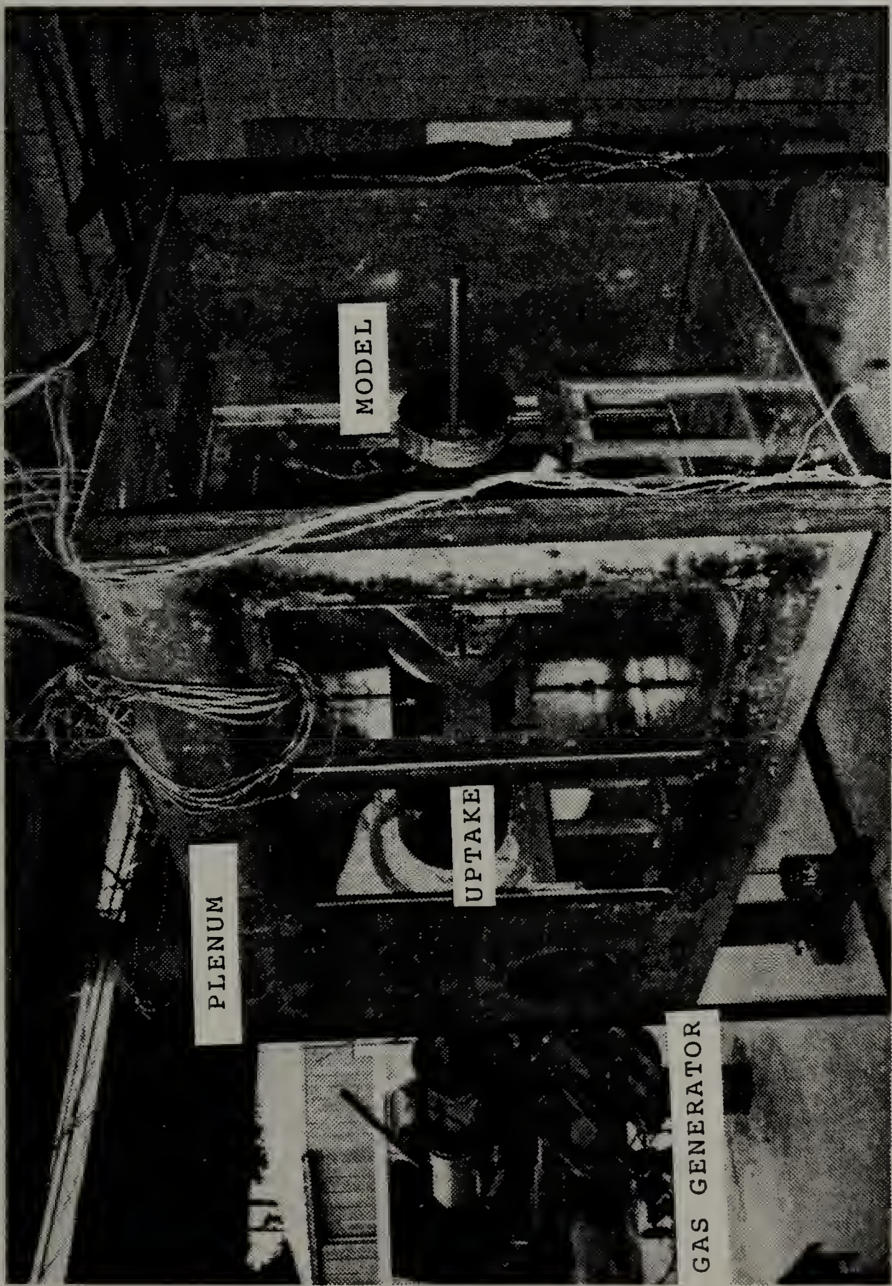

Figure 5. Hot Flow Test Facility

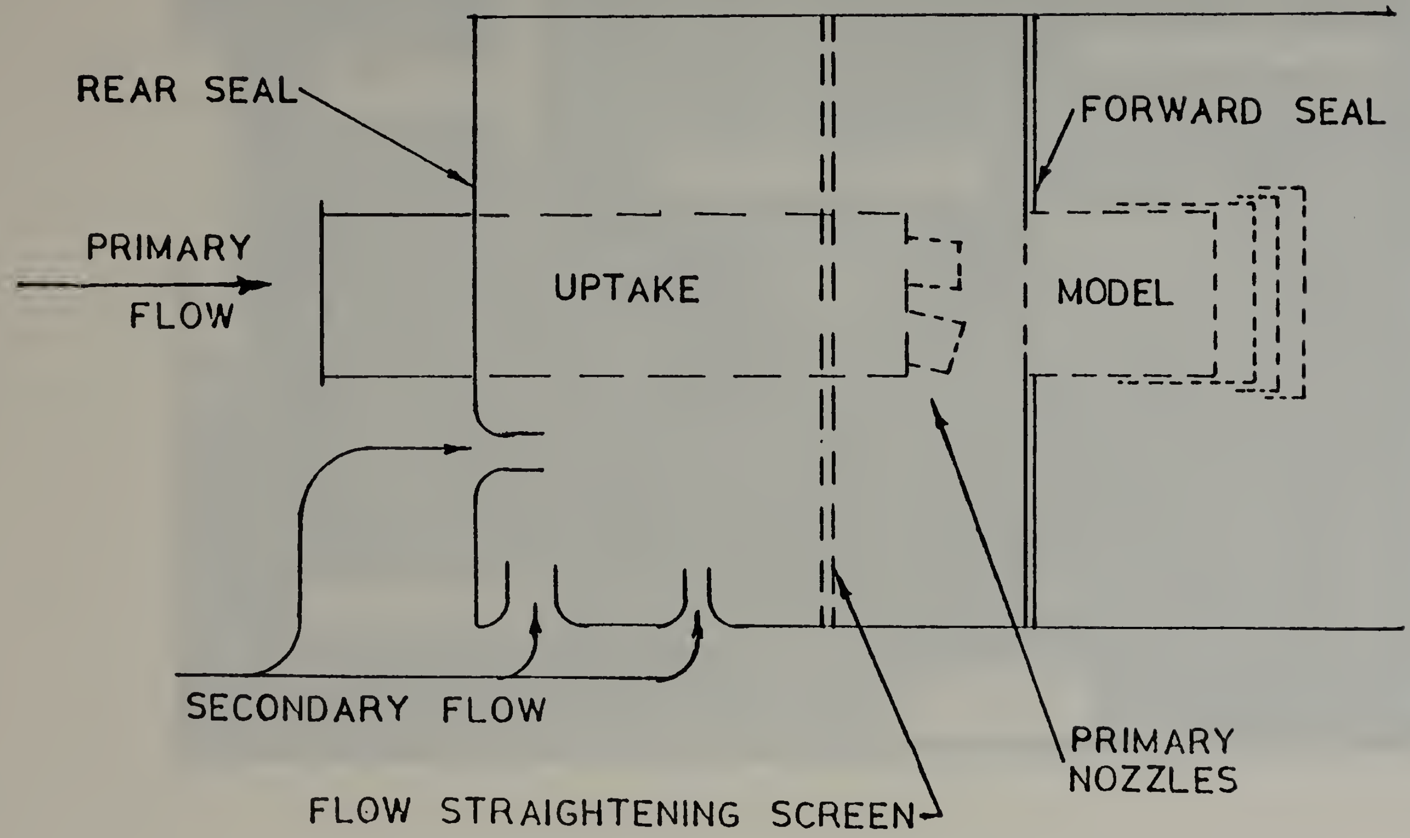

Figure 6. Plan of Uptake, Model, and Measurement Plenum

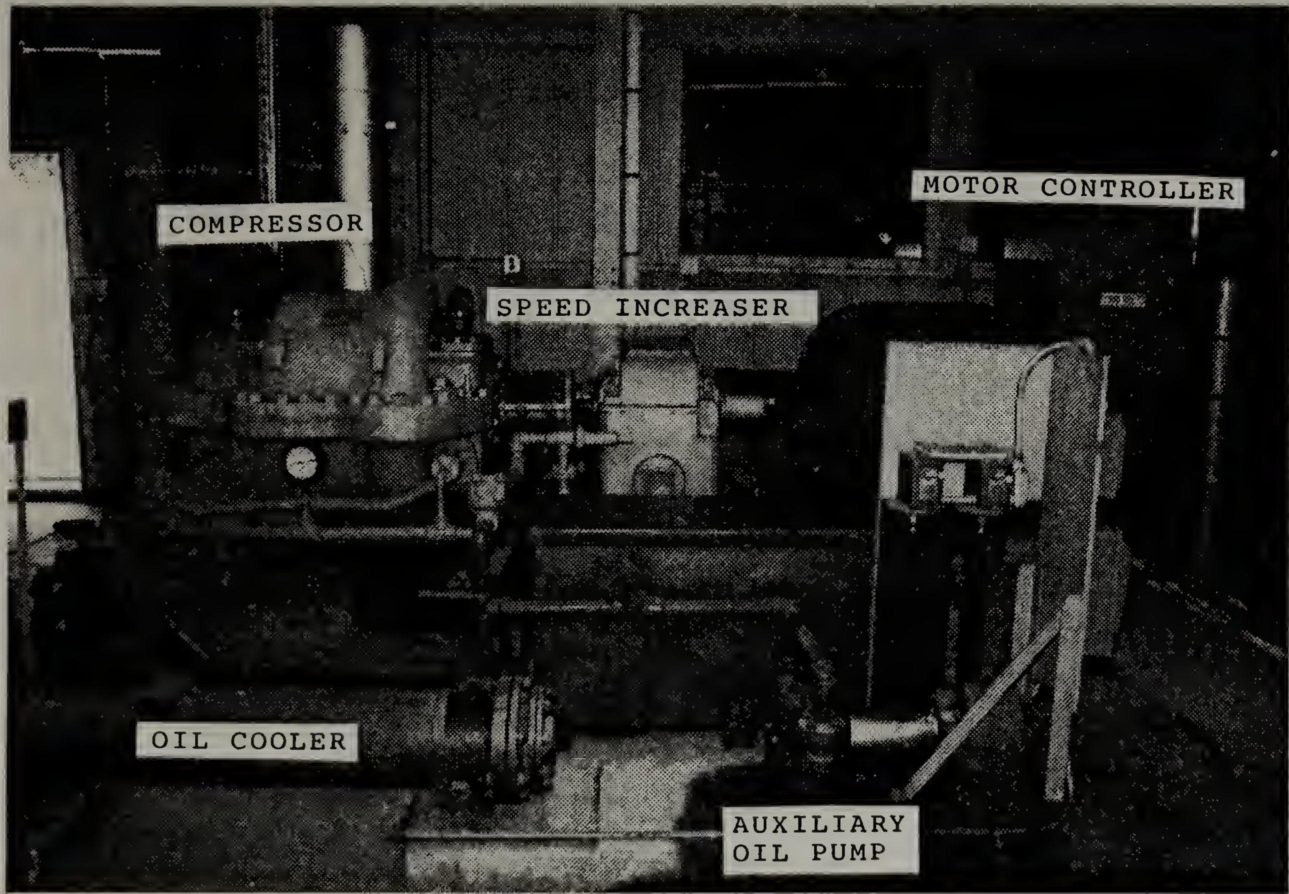

Figure 7. Carrier Air Compressor

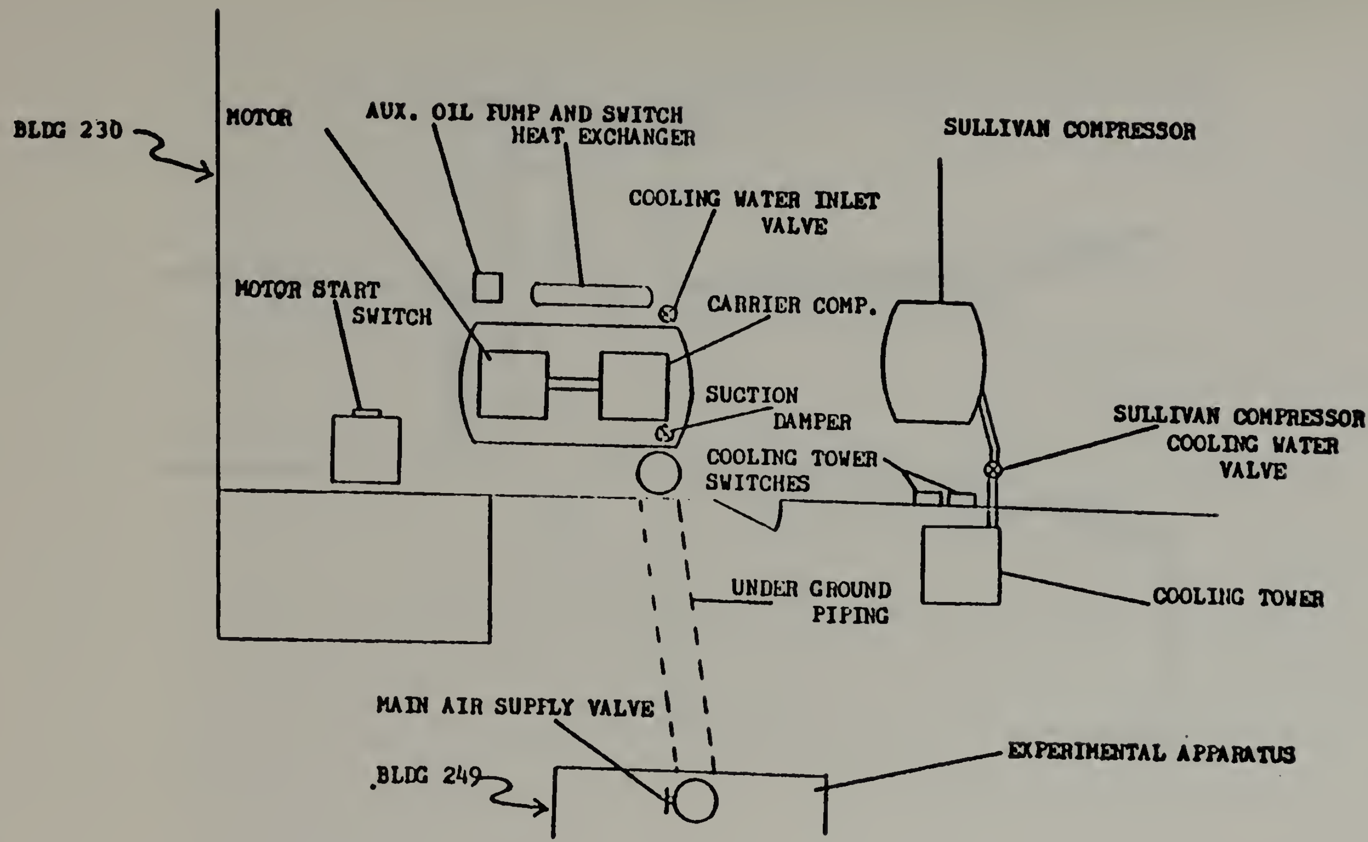

Figure 8. Compressor Layout

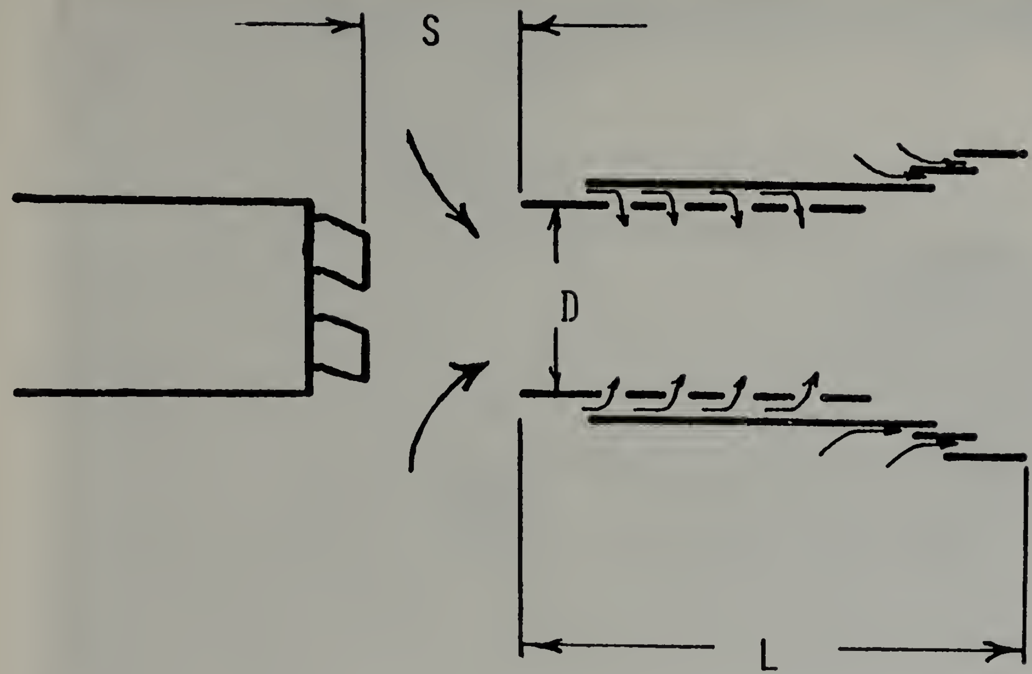

Figure 9. Characteristic Eductor Dimension

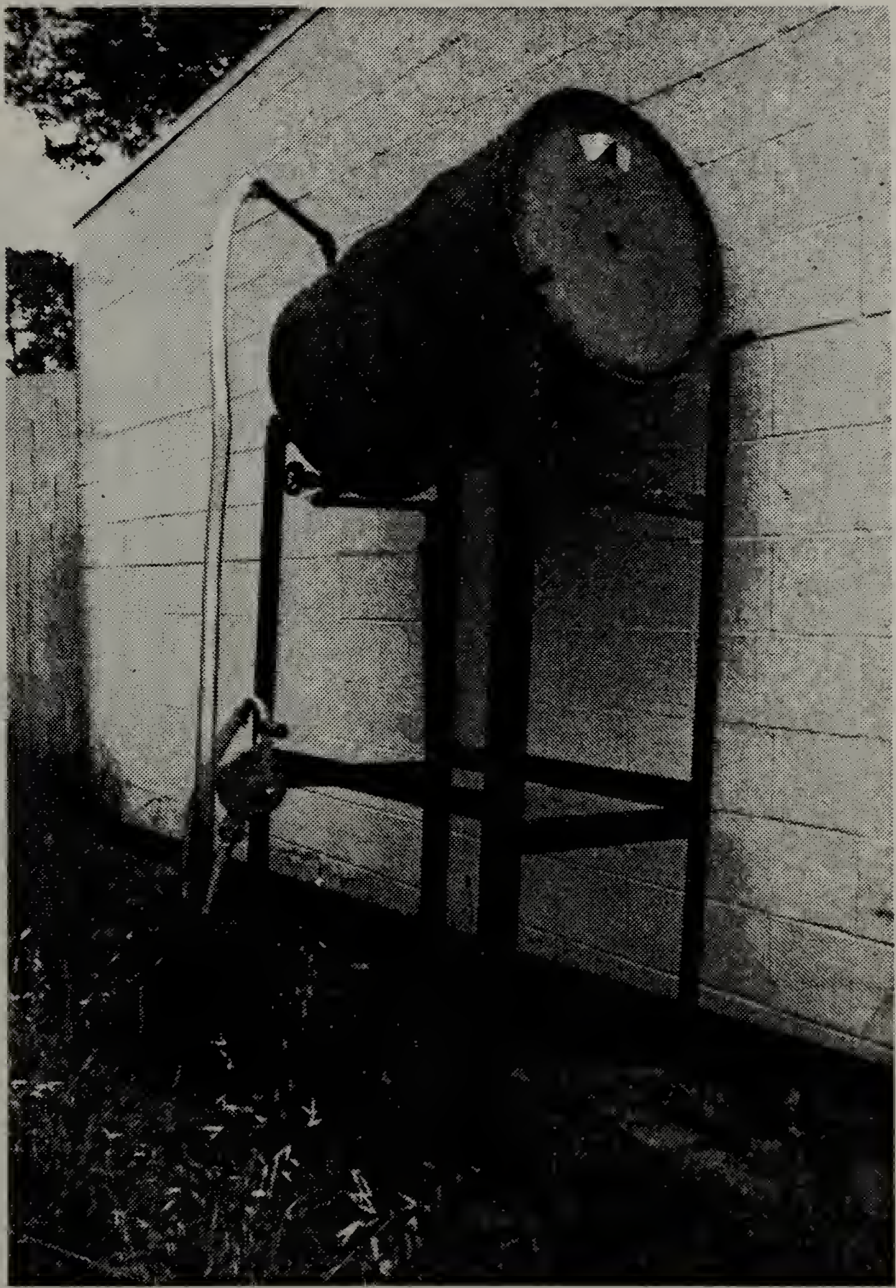

Figure 10. Fuel Service Tank

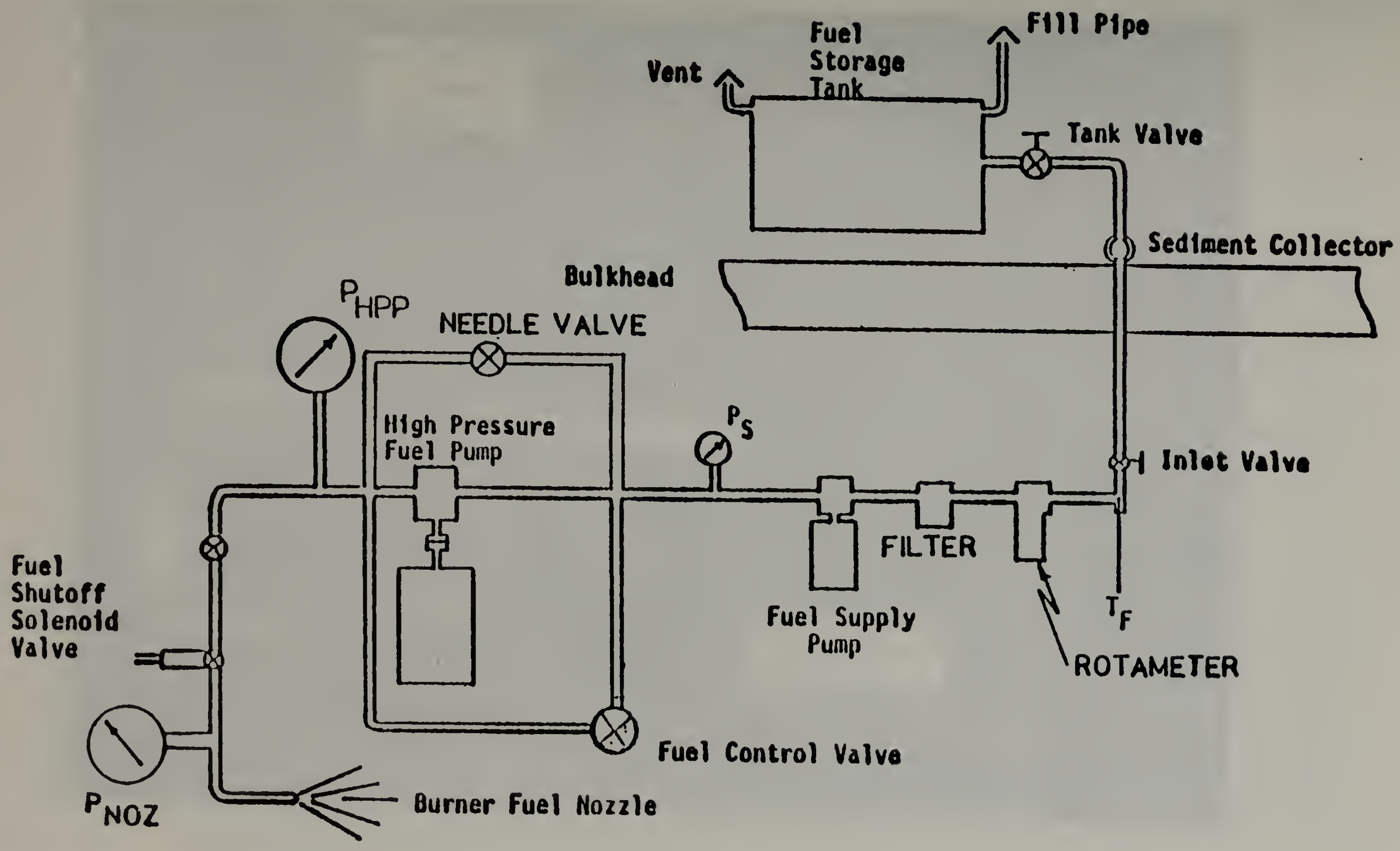

Figure 11. Gas Generator Fuel System

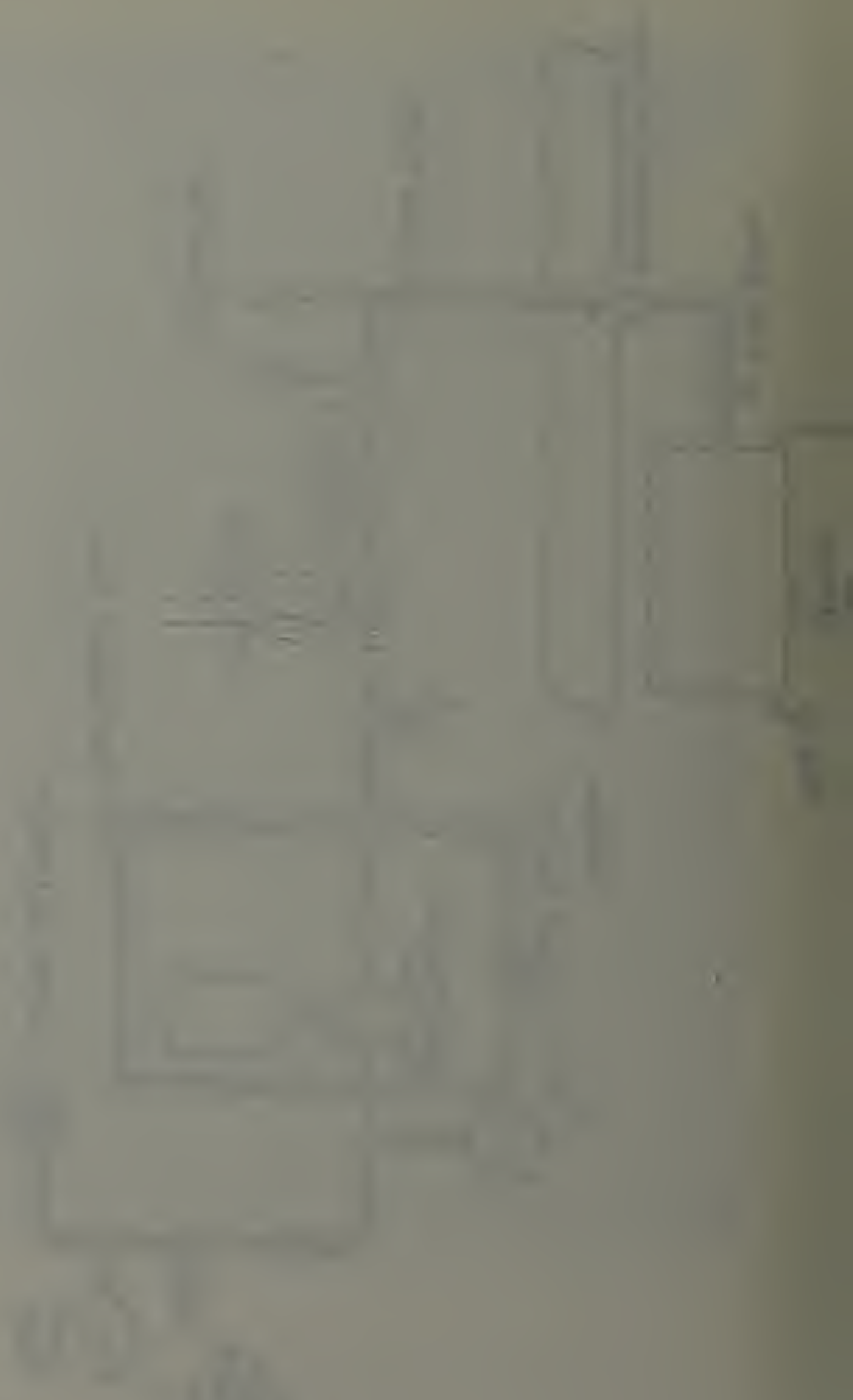

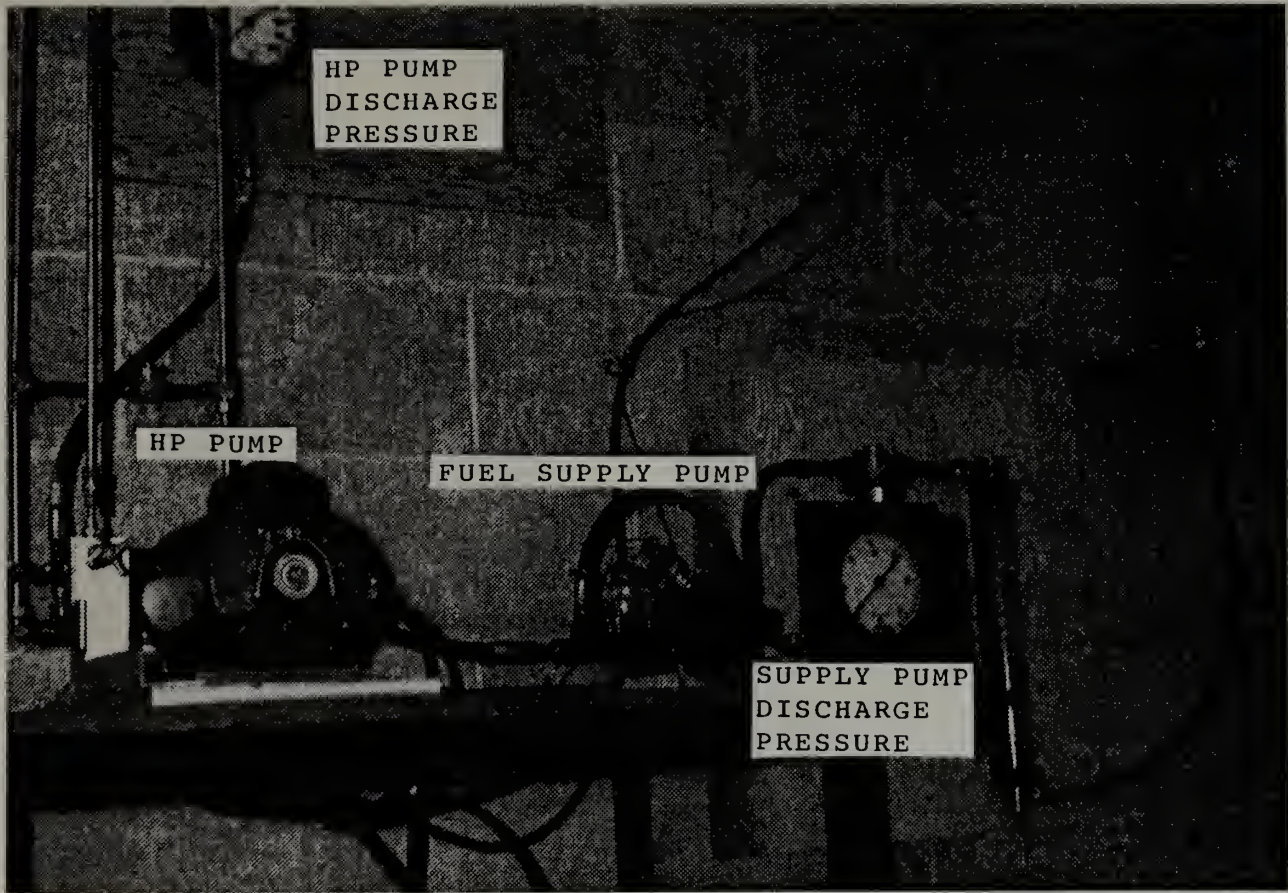

Figure 12. Fuel Pump Installation

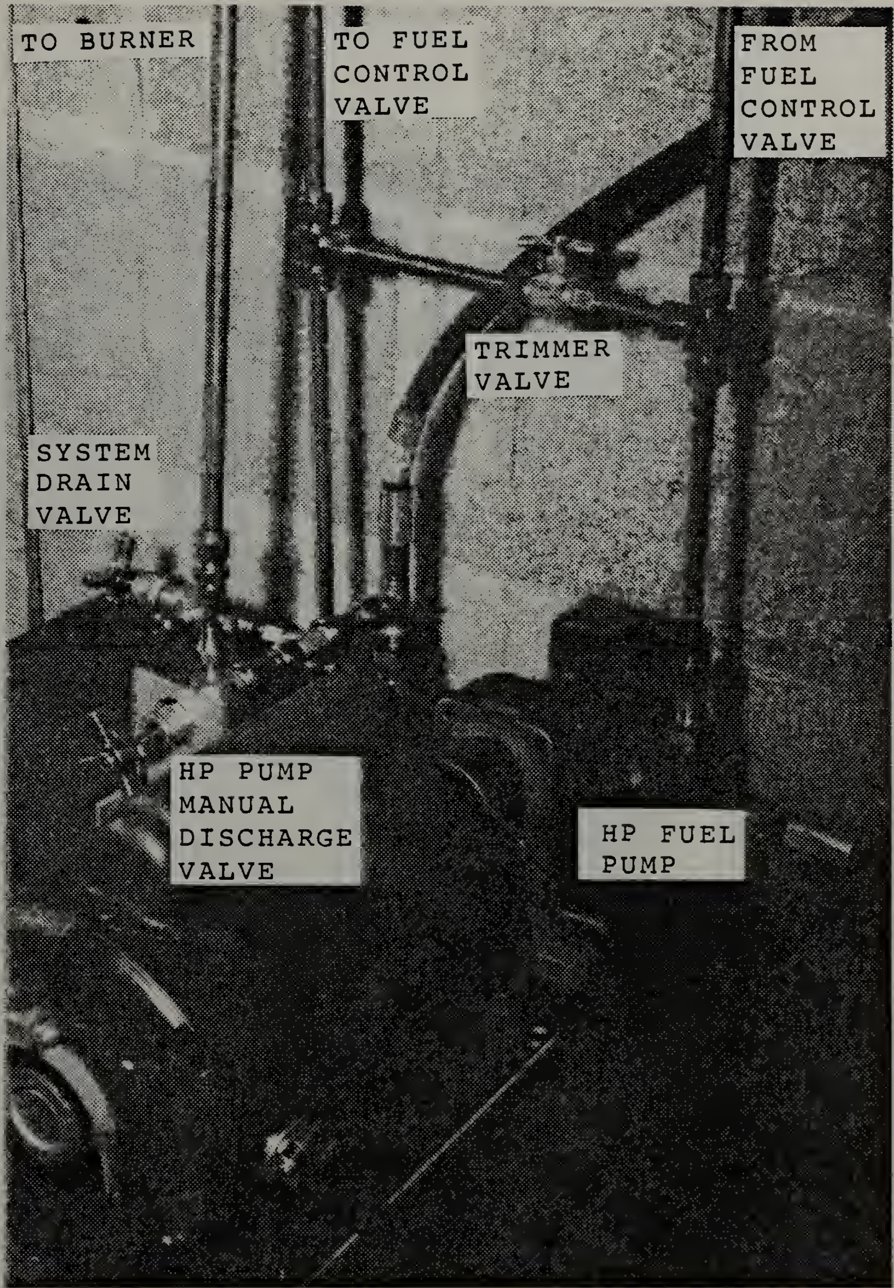

Figure 13. HP Fuel Piping and Valves

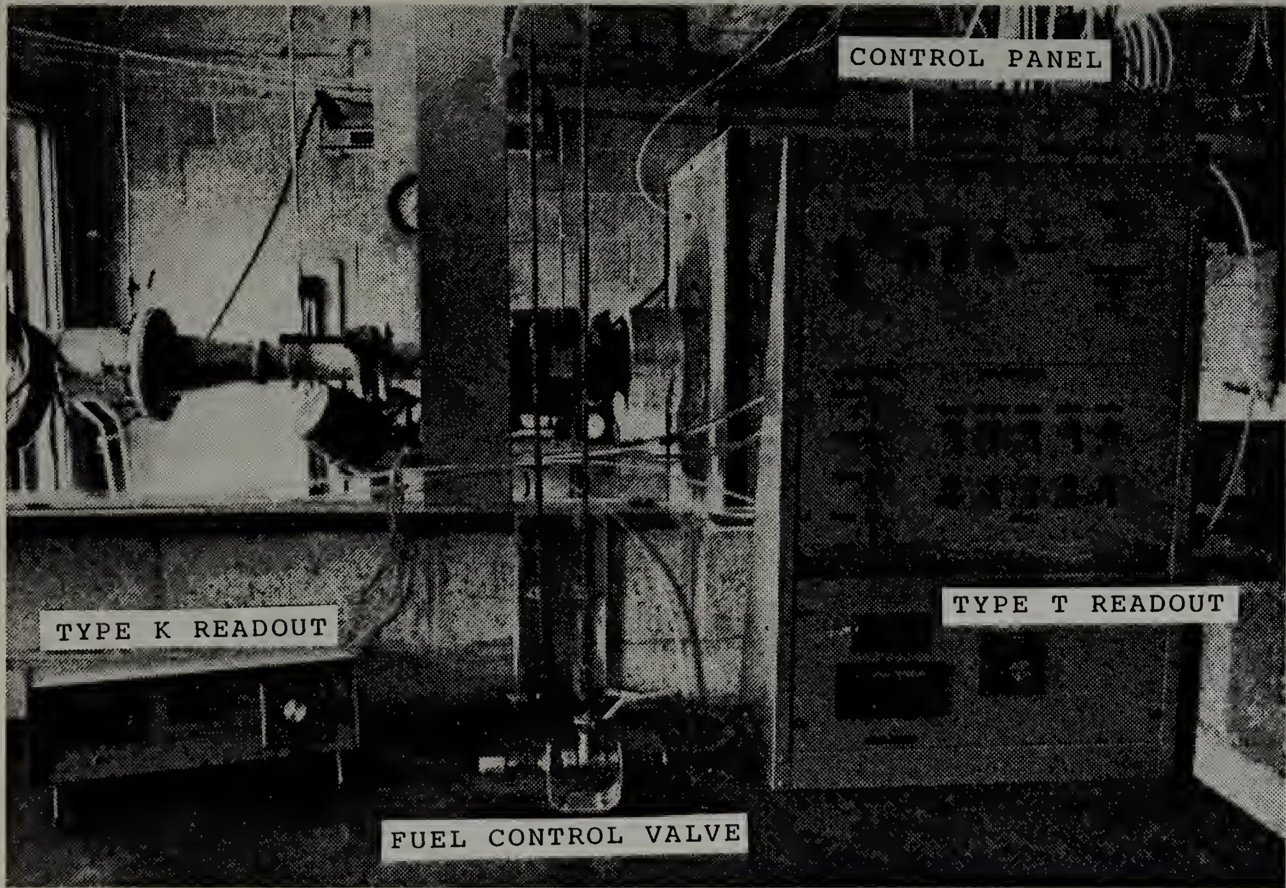

Figure 14. Gas Generator Control Station

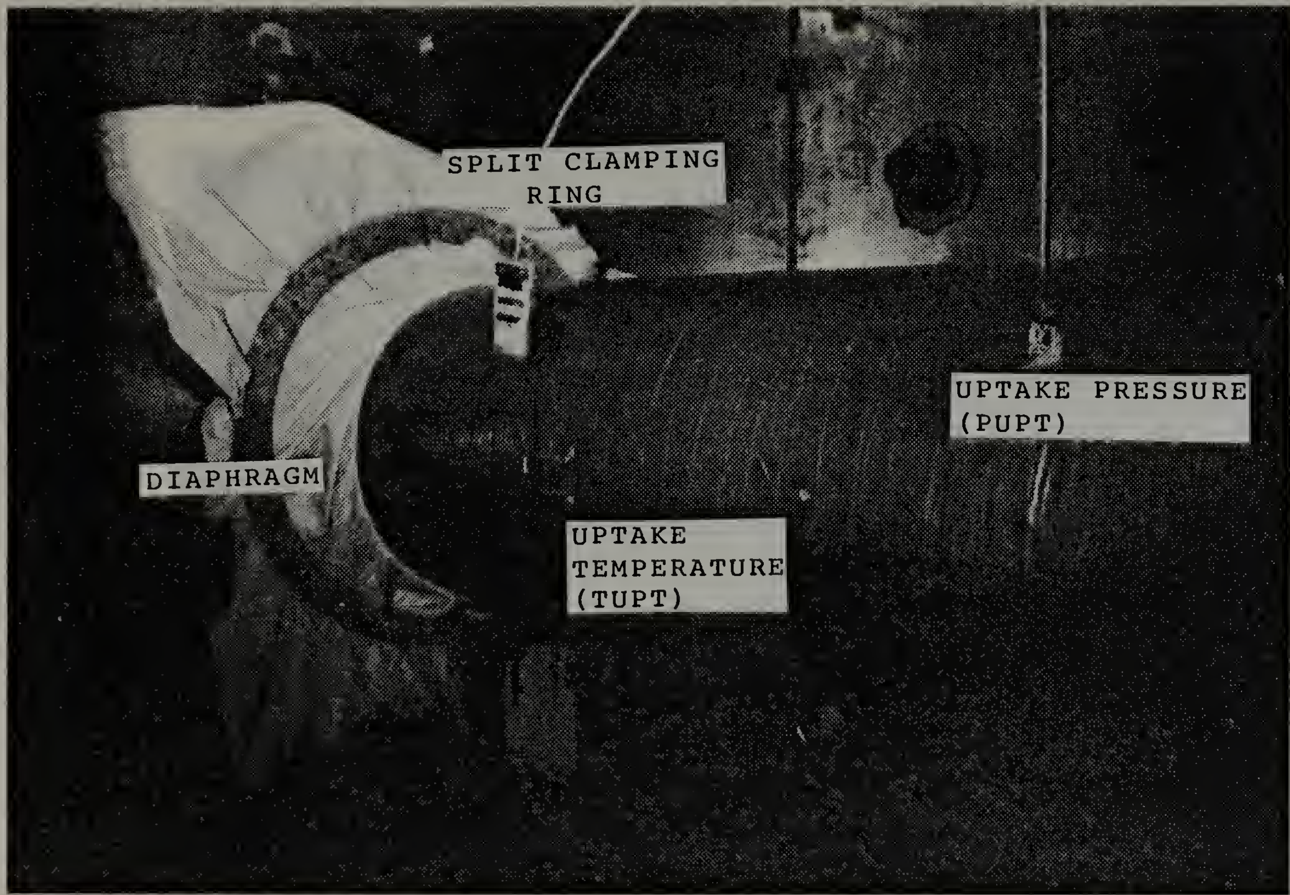

Figure 15. Uptake Section

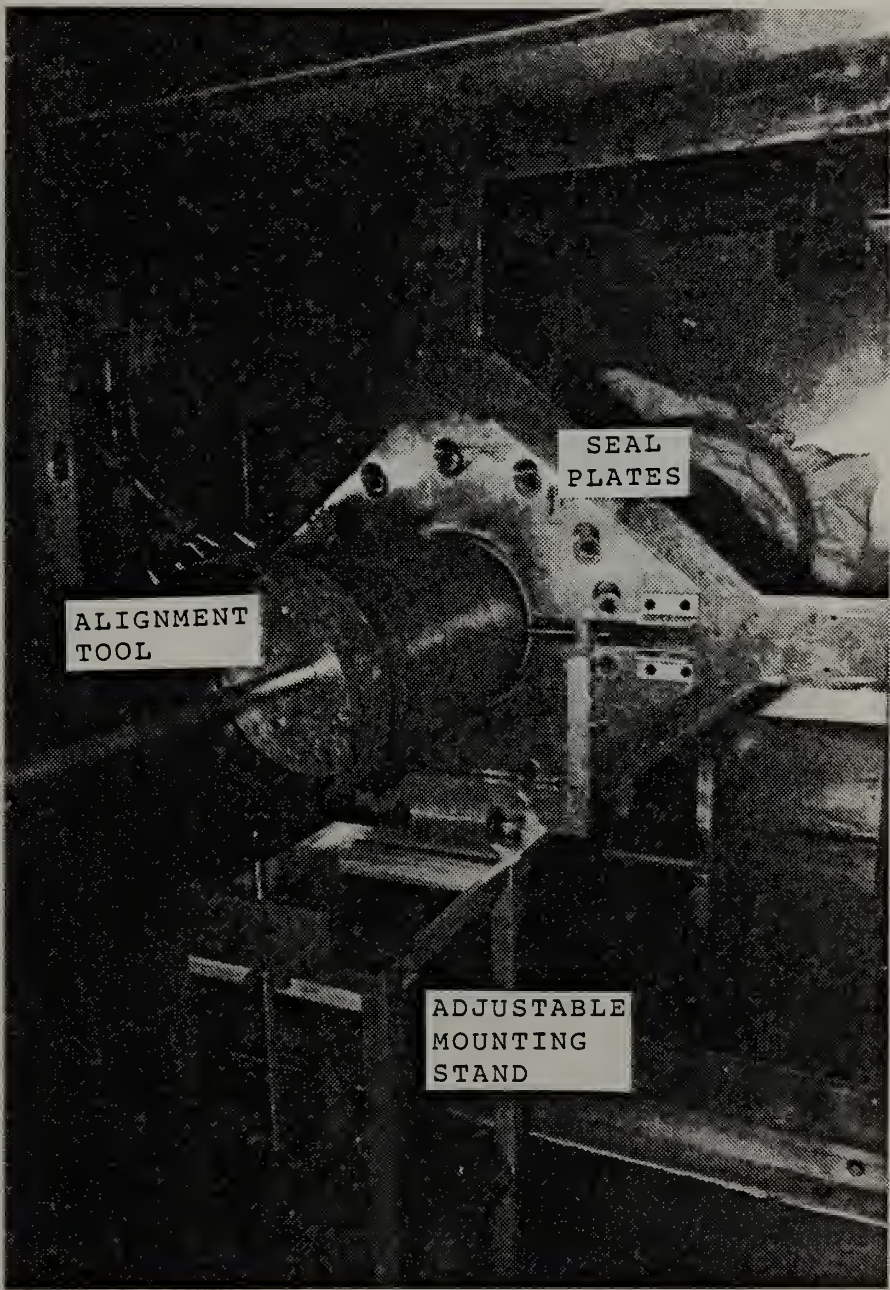

Figure 16. Model Installation

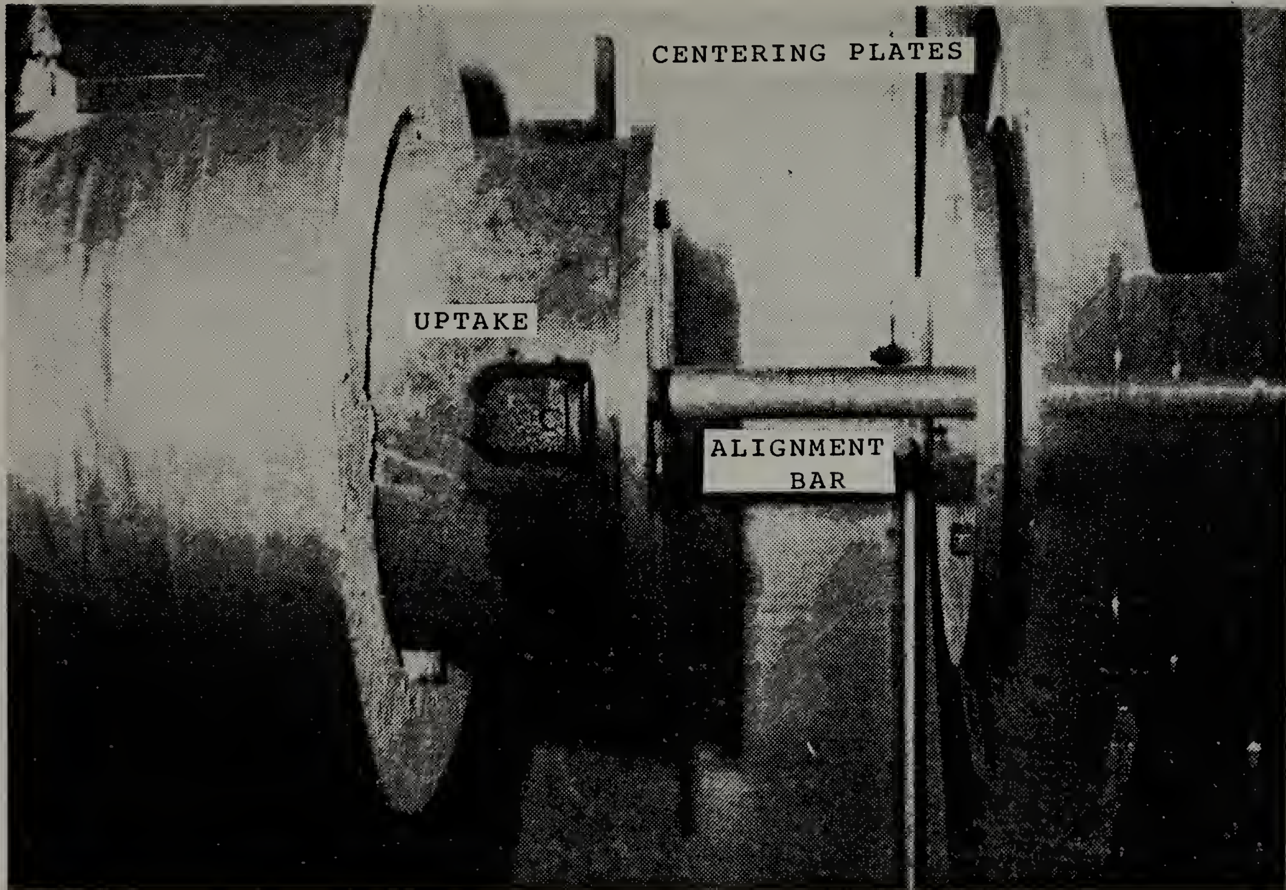

Figure 17. Model Alignment

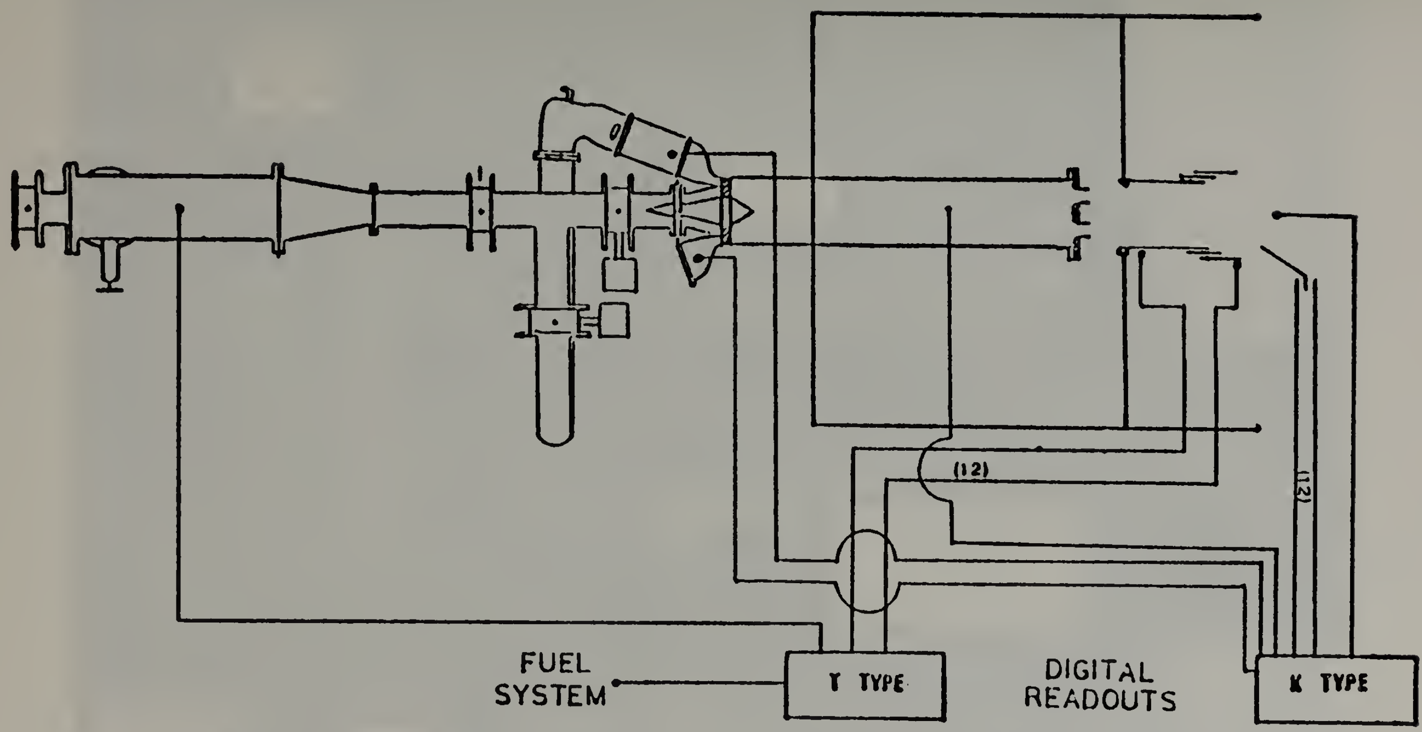

Figure 18. Schematic Diagram of Temperature Measurement System

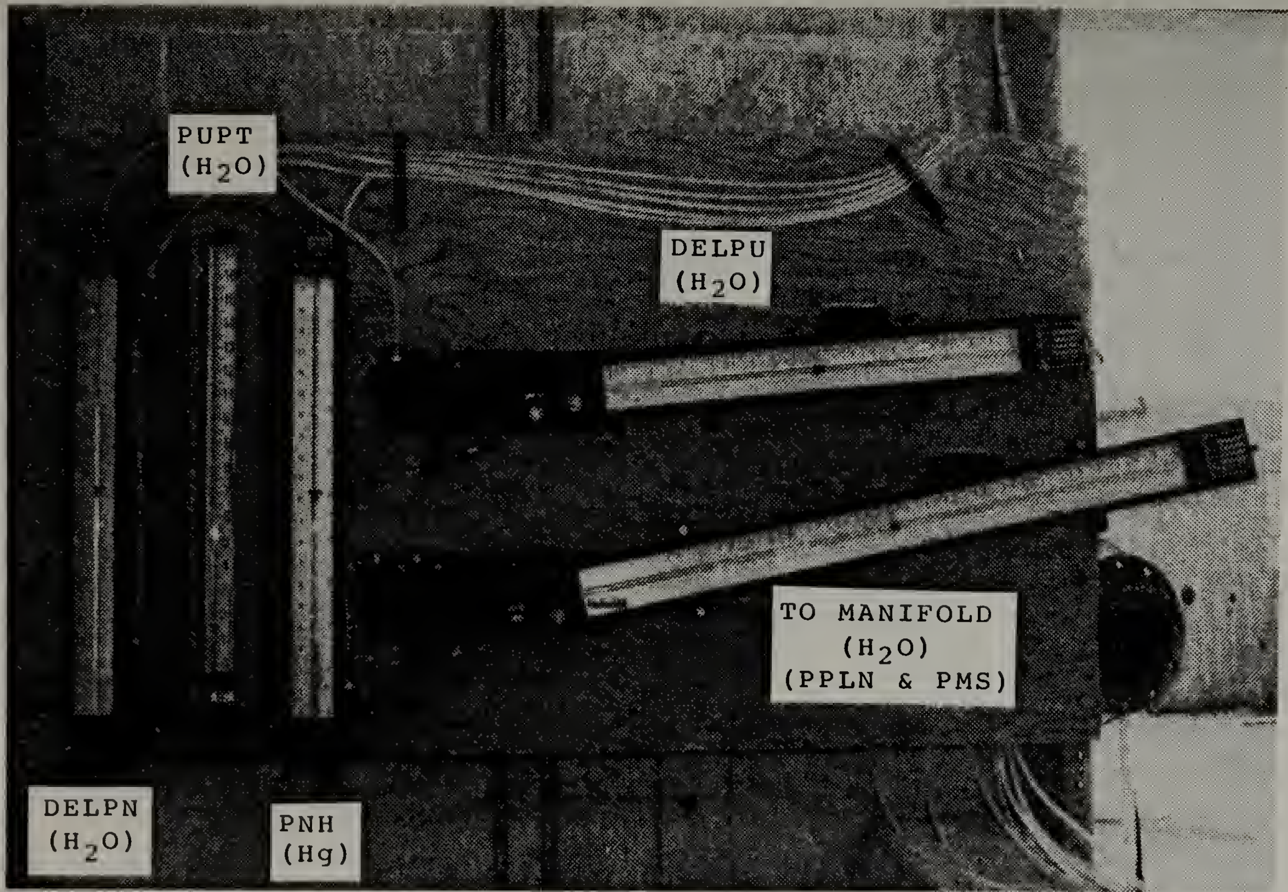

Figure 19. Manometer Installation

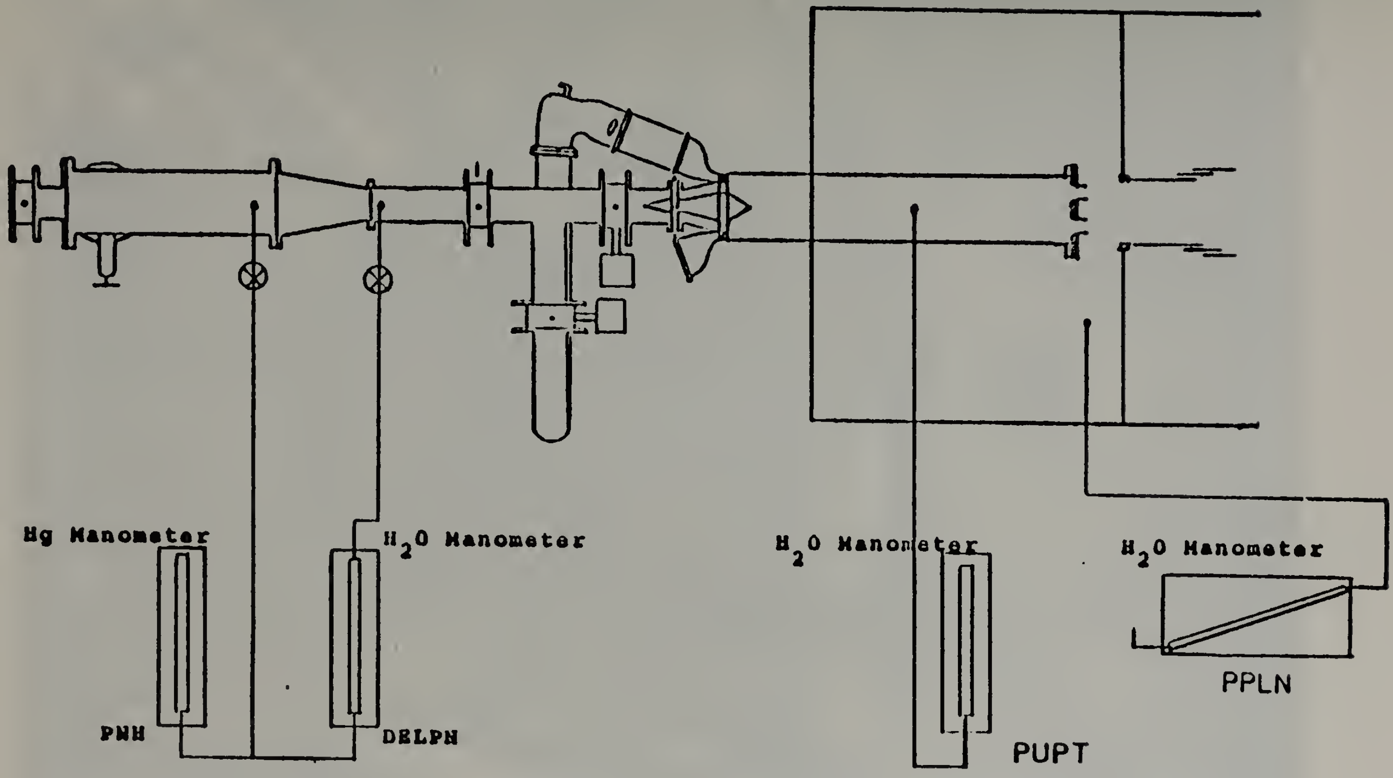

Figure 20. Schematic Diagram of Pressure Measurement System

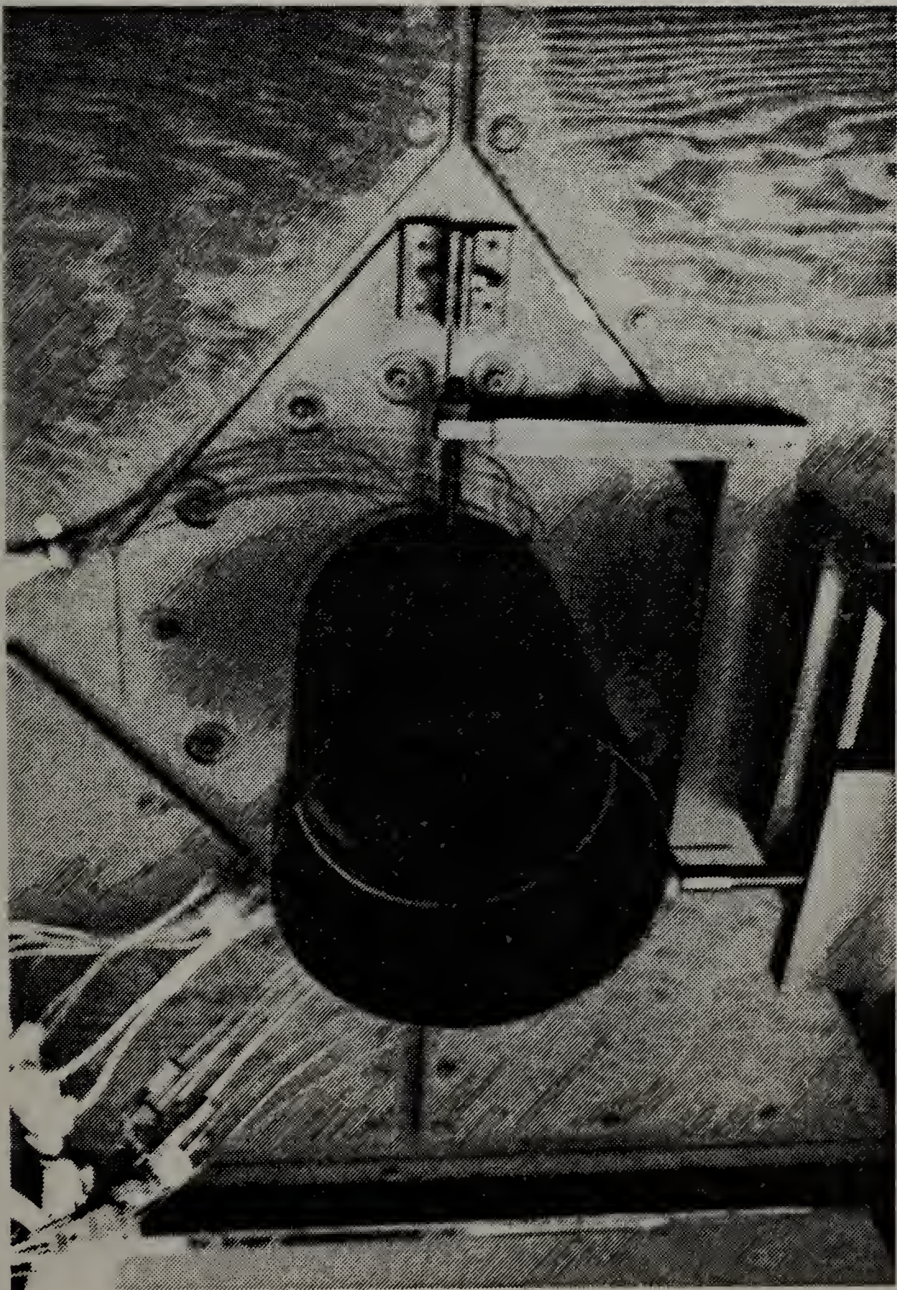

Figure 21. Model A Installed

Figure 22. Tilted-Angled Nozzle Plate

All dimensions in inches

$A_m/A_p = 2.5$

A	10.000
B	45°
R_1	1.126
R_2	1.251

R_3	2.070
R_4	4.509
R_5	3.729
R_6	4.108

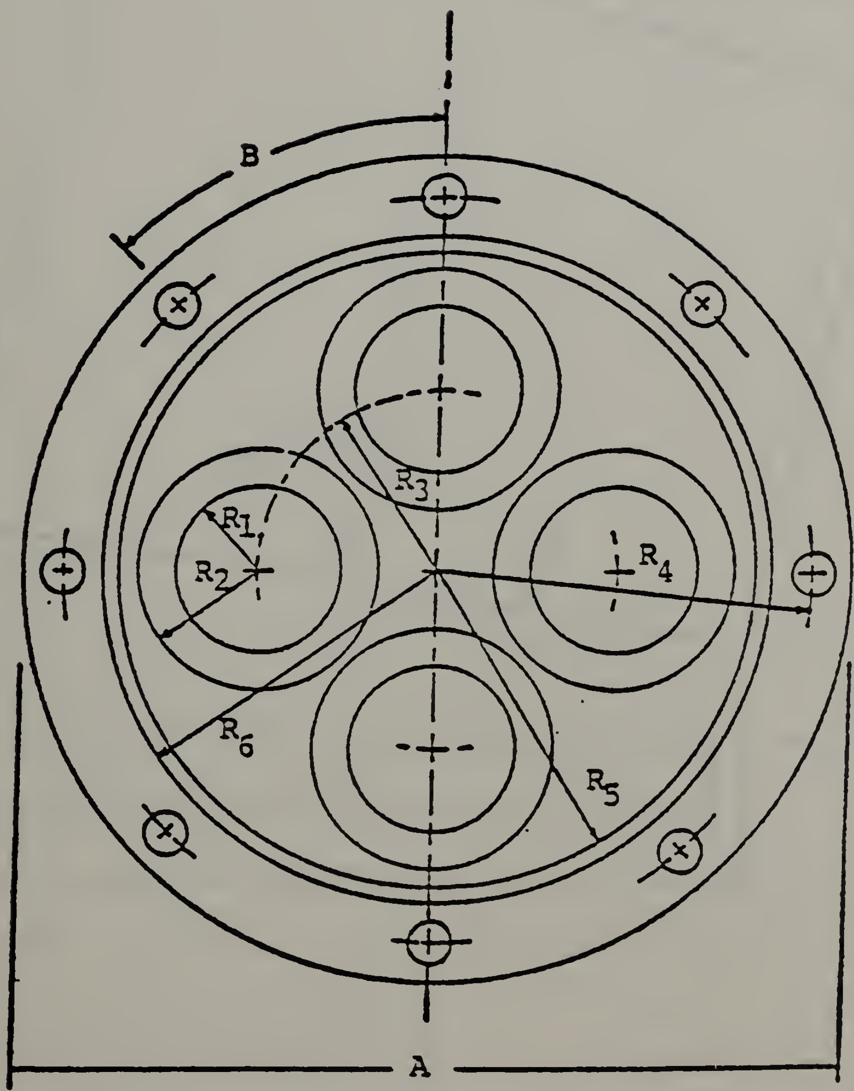

Figure 23. Dimensional Diagram of Primary Flow Nozzle Plate

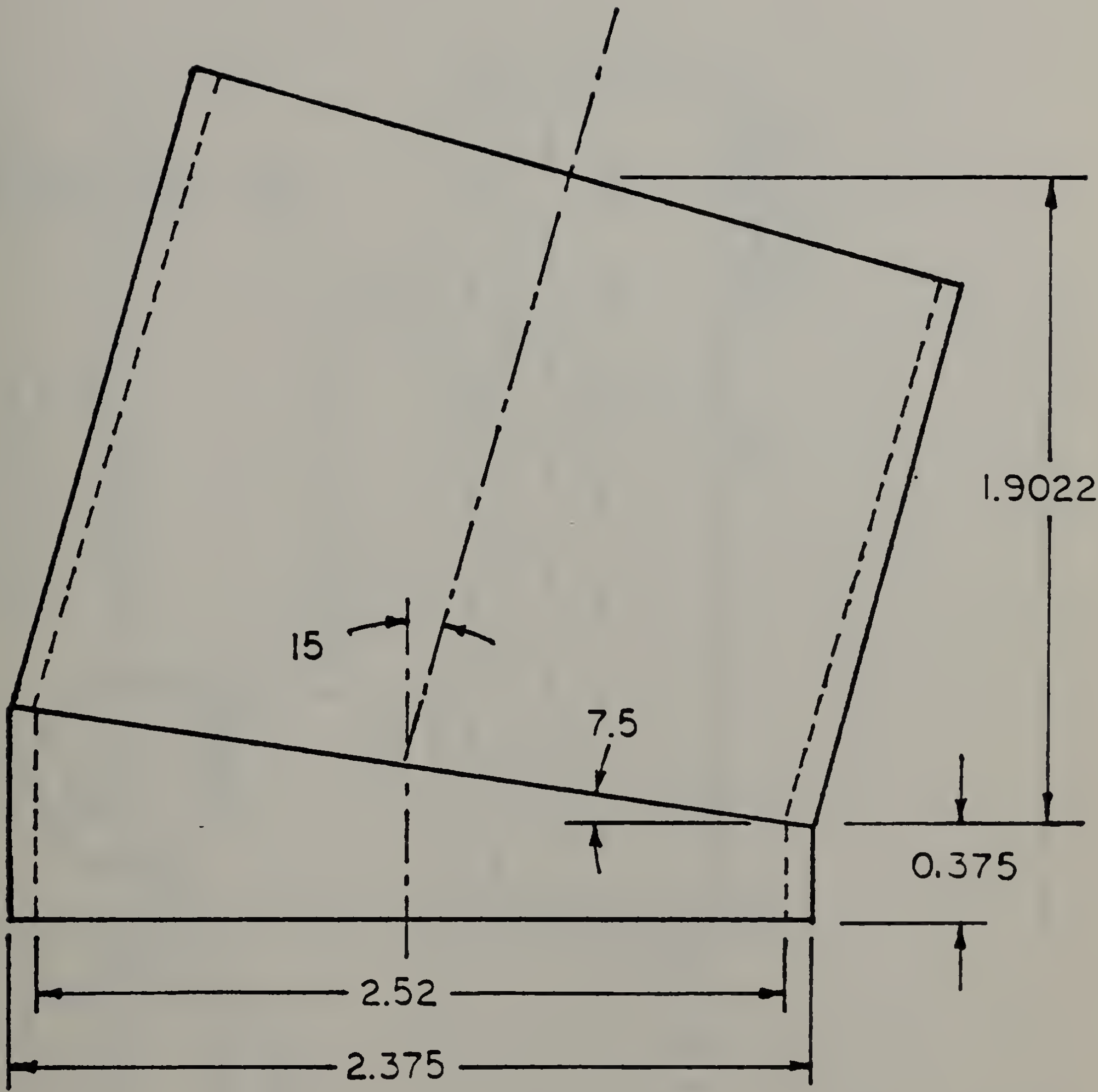

Figure 24. Tilted Nozzle Geometry

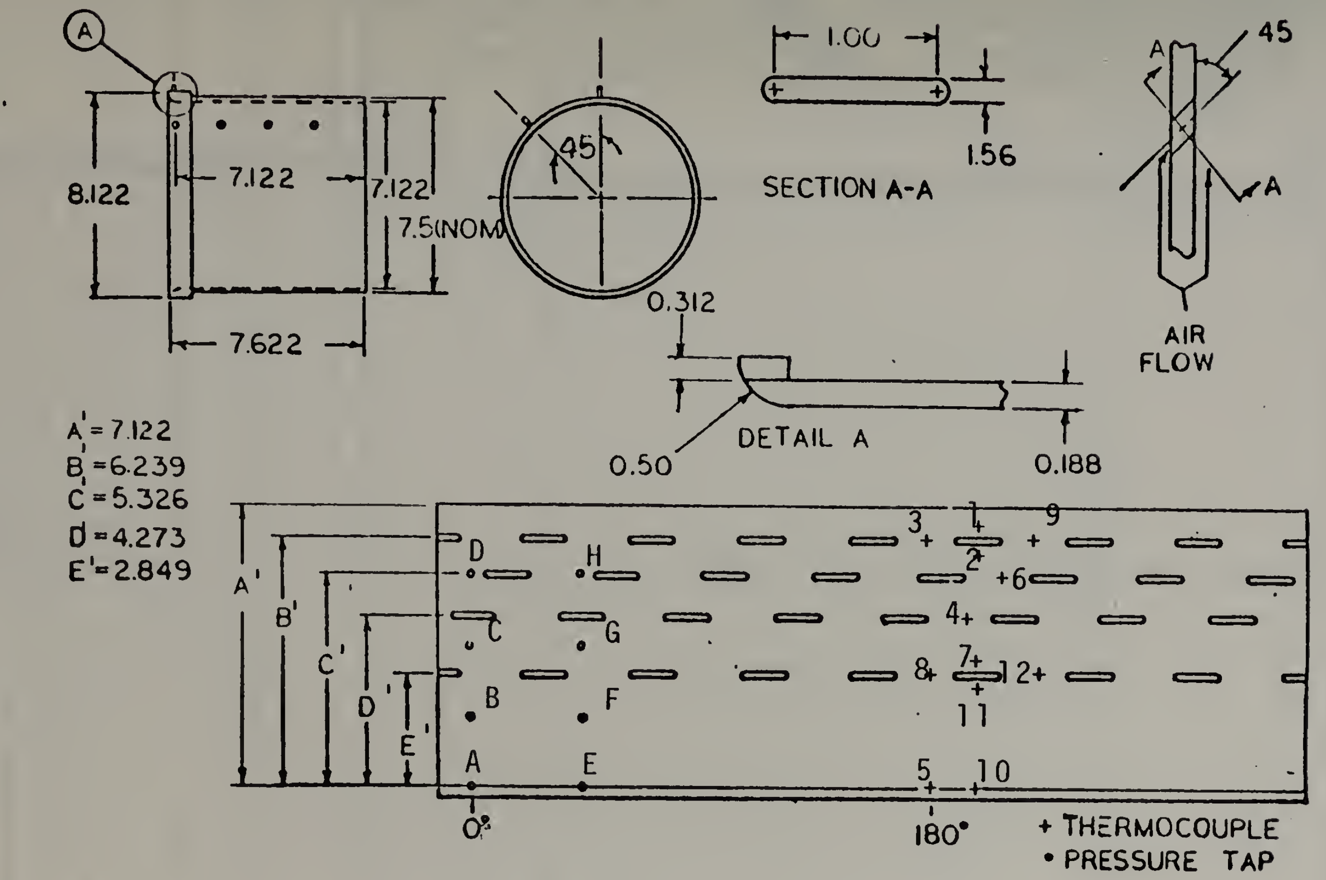

Figure 25. Dimensional Diagram of Slotted Mixing Stack

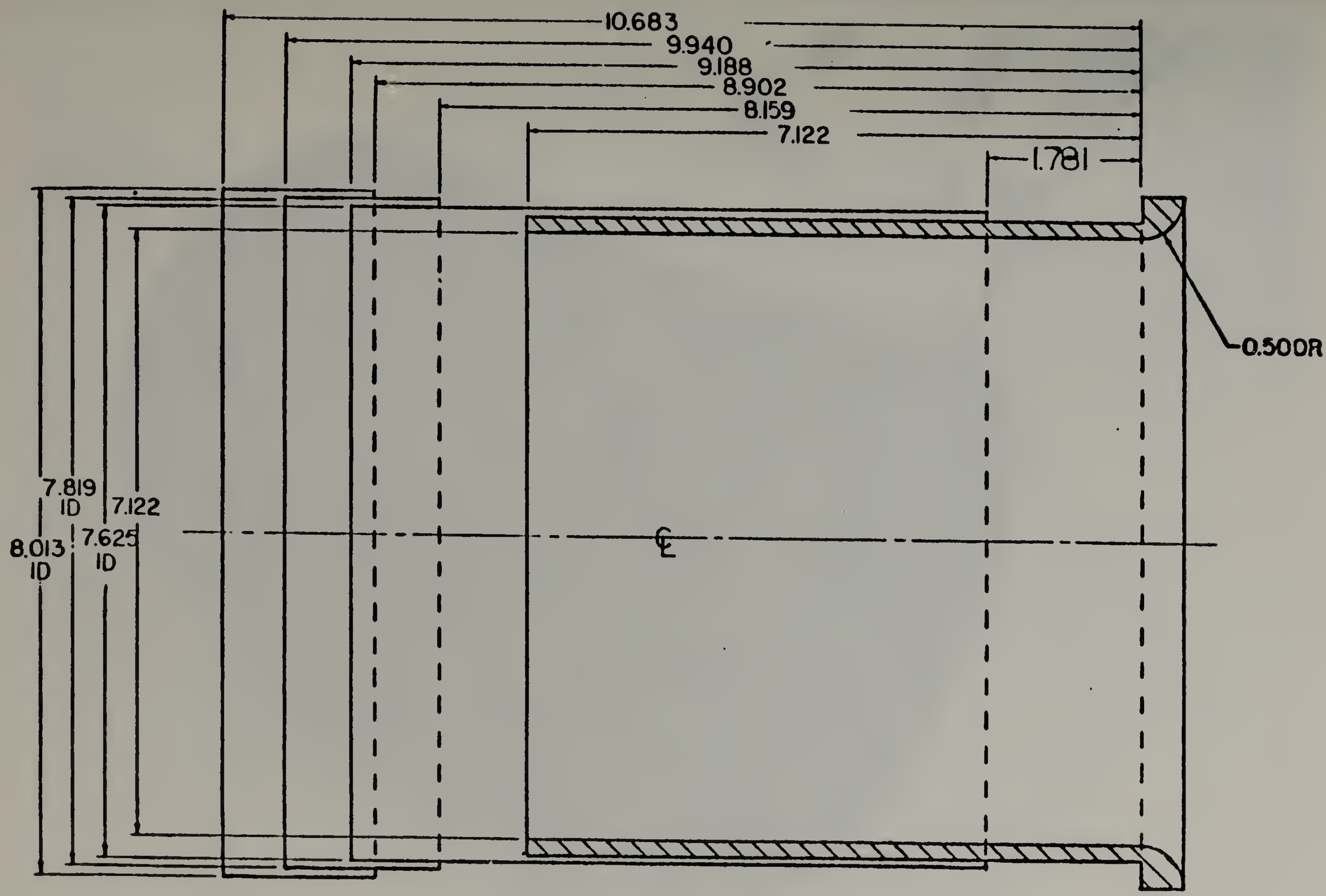

Figure 26. Mixing Stack With Shroud and Two Diffuser Rings (Model A)

Figure 27. Model B Entrance

Figure 28. Model B Exit

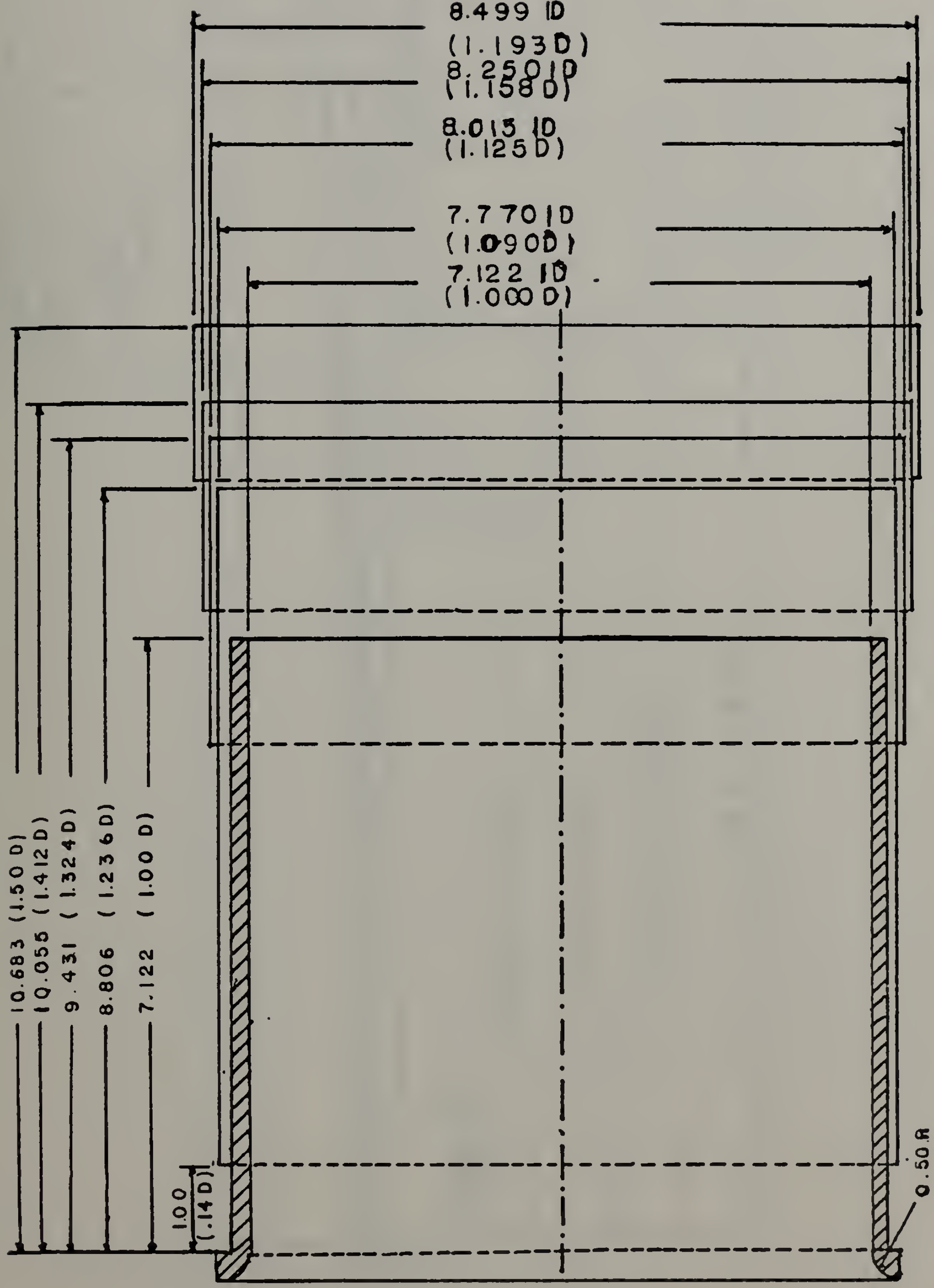

Figure 29. Mixing Stack With Shroud and Three Diffuser Rings (Model B)

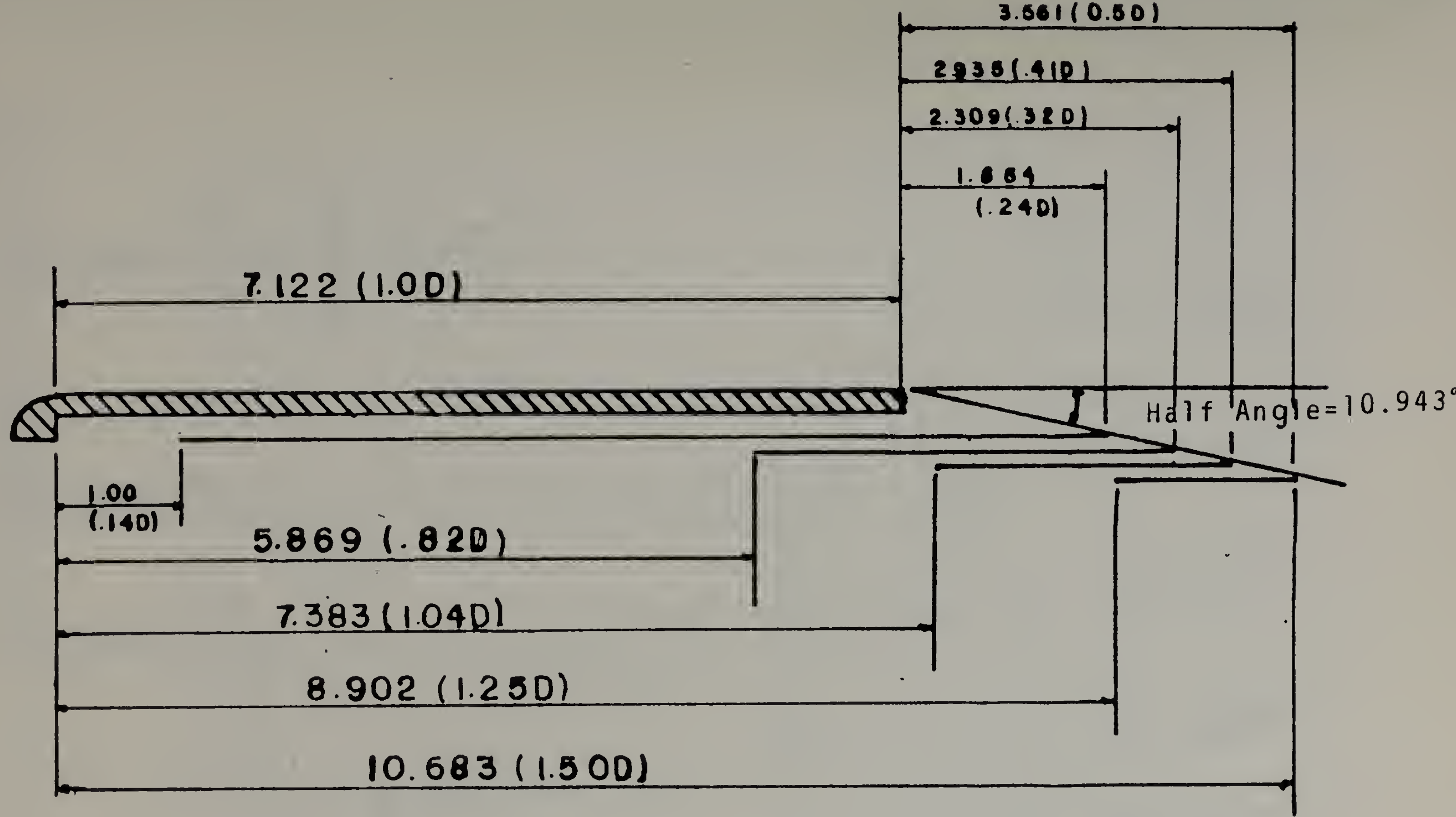

Figure 30, Dimensional Diagram of Model B

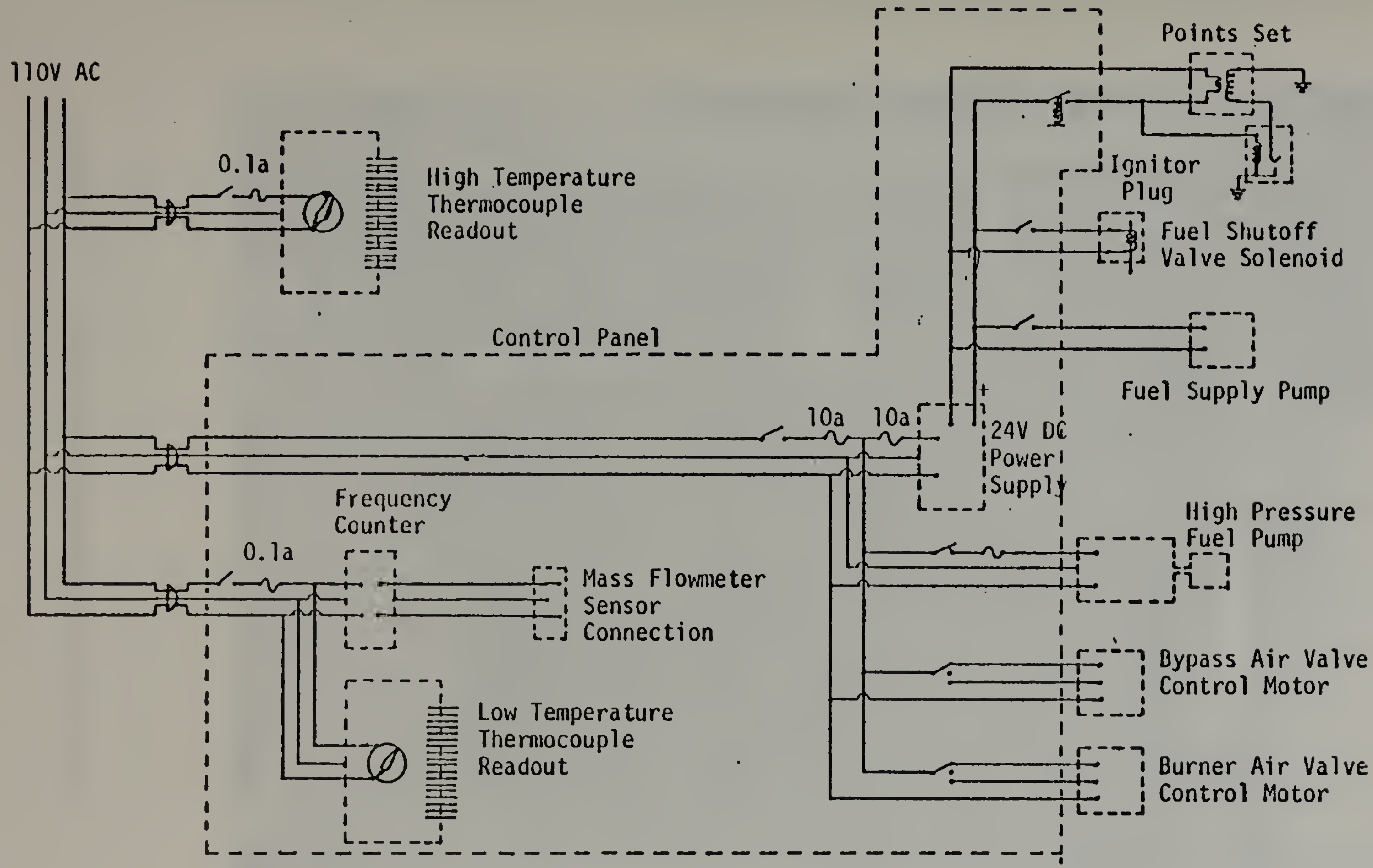

Figure 31. Gas Generator Electrical System

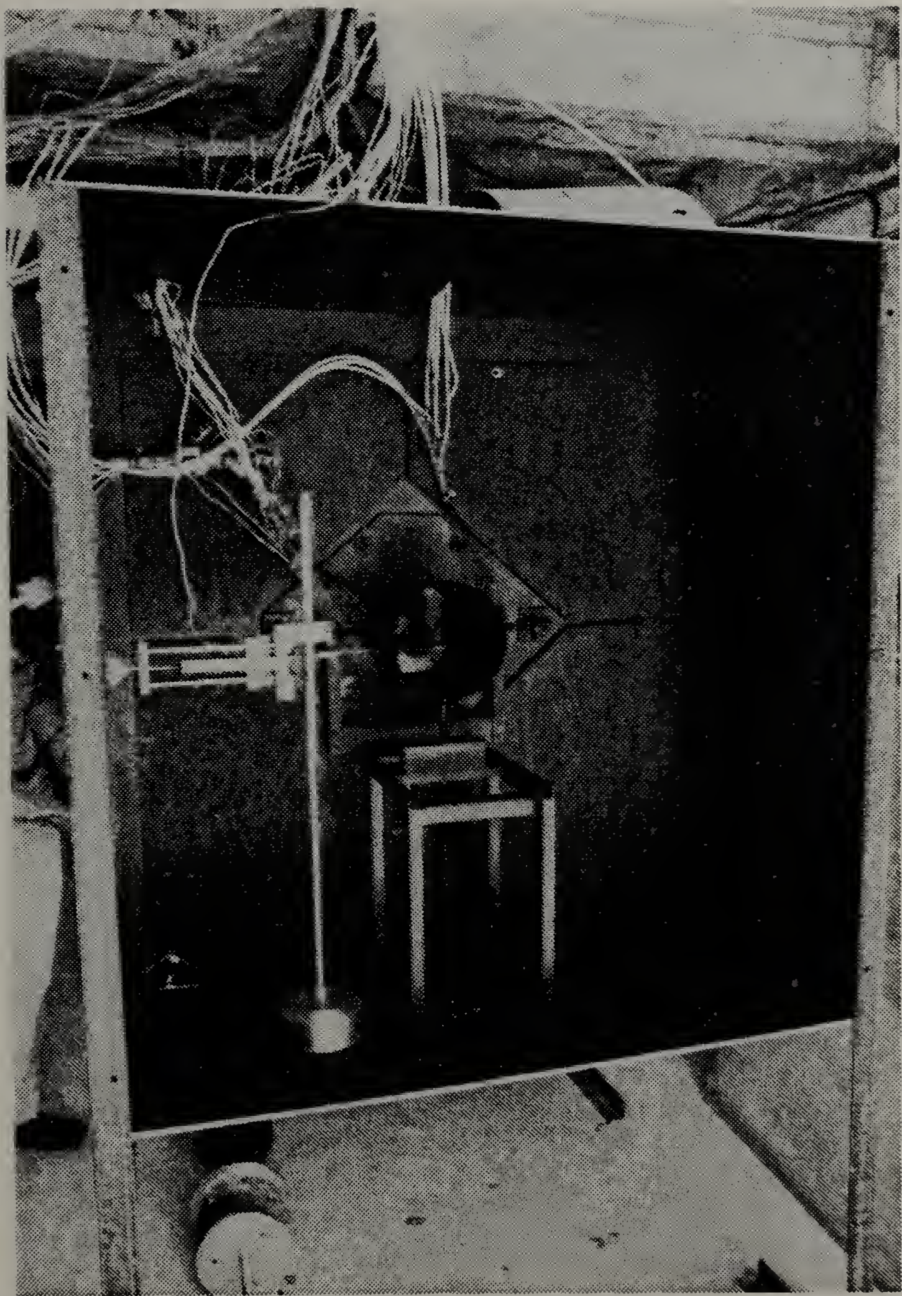

Figure 32. Exit Plane Temperature Measurement

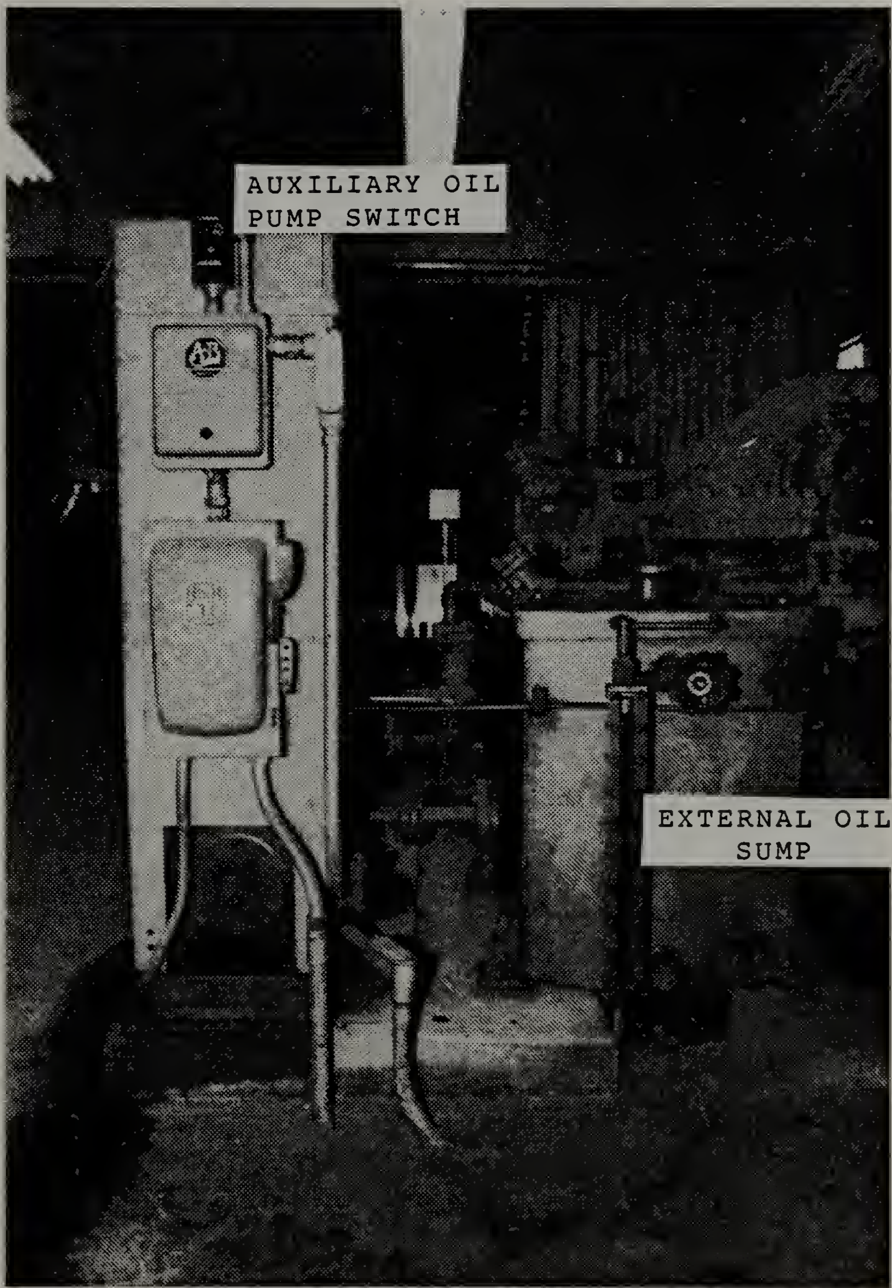

Figure 33. Auxiliary Oil Pump Control

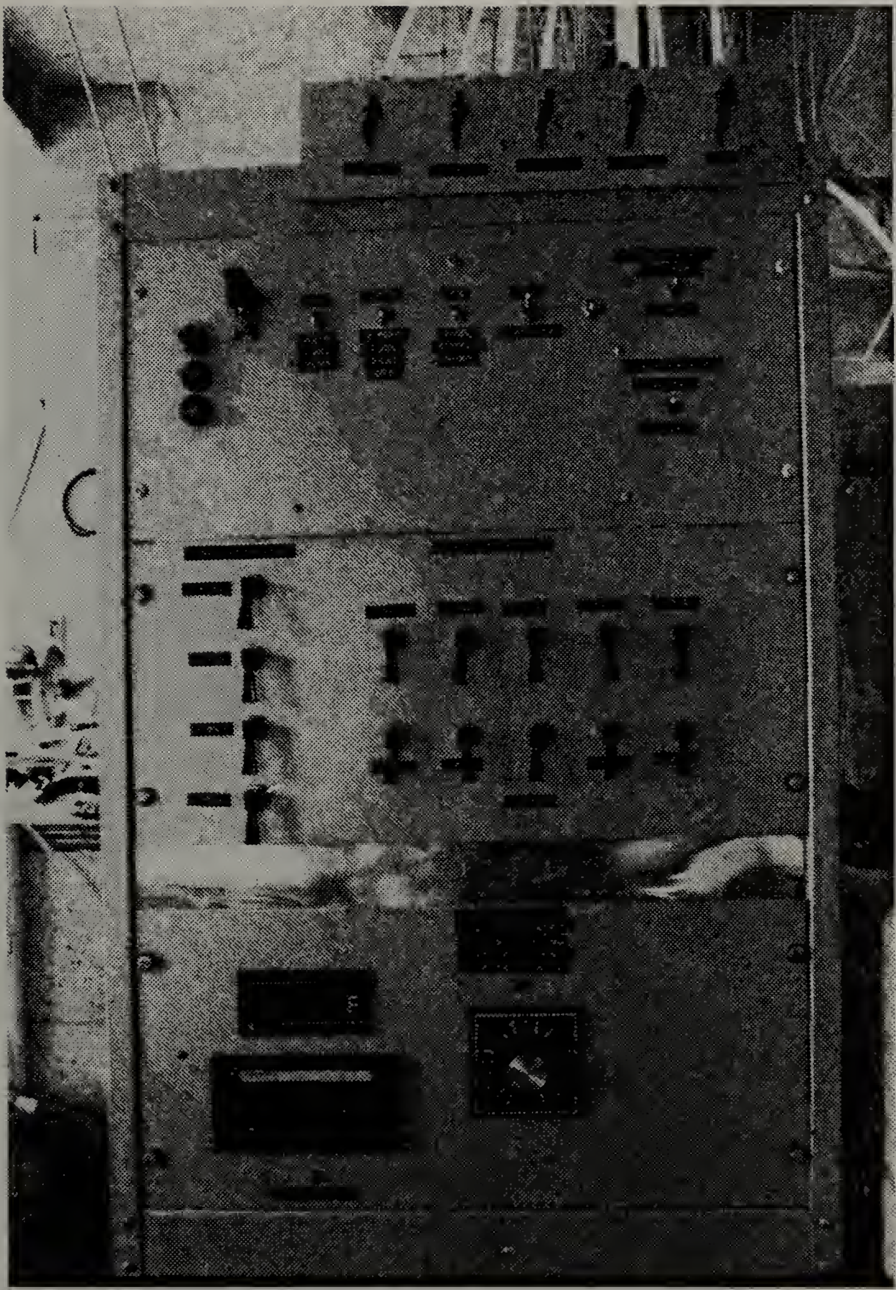

Figure 34. Main Power Supply and Control Panel

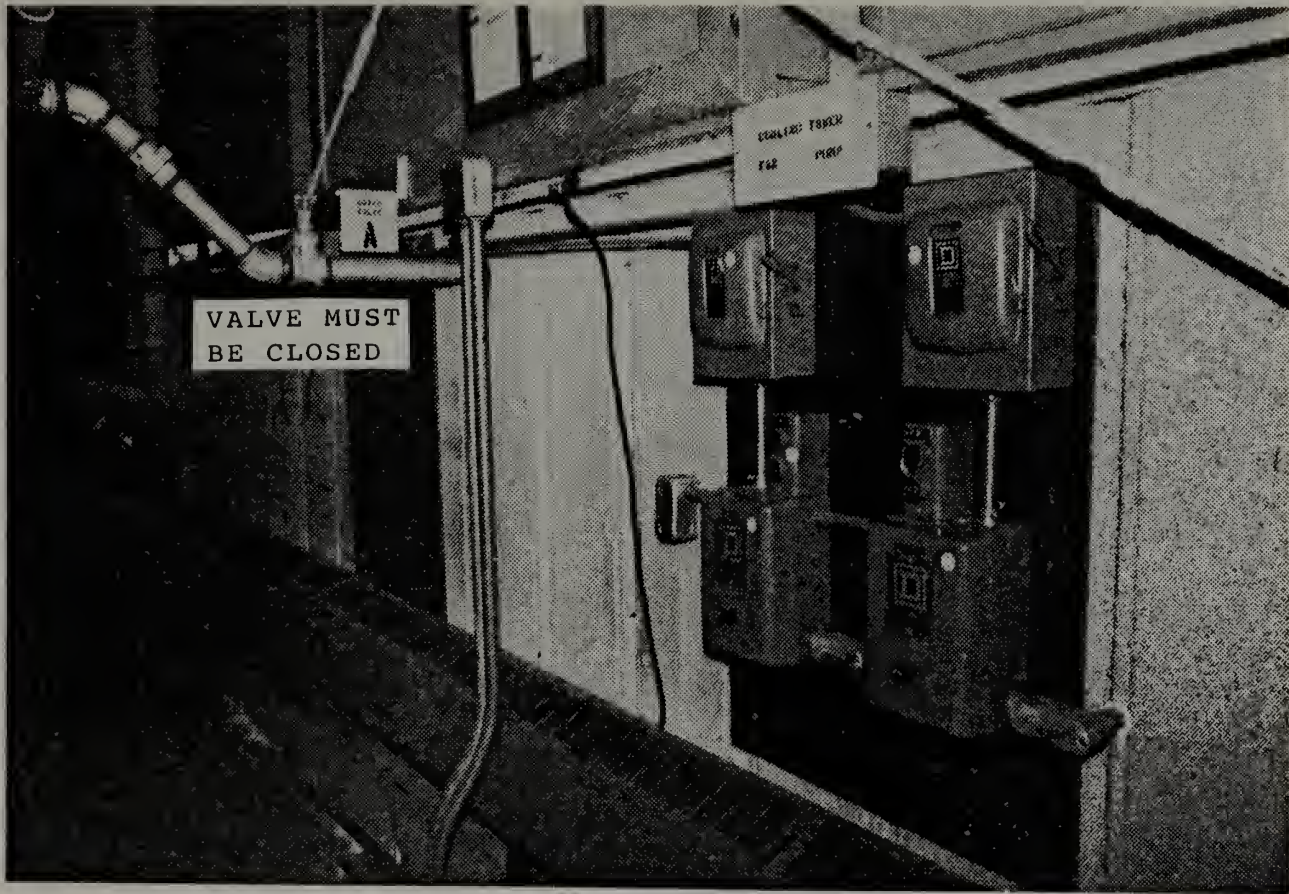

Figure 35. Cooling Water Pump and Tower Fan Controllers

Figure 36. Air Cooling Bank and Bypass Discharge

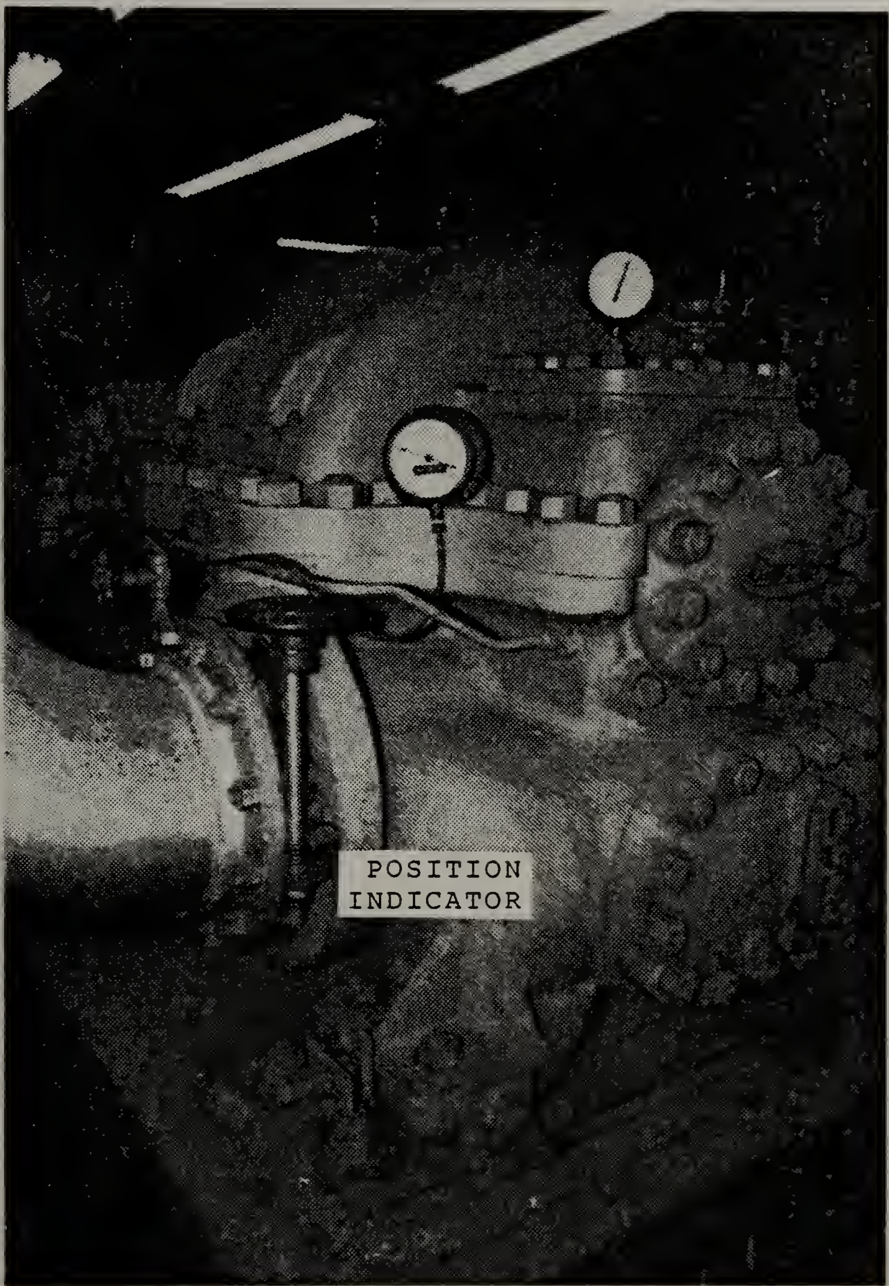

Figure 37. Air Compressor Suction Valve

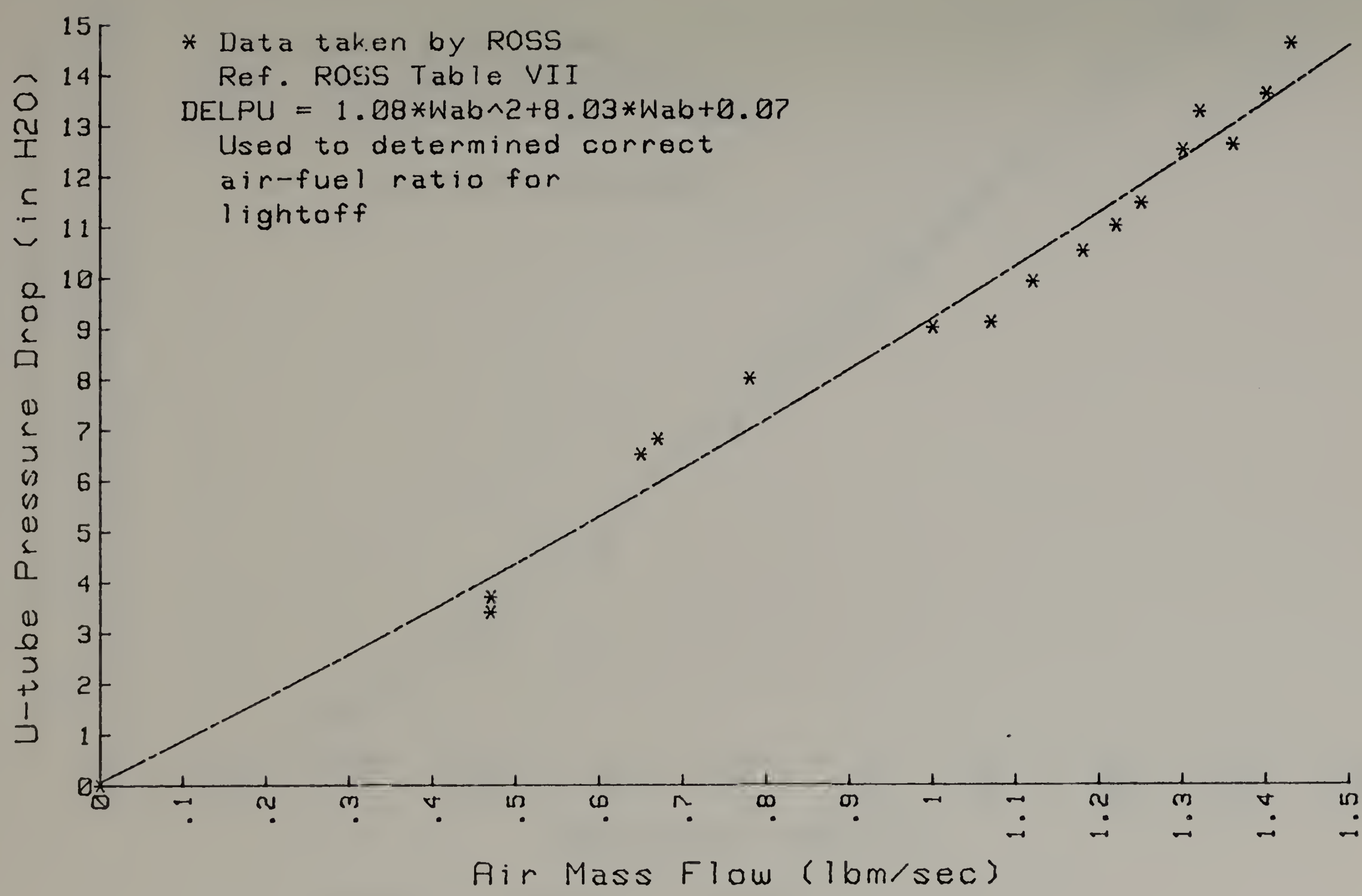

Figure 38. DELPU vs. Burner Air Flow

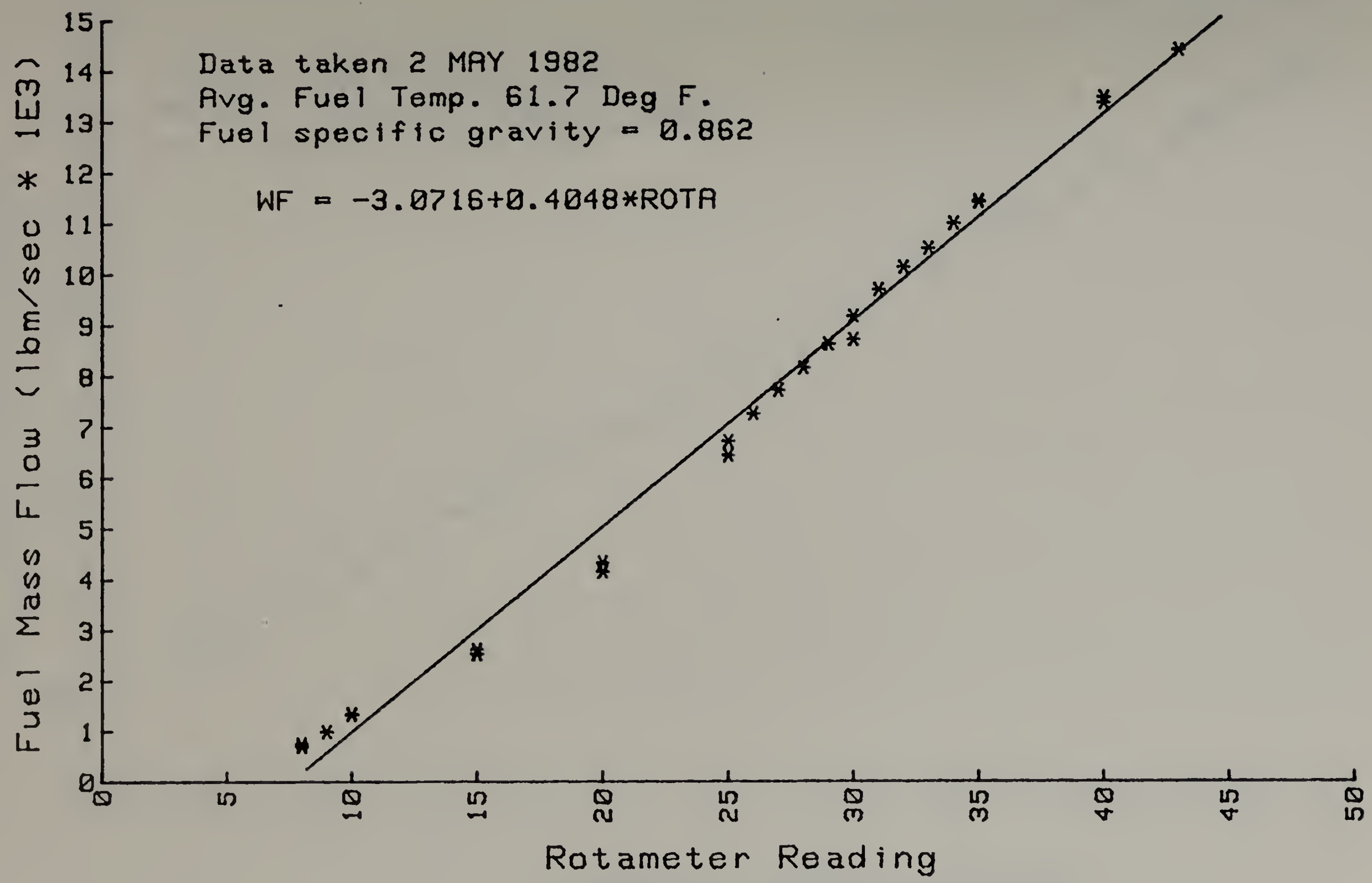

Figure 39. Rotameter Calibration

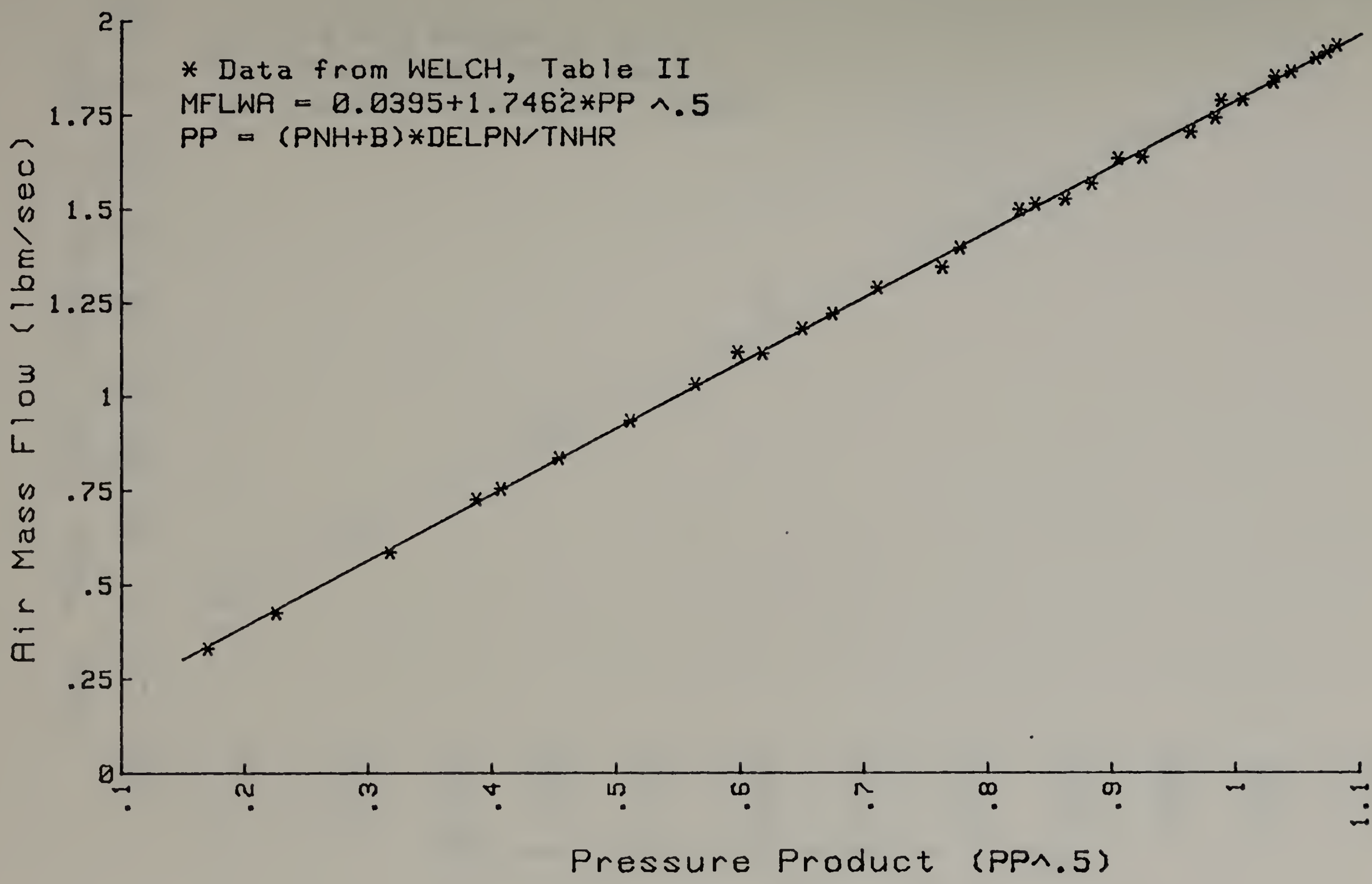

Figure 40. Total Air Mass Flow vs. Pressure Product

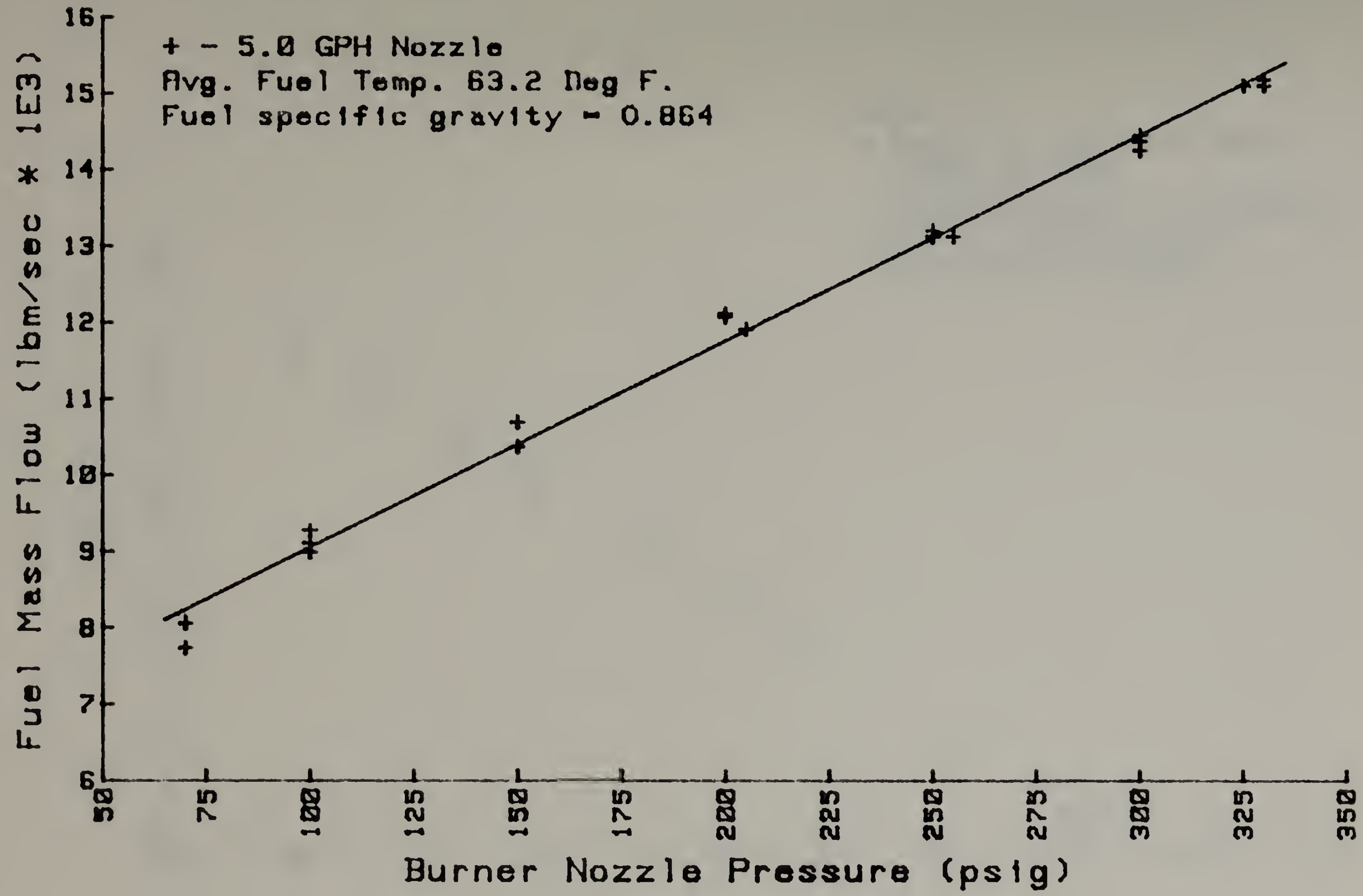

Figure 41. Burner Nozzle Calibration Curve

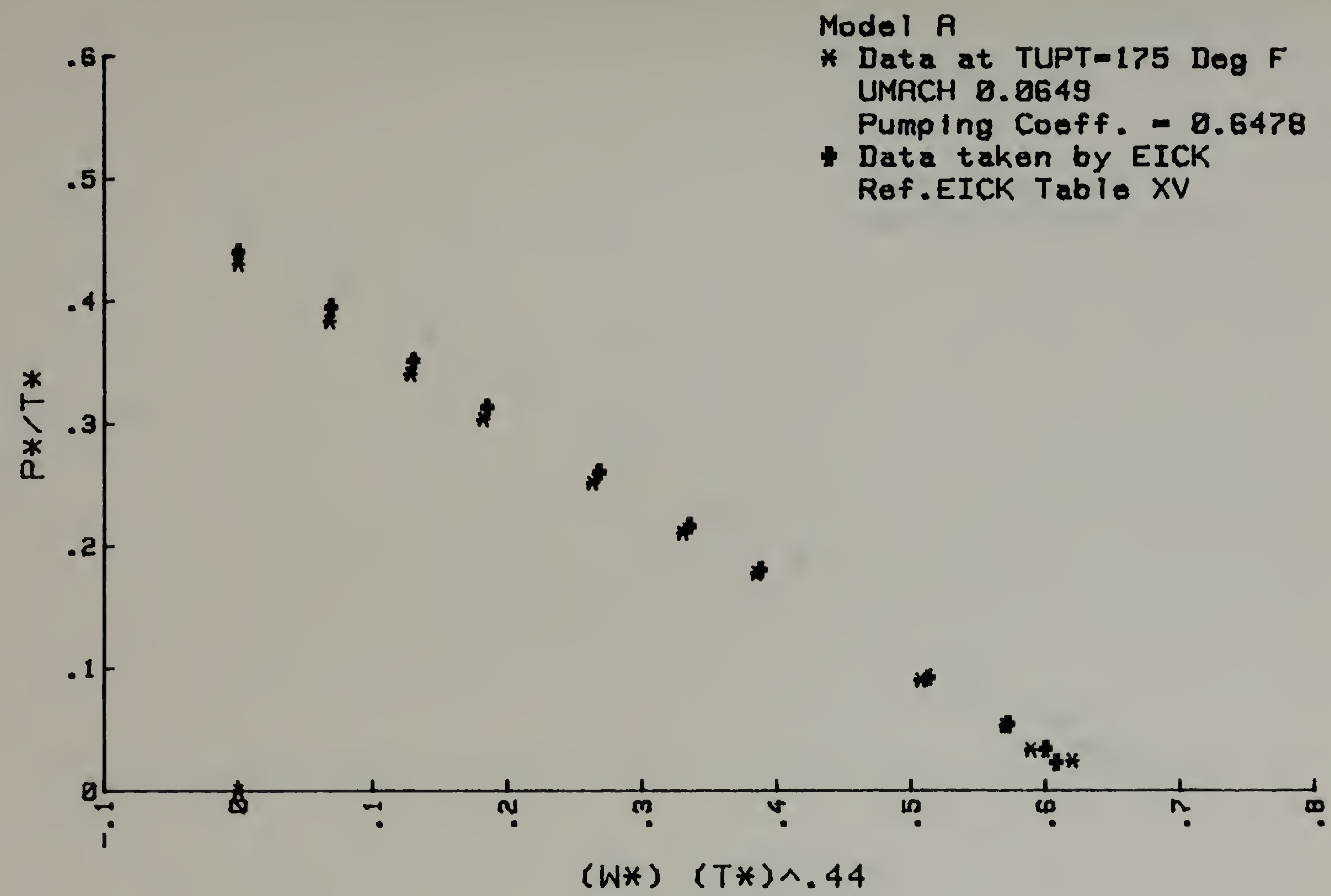

Figure 42. Pumping Coefficient, Model A (175^{o} F)

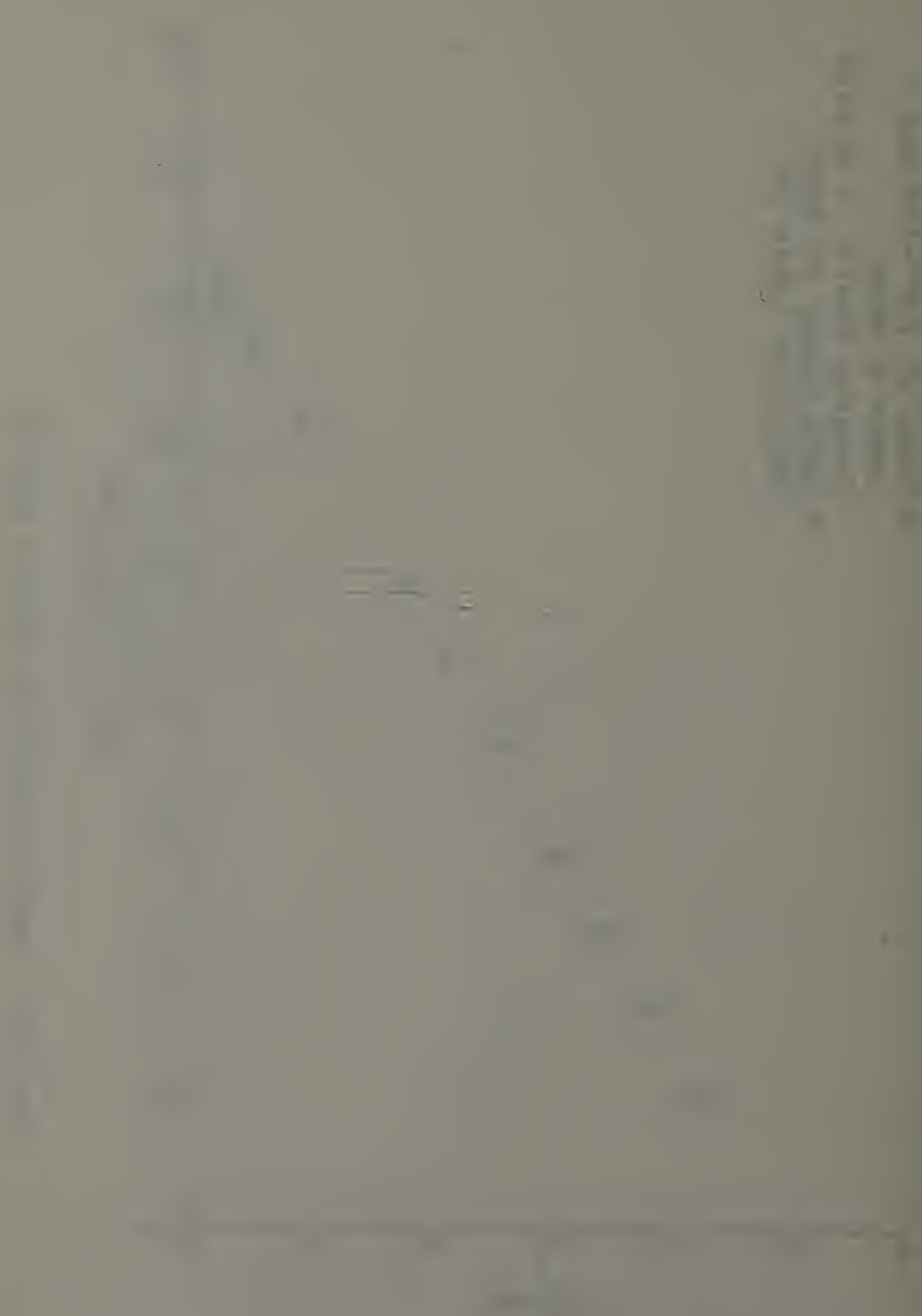

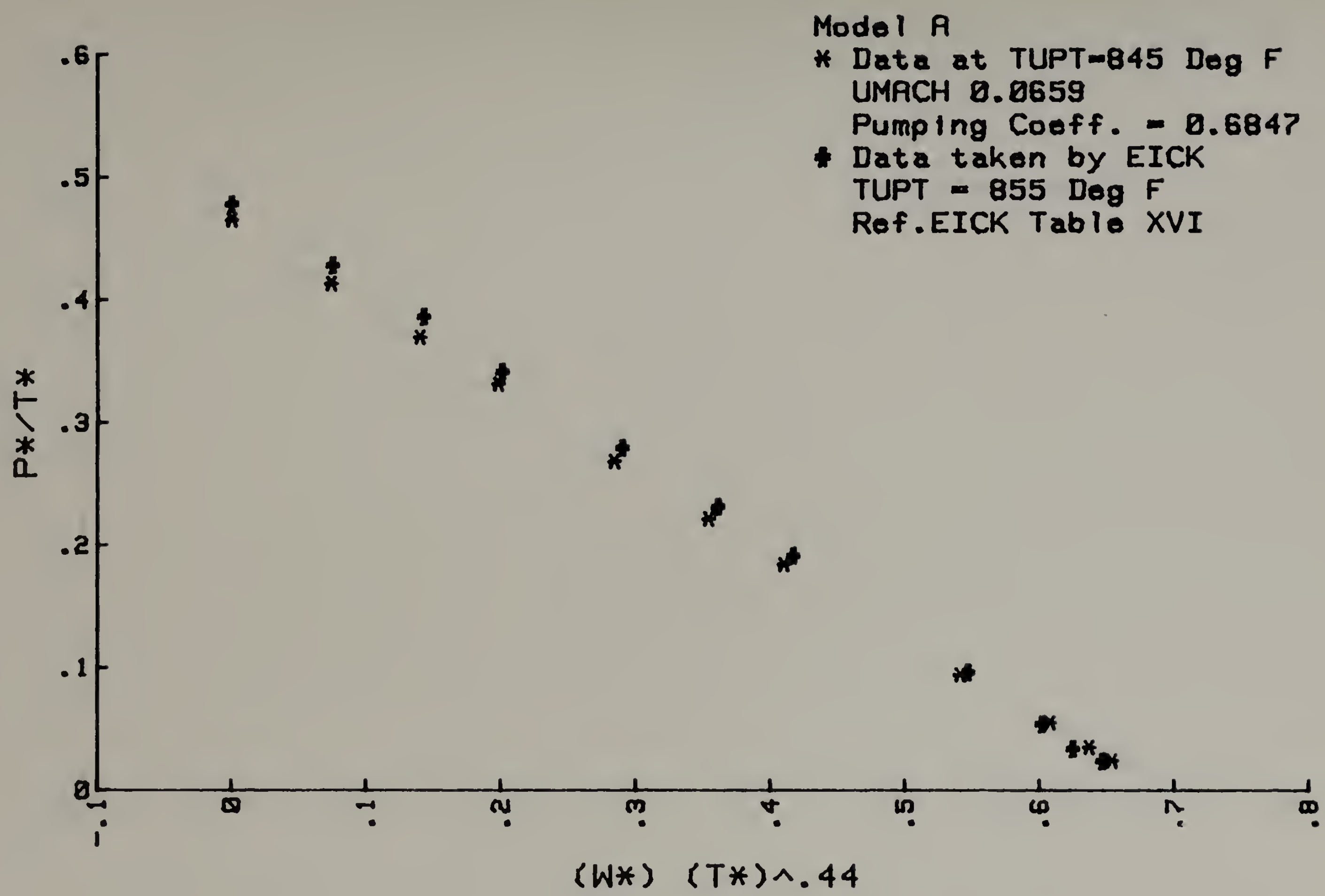

Figure 43. Pumping Coefficient, Model A (845^{o} F)

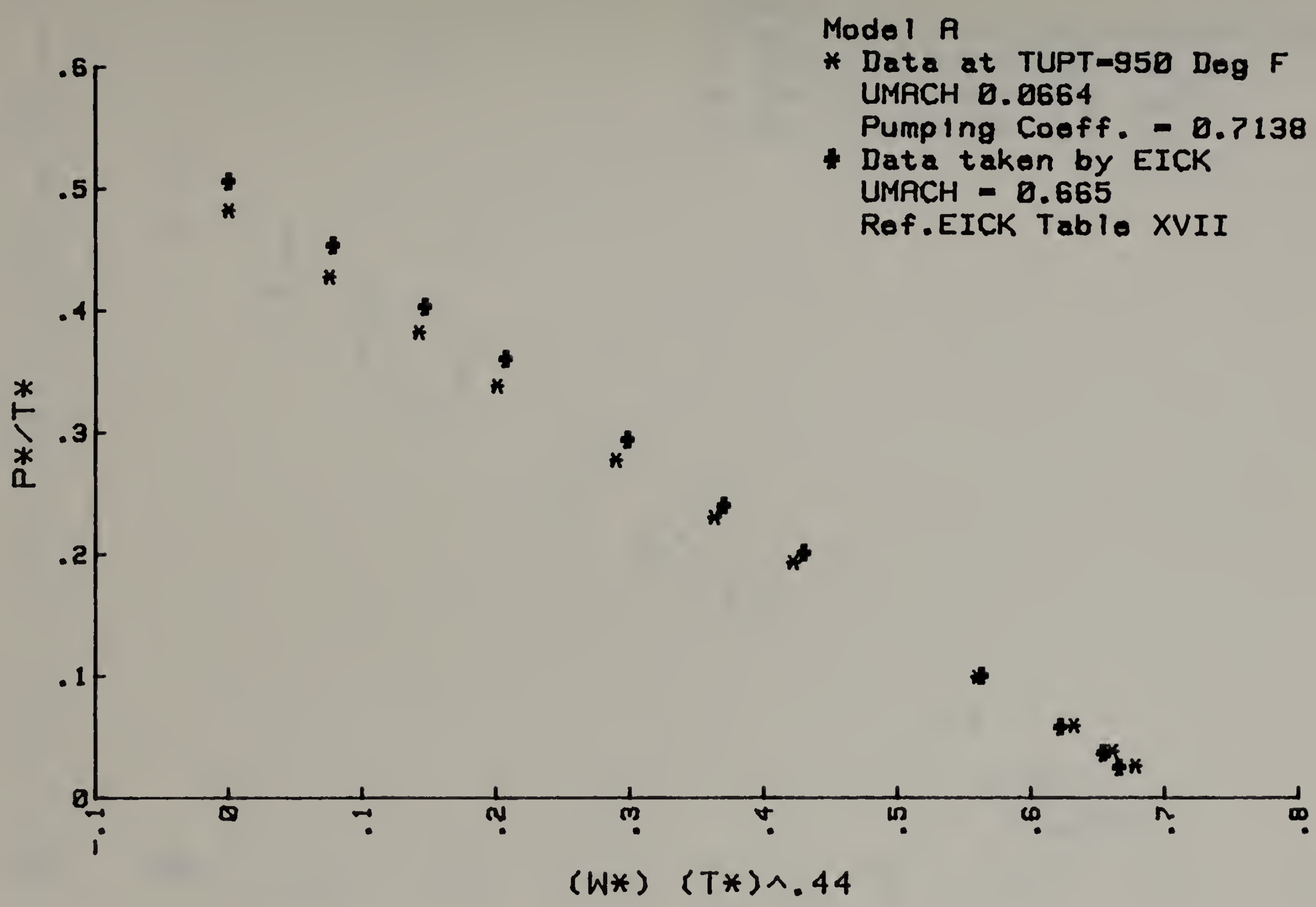

Figure 44. Pumping Coefficient, Model A (950^{o} F)

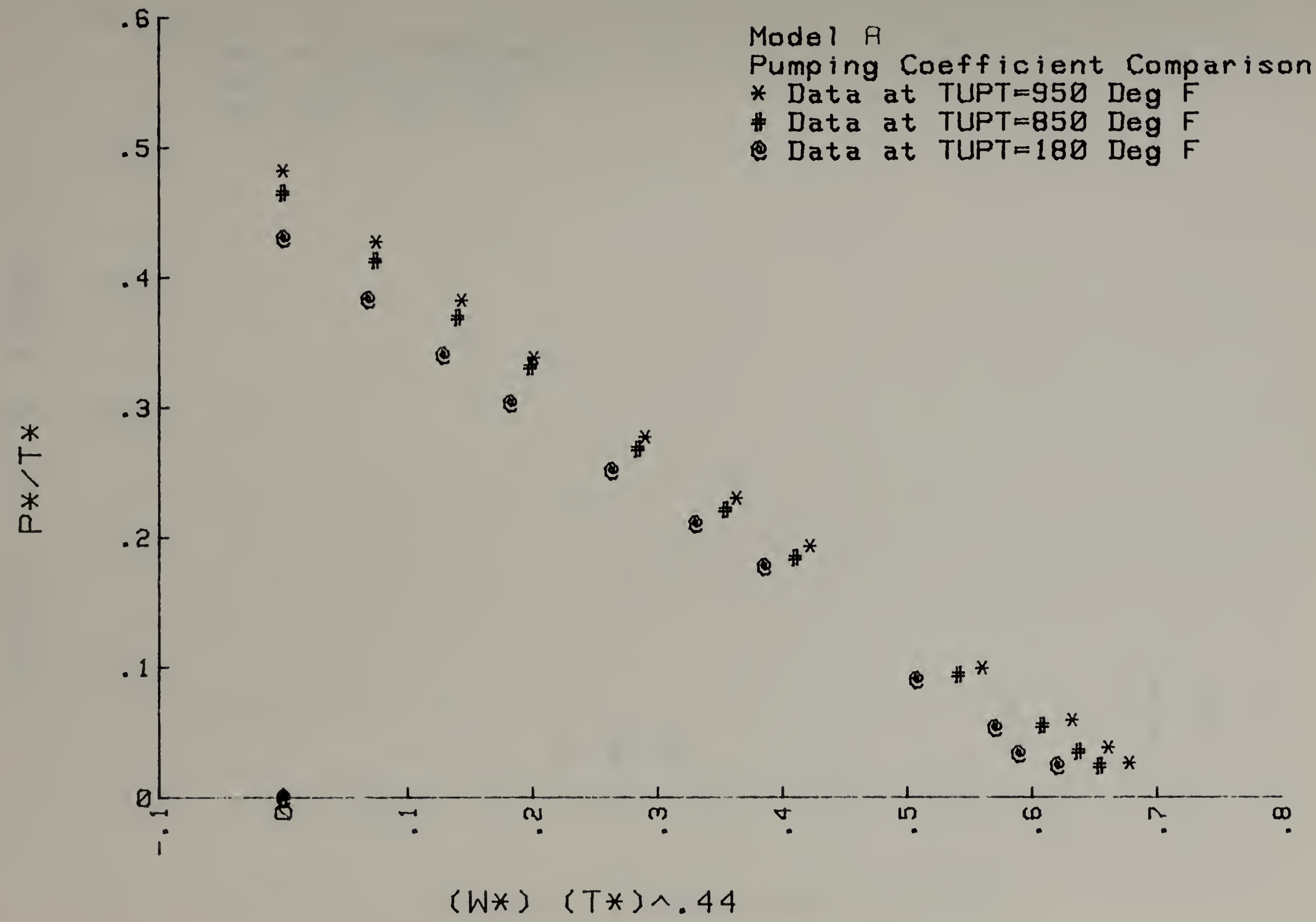

Figure 45. Pumping Coefficient Comparison, Model A

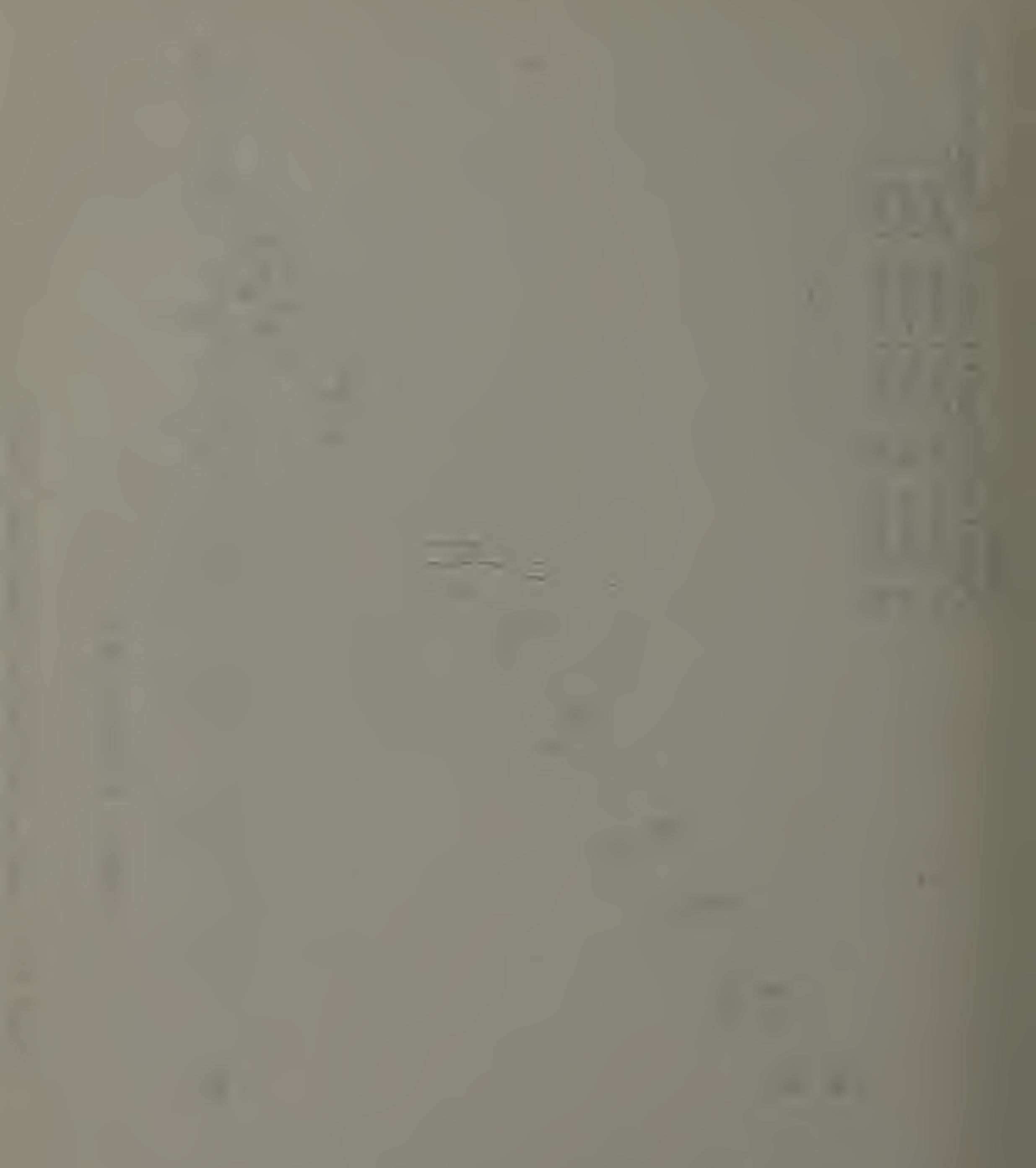

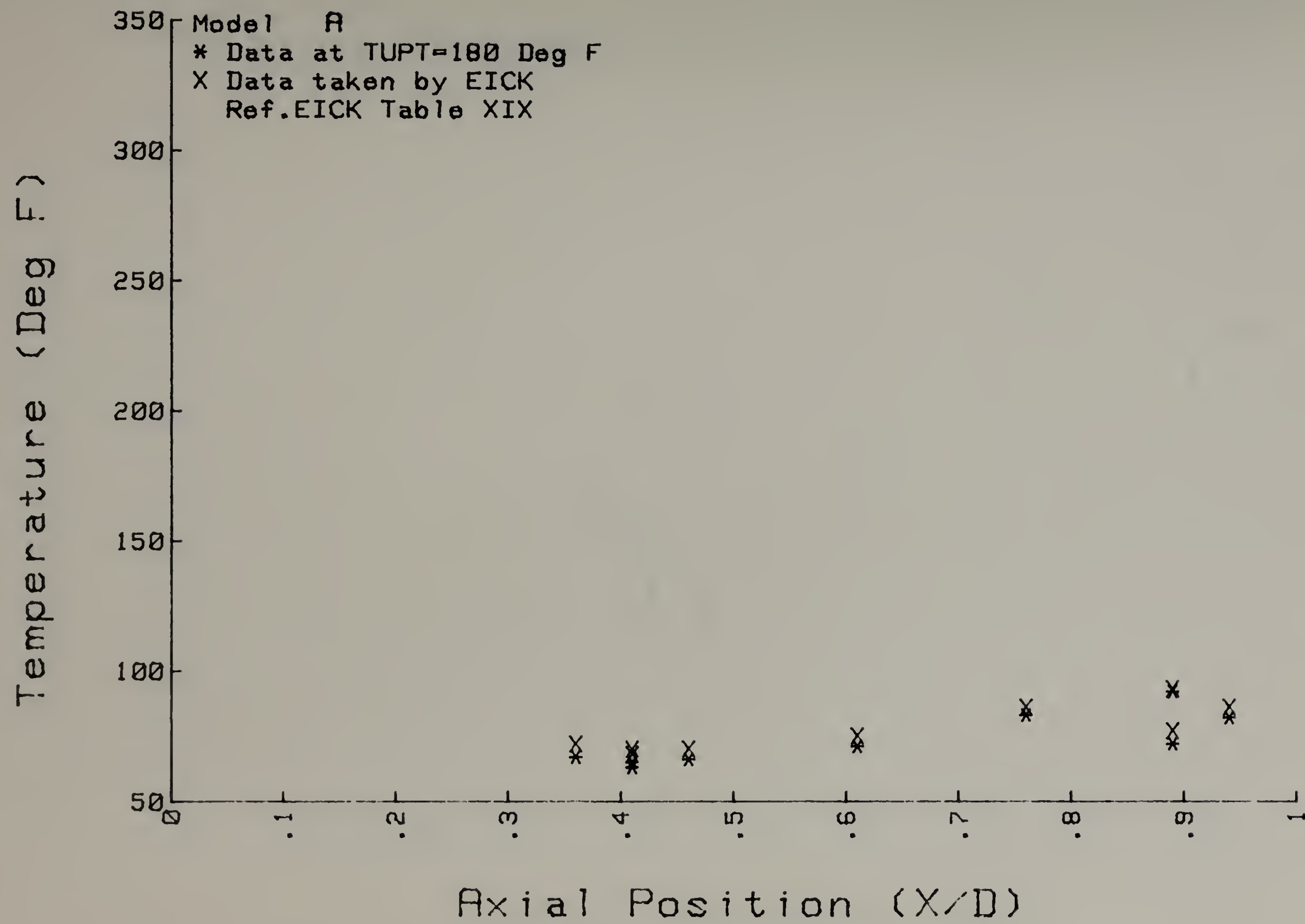

Figure 46. Mixing Stack Temperatures, Model A (180° F)

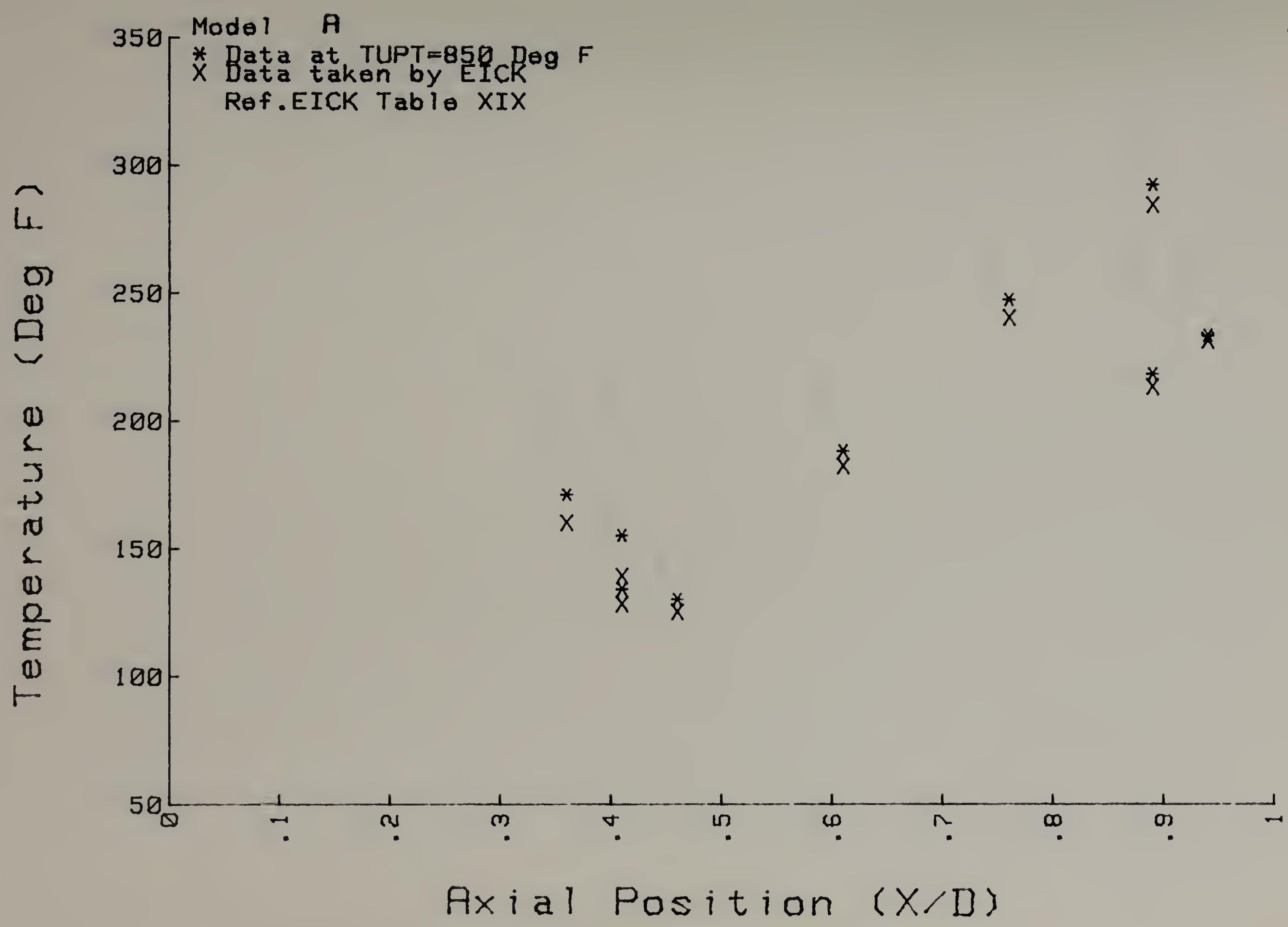

Figure 47. Mixing Stack Temperatures, Model A (850^{o} F)

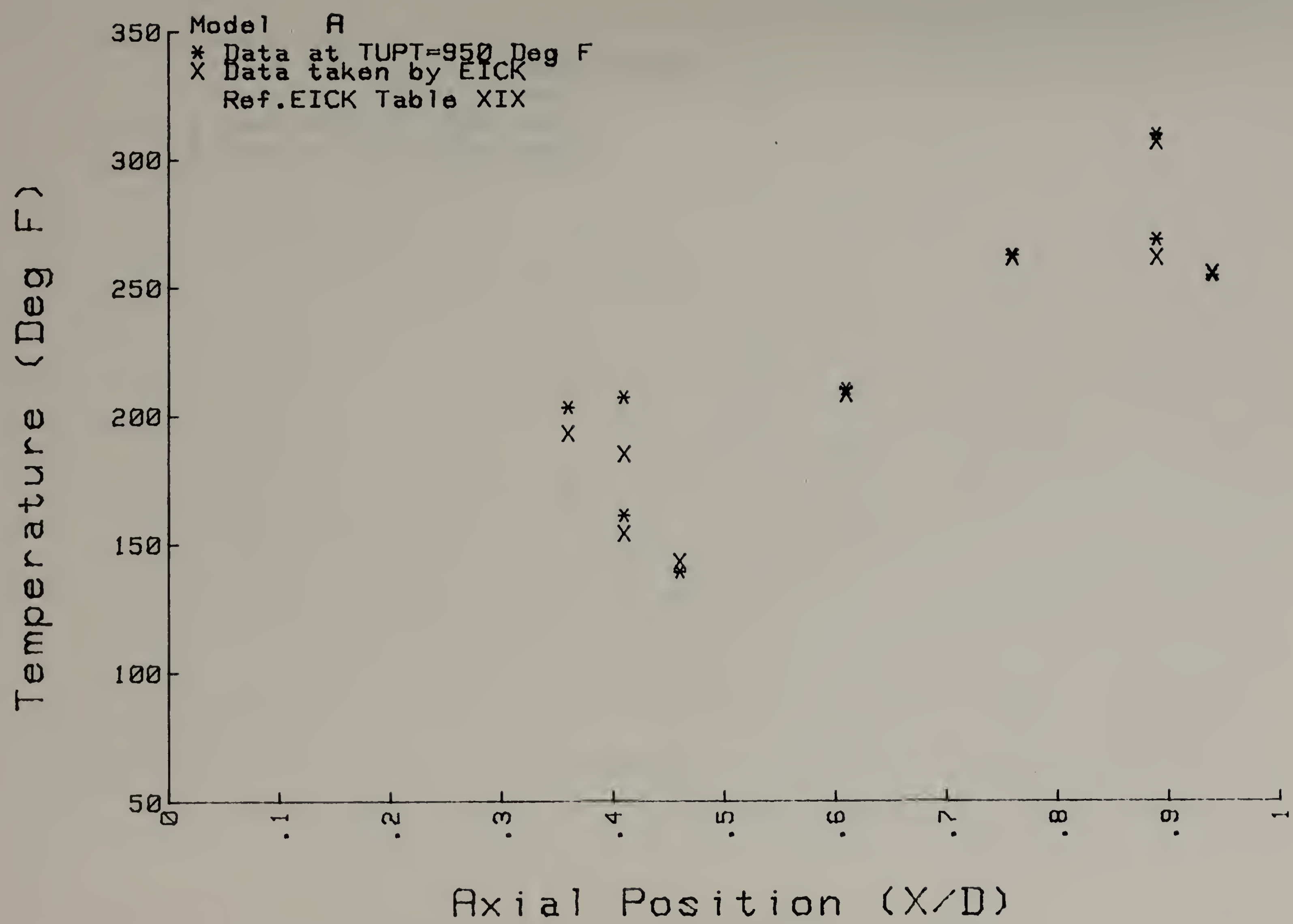

Figure 48. Mixing Stack Temperatures, Model A (950^{o} F)

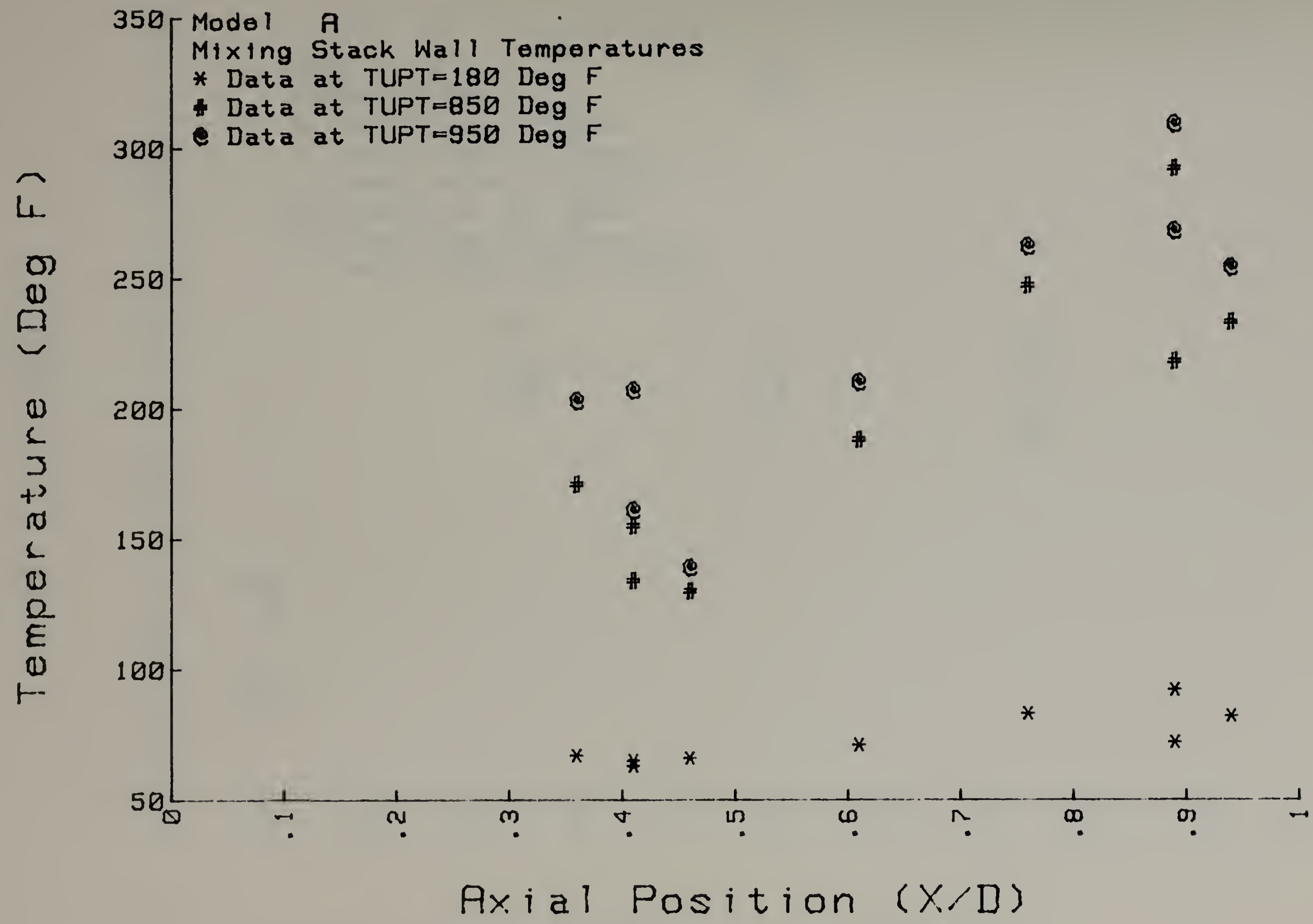

Figure 49. Mixing Stack Temperatures Comparison, Model A

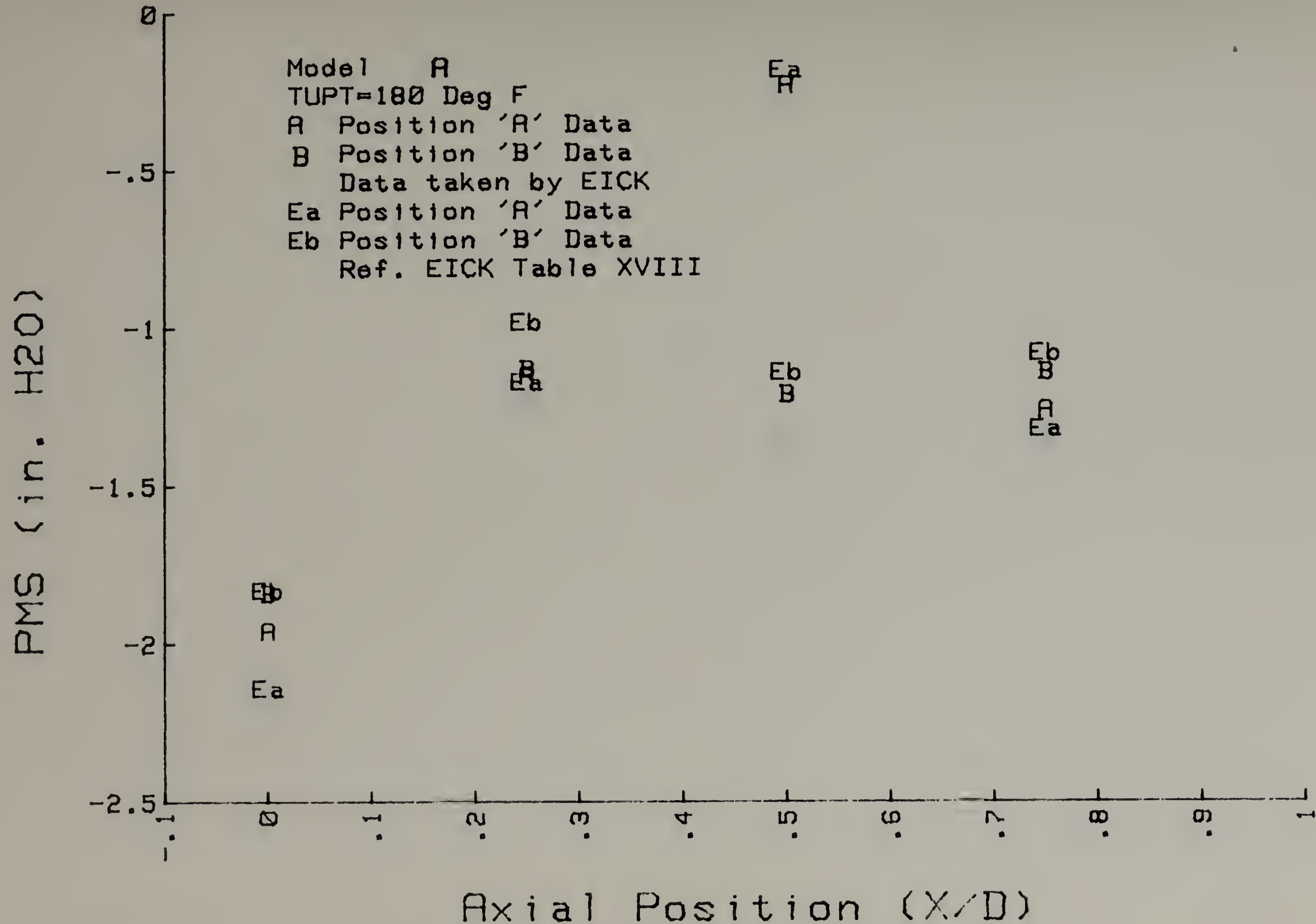

Figure 50. Mixing Stack Pressure, Model A (180° F)

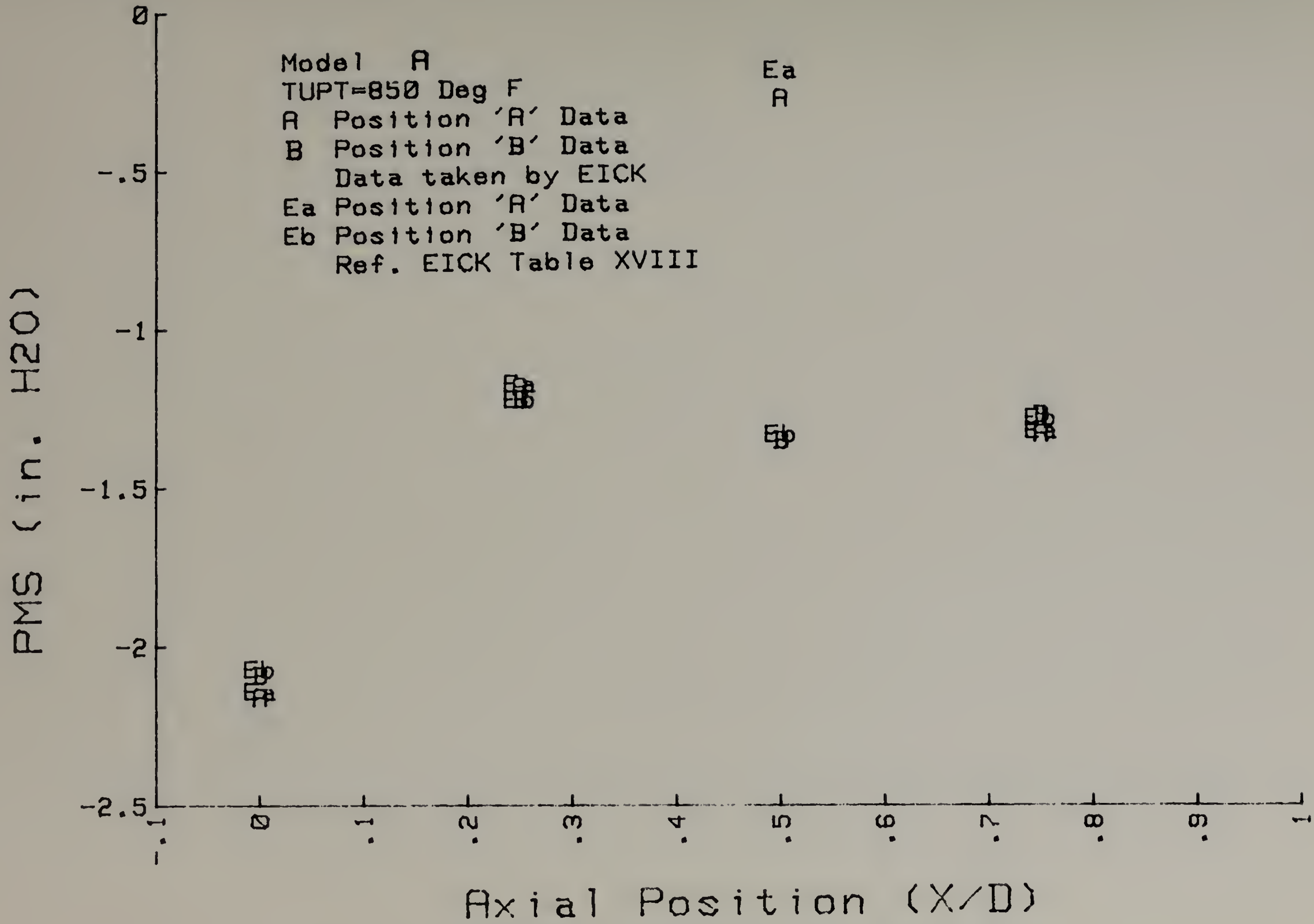

Figure 51. Mixing Stack Pressure, Model A (850^{o} F)

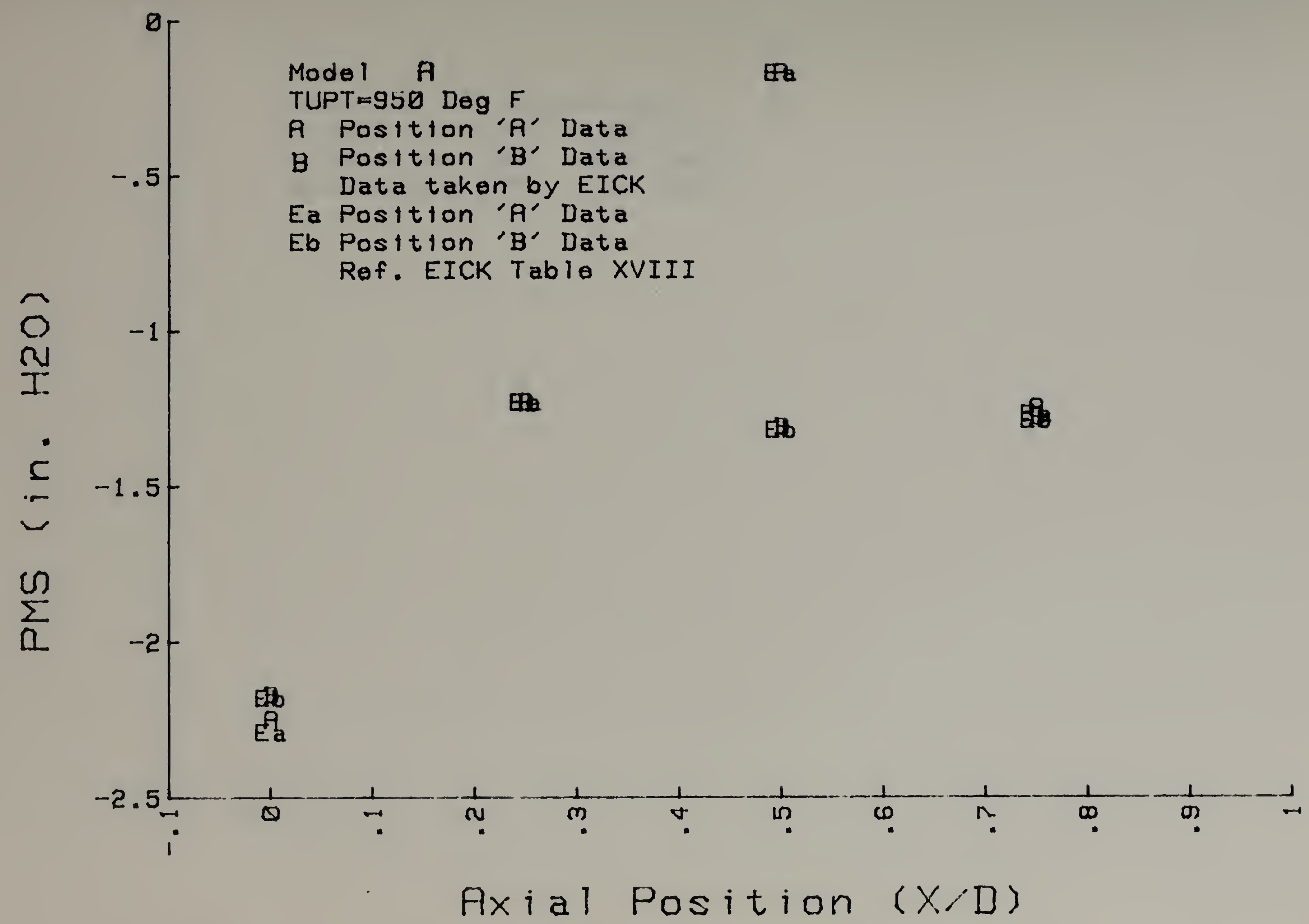

Figure 52, Mixing Stack Pressure, Model A (950^{o} F)

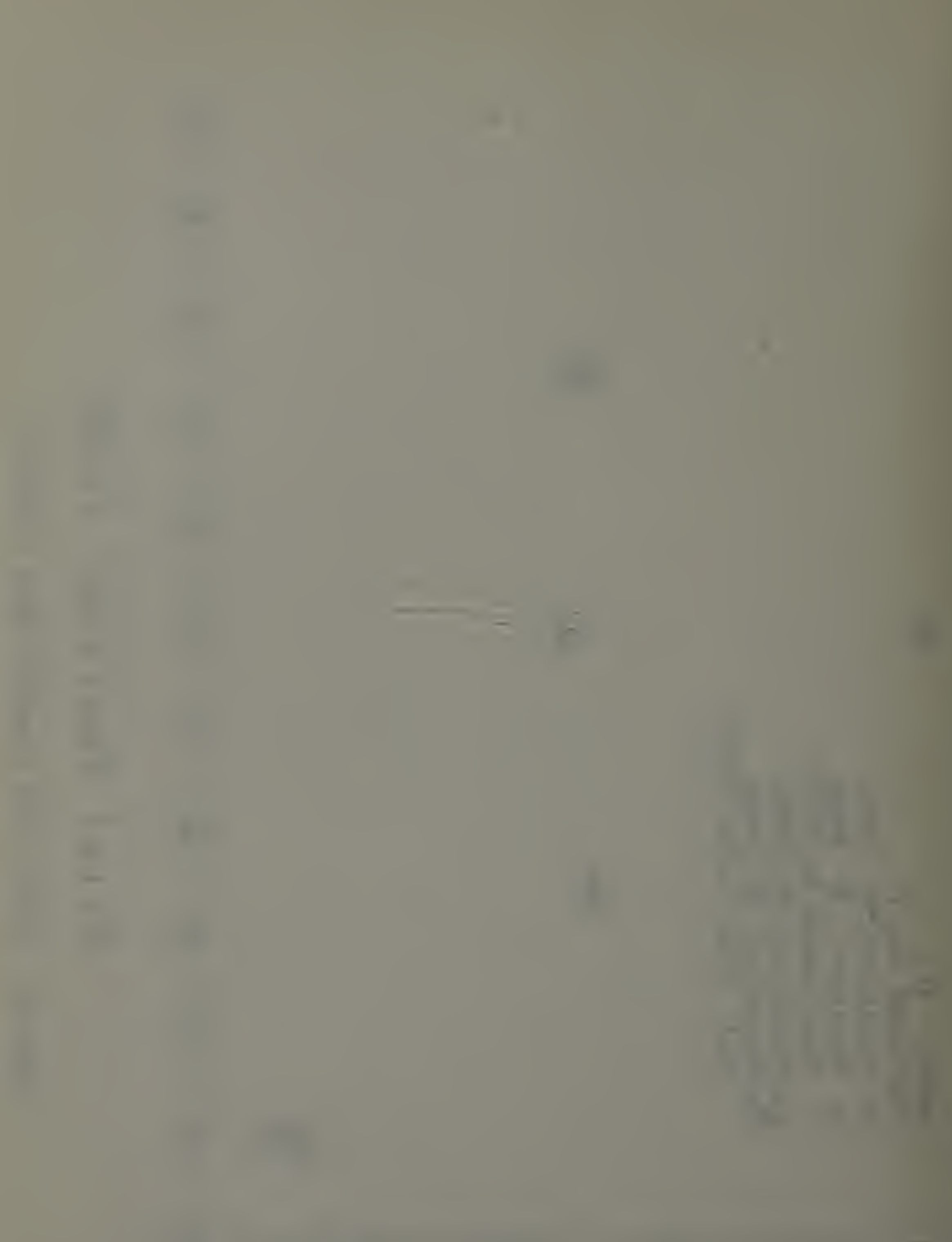

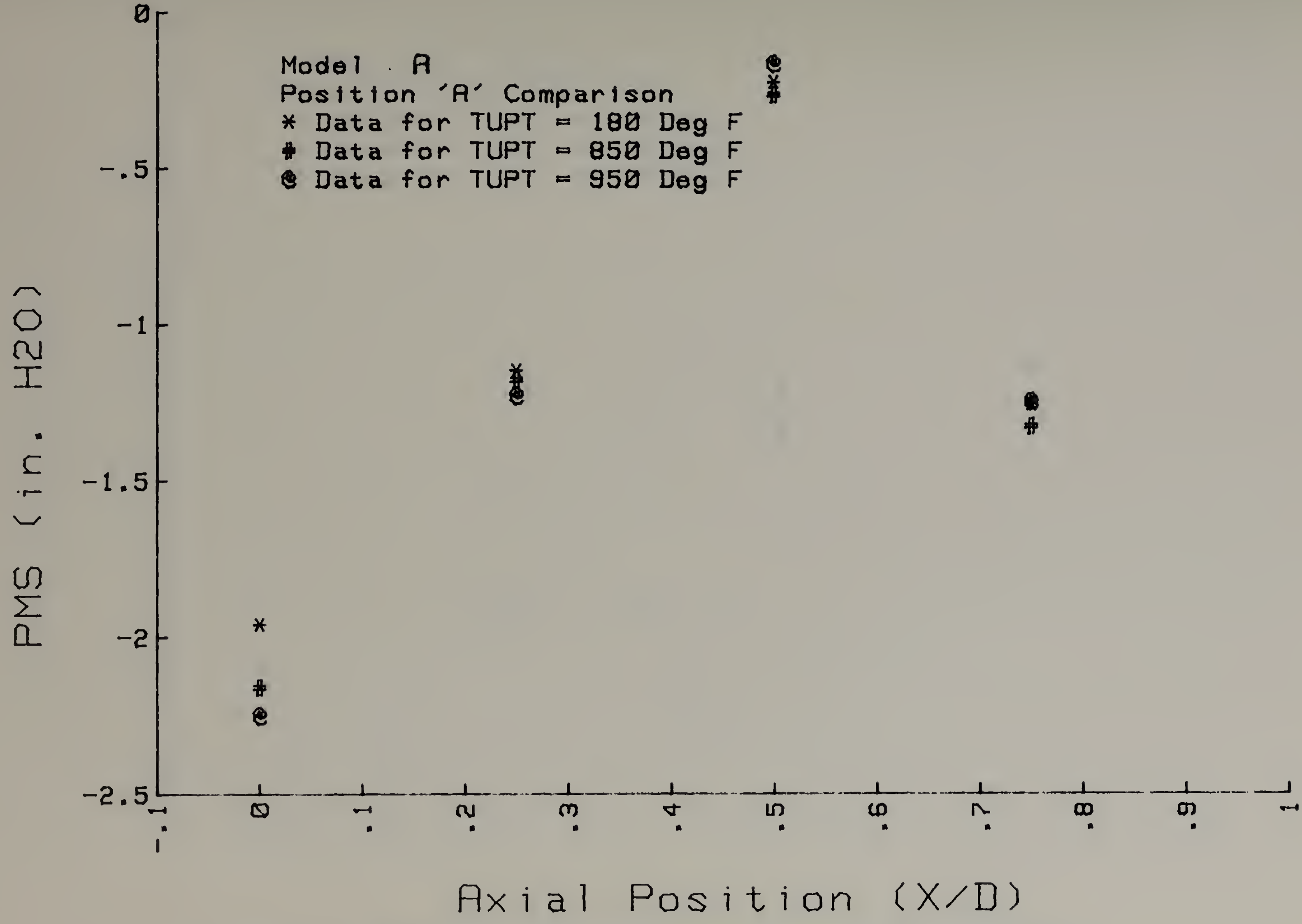

Figure 53. Mixing Stack Pressure Comparison, Model A (Position A)

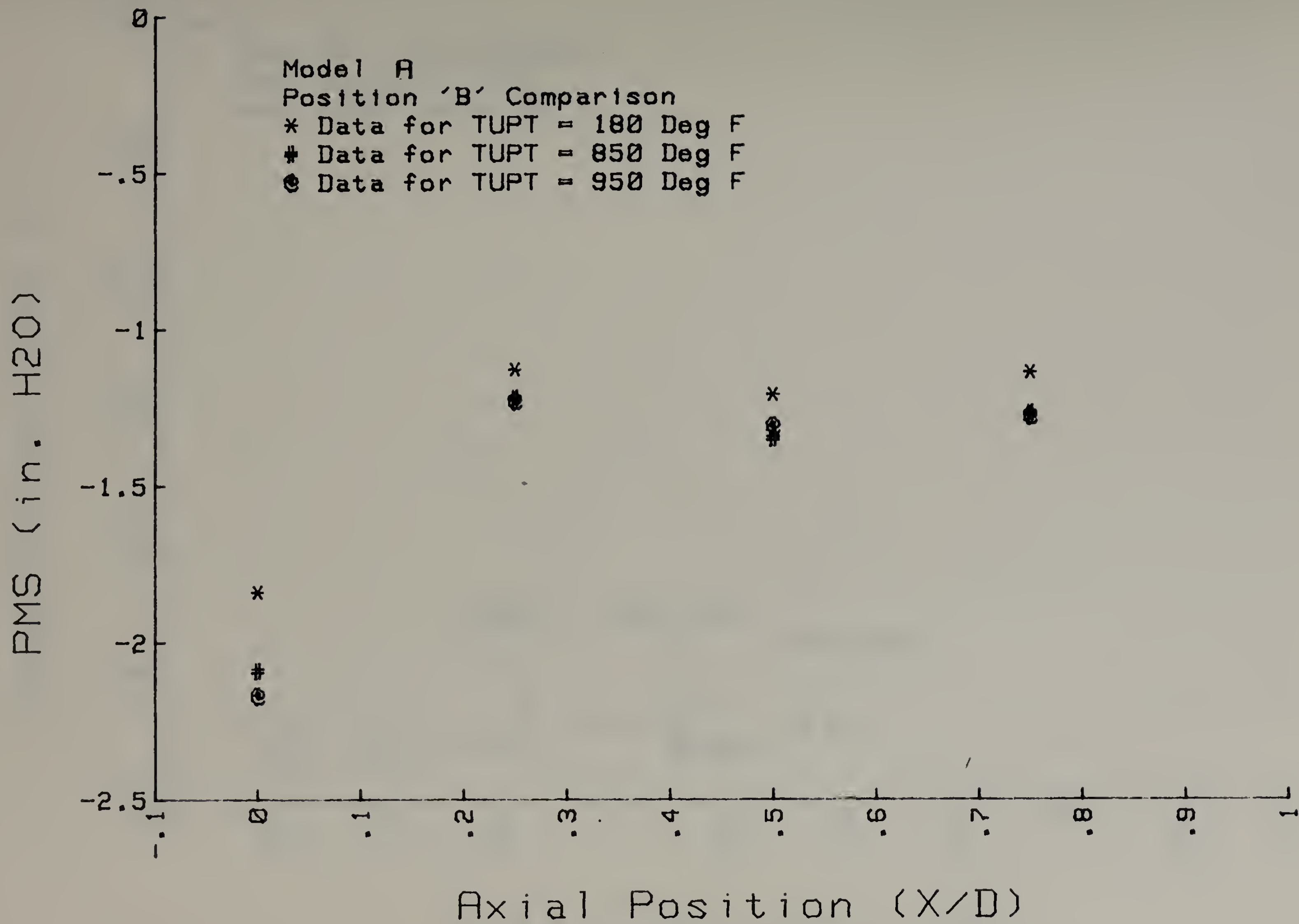

Figure 54. Mixing Stack Pressure Comparison, Model A (Position B)

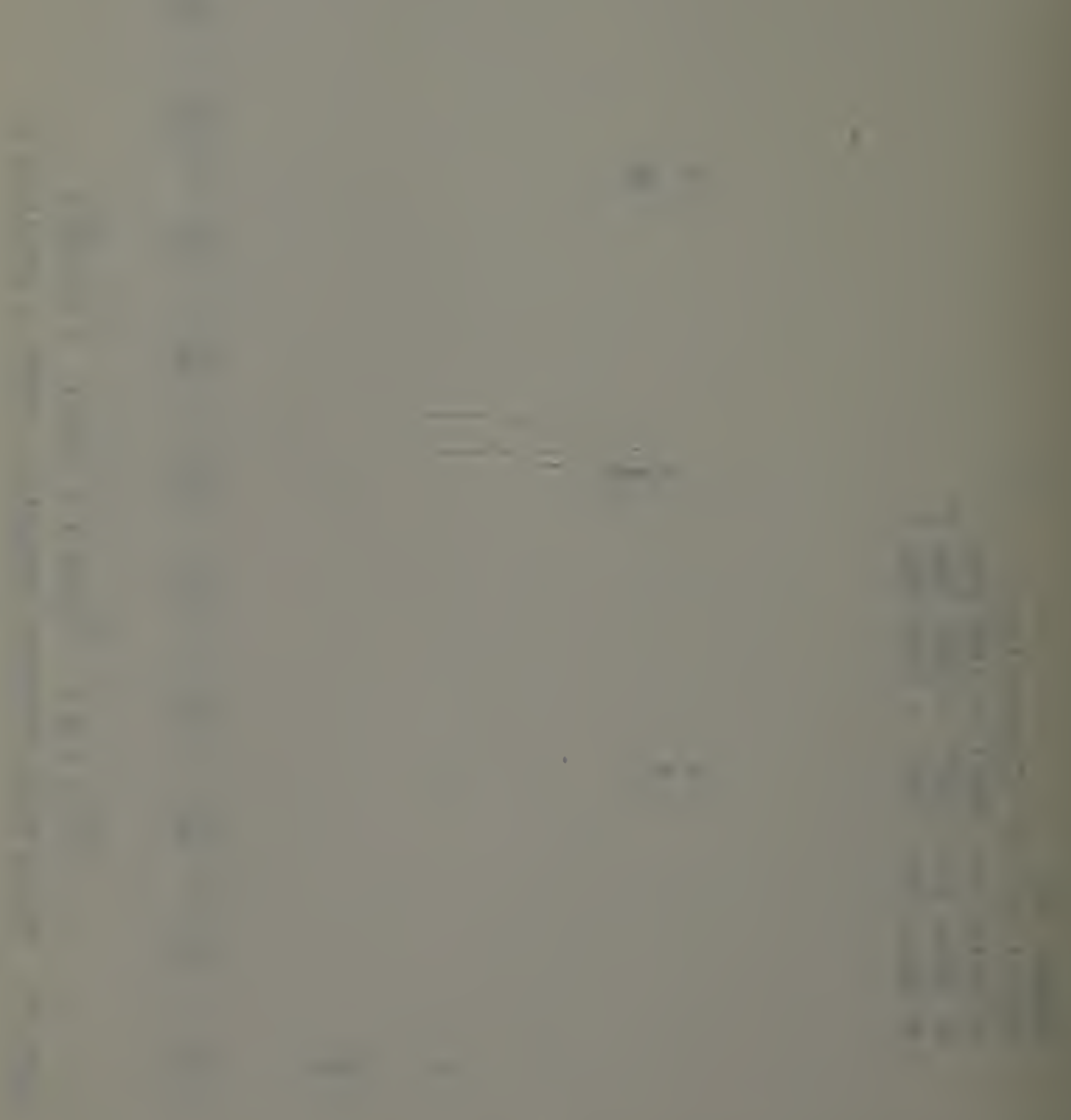

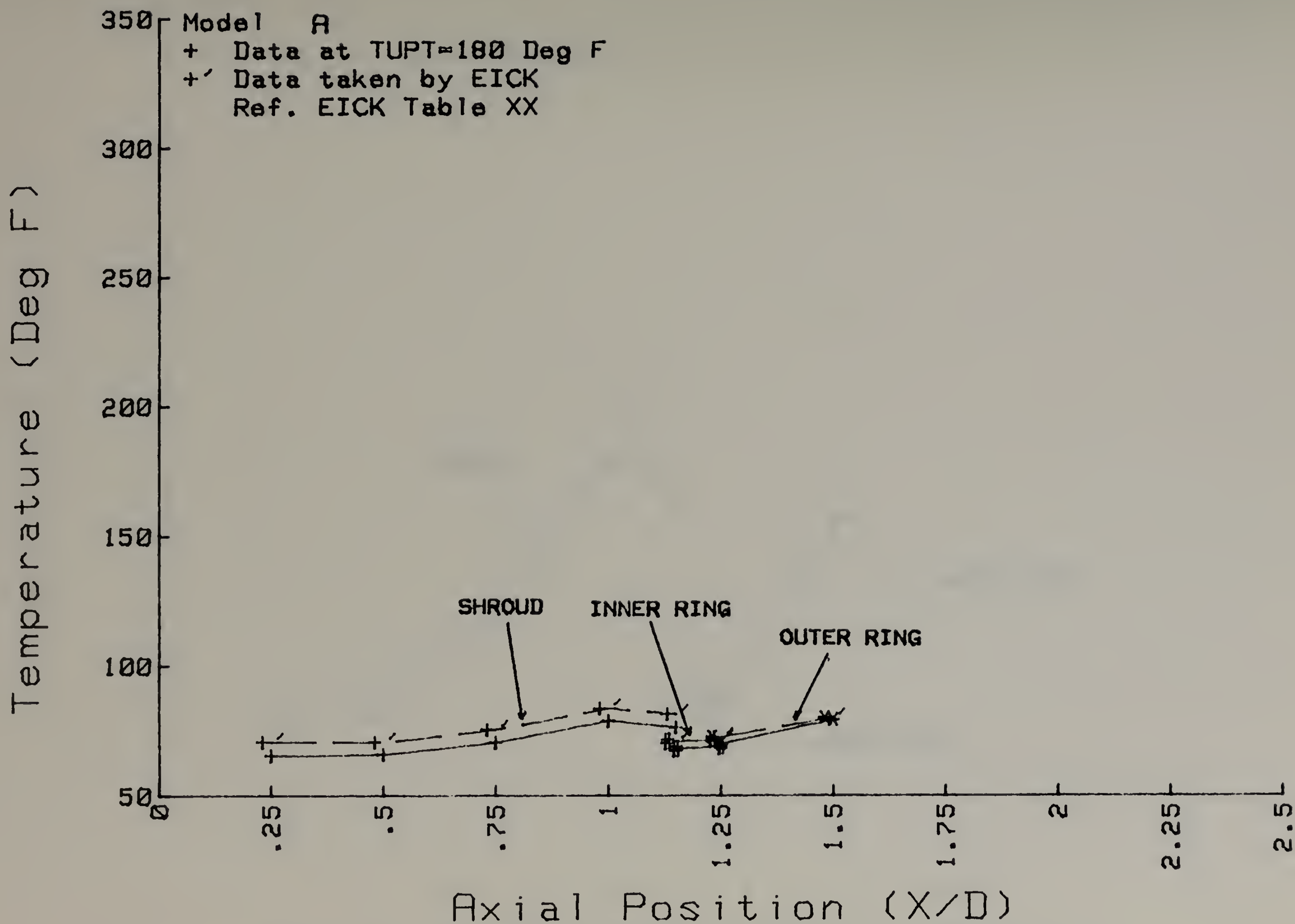

Figure 55. Shroud and Diffuser Temperatures, Model A (180° F)

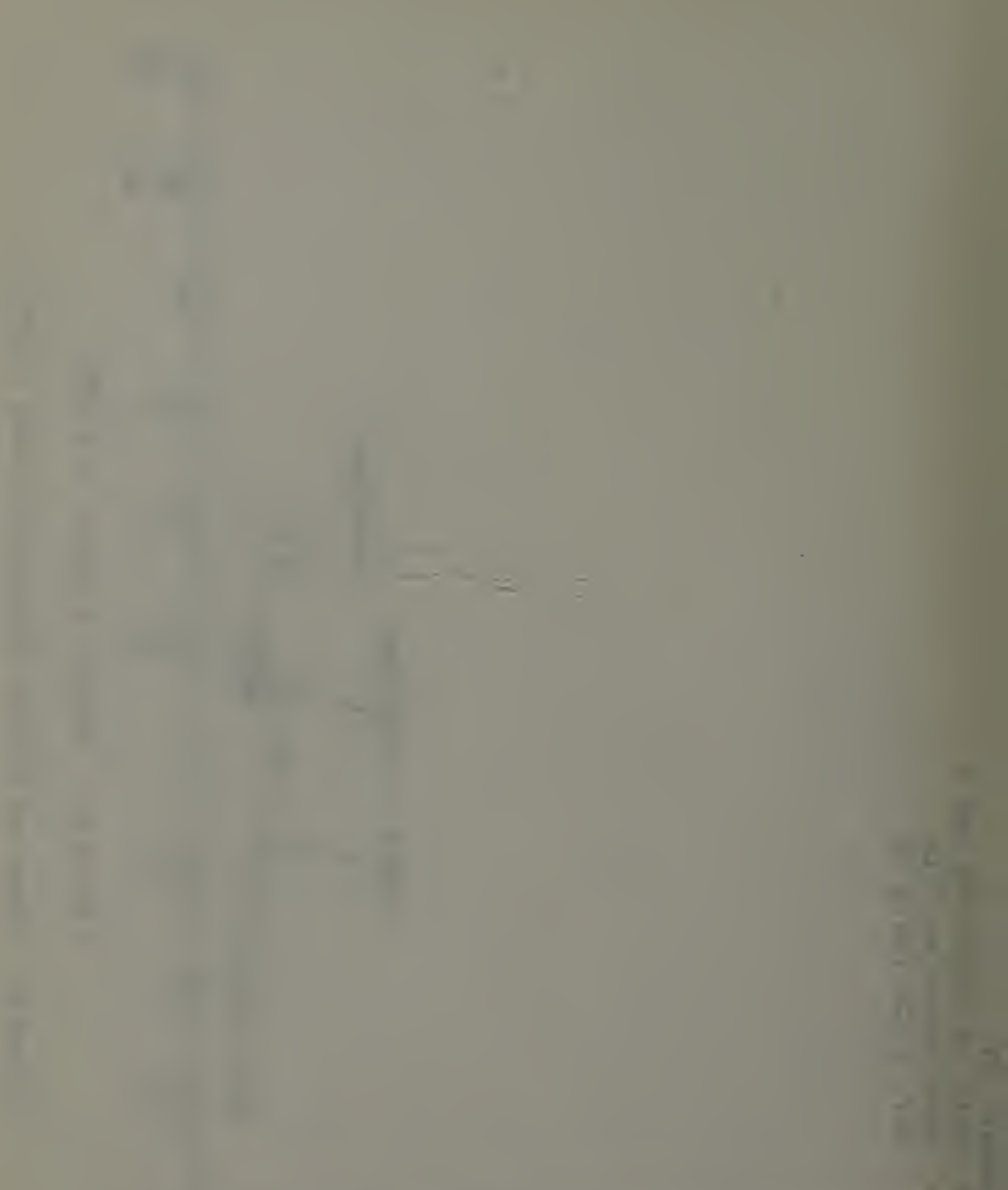

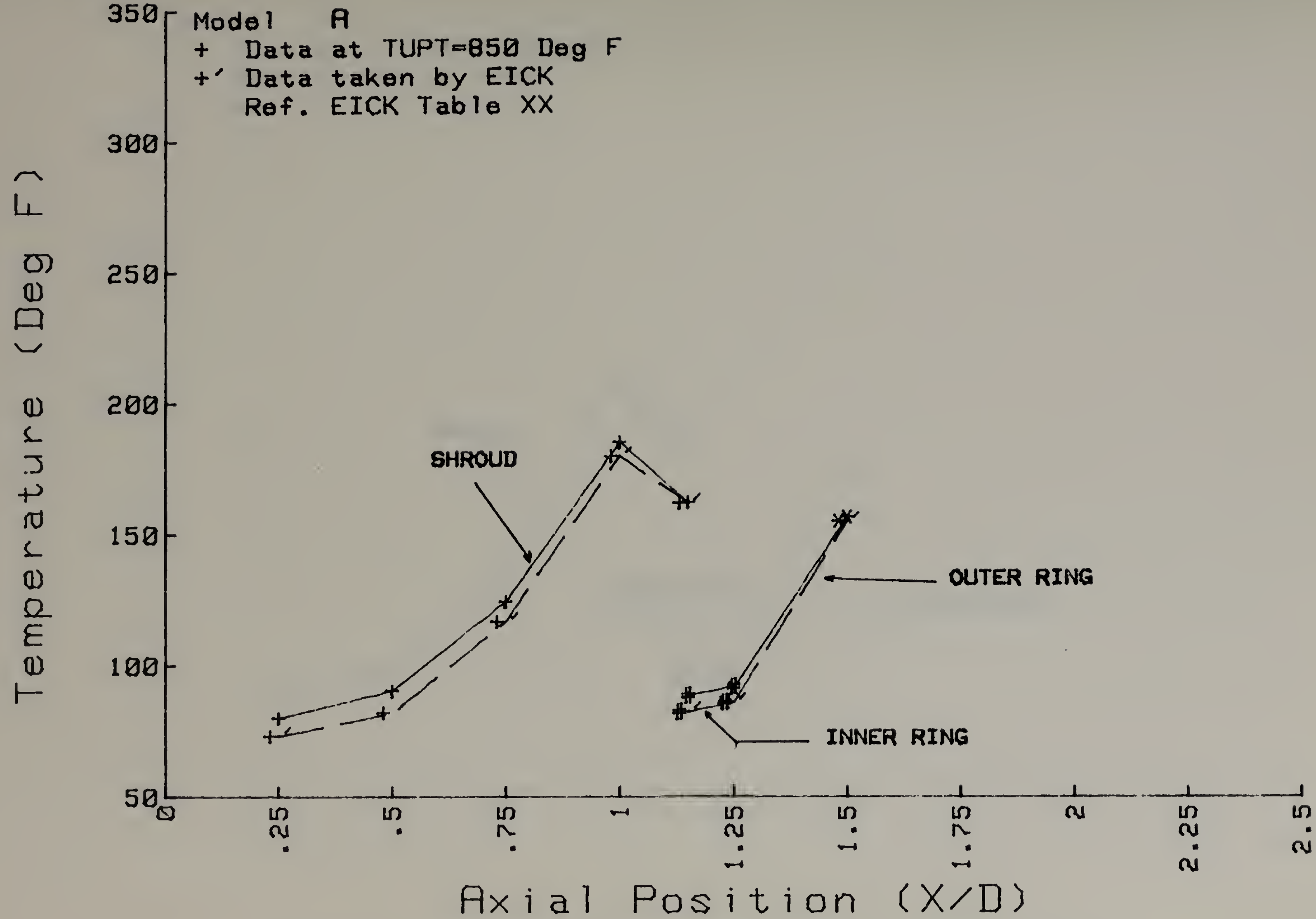

Figure 56. Shroud and Diffuser Temperatures, Model A (850^{o} F)

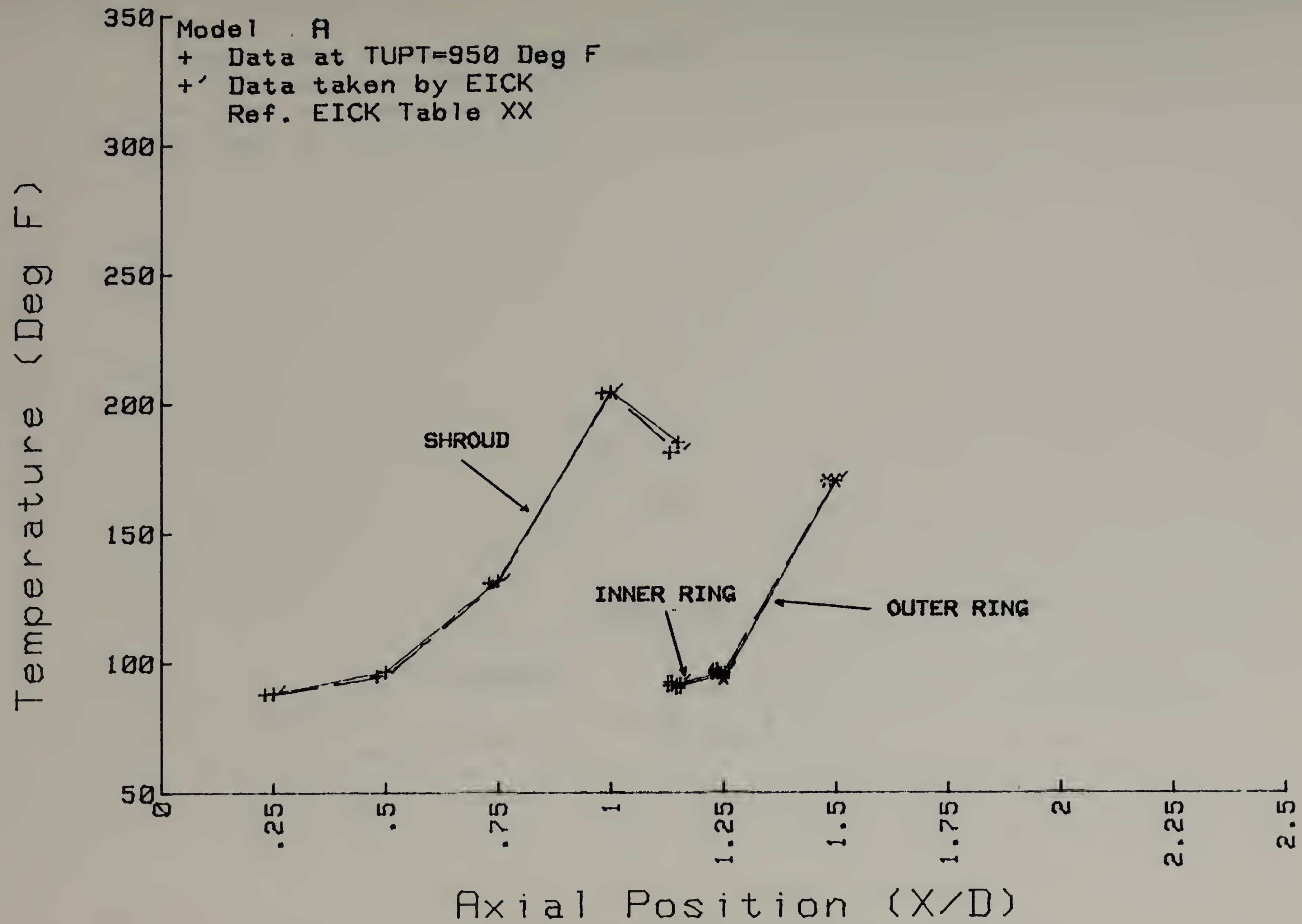

Figure 57. Shroud and Diffuser Temperatures, Model A (950^{O} F)

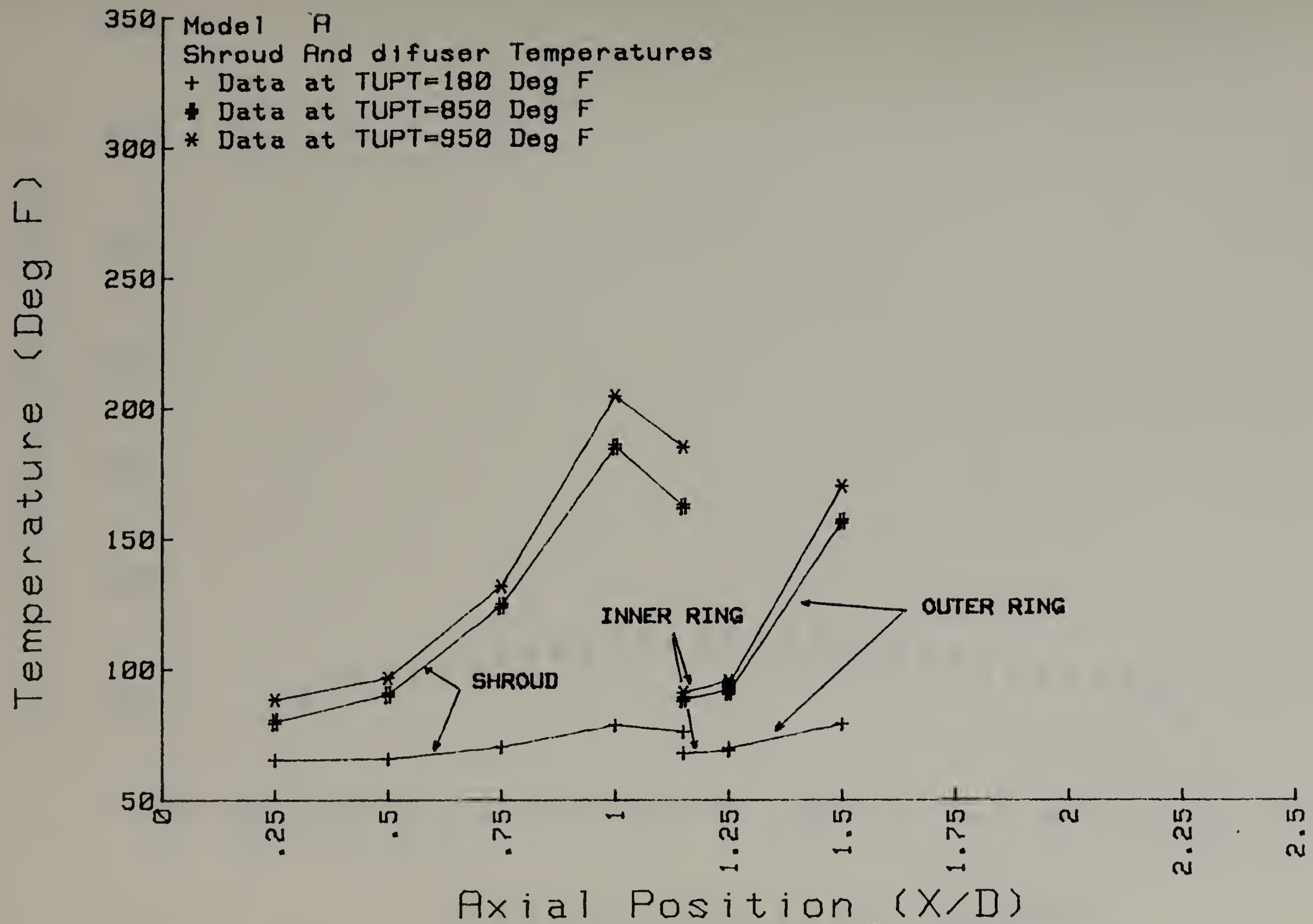

Figure 58. Shroud and Diffuser Temperatures Comparison, Model A

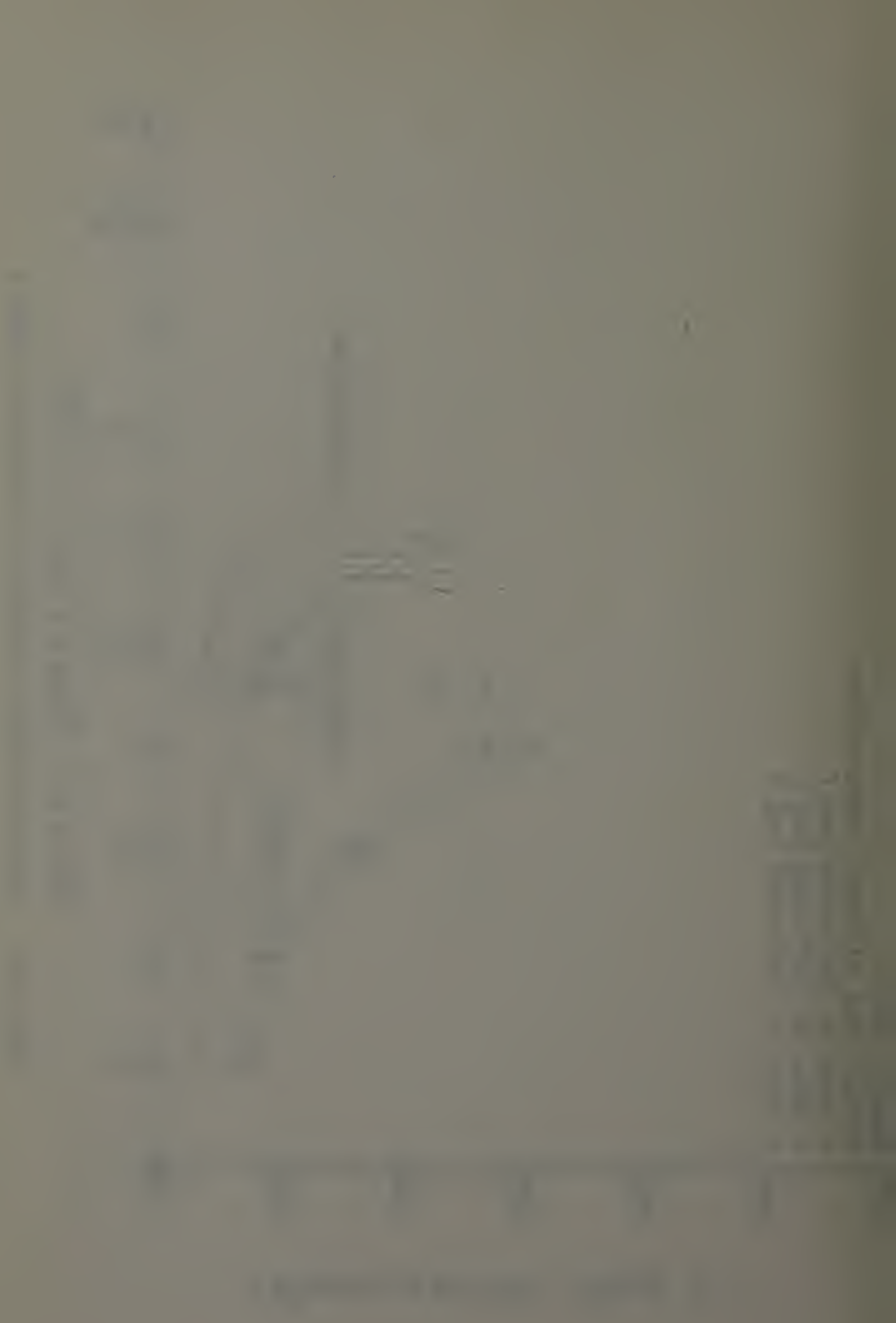

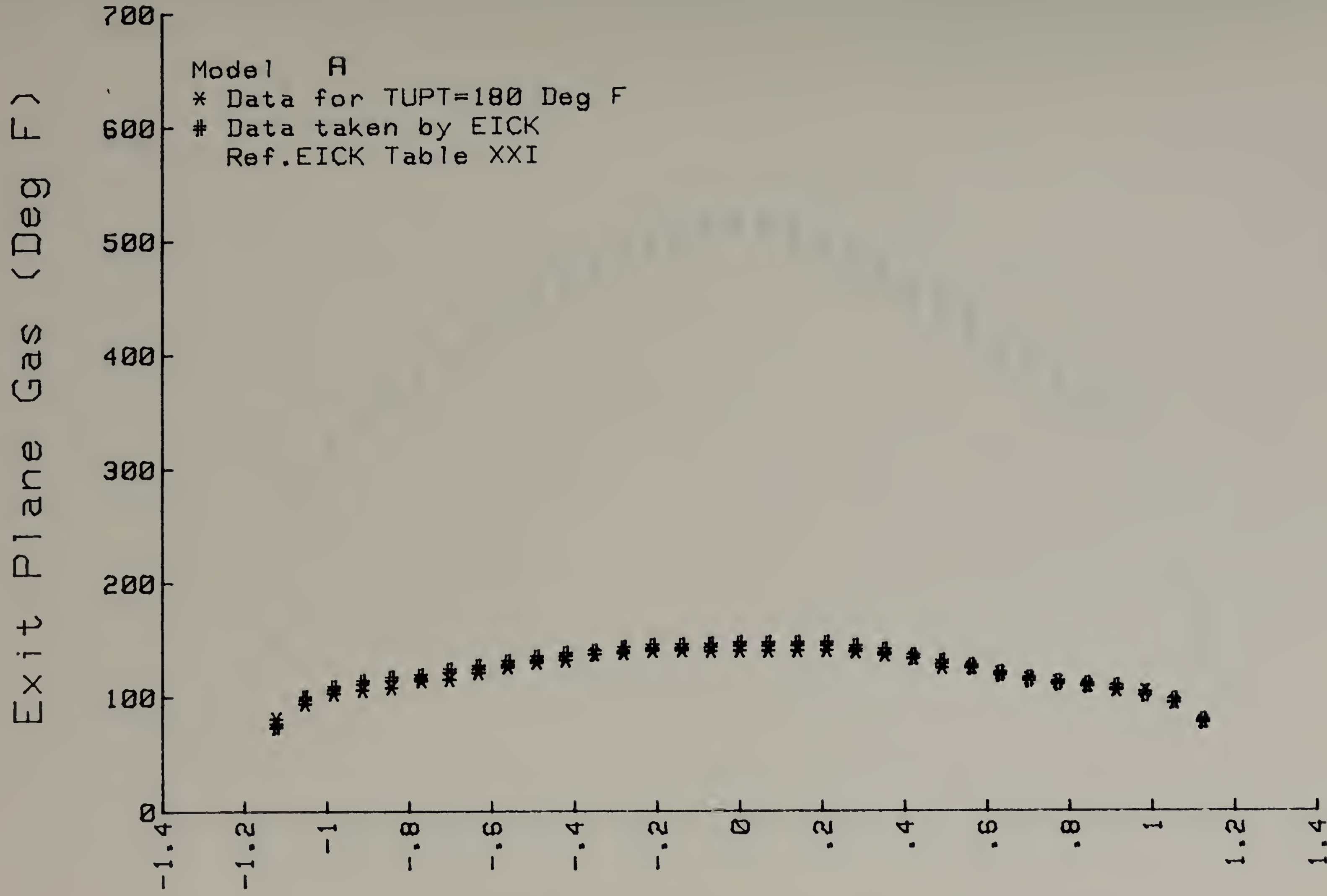

Figure 59. Exit Plane Temperature, Model A (180^{o} F)

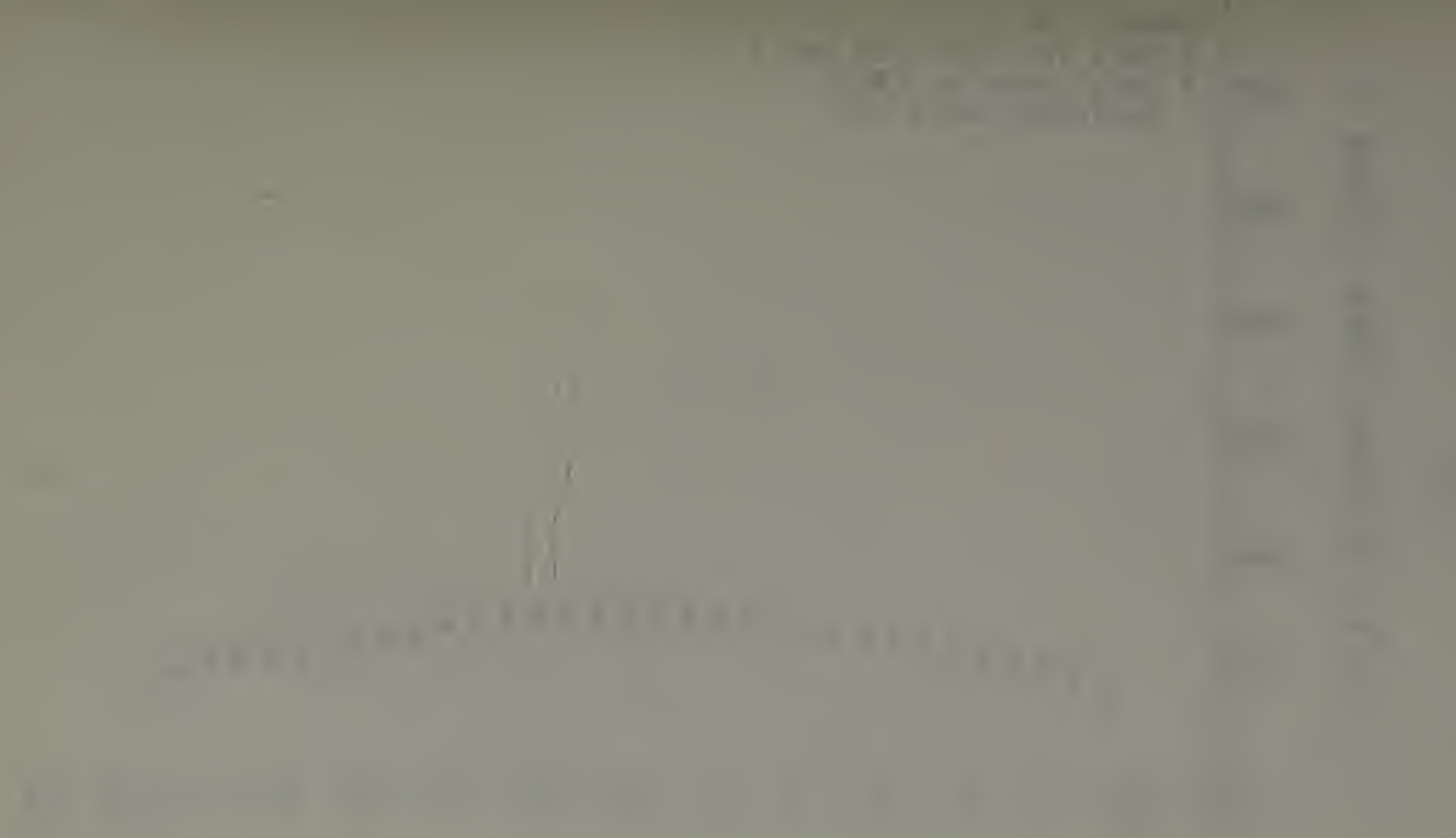

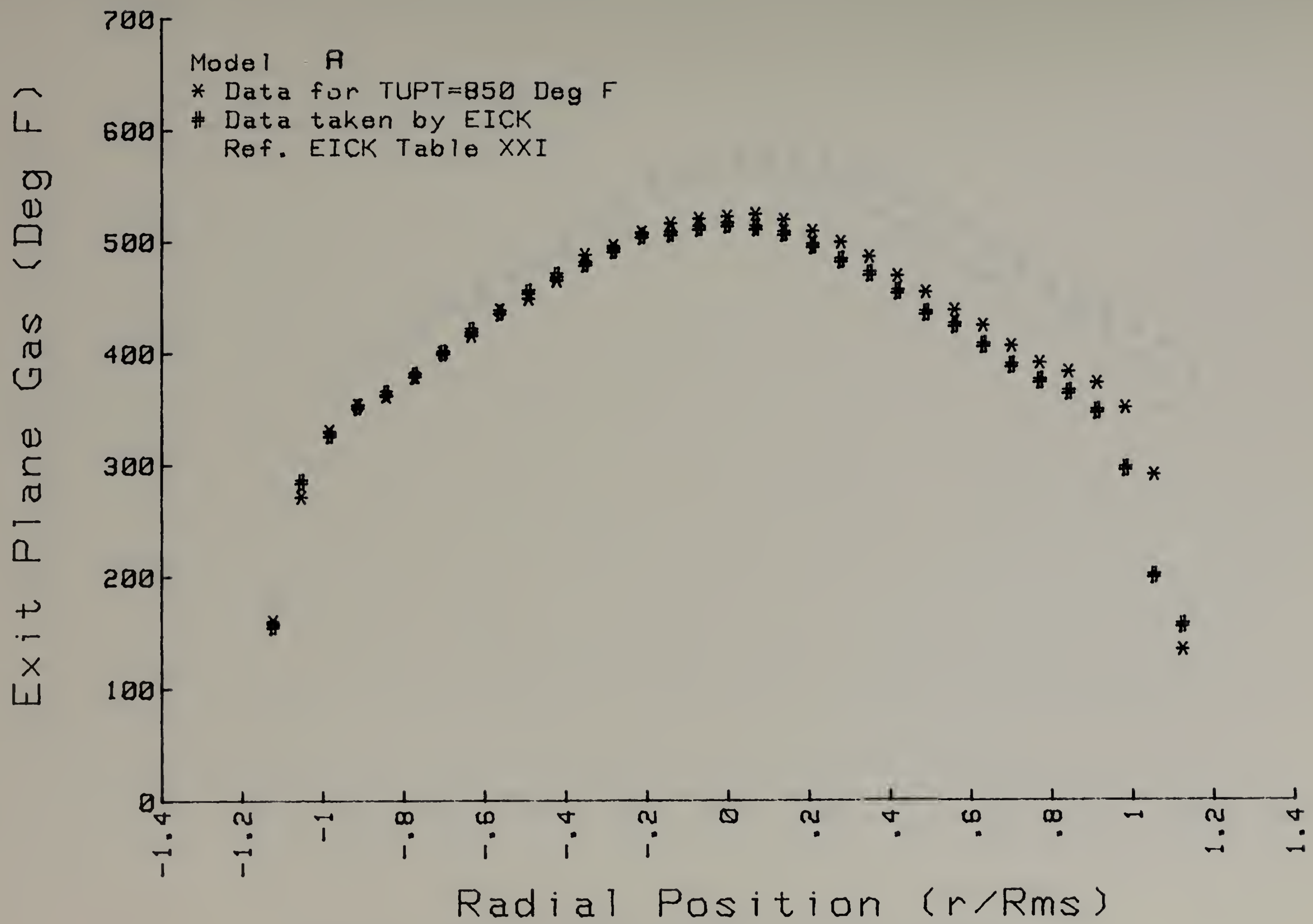

Figure 60. Exit Plane Temperature, Model A (850° F)

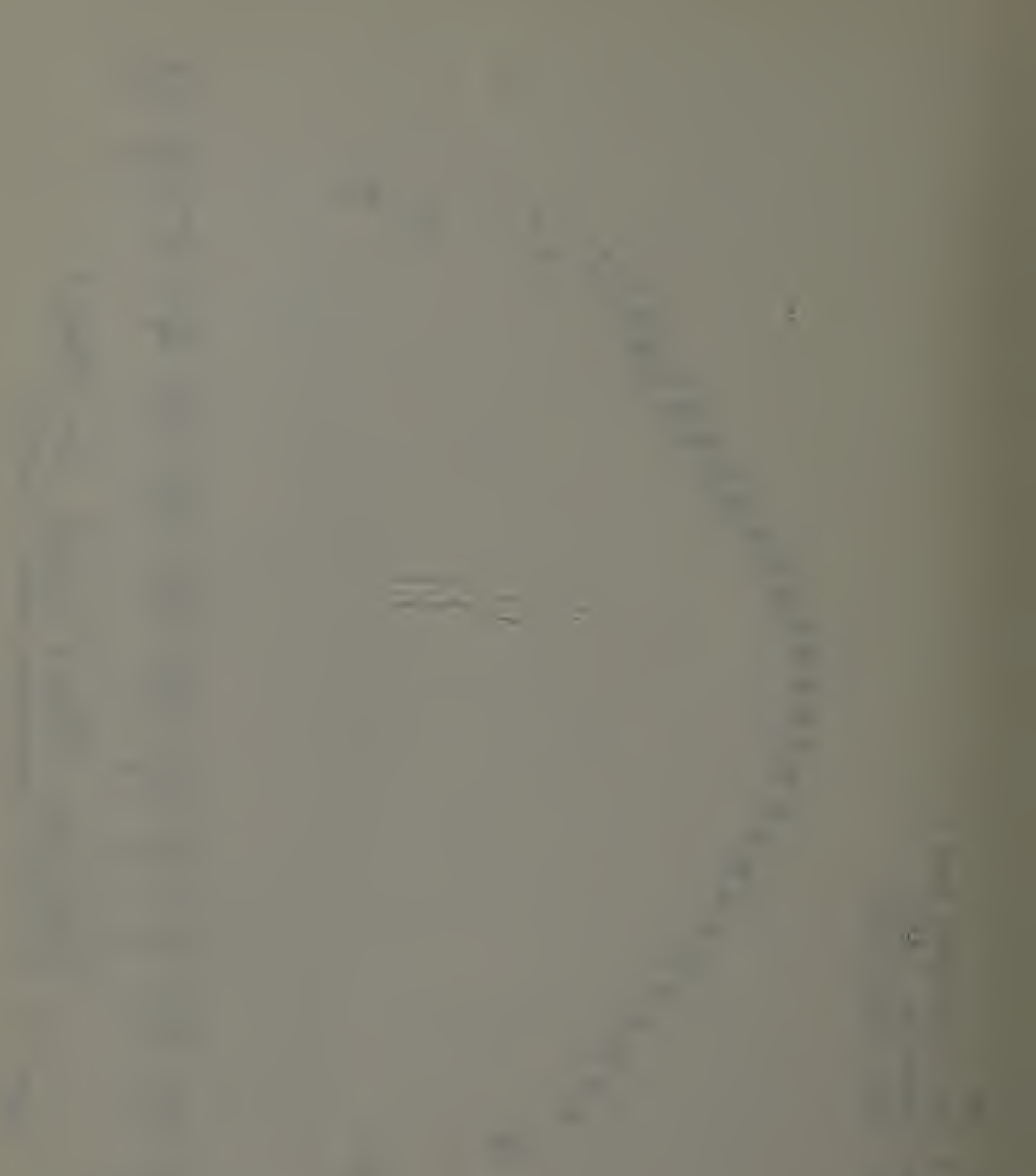

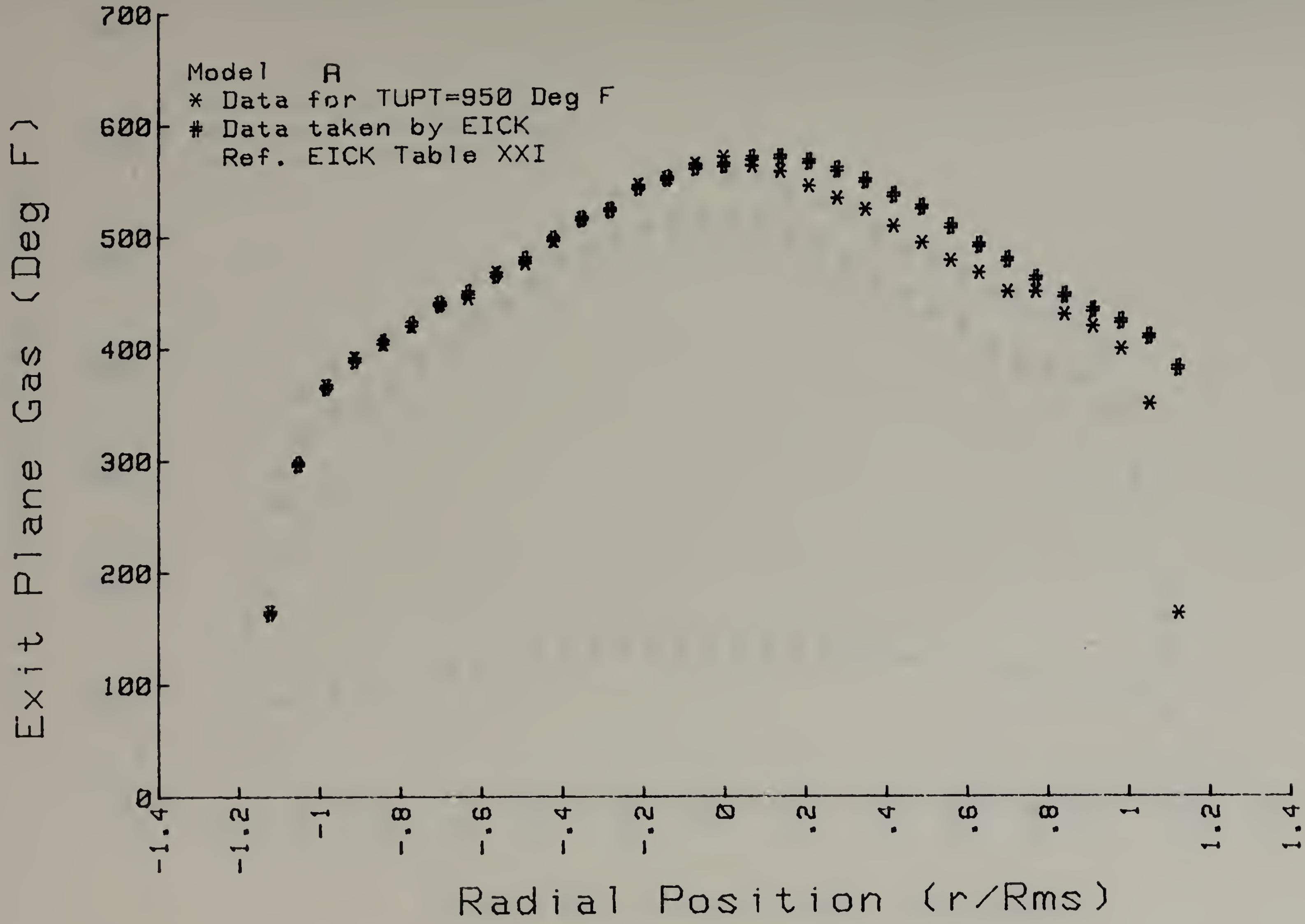

Figure 61. Exit Plane Temperature, Model A (950^{o} F)

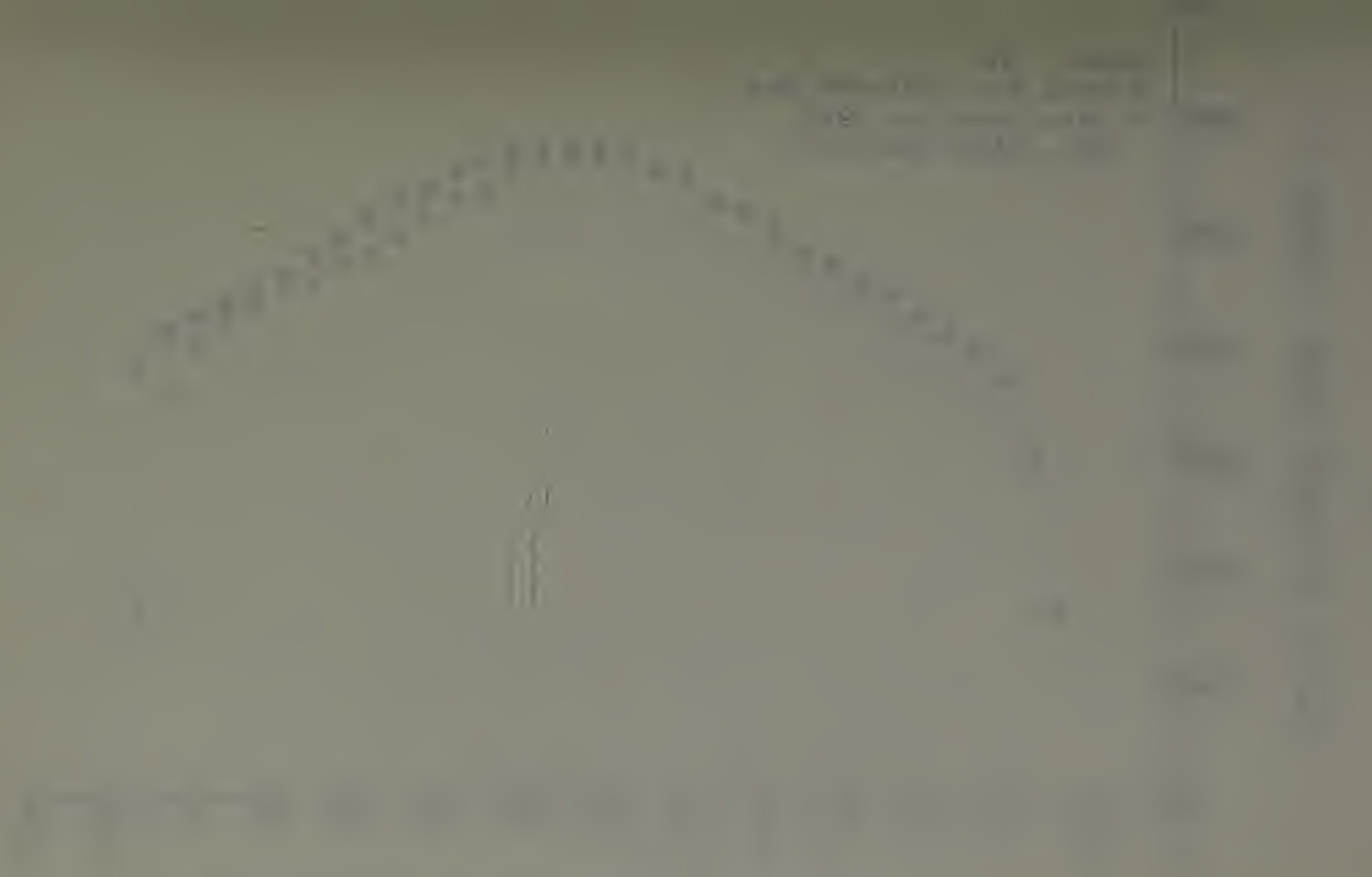

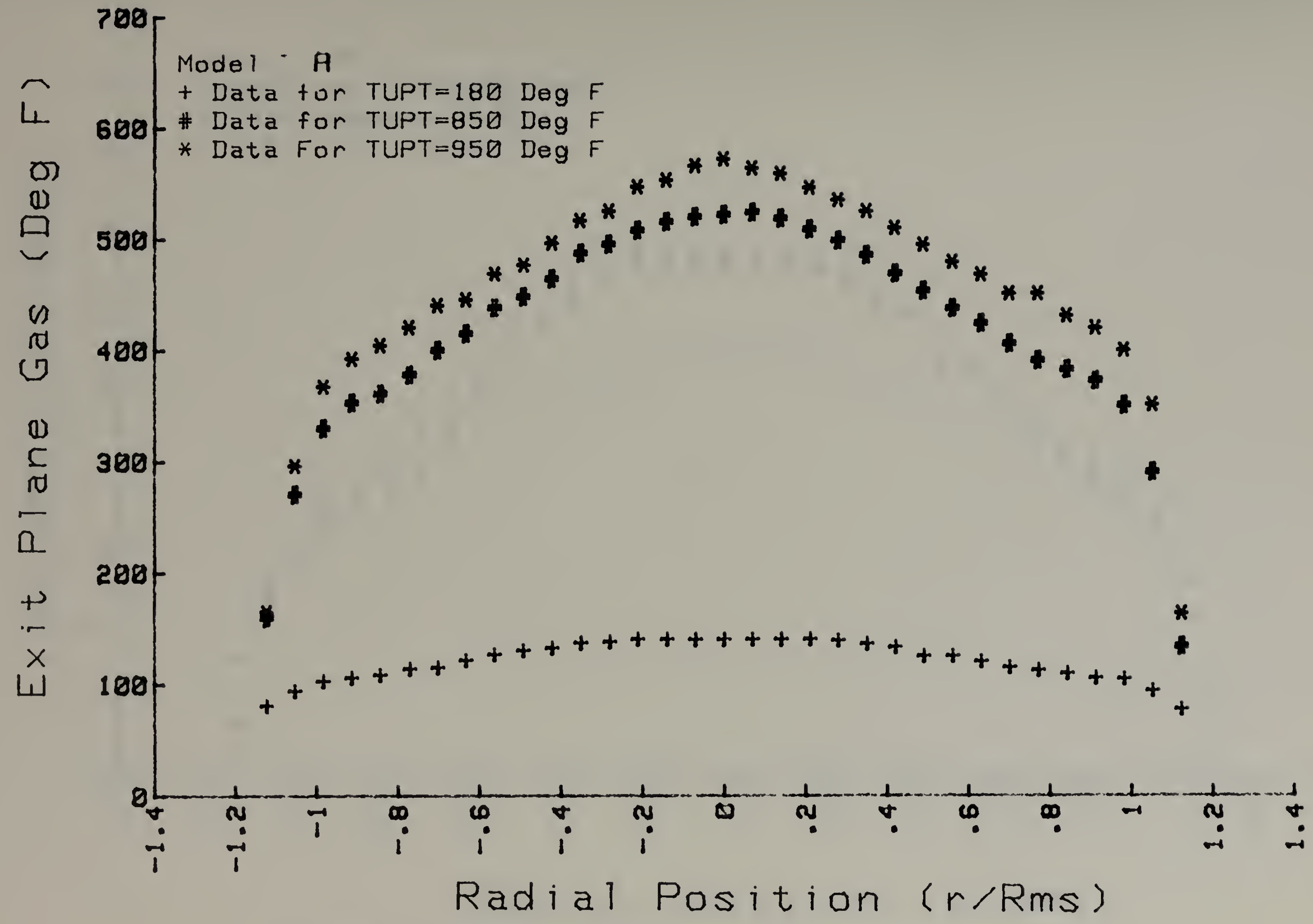

Figure 62. Exit Plane Temperature Comparison, Model A

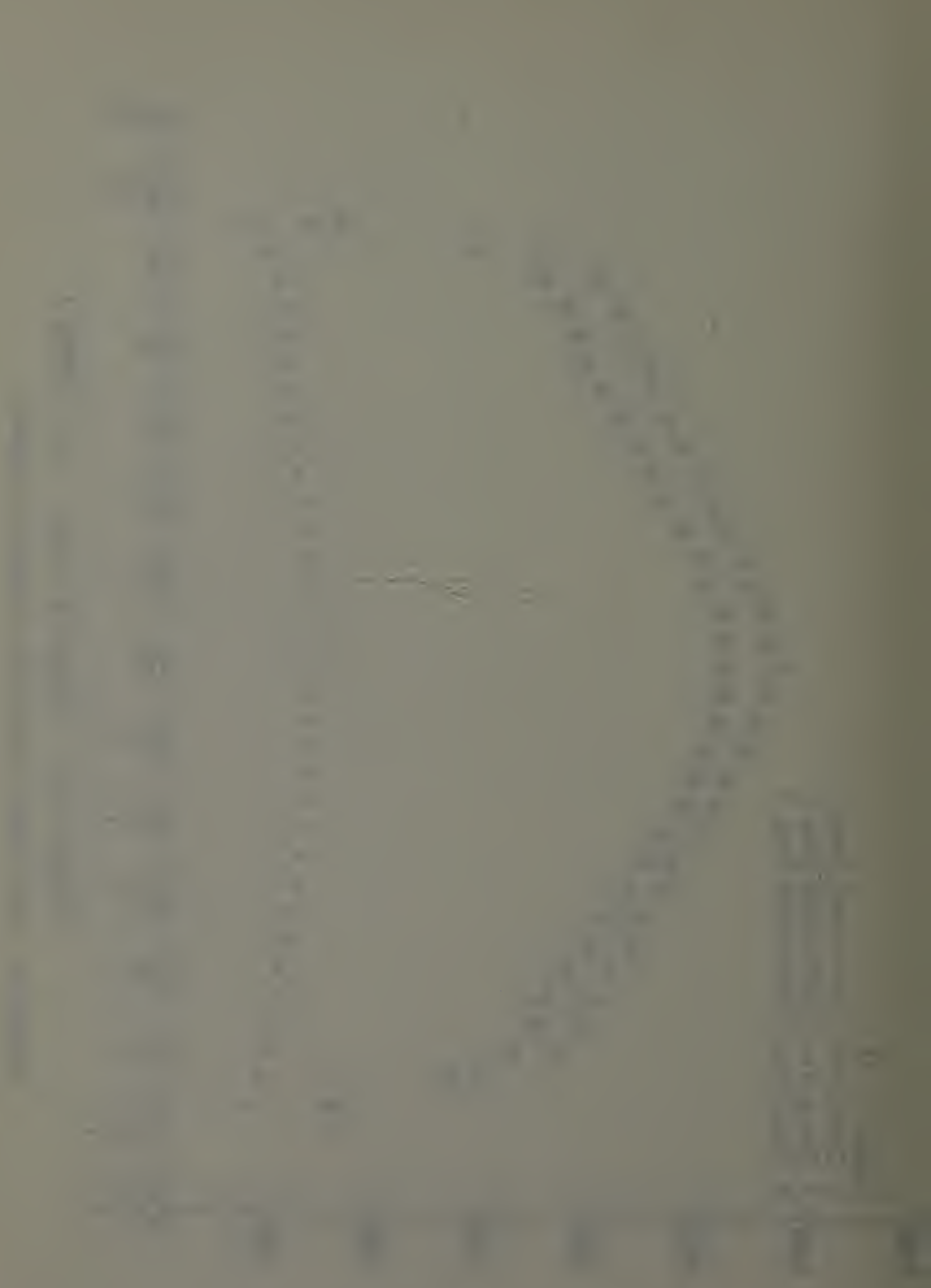

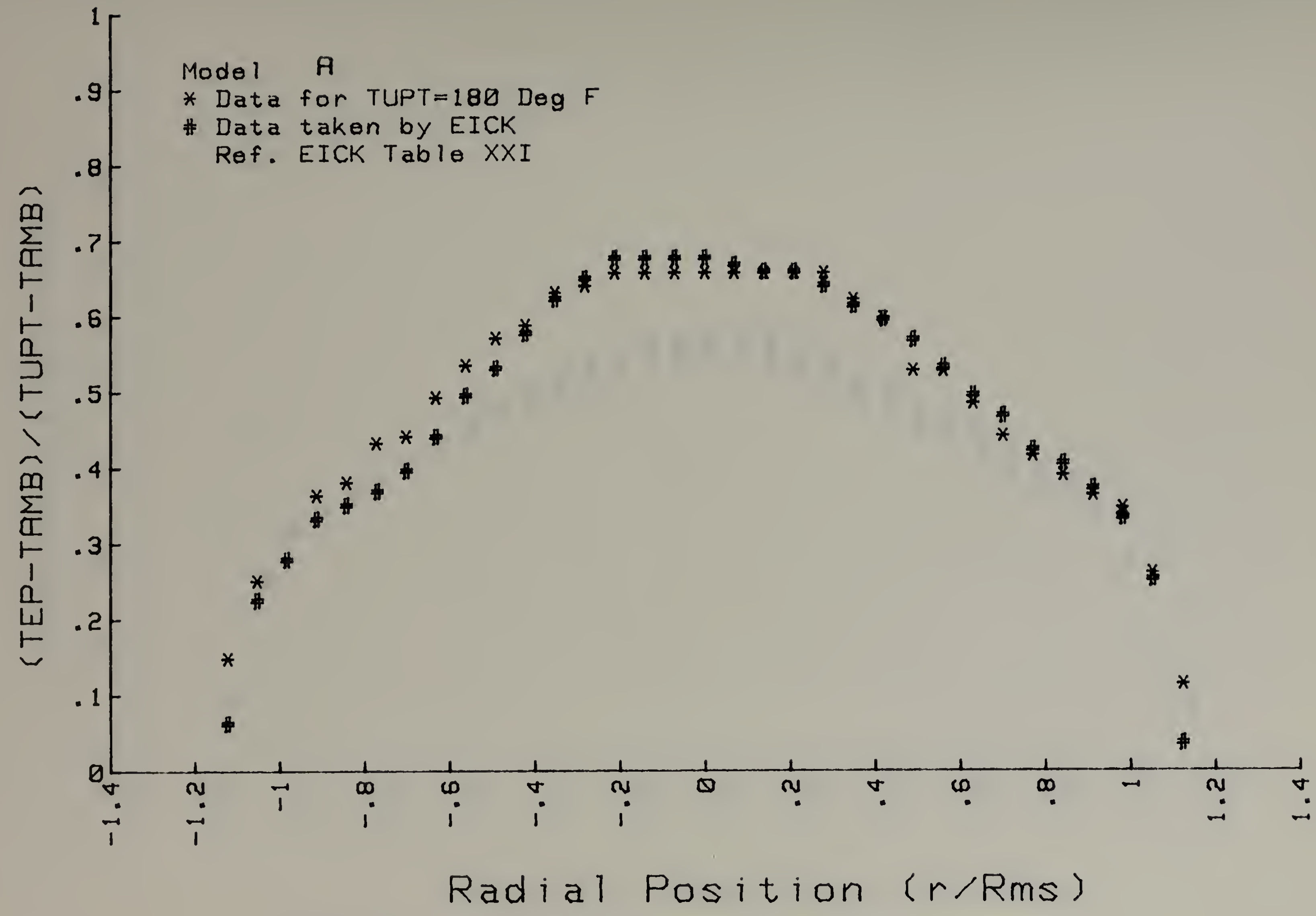

Figure 63. Exit Plane Coefficients, Model A (180^{o} F)

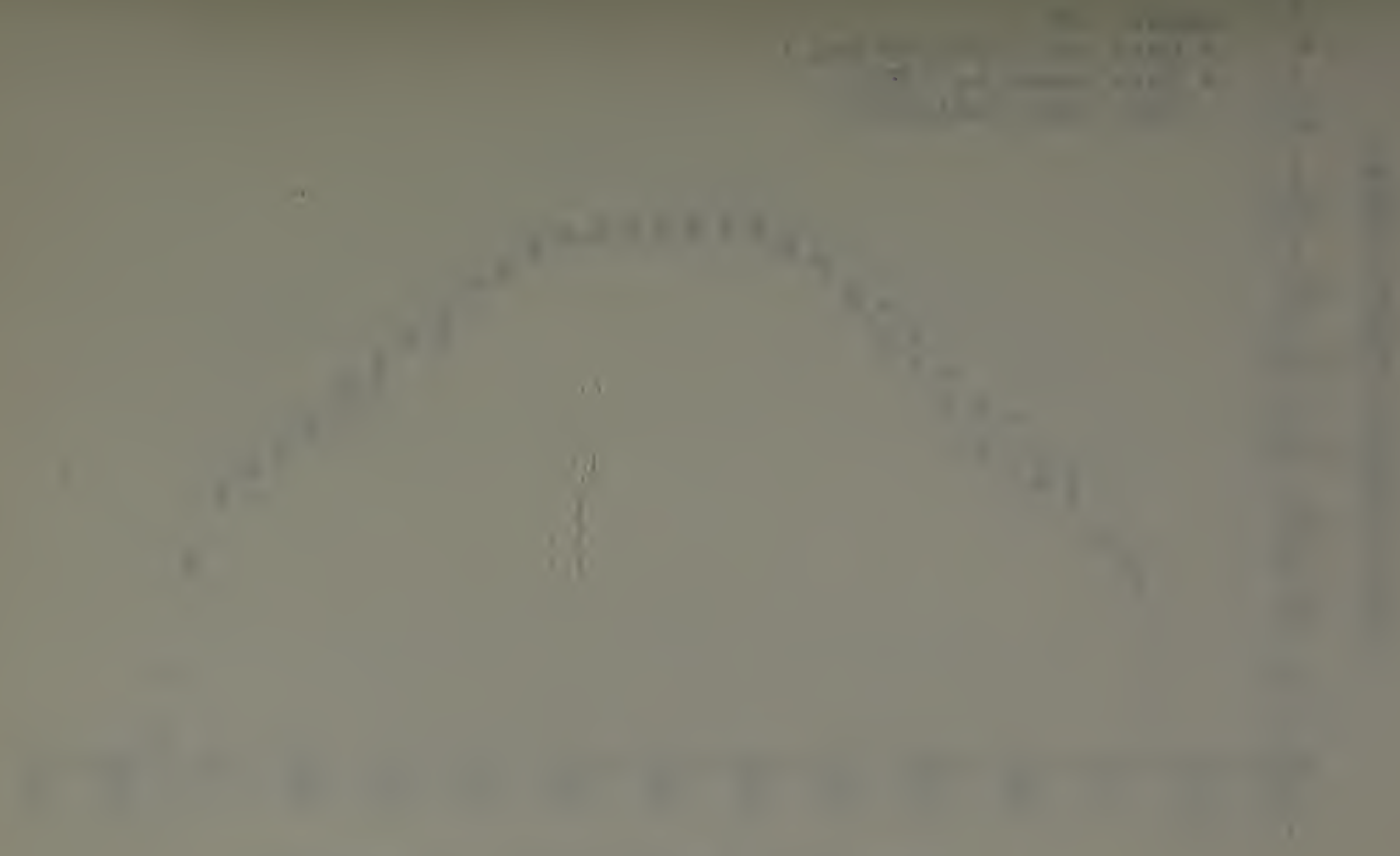

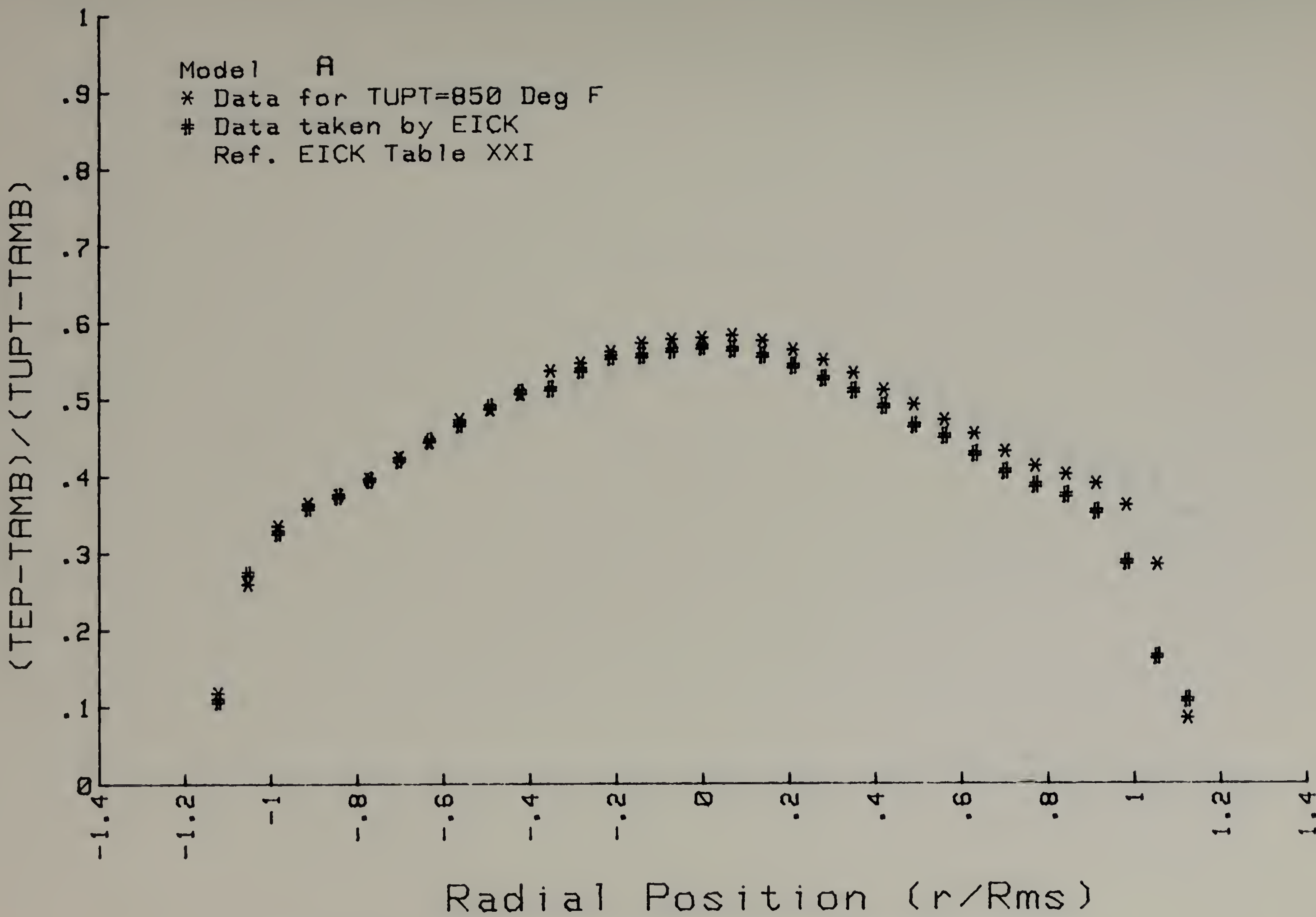

Figure 64. Exit Plane Coefficients, Model A (850^{o} F)

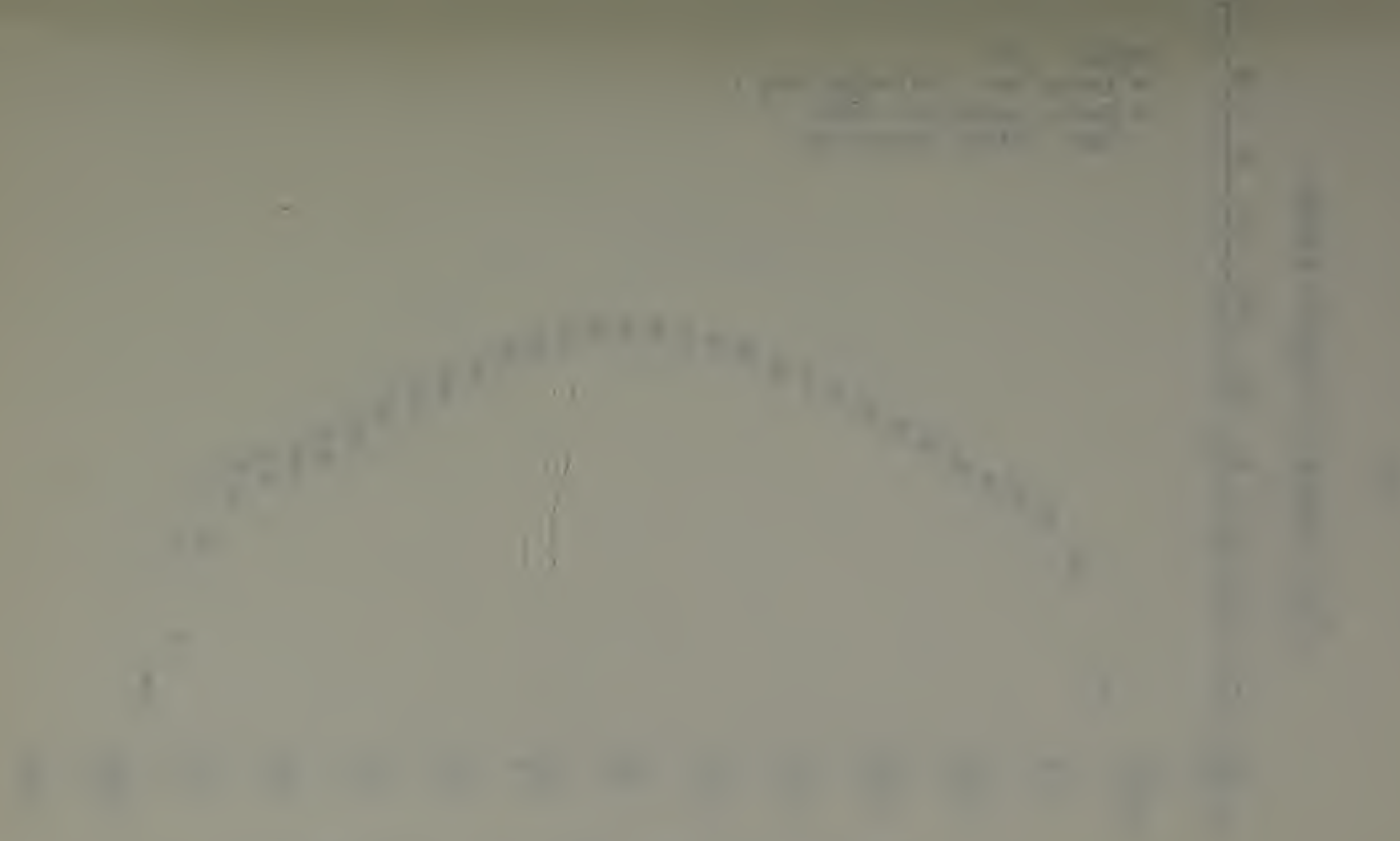

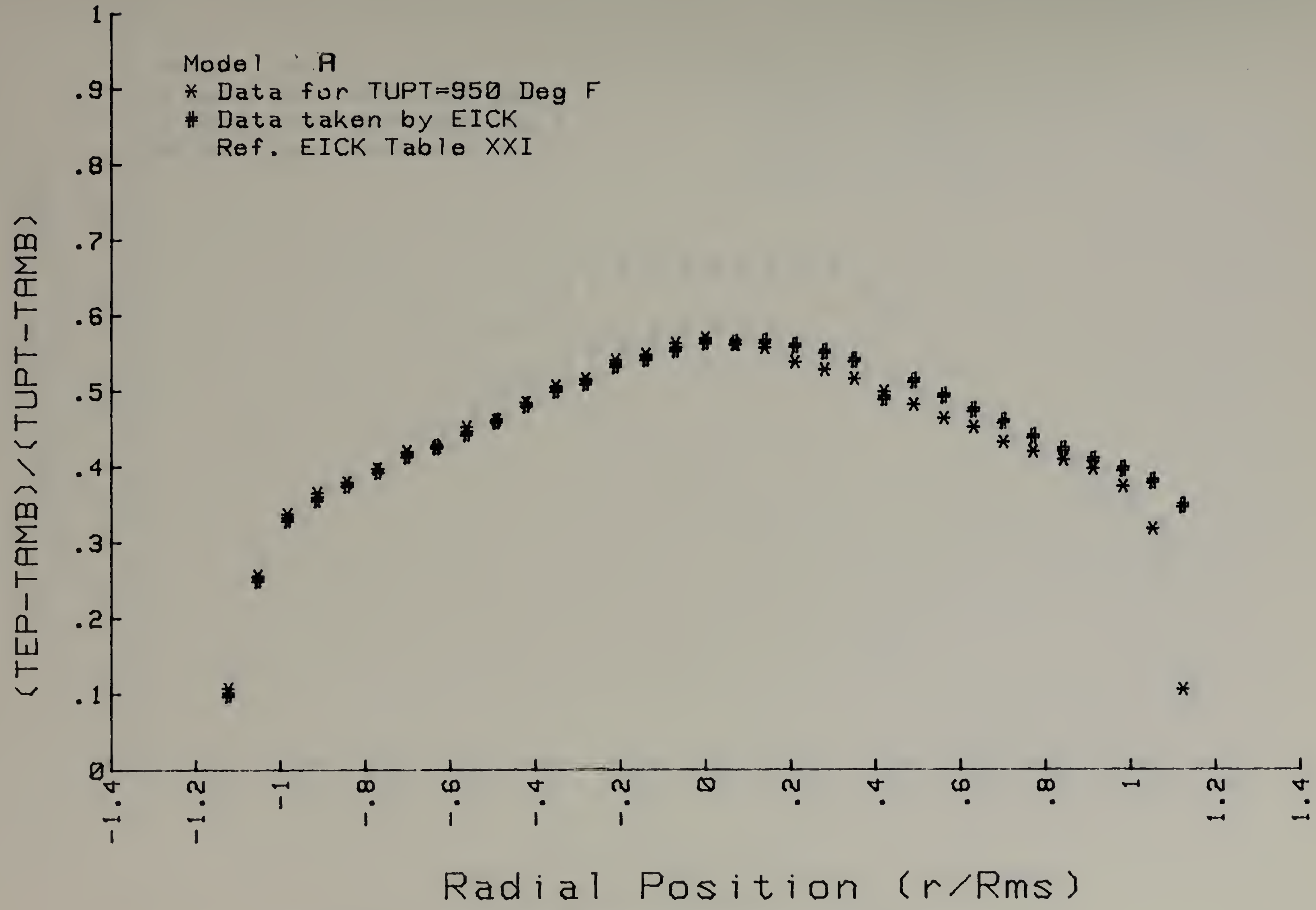

Figure 65. Exit Plane Coefficients, Model A (950^{o} F)

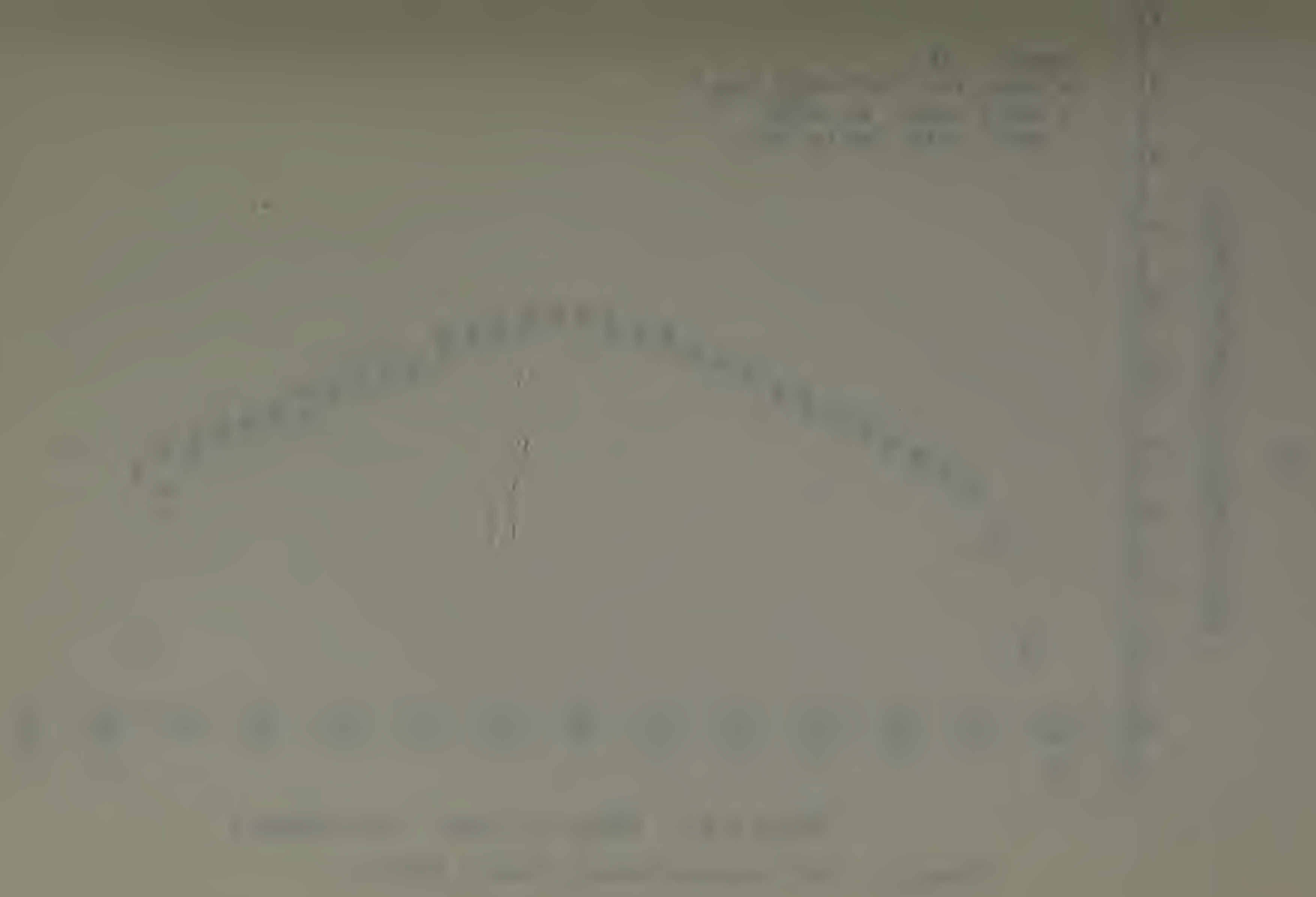

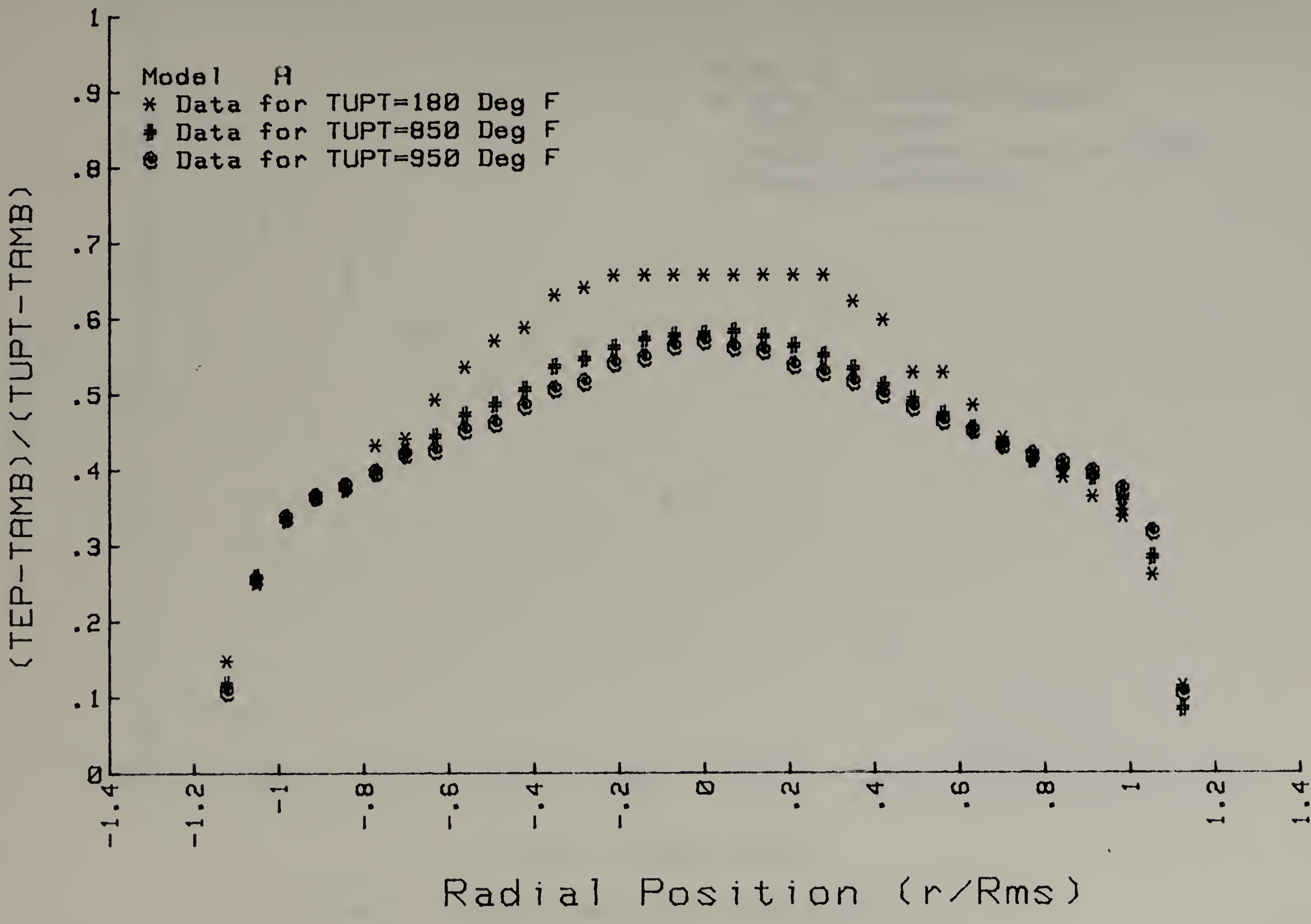

Figure 66. Exit Plane Coefficients Comparison, Model A

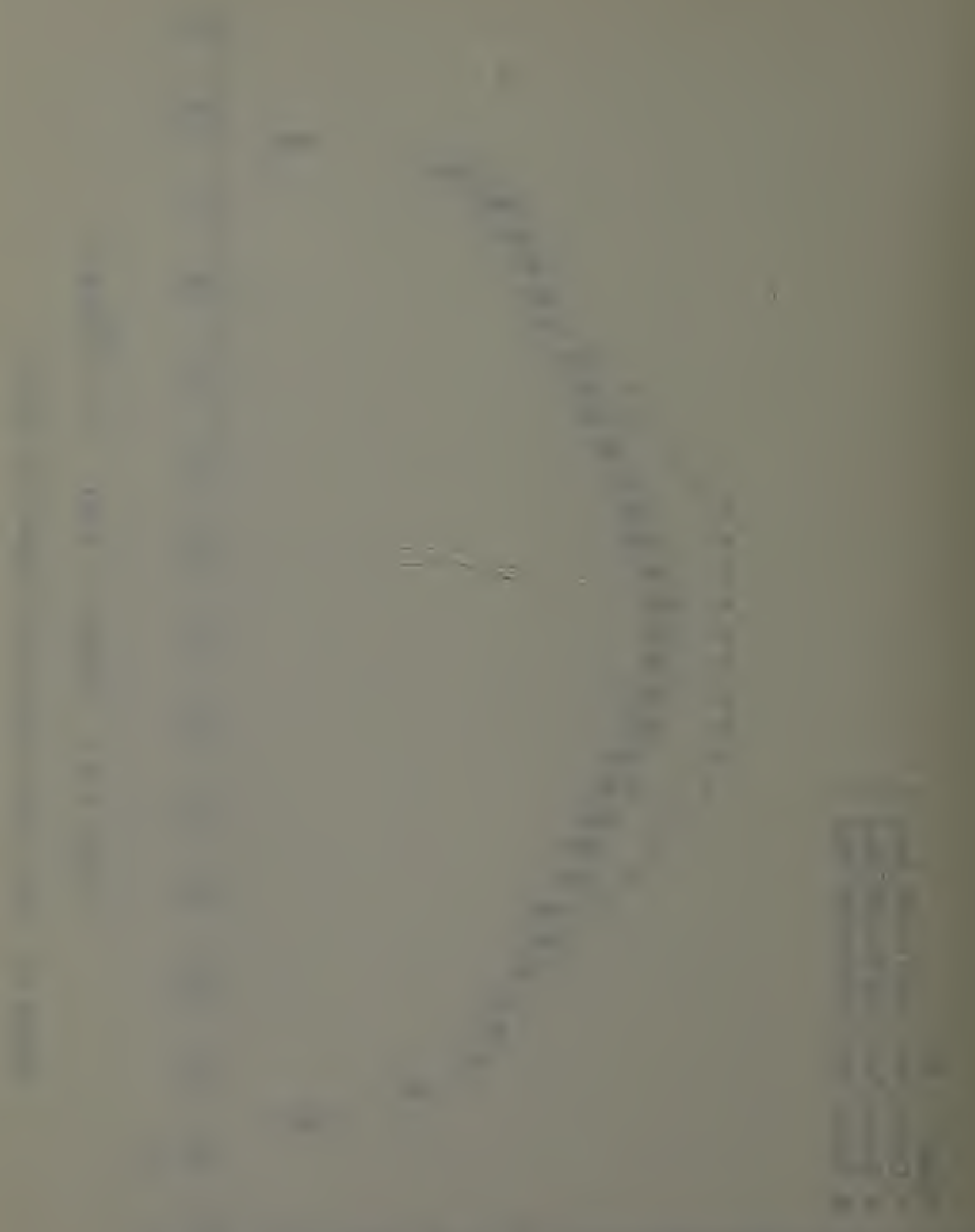

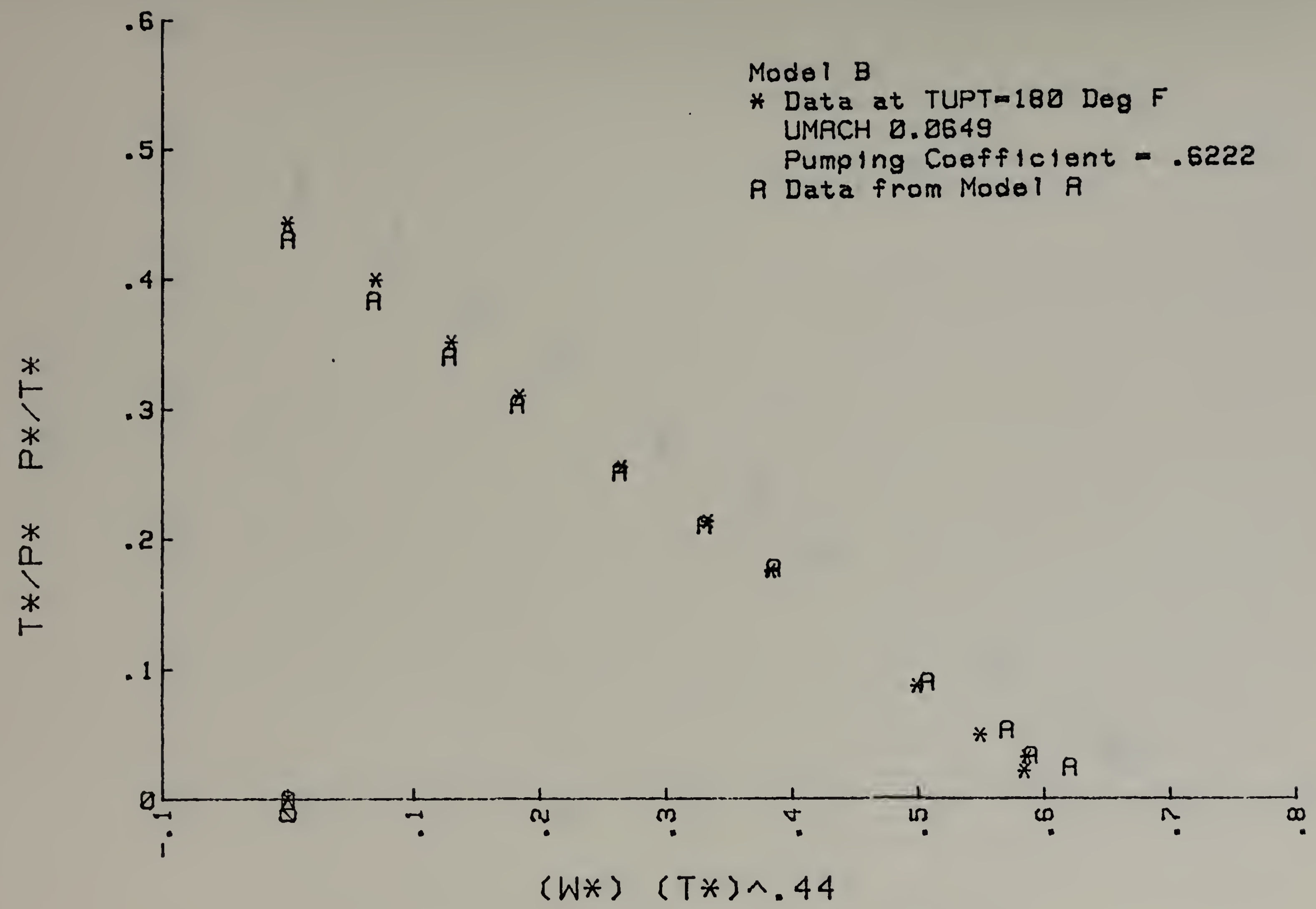

Figure 67. Pumping Coefficient, Model B (180^{o} F)

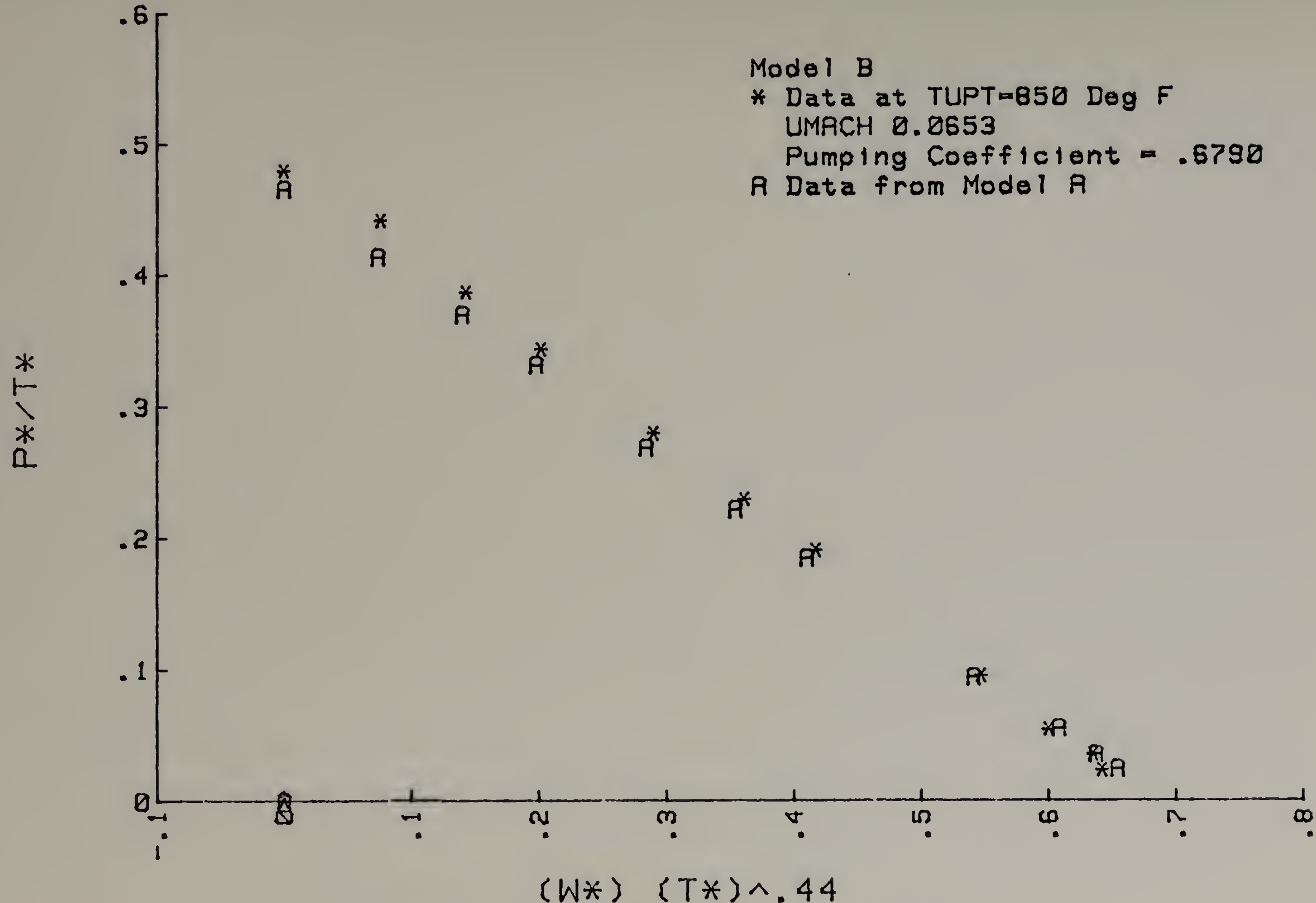

Figure 68. Pumping Coefficient, Model B (850^{o} F)

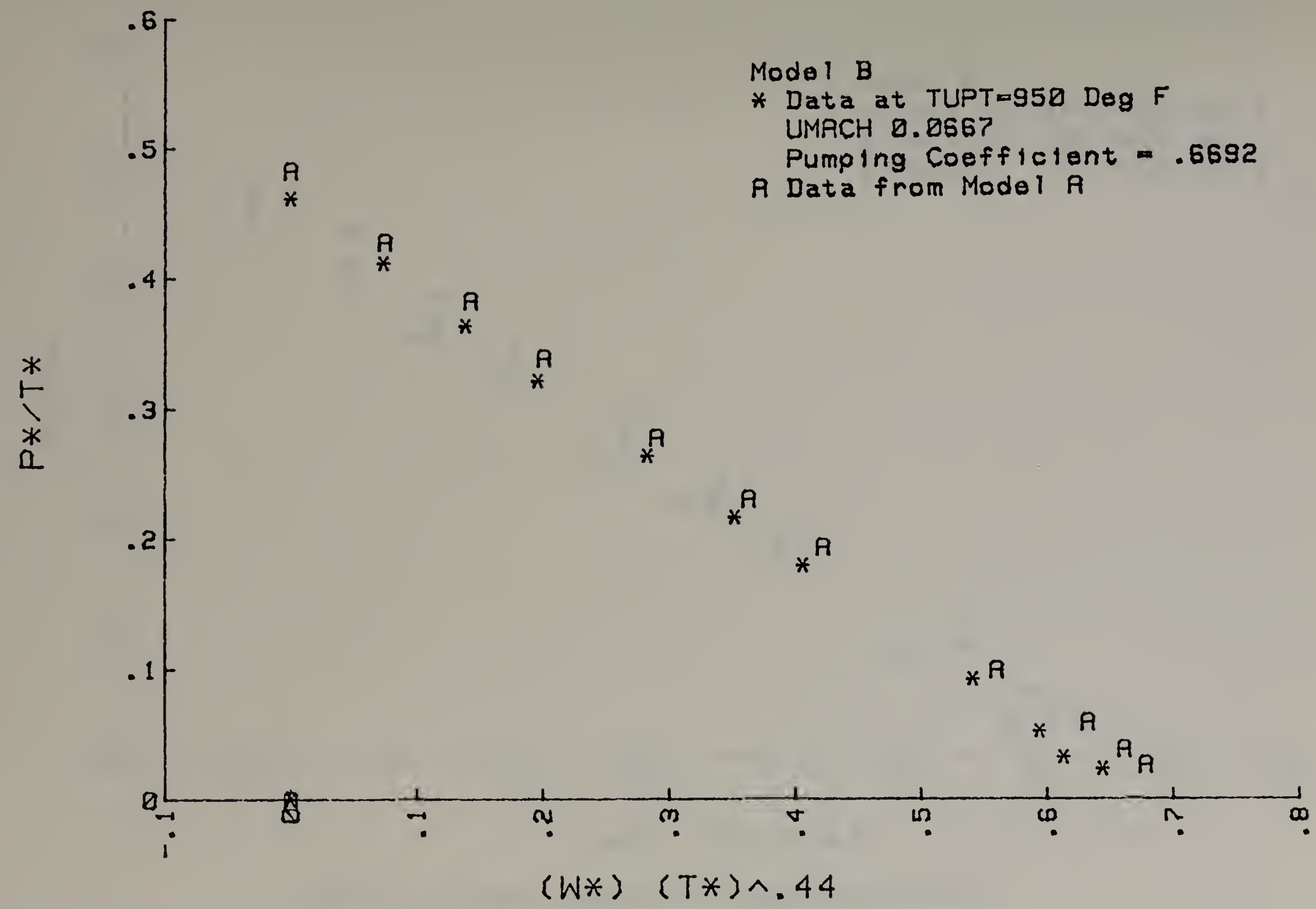

Figure 69. Pumping Coefficient, Model B (950^o F)

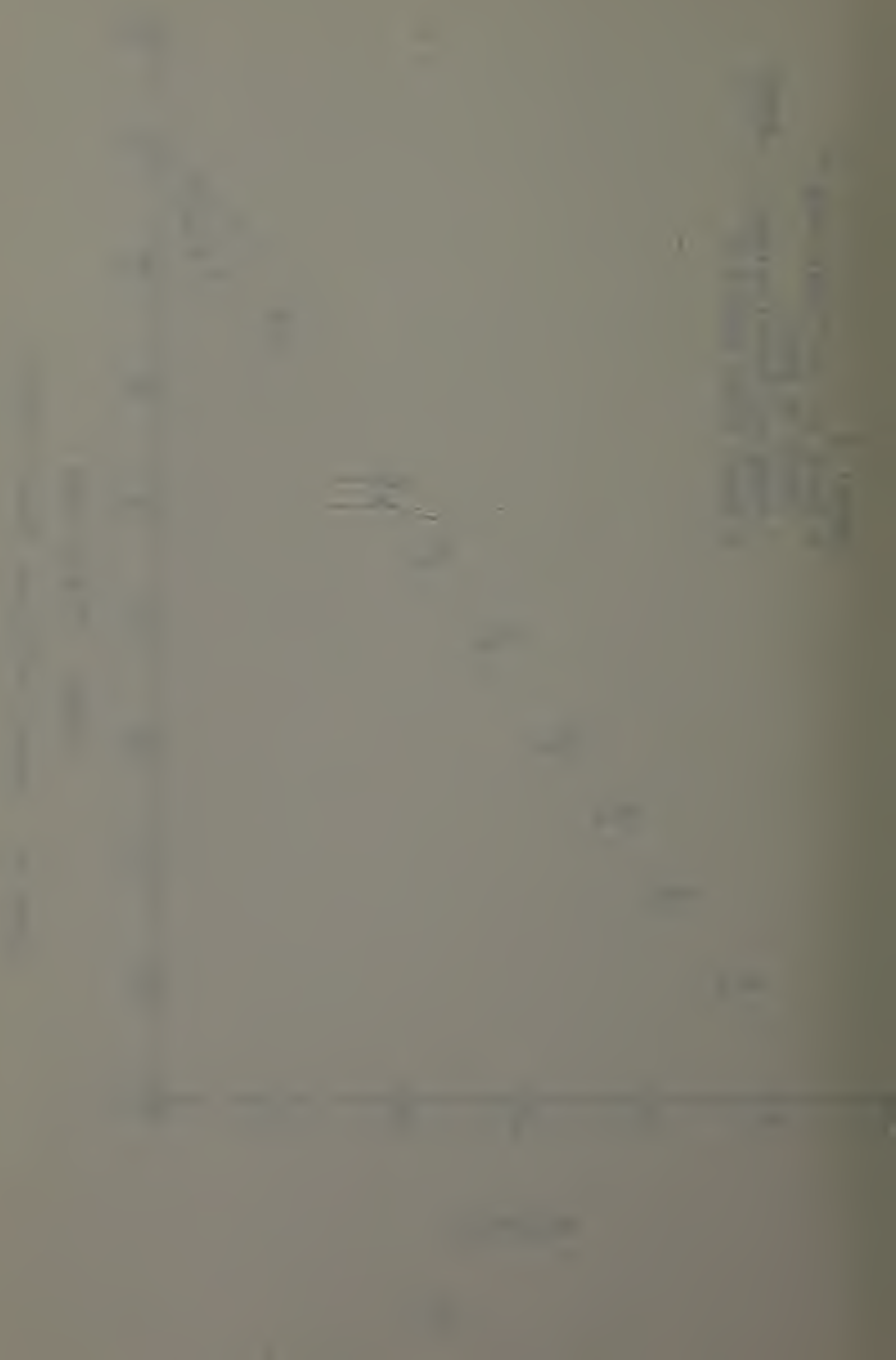

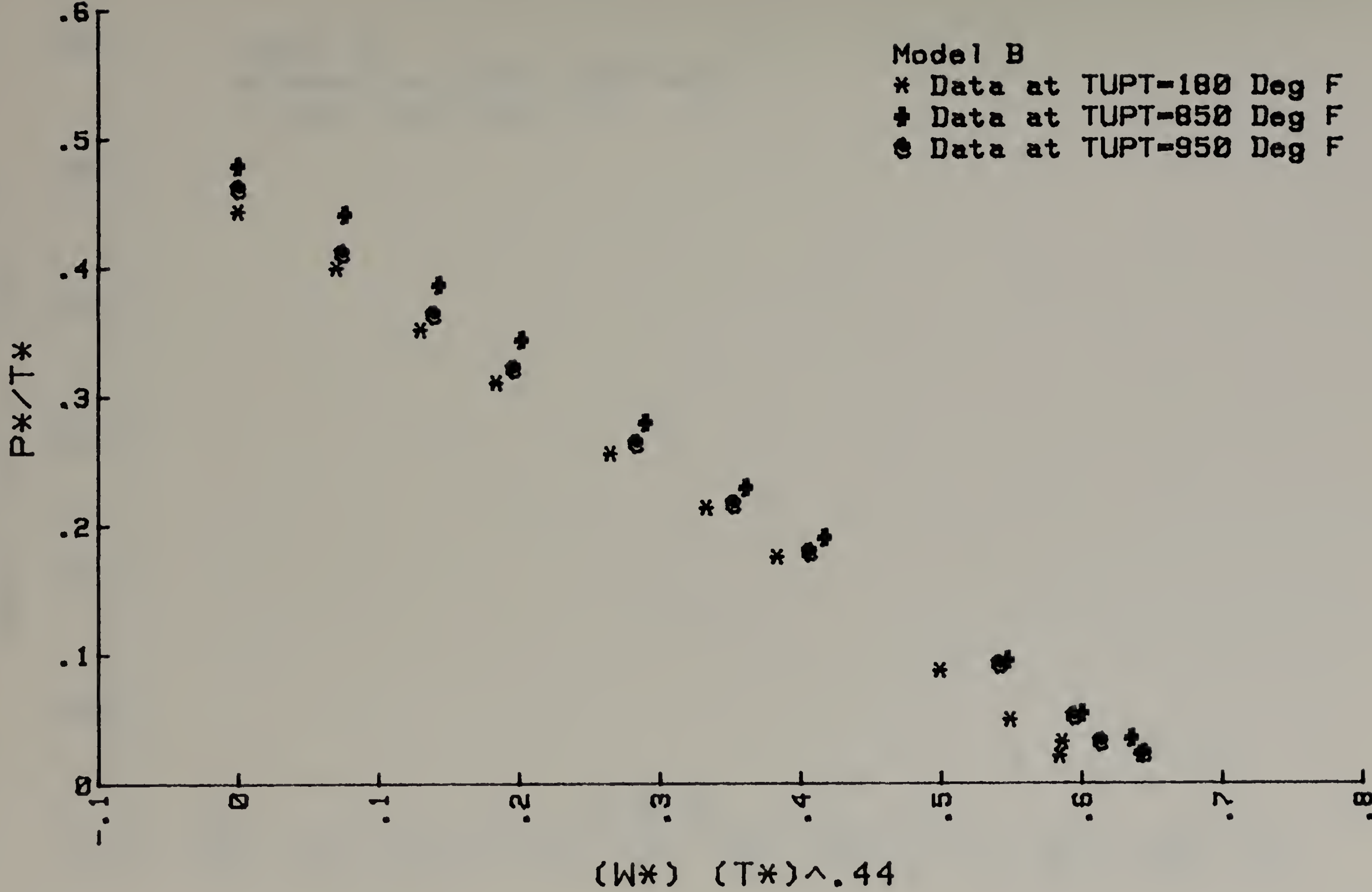

Figure 70. Pumping Coefficient Comparison, Model B

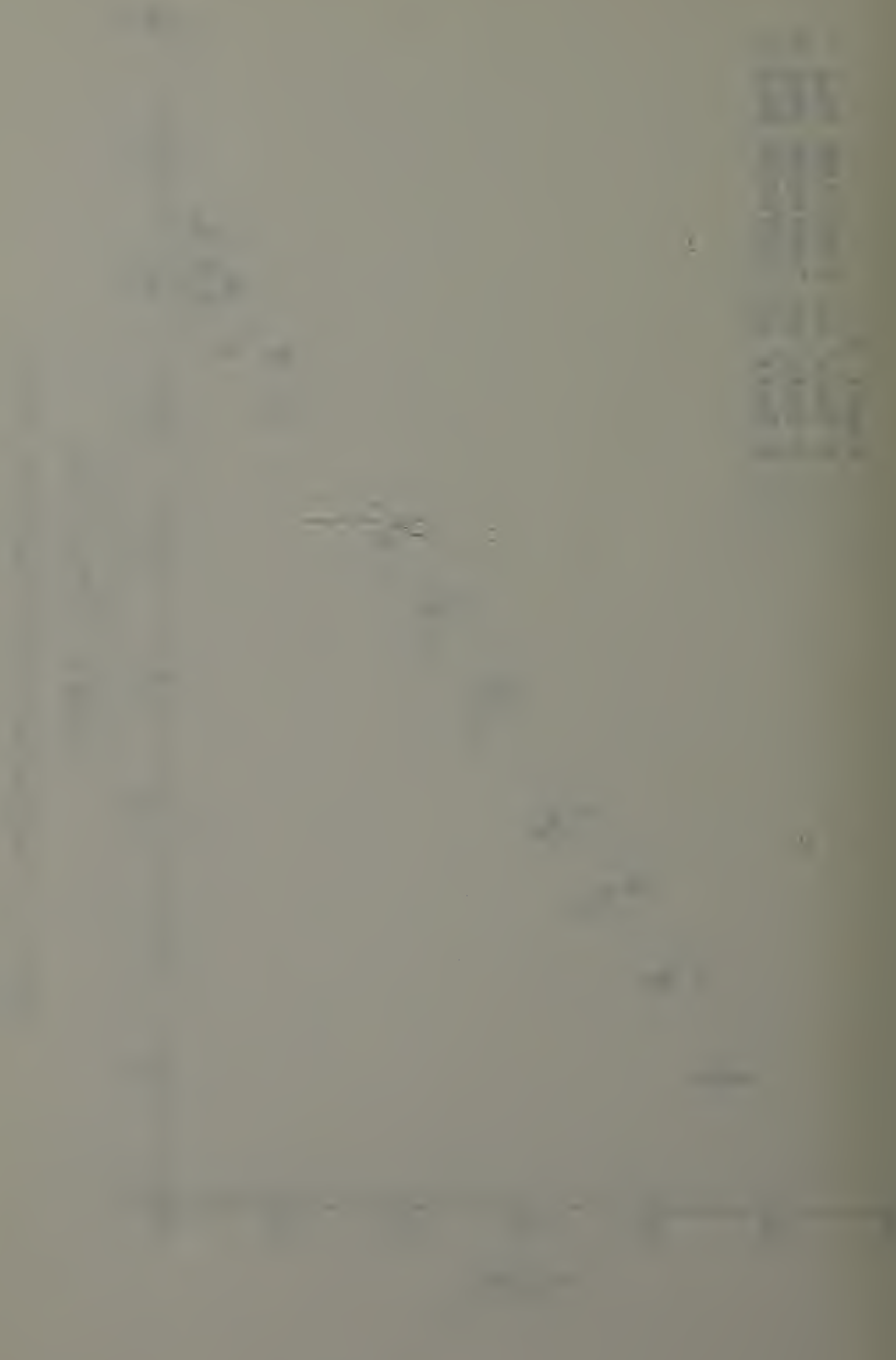

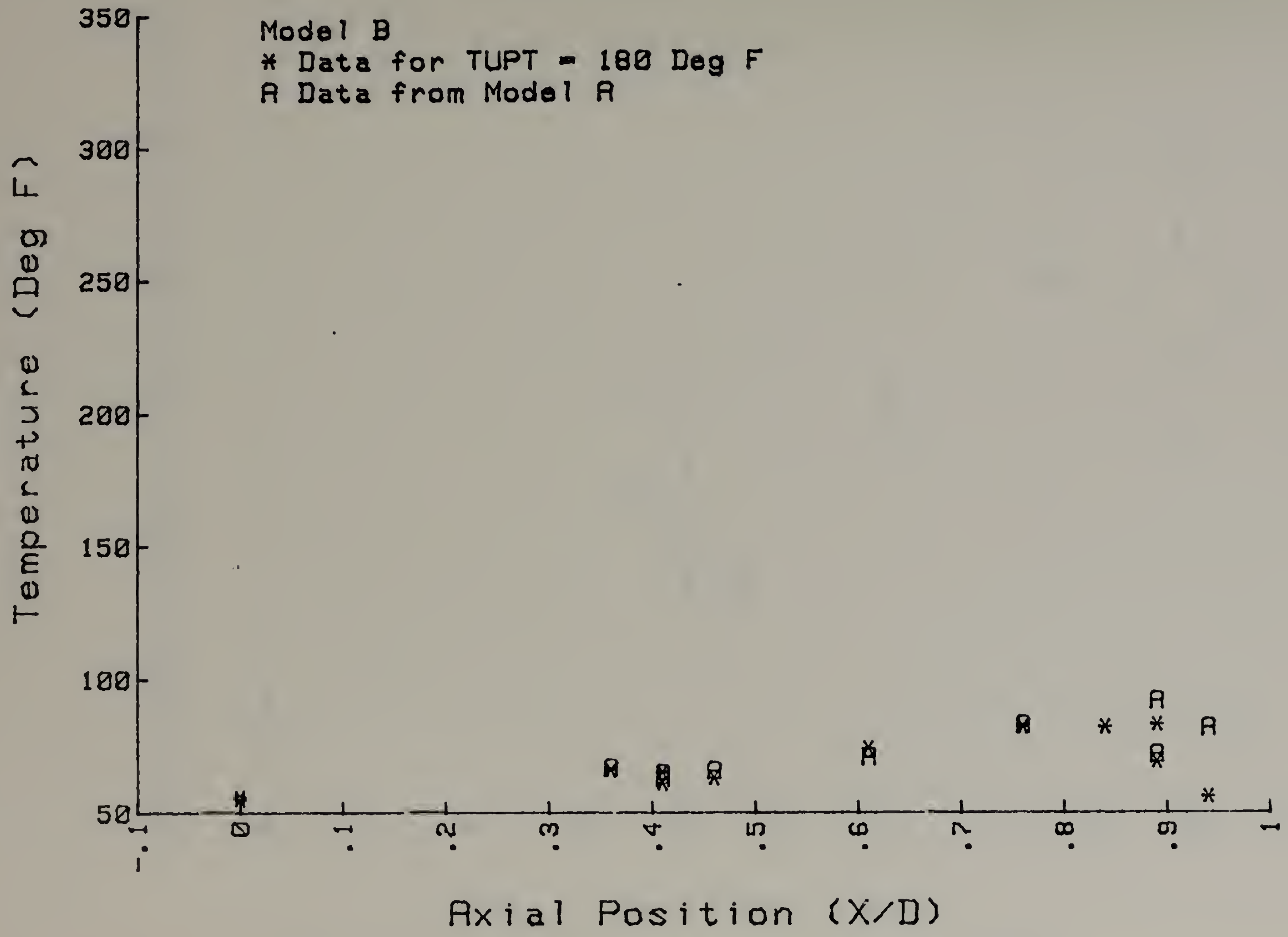

Figure 71. Mixing Stack Temperatures, Model B (180^{o} F)

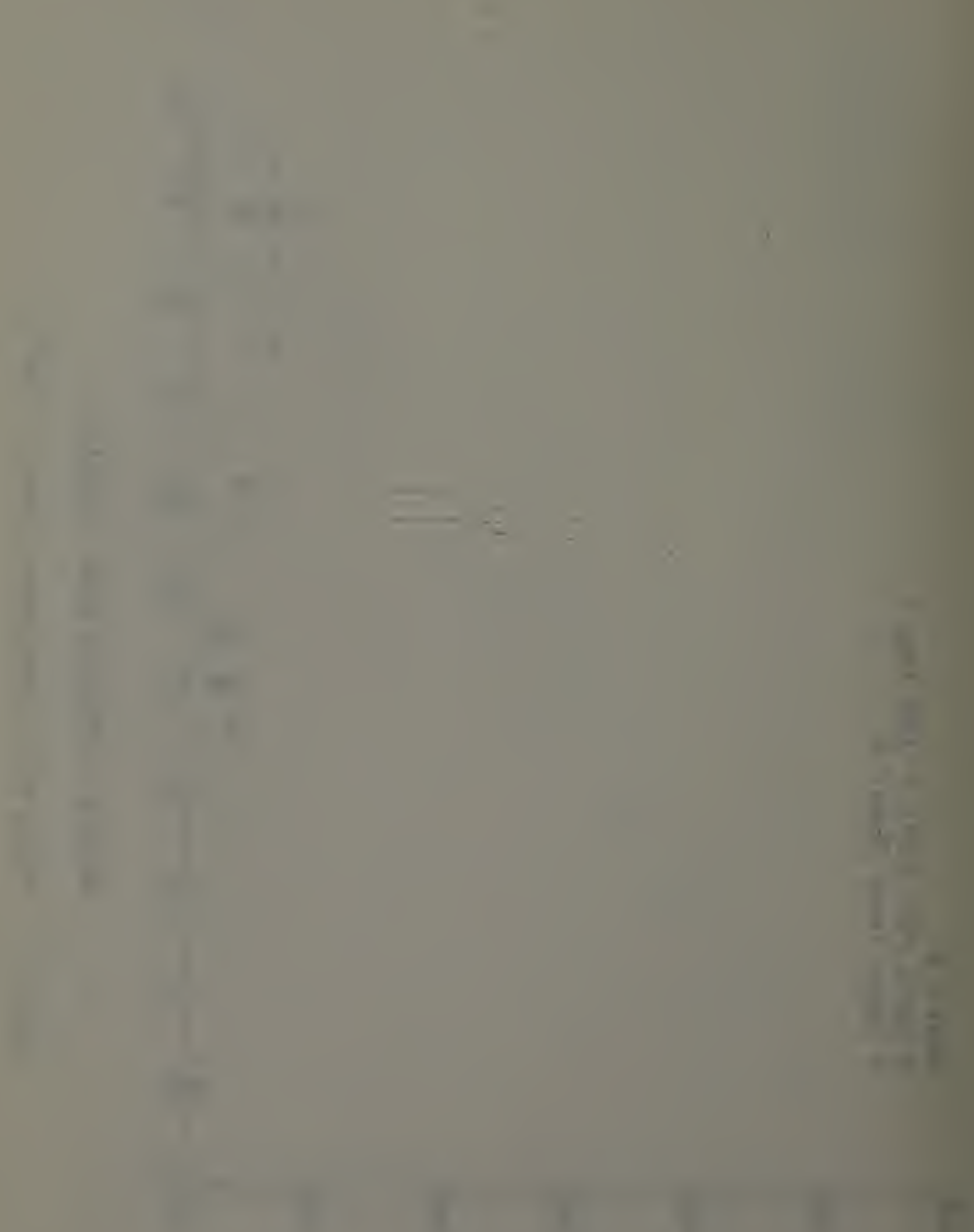

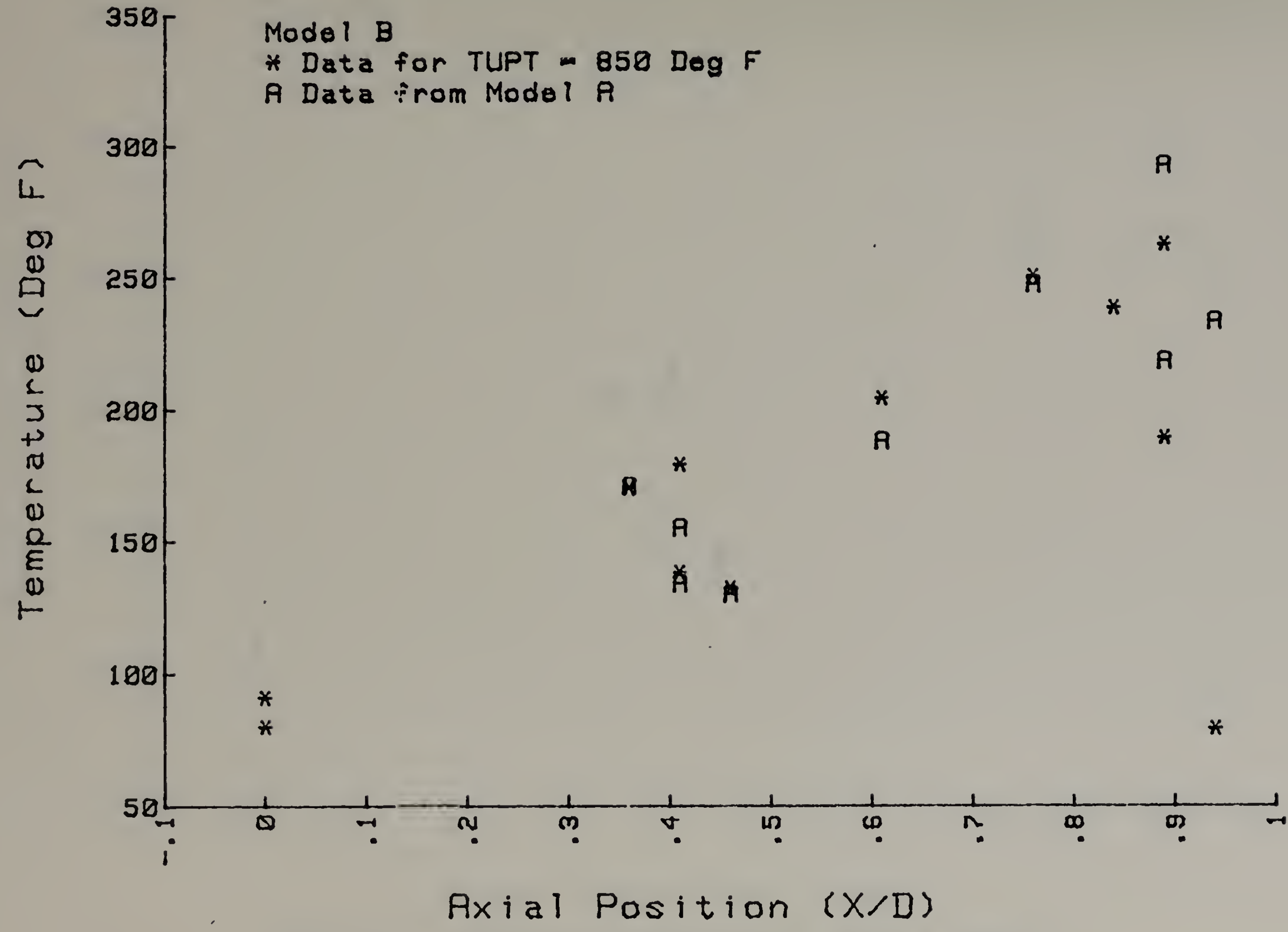

Figure 72. Mixing Stack Temperatures, Model B (850° F)

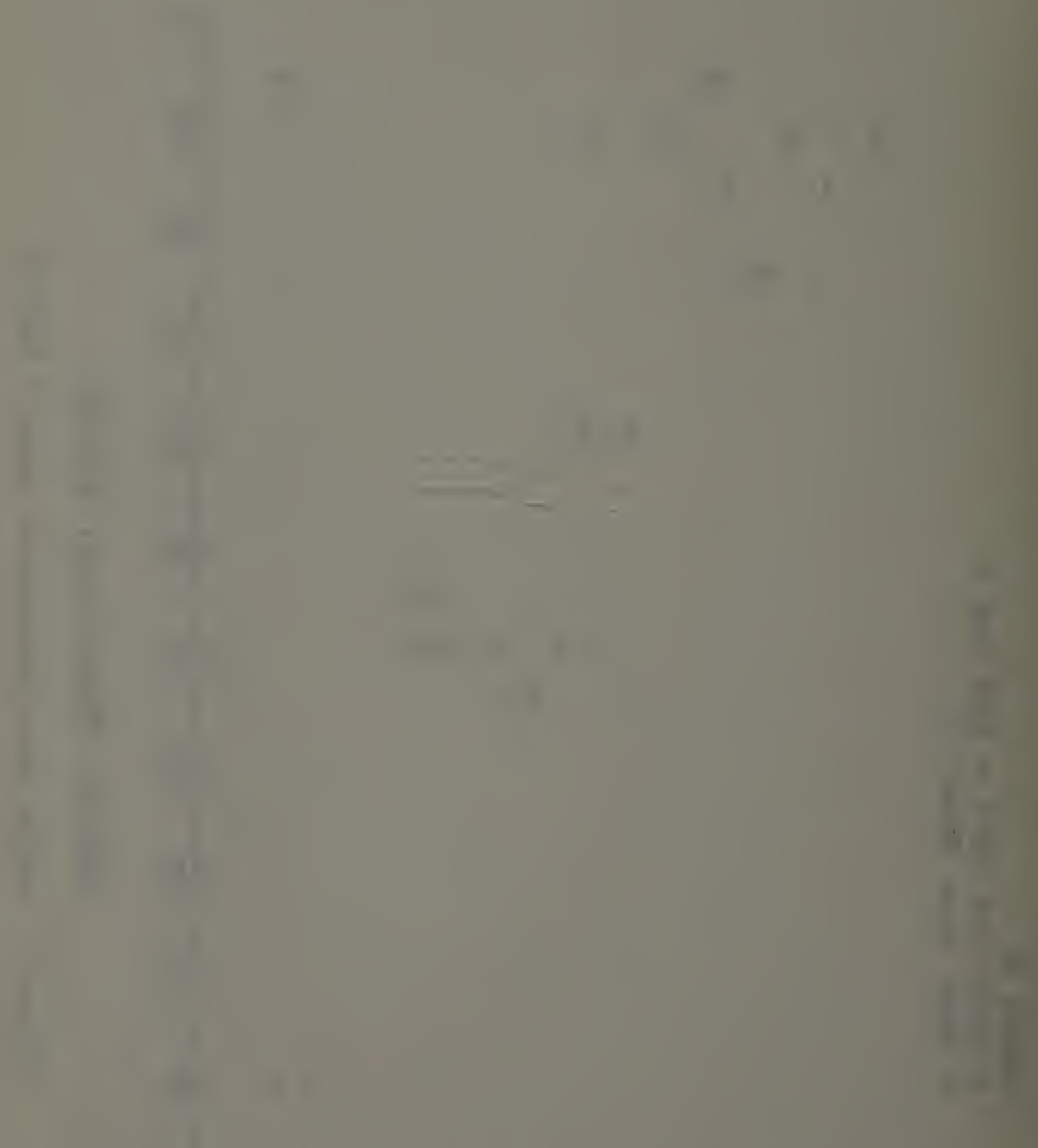

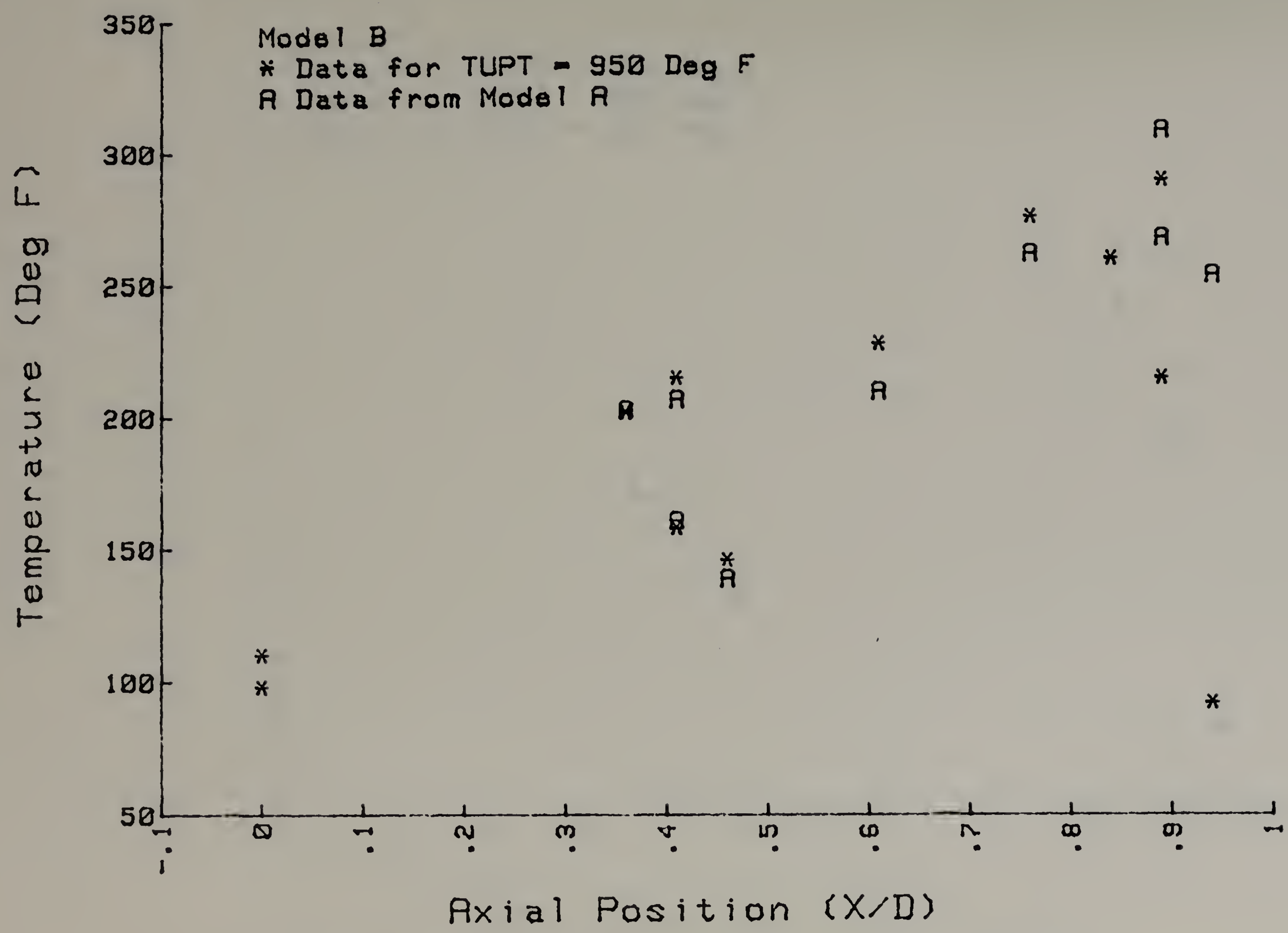

Figure 73. Mixing Stack Temperatures, Model B (950^{o} F)

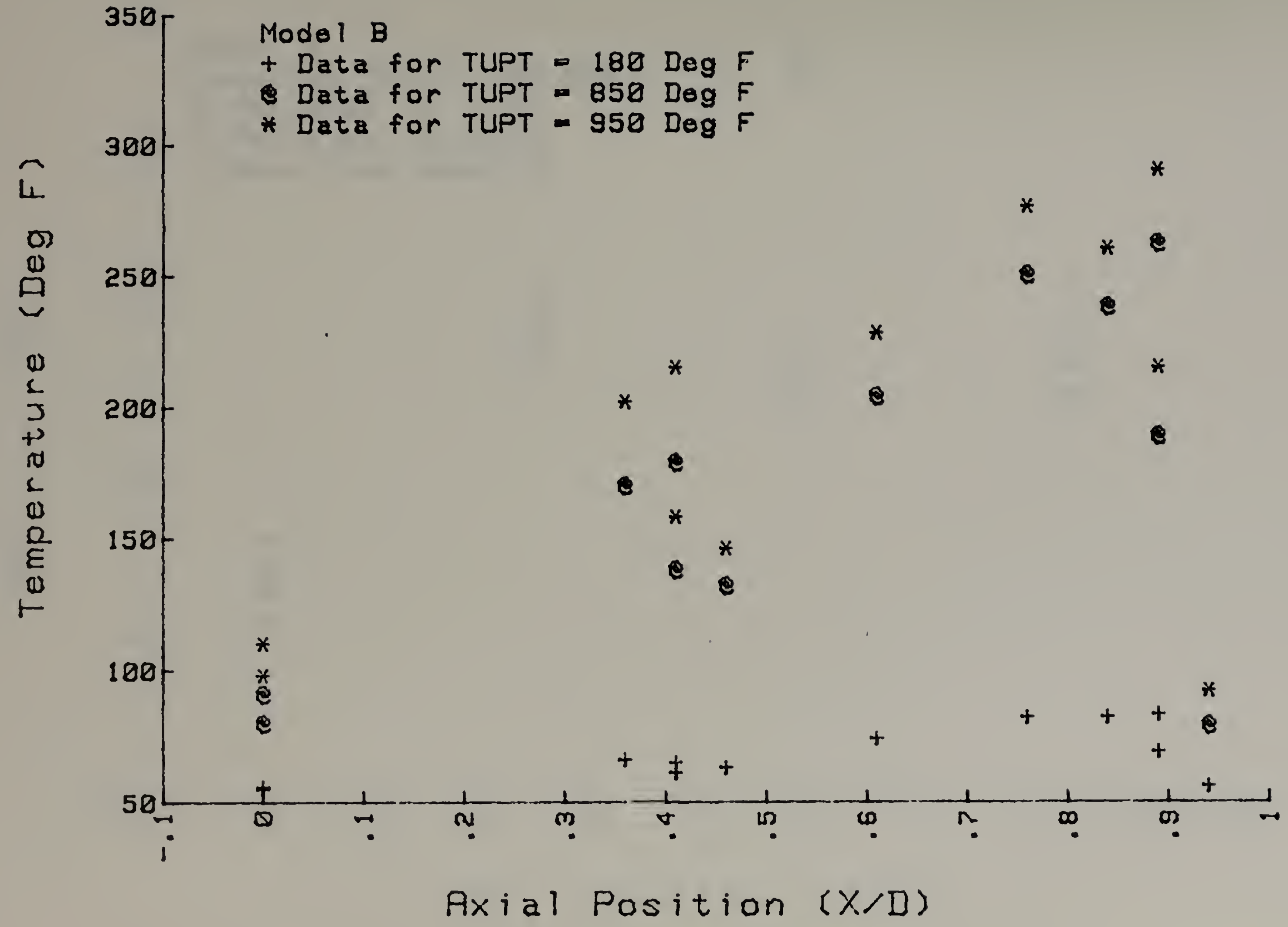

Figure 74. Mixing Stack Temperatures Comparison, Model B

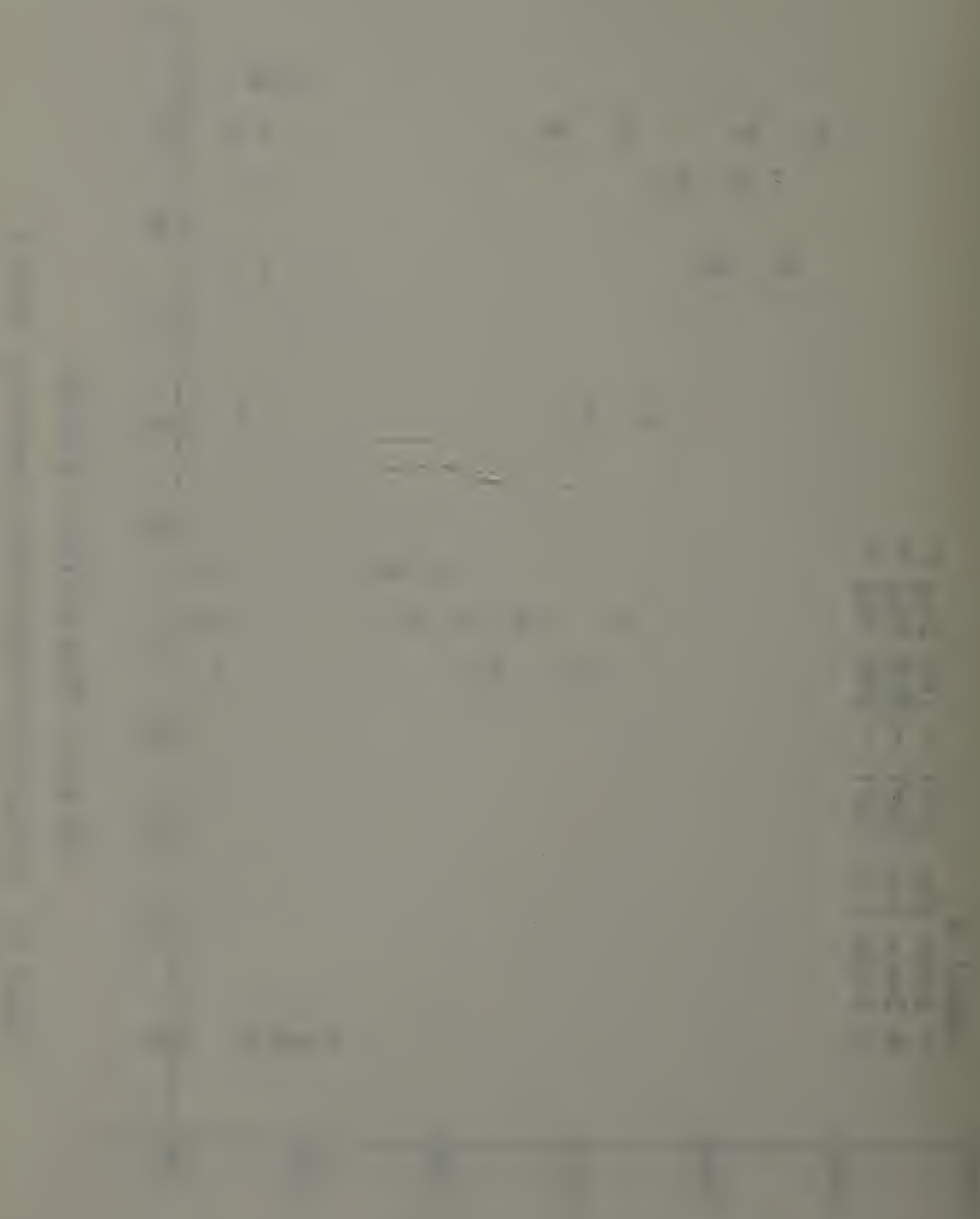

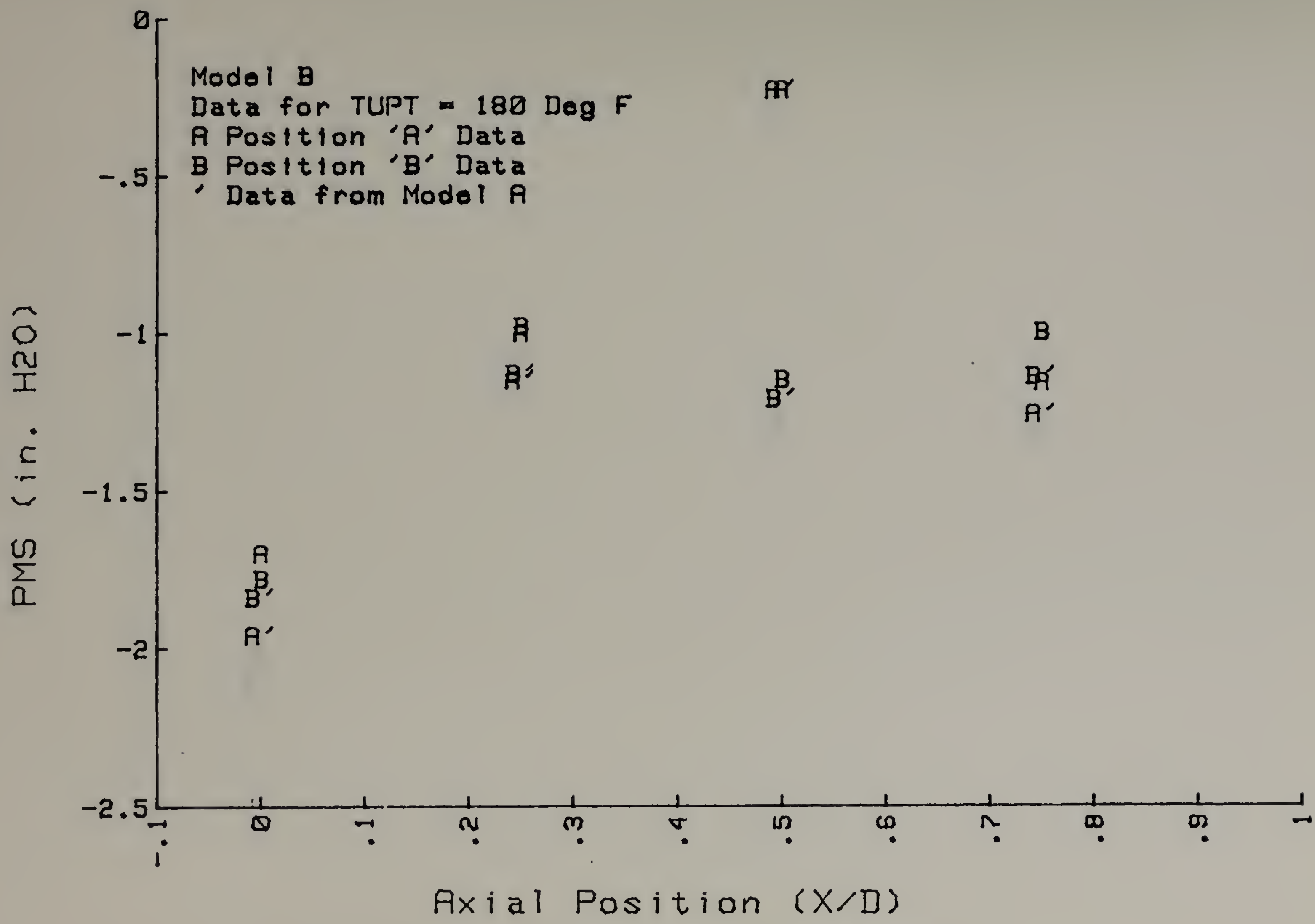

Figure 75. Mixing Stack Pressure, Model B (180^{o} F)

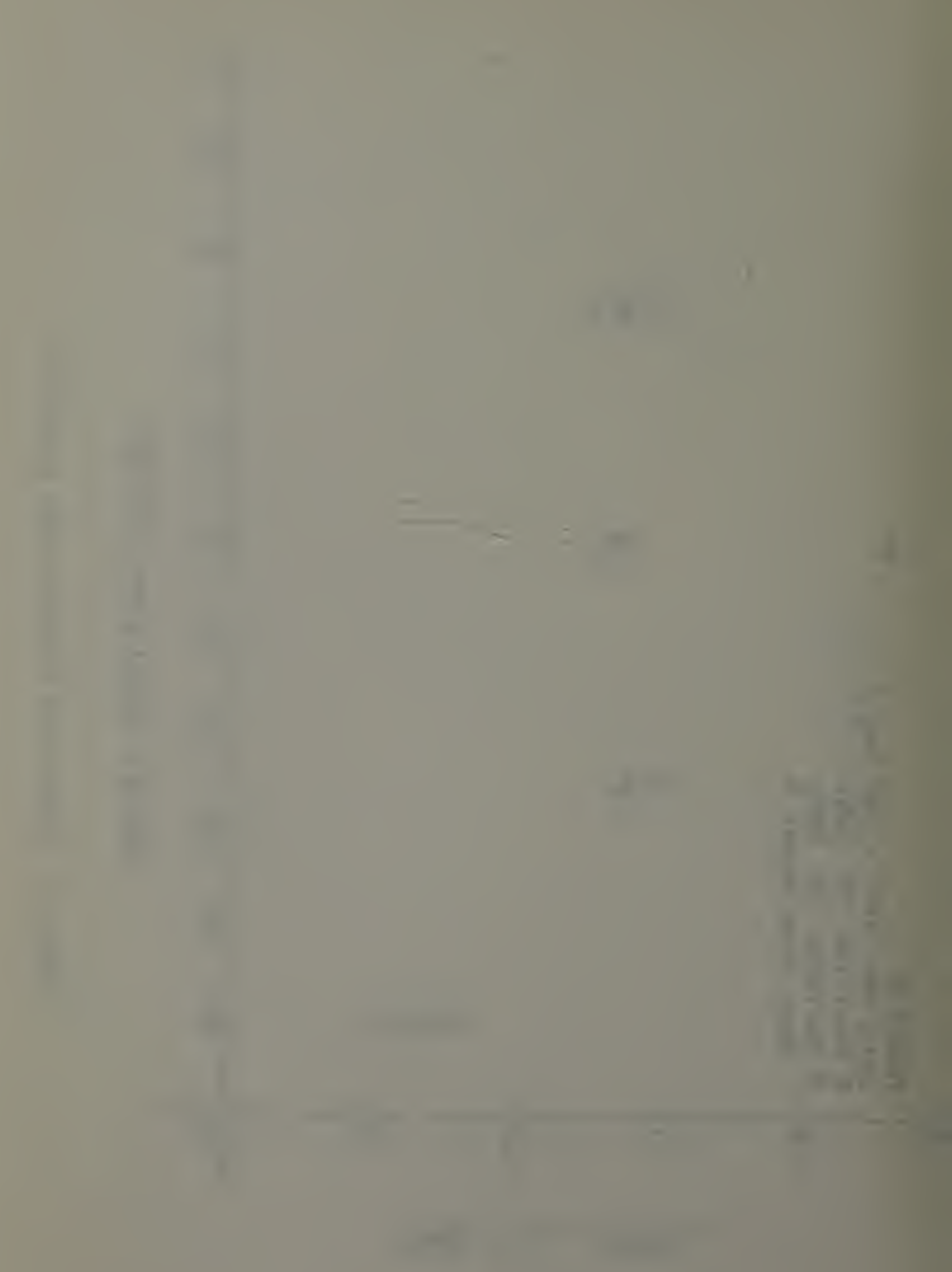

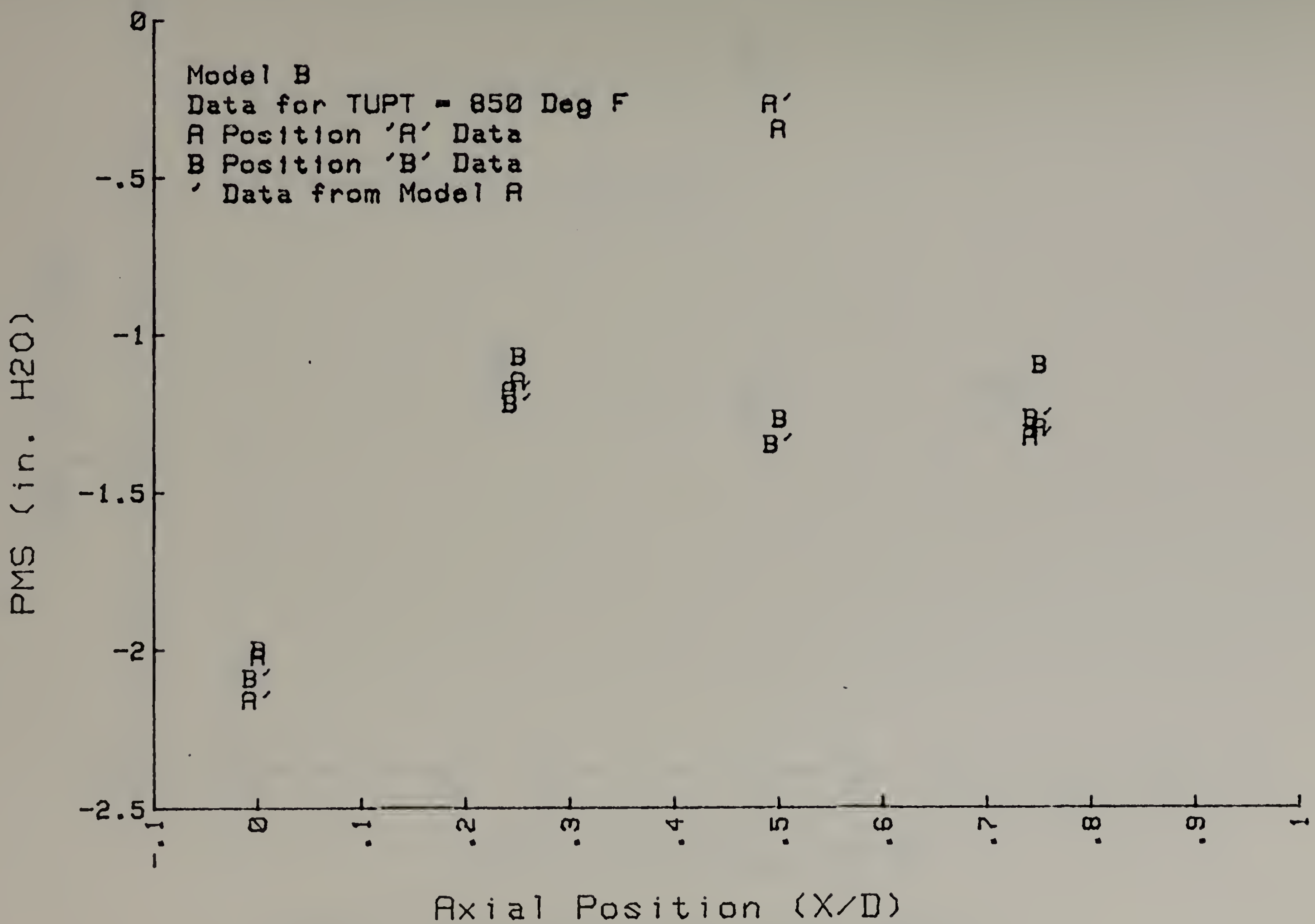

Figure 76. Mixing Stack Pressure, Model B (850^{o} F)

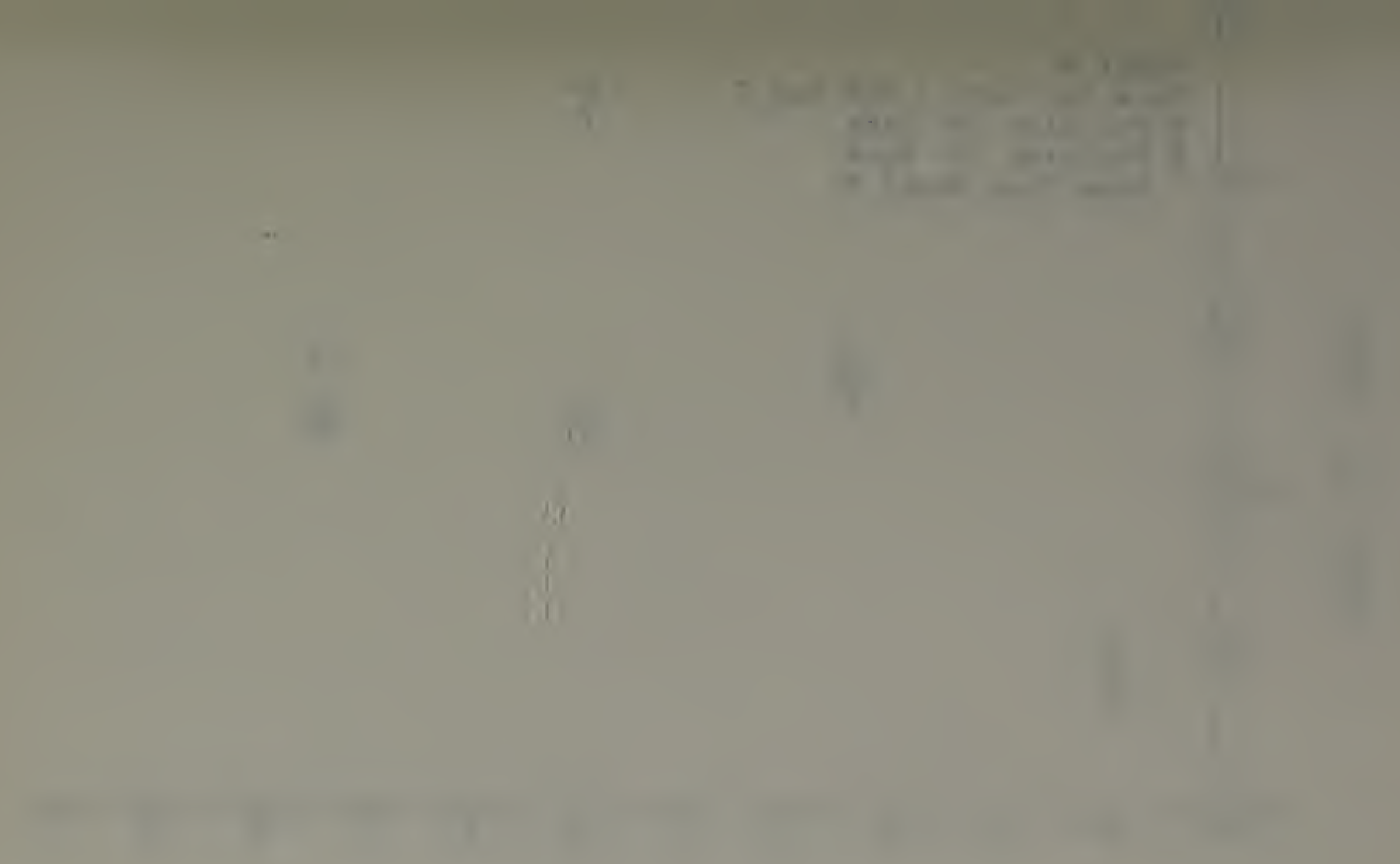

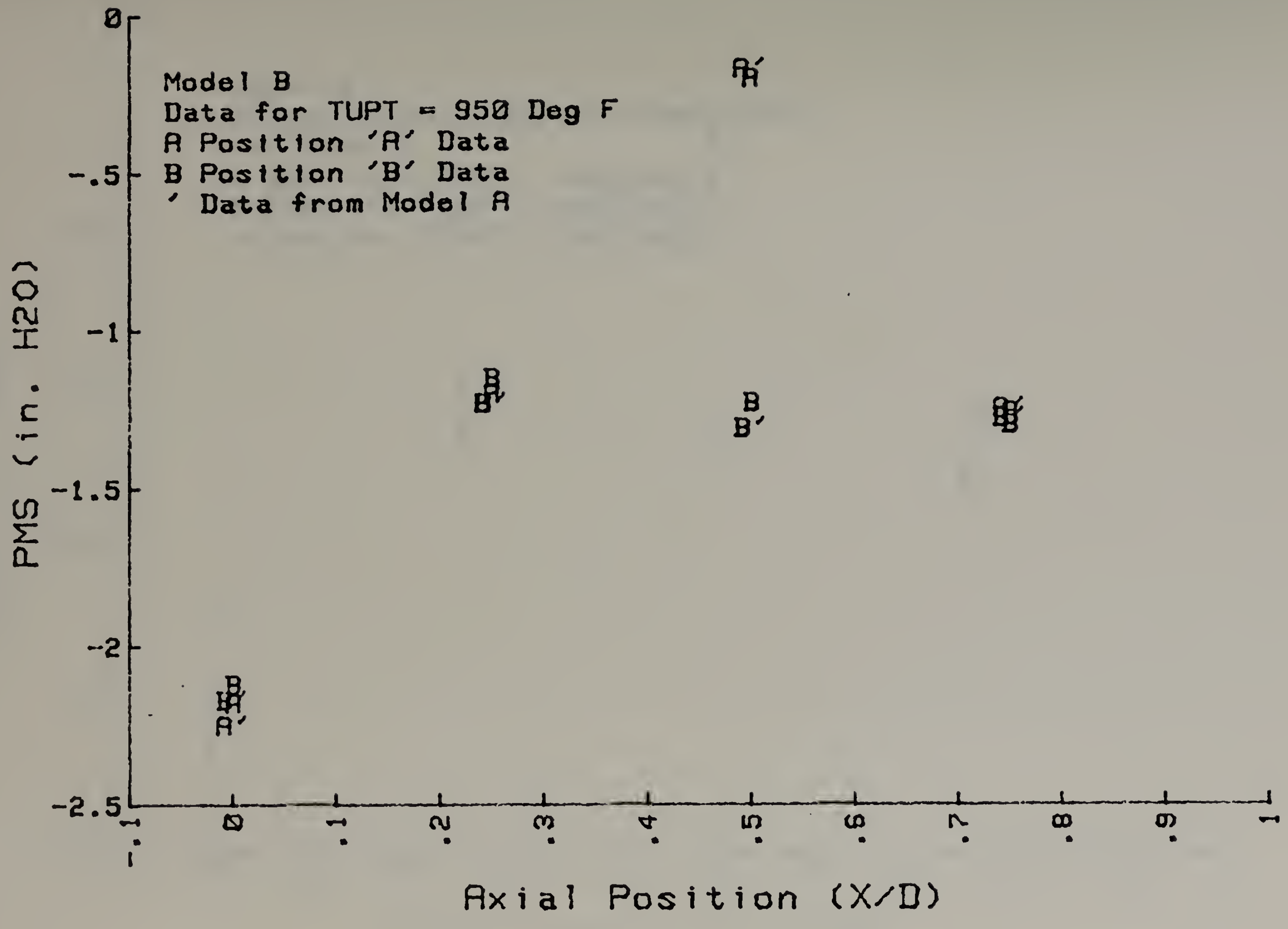

Figure 77. Mixing Stack Pressure, Model B (950^{o} F)

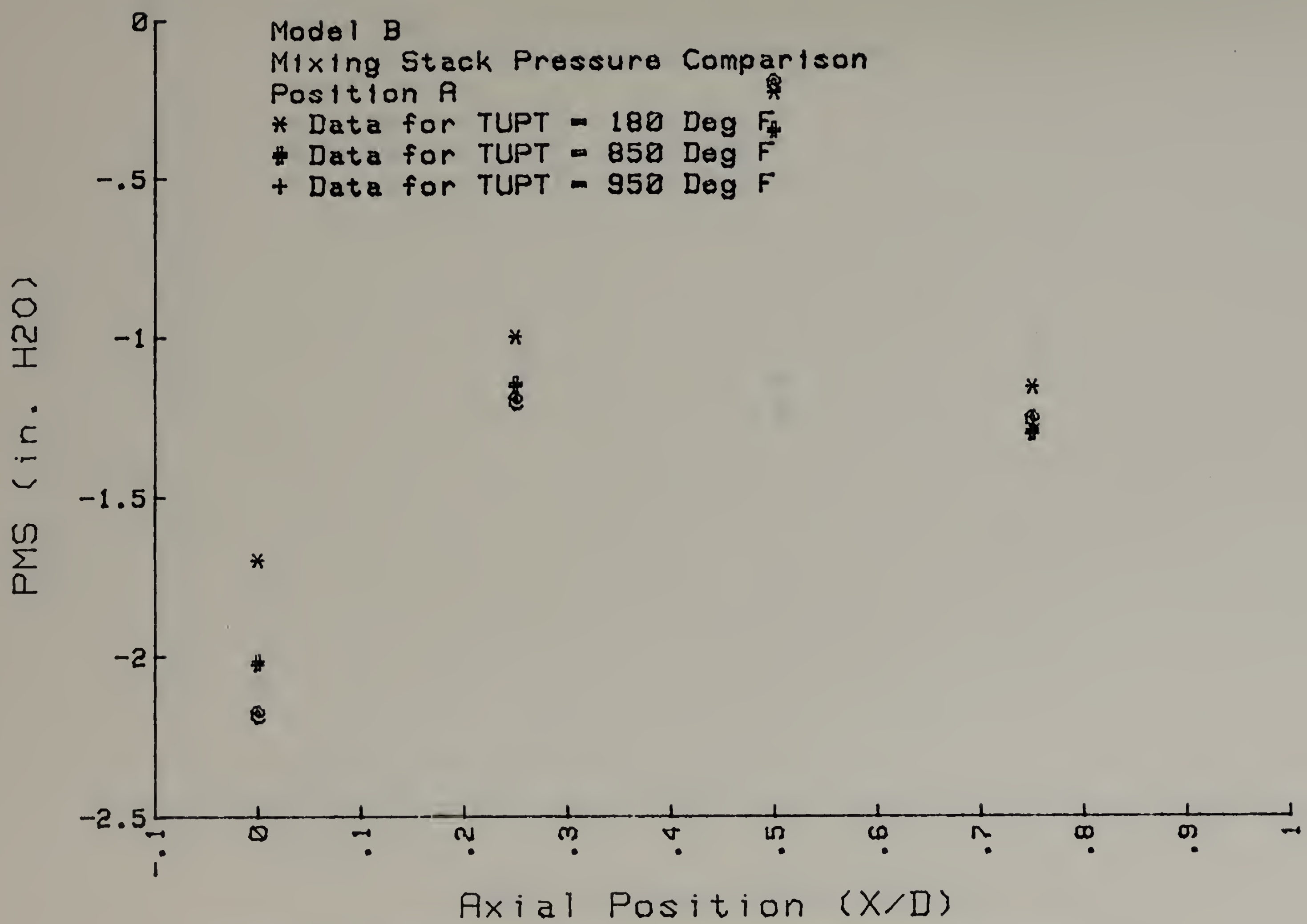

Figure 78. Mixing Stack Pressure Comparison, Model B (Position A)

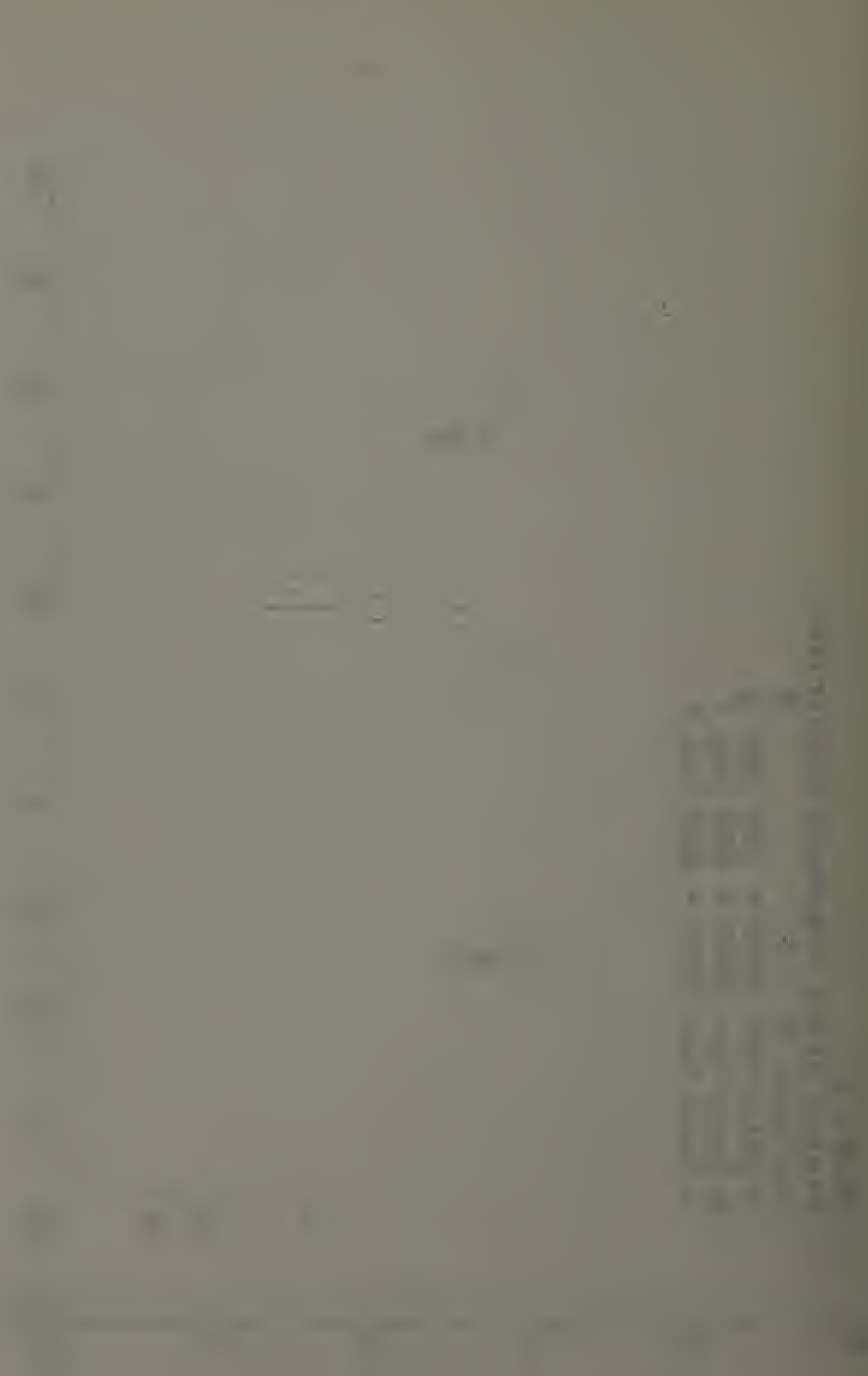

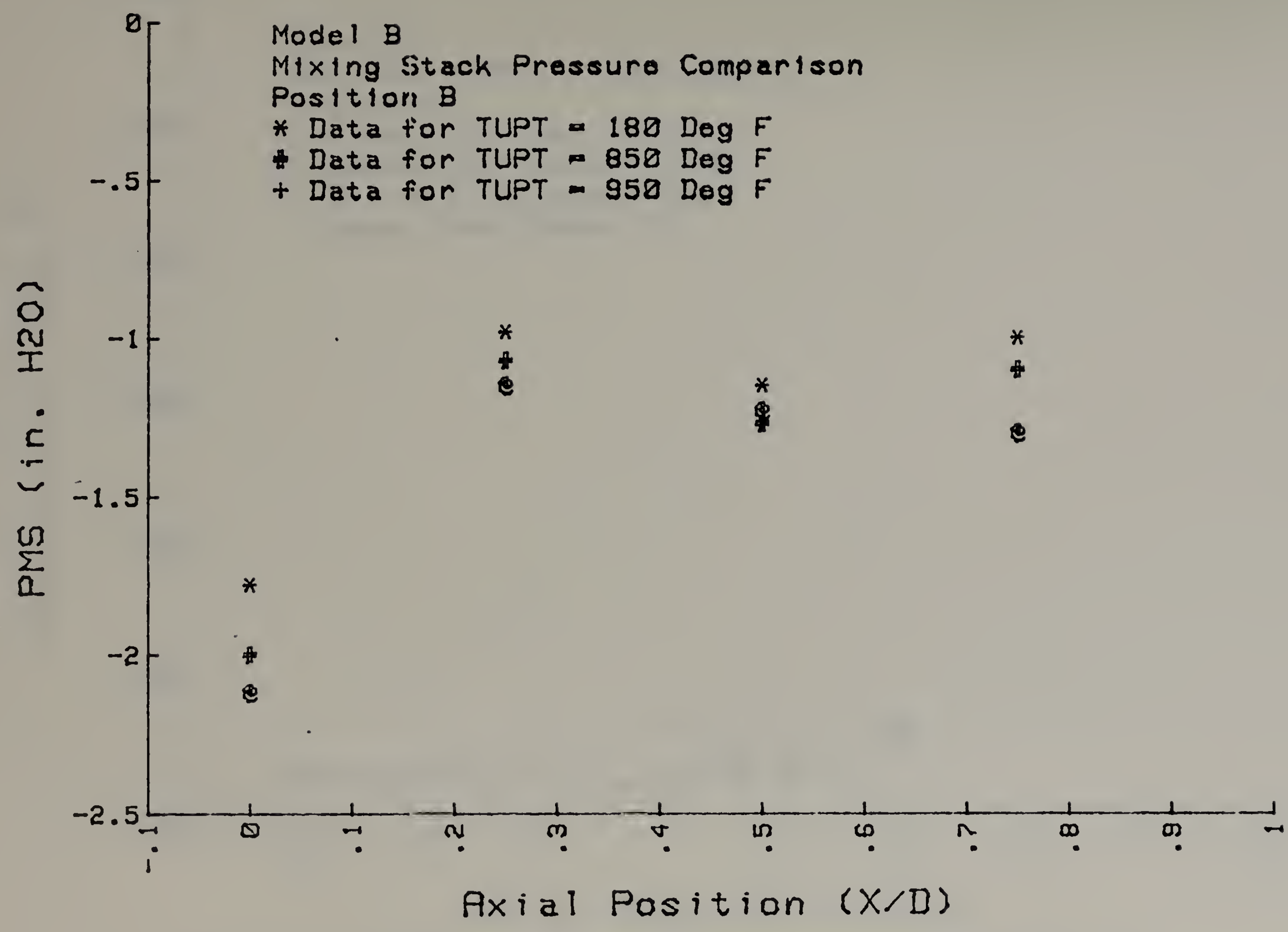

Figure 79. Mixing Stack Pressure Comparison, Model B (Position B)

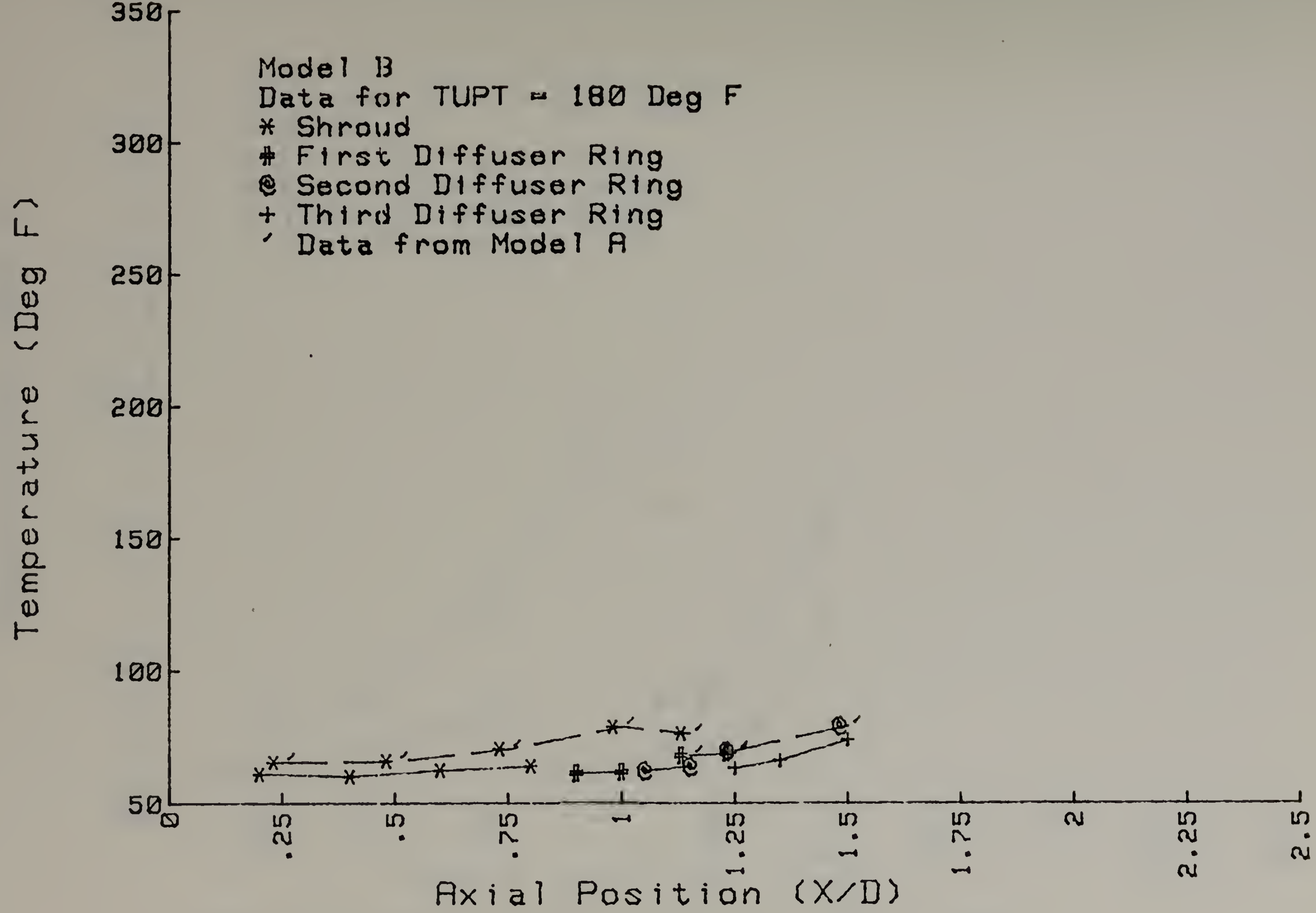

Figure 80. Shroud and Diffuser Temperatures, Model B (180^{o} F)

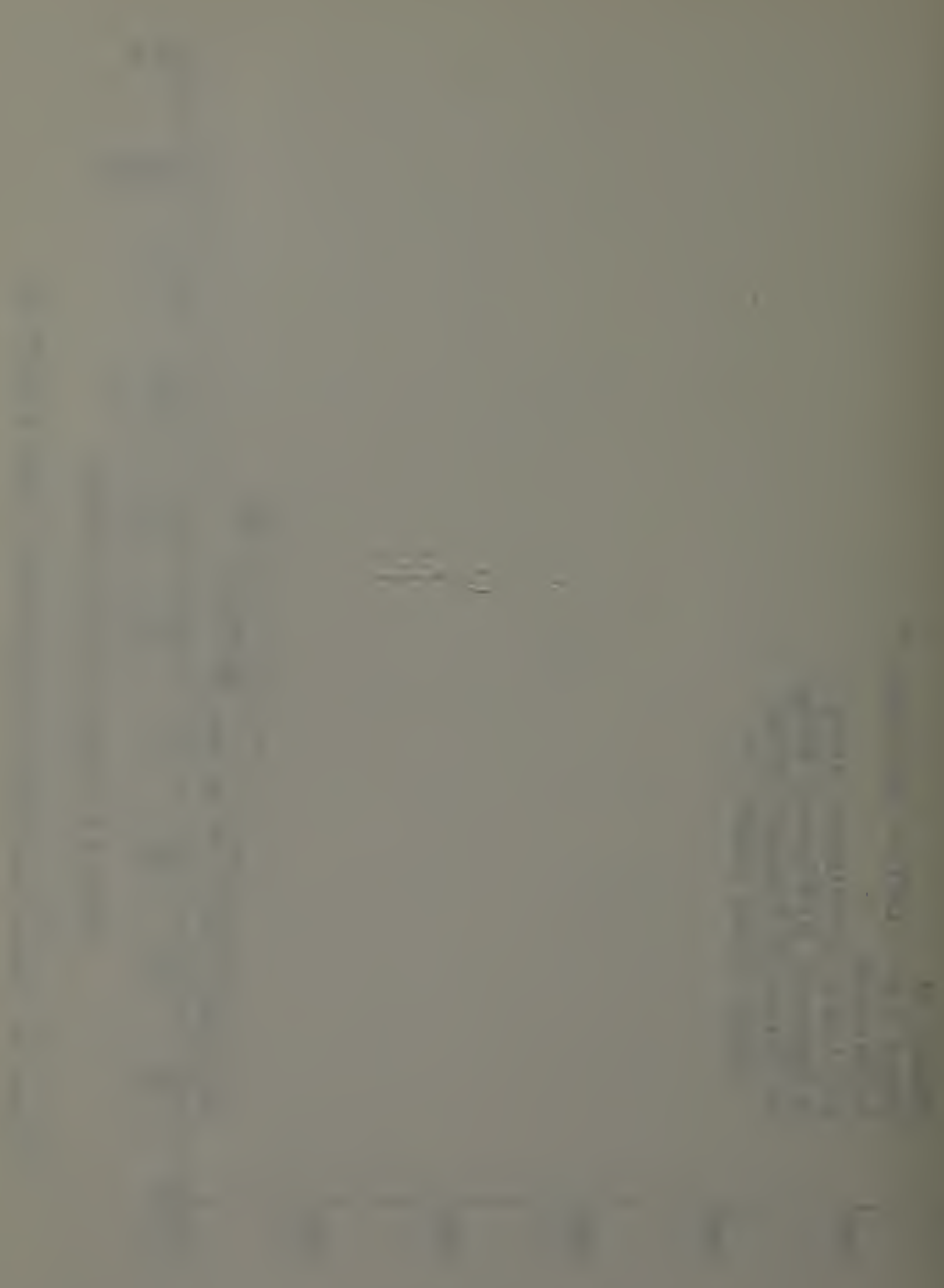

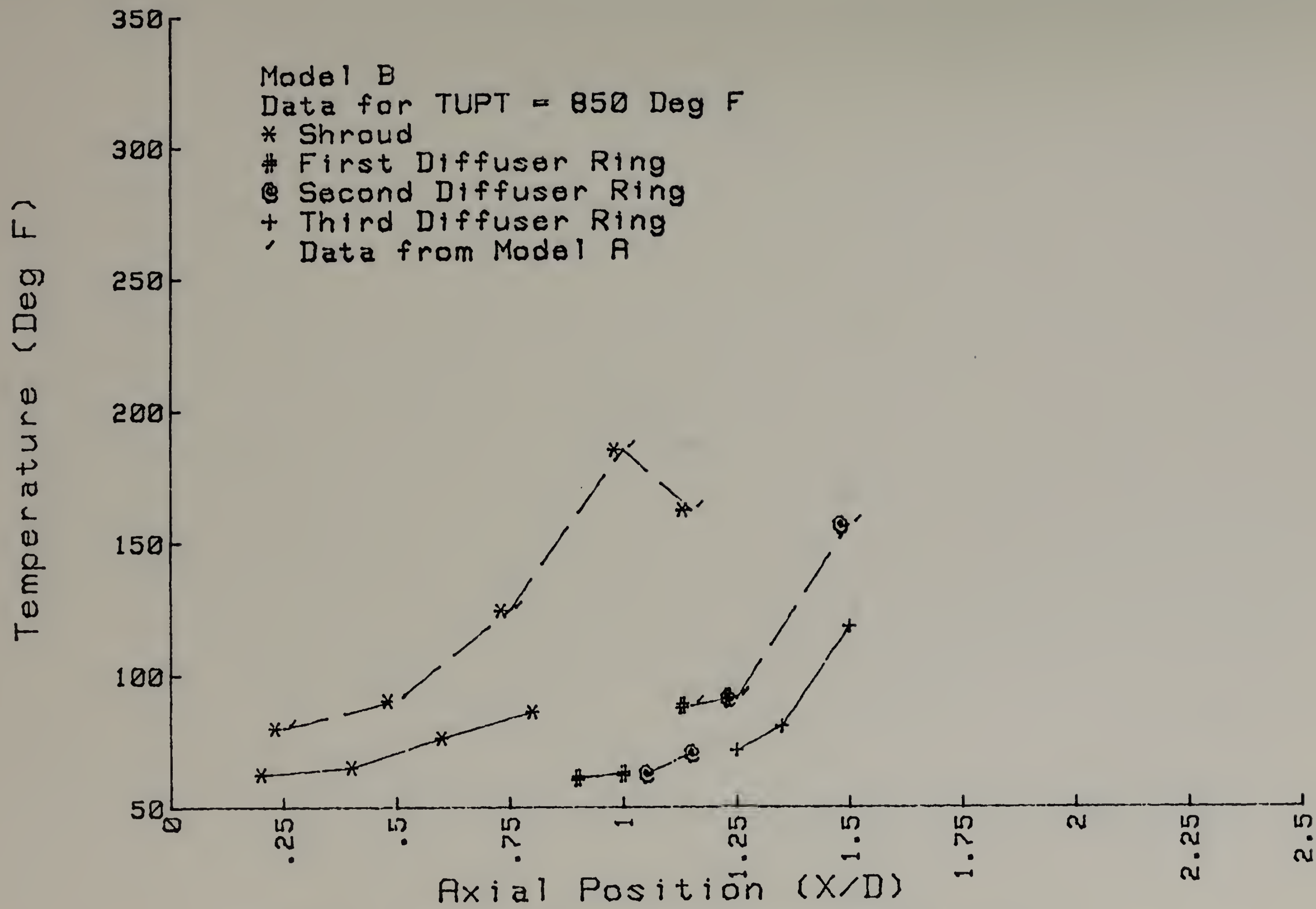

Figure 81. Shroud and Diffuser Temperatures, Model B (850° F)

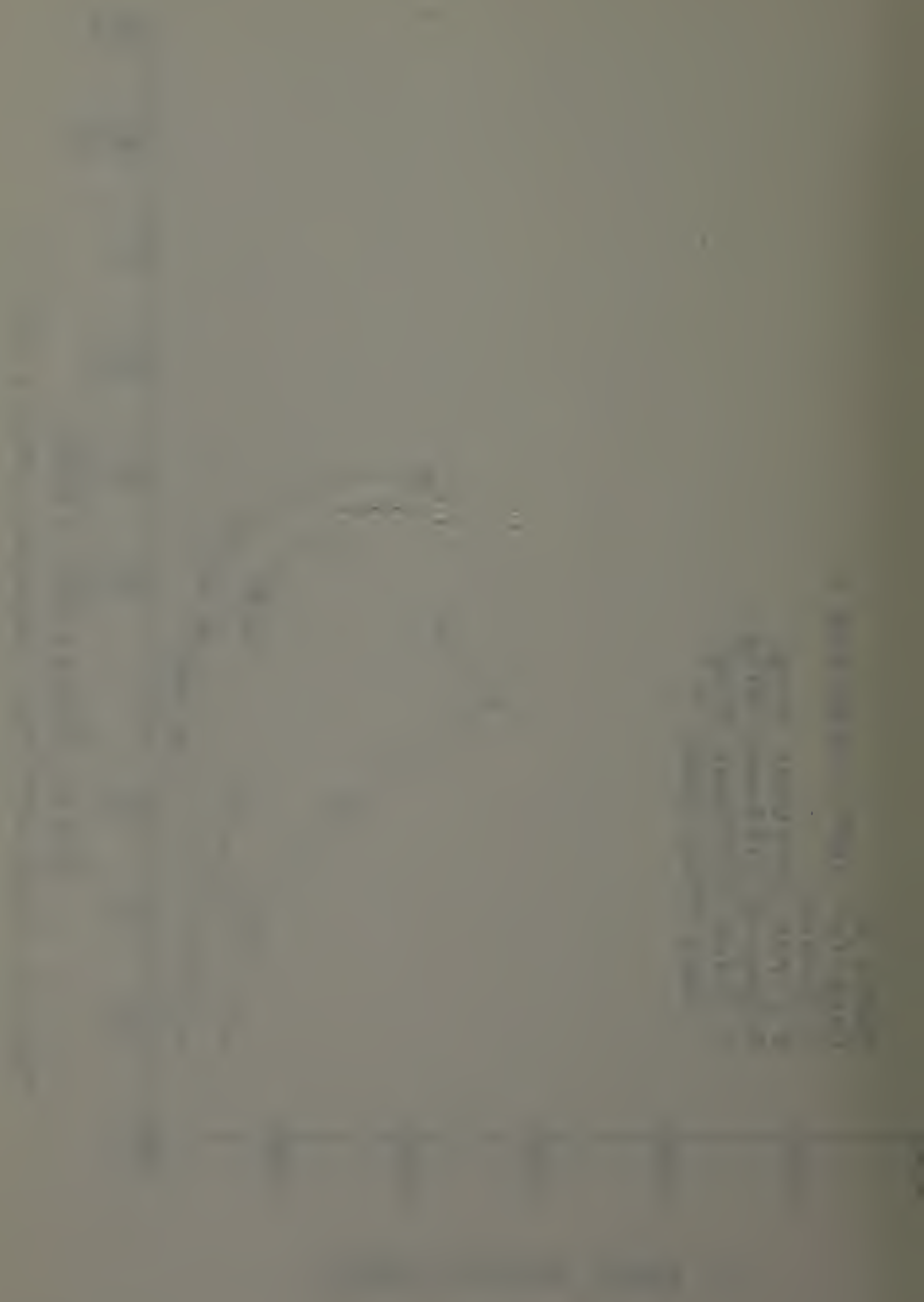

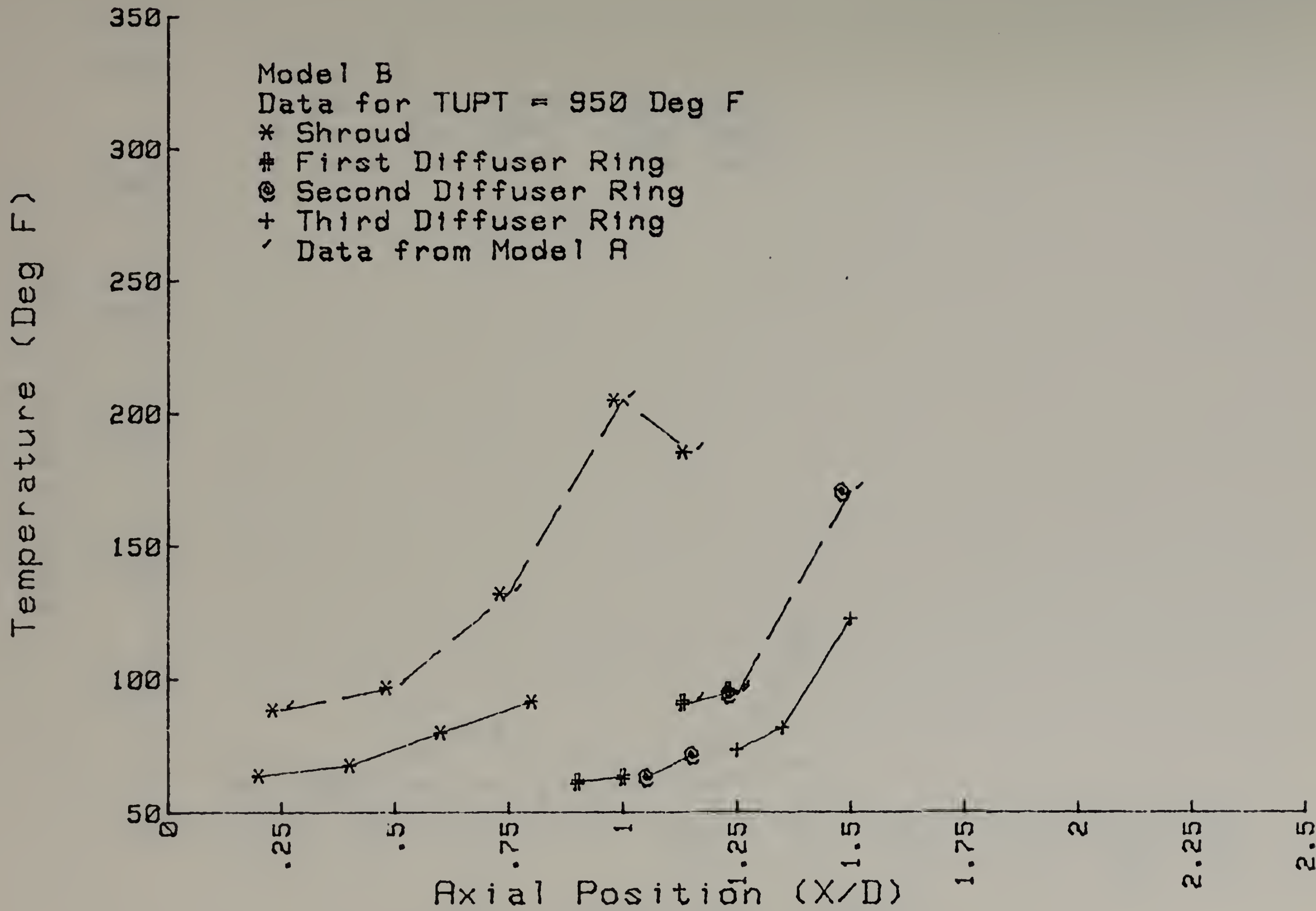

Figure 82. Shroud and Diffuser Temperatures, Model B (950^{o} F)

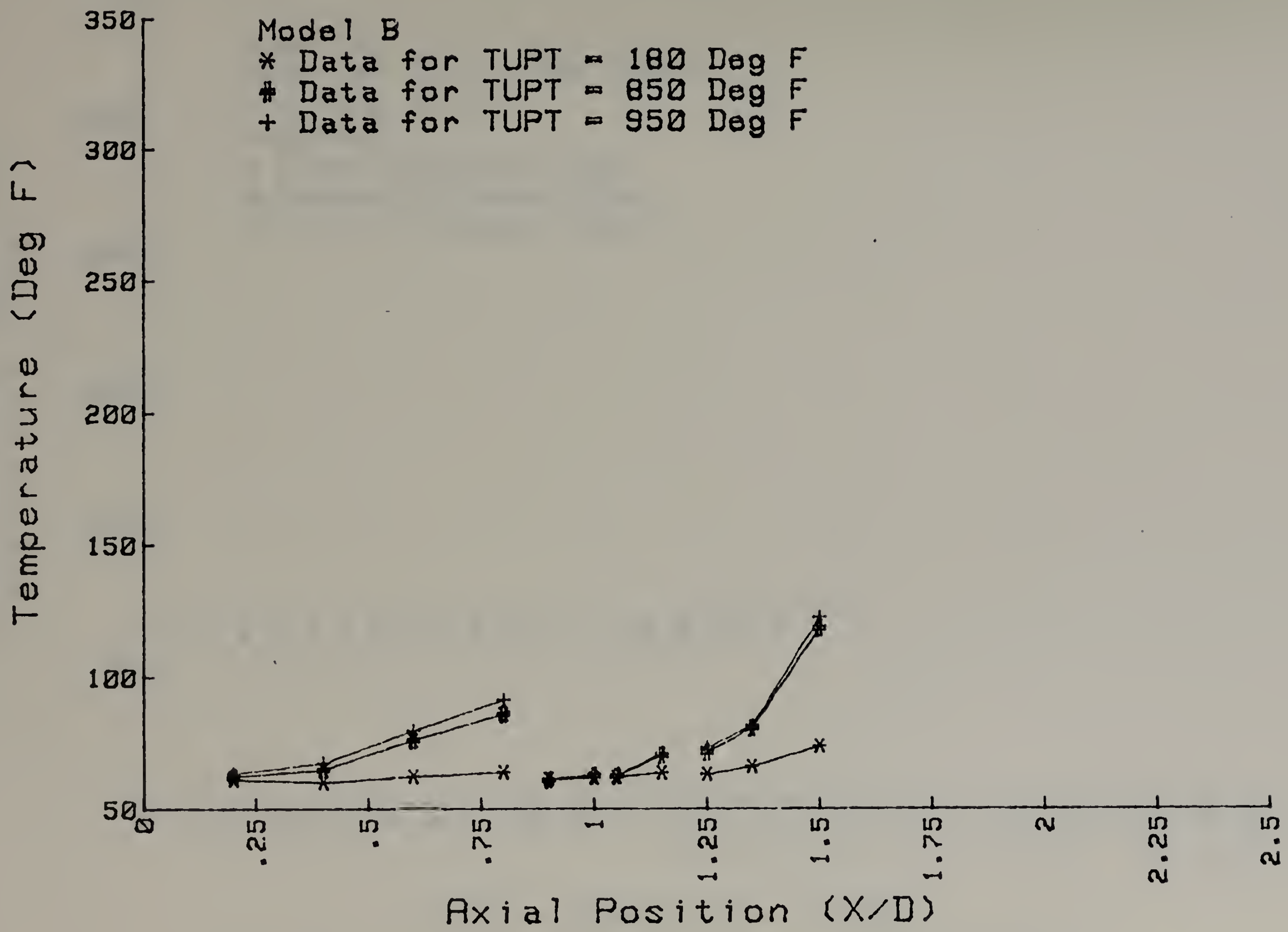

Figure 83. Shroud and Diffuser Temperatures Comparison, Model B

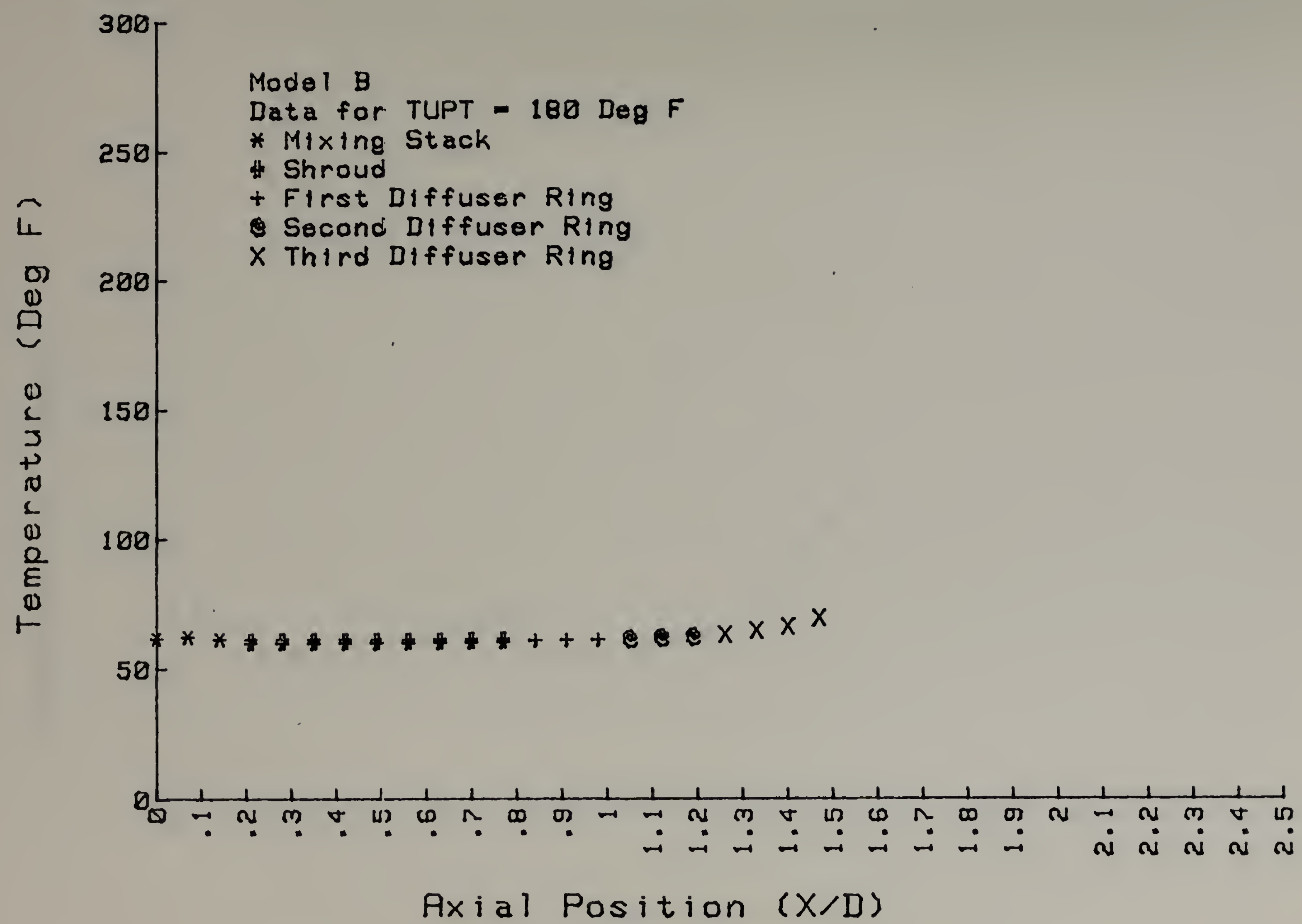

Figure 84. External Surface Temperatures, Model B (180^{o} F)

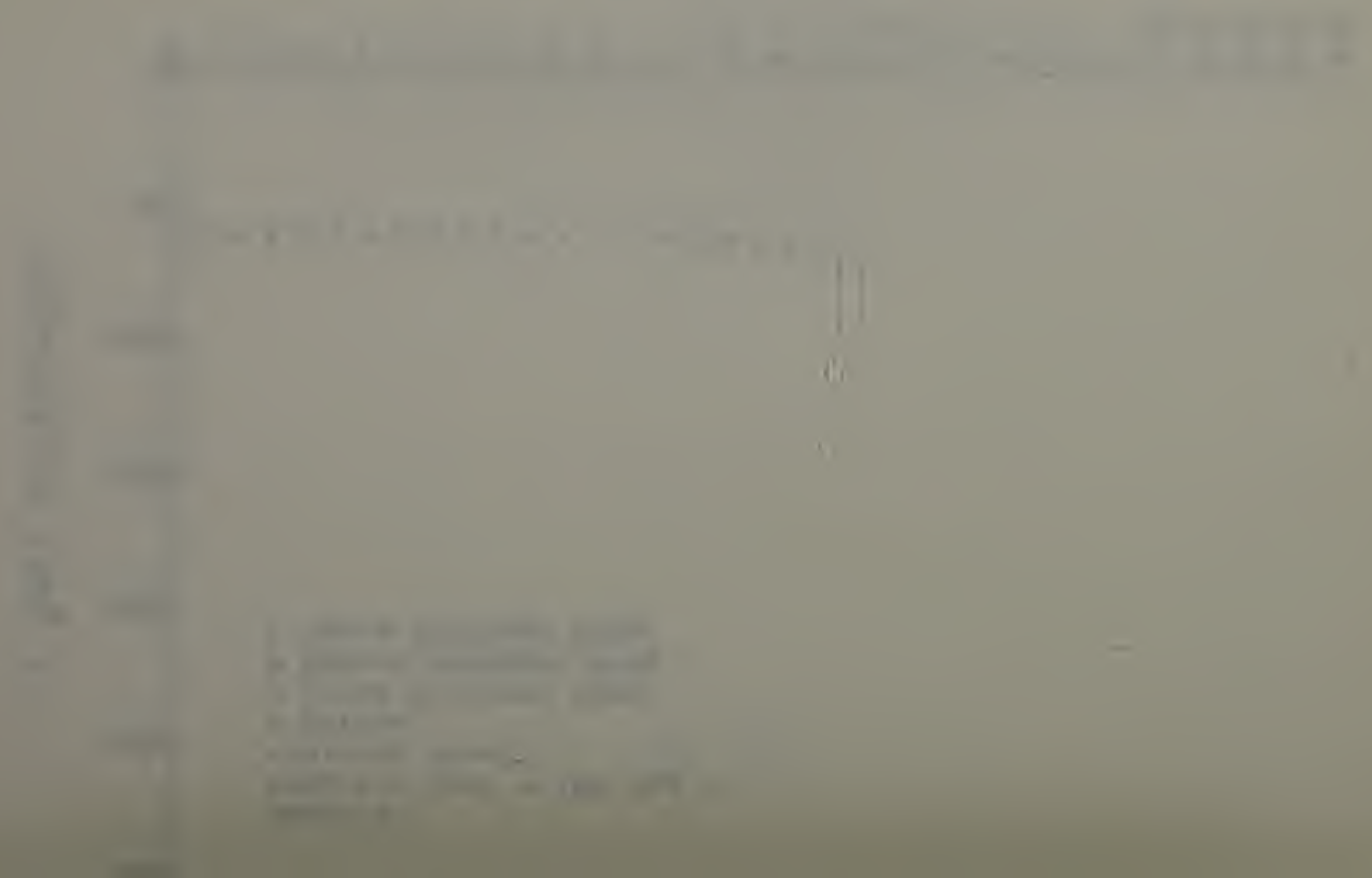

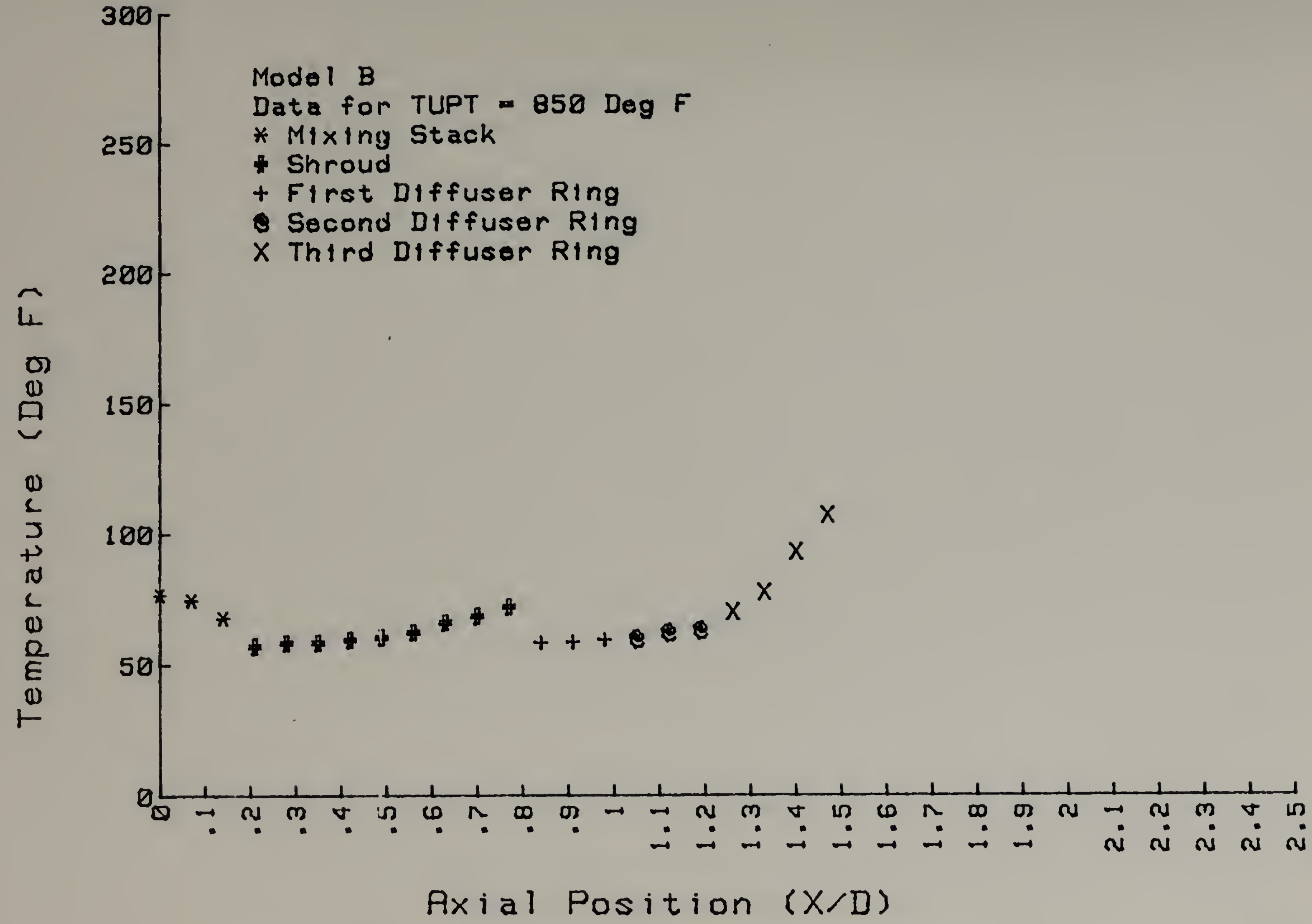

Figure 85. External Surface Temperatures, Model B (850° F)

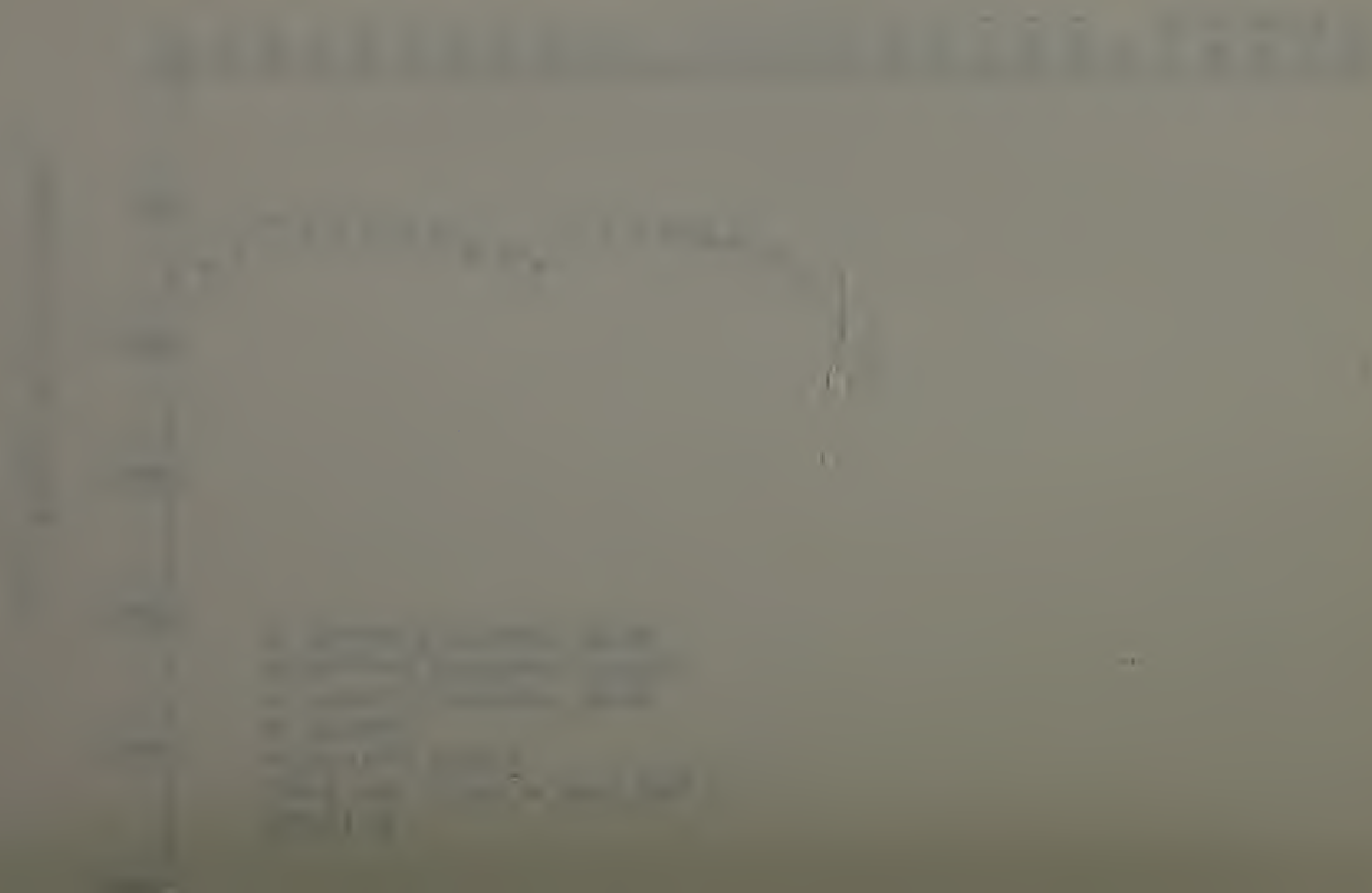

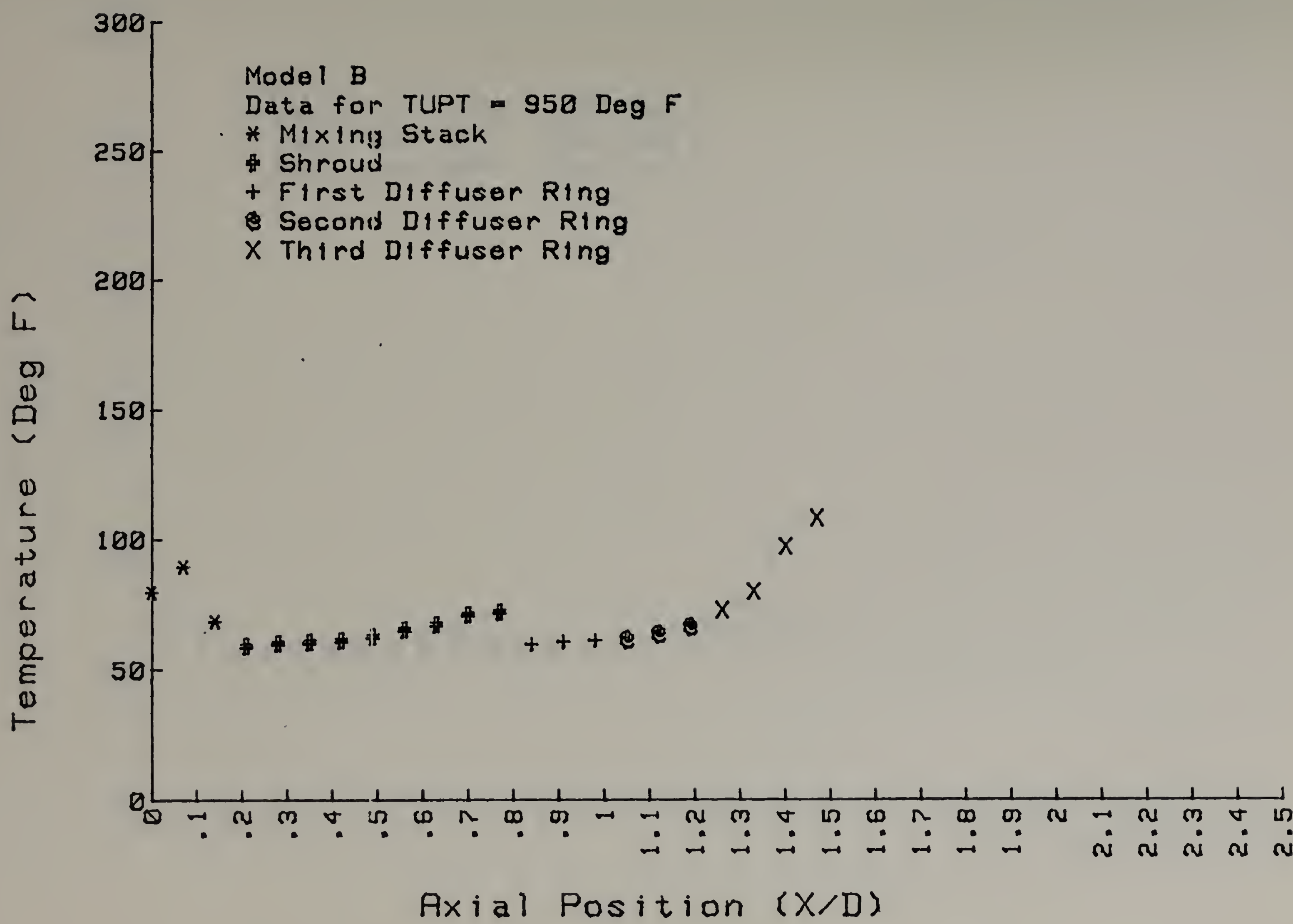

Figure 86. External Surface Temperatures, Model B (950^{o} F)

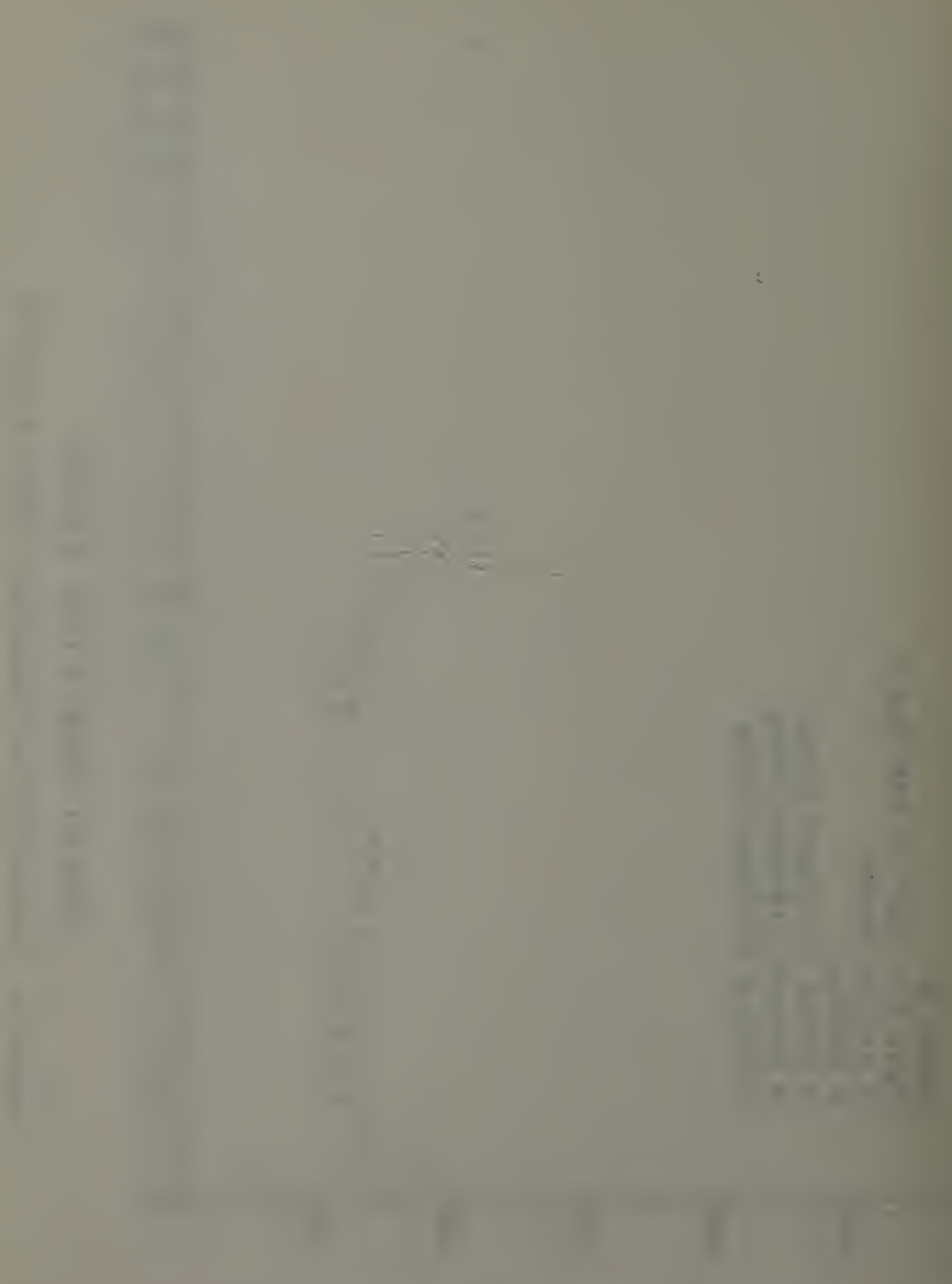

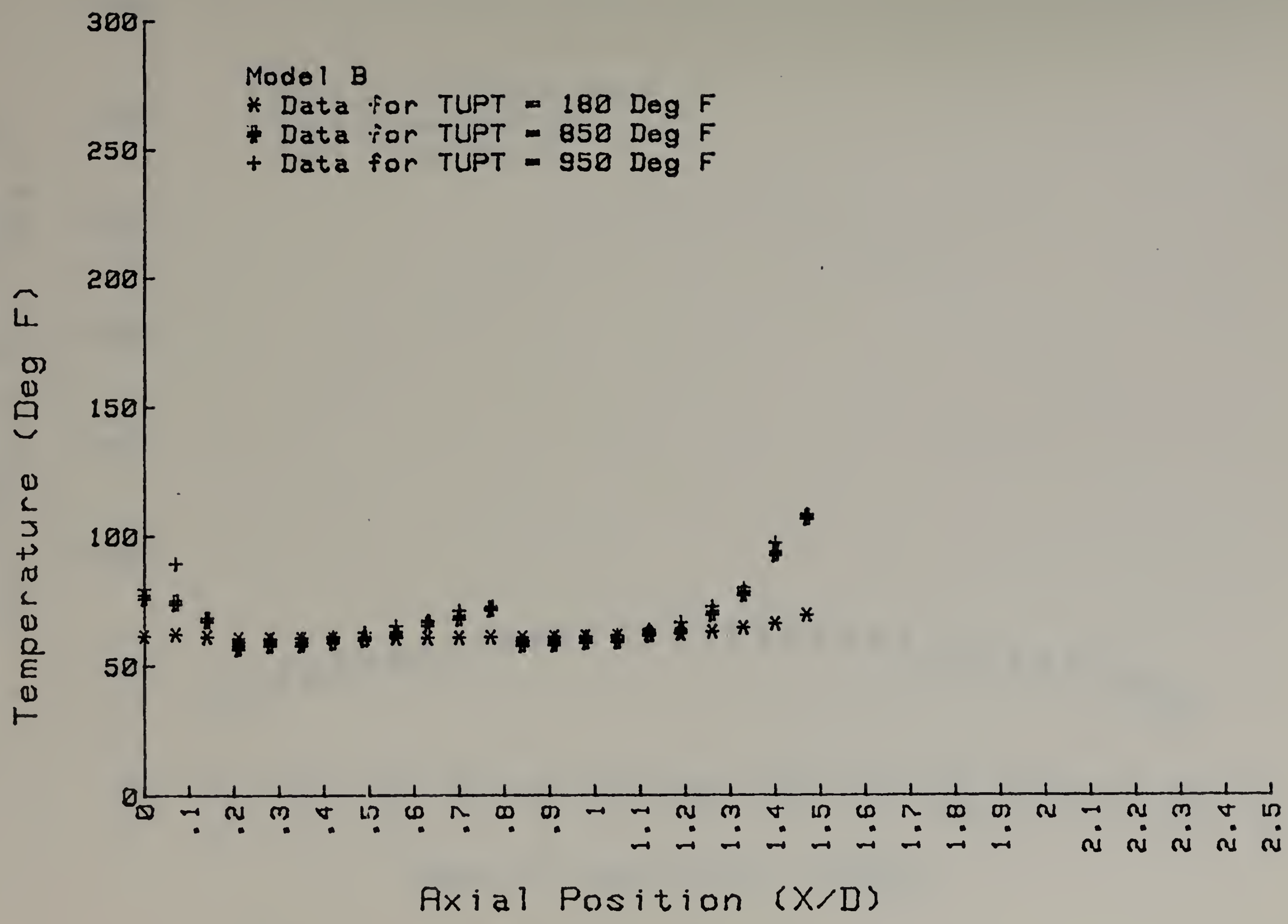

Figure 87. External Surface Temperatures Comparison, Model B

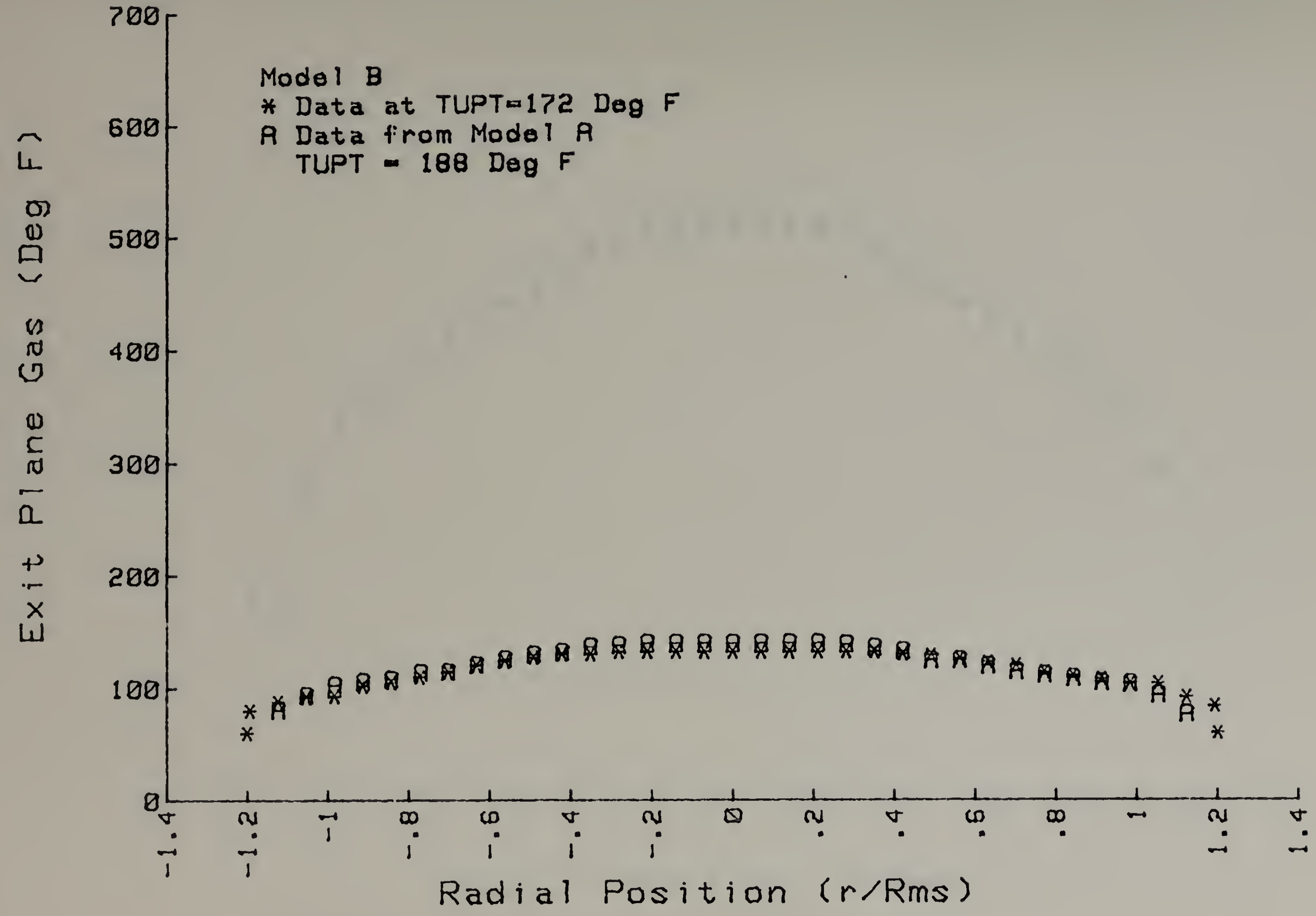

Figure 88. Exit Plane Temperatures, Model B (172° F)

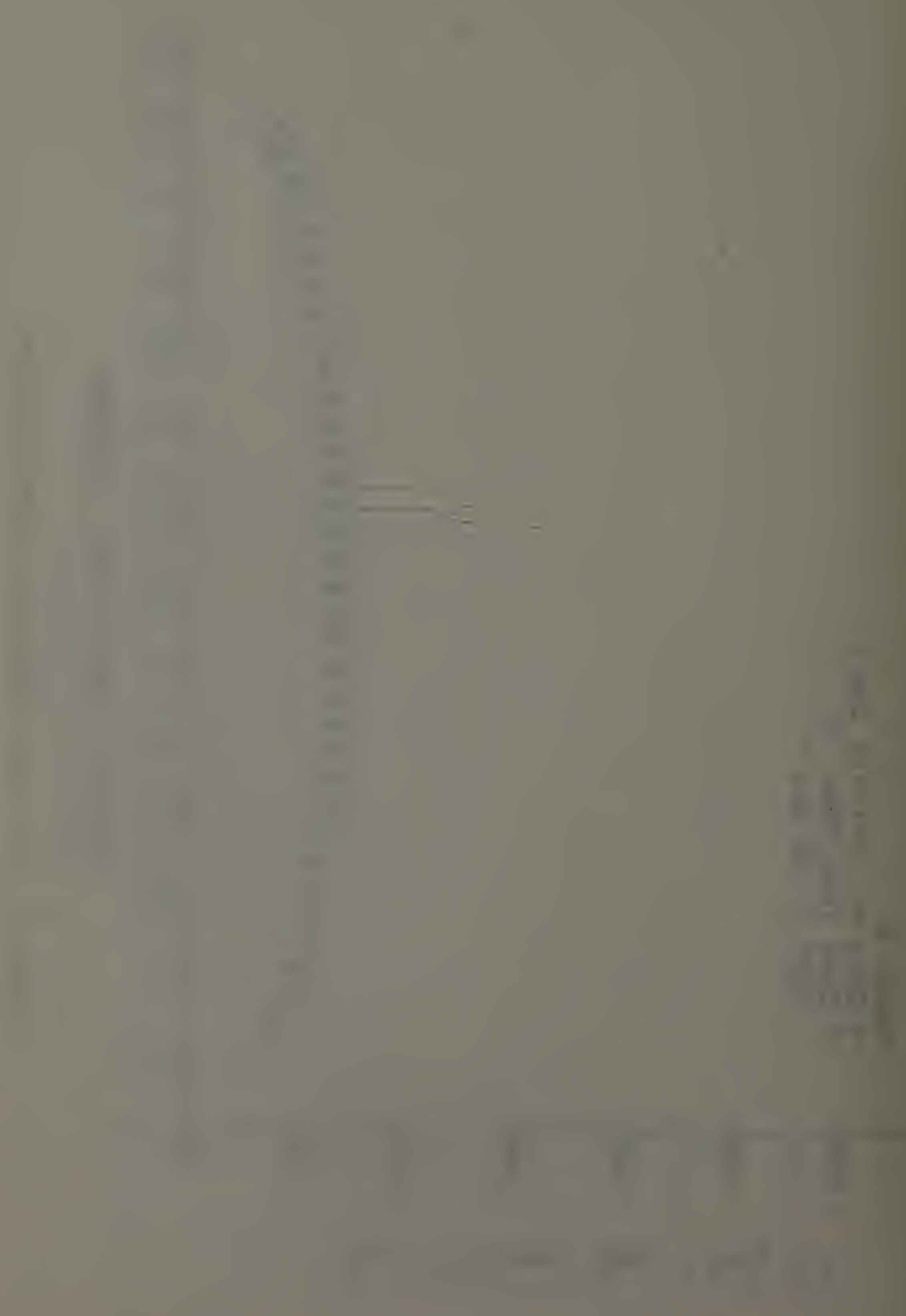

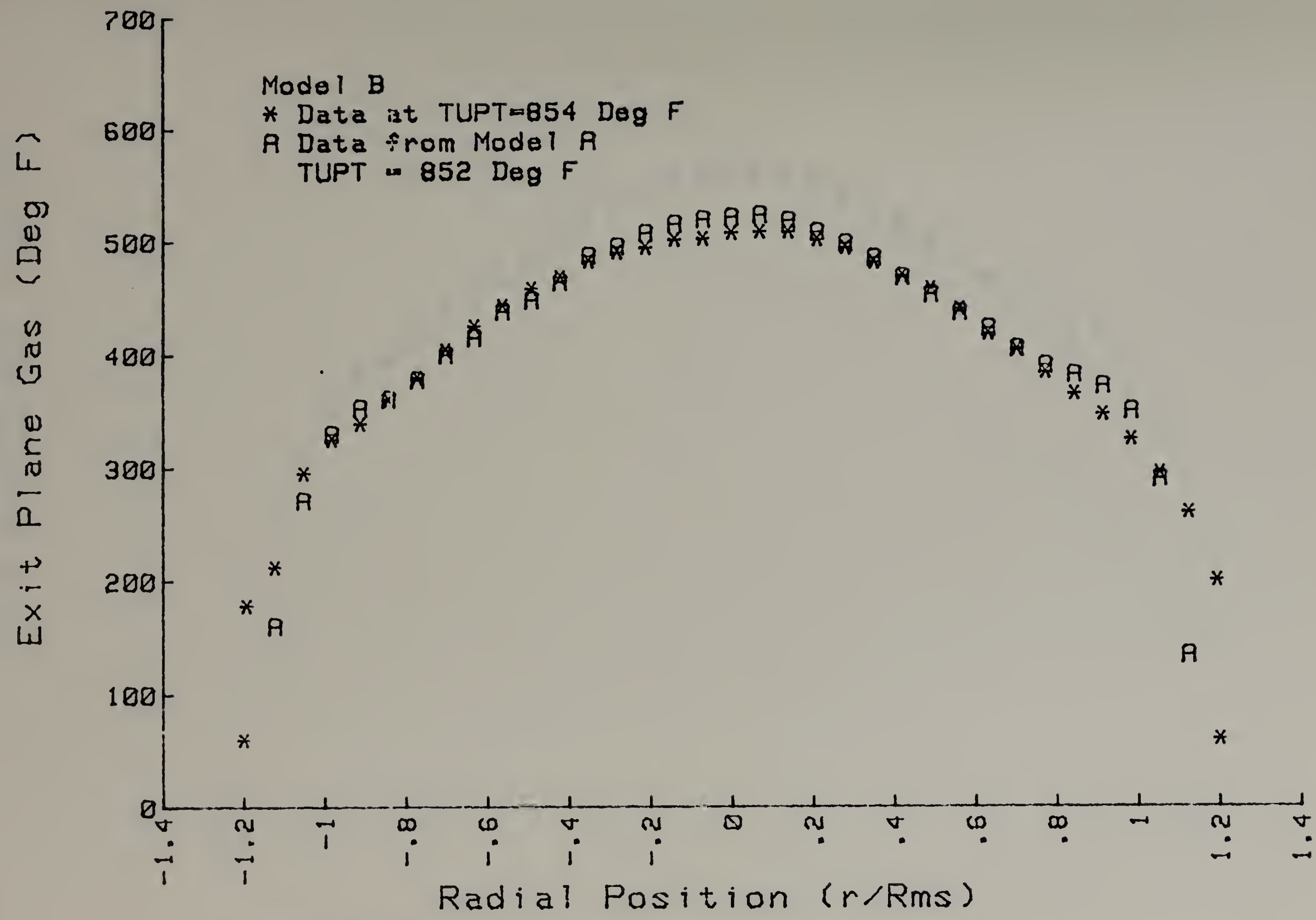

Figure 89. Exit Plane Temperatures, Model B (854° F)

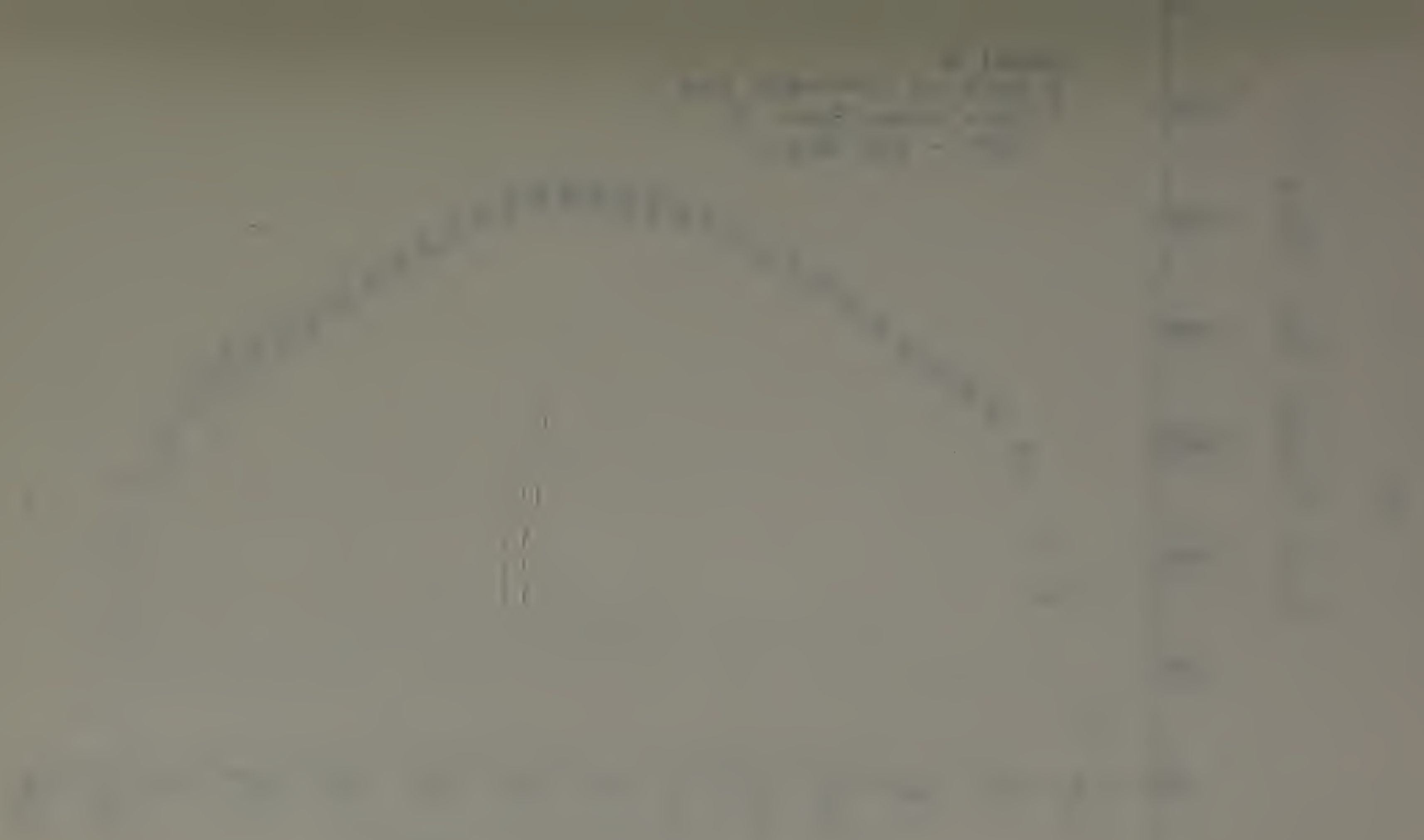

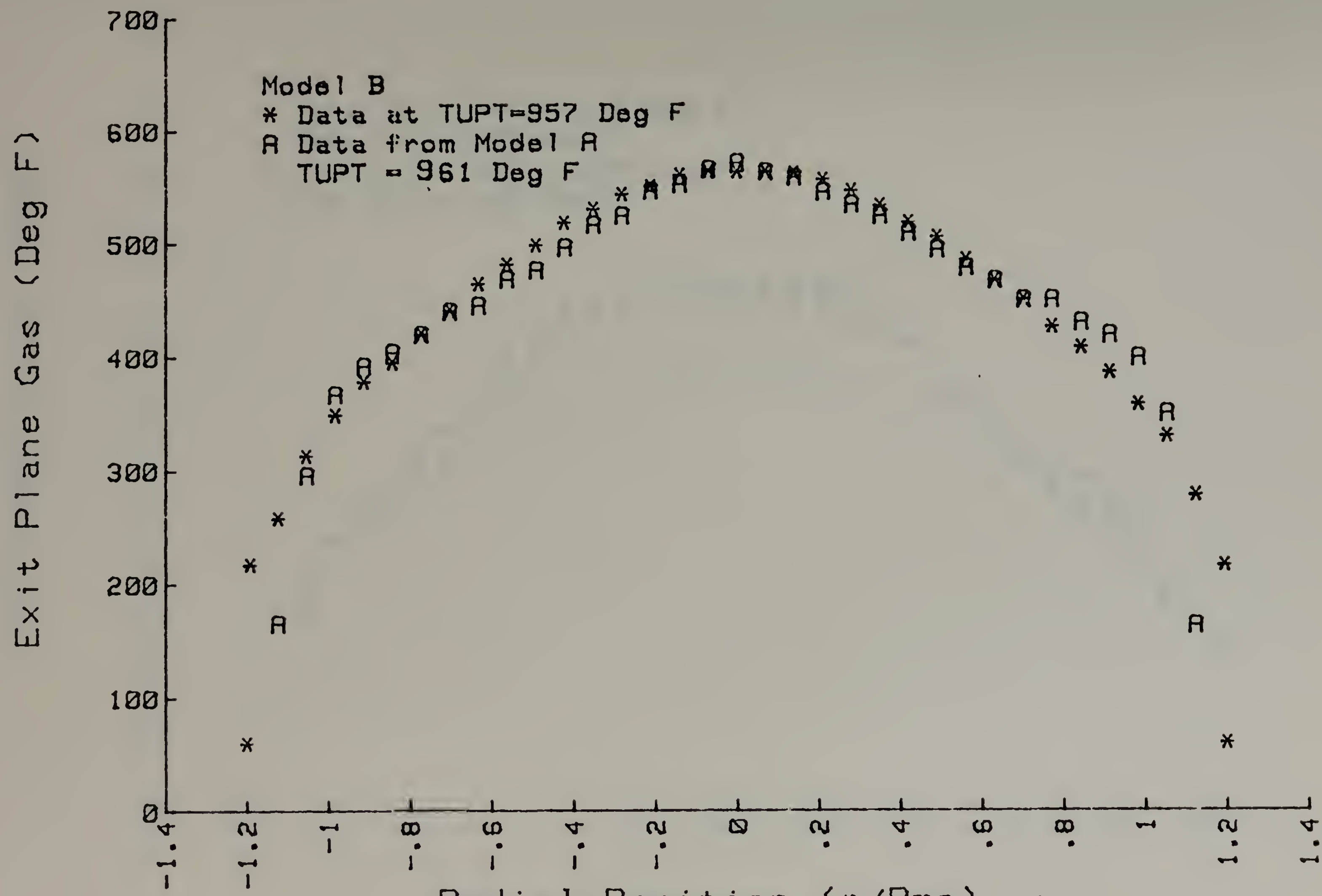

Figure 90. Exit Plane Temperatures, Model B (957^{o} F)

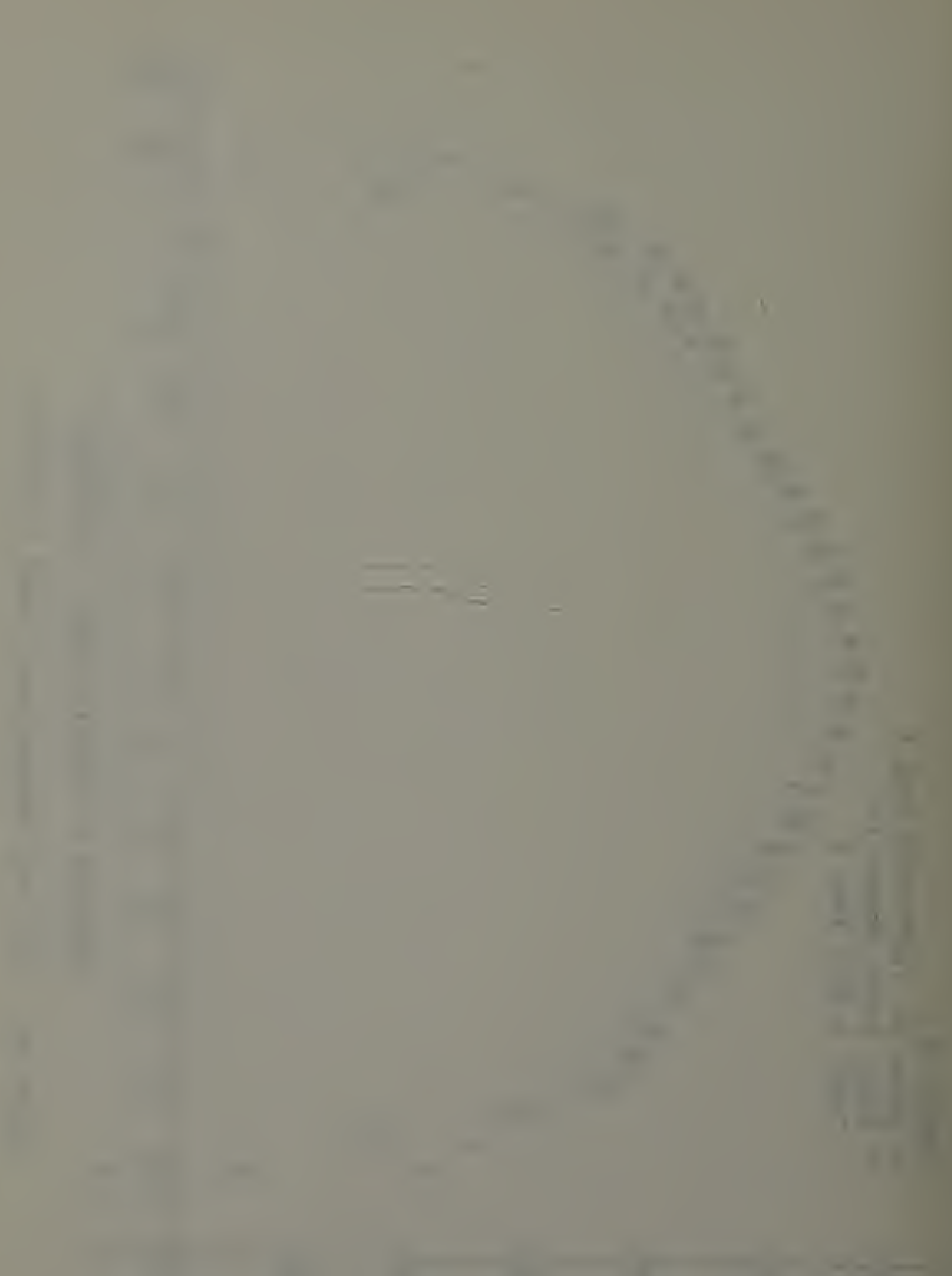

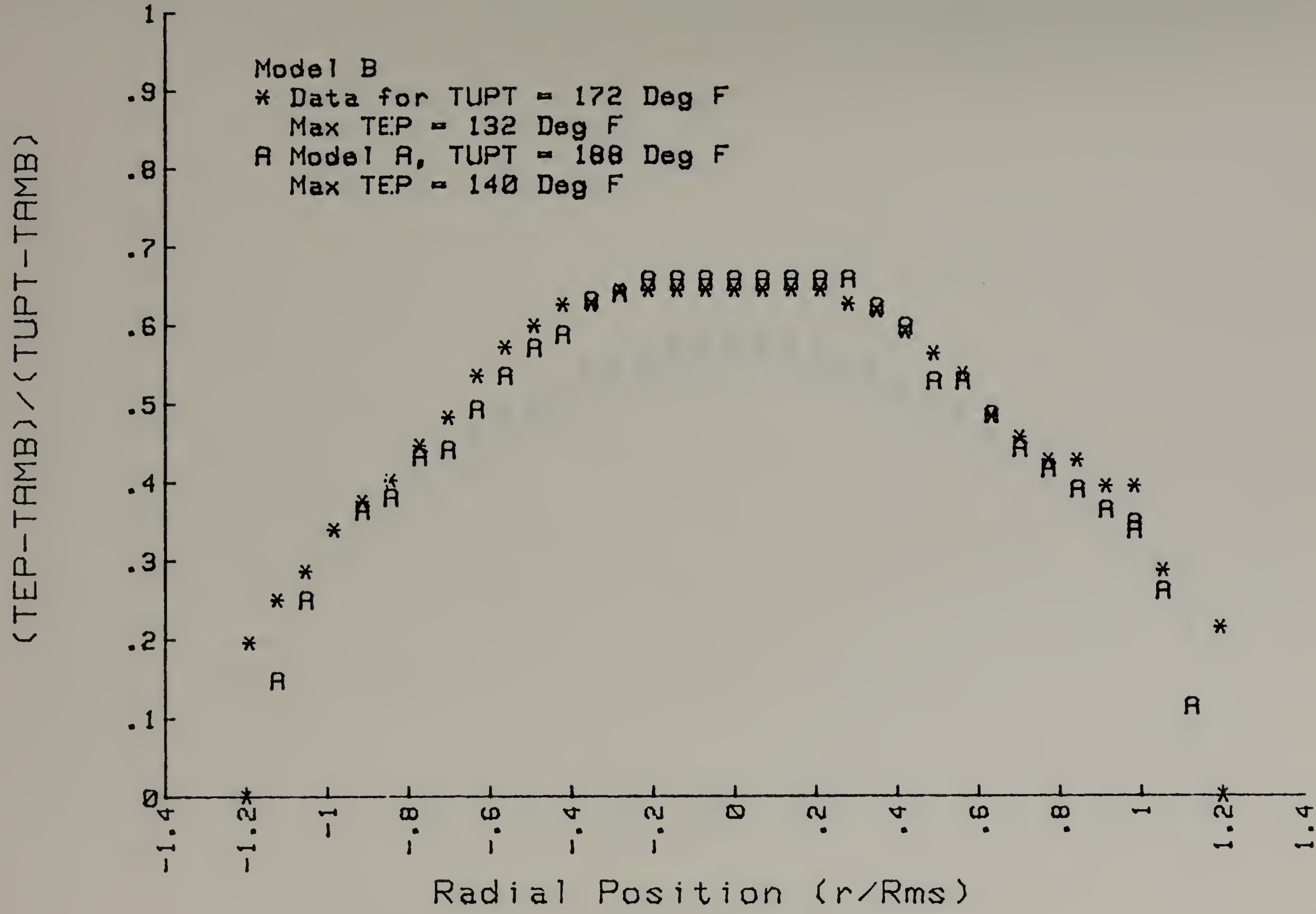

Figure 91. Exit Plane Coefficients, Model B (172° F).

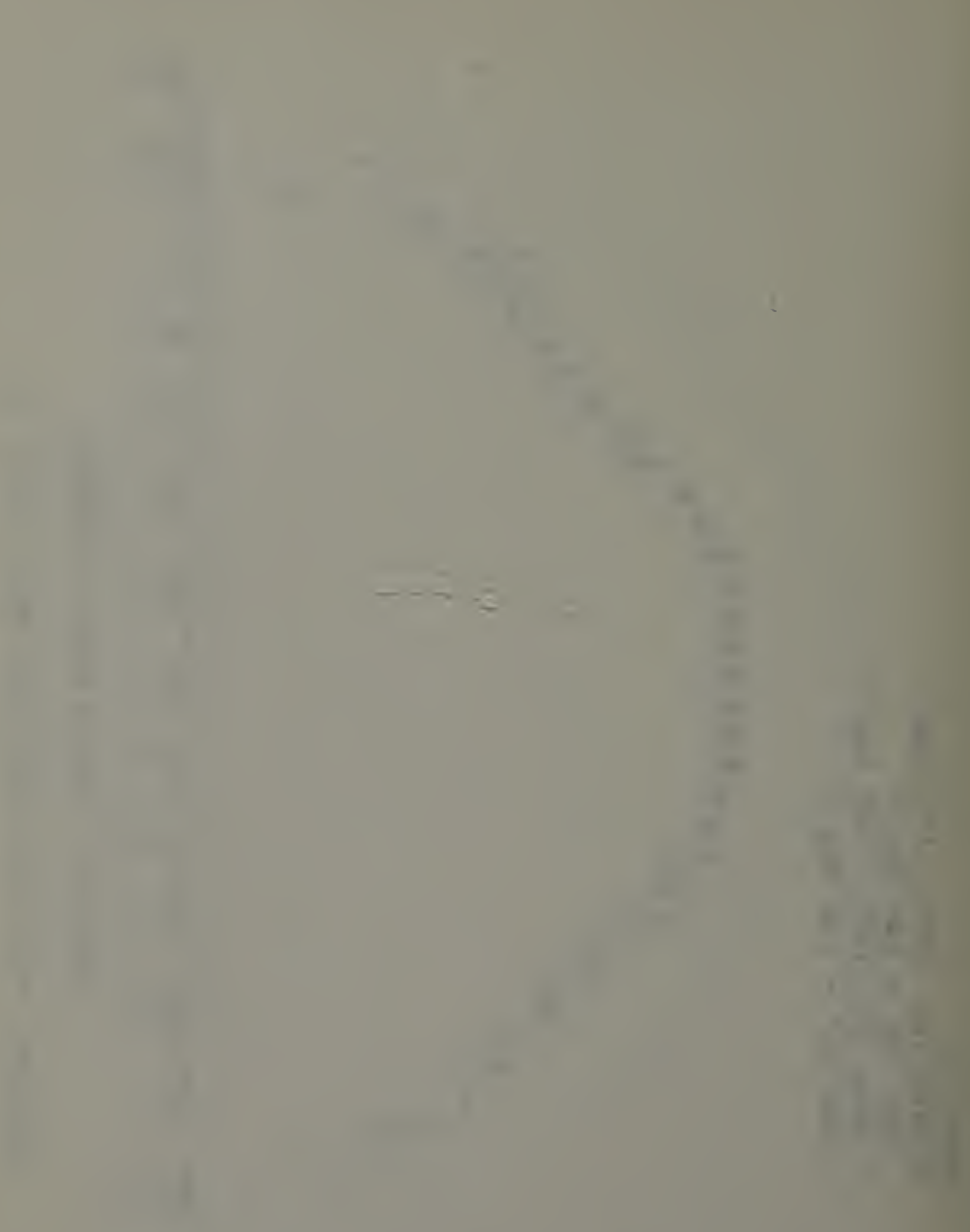

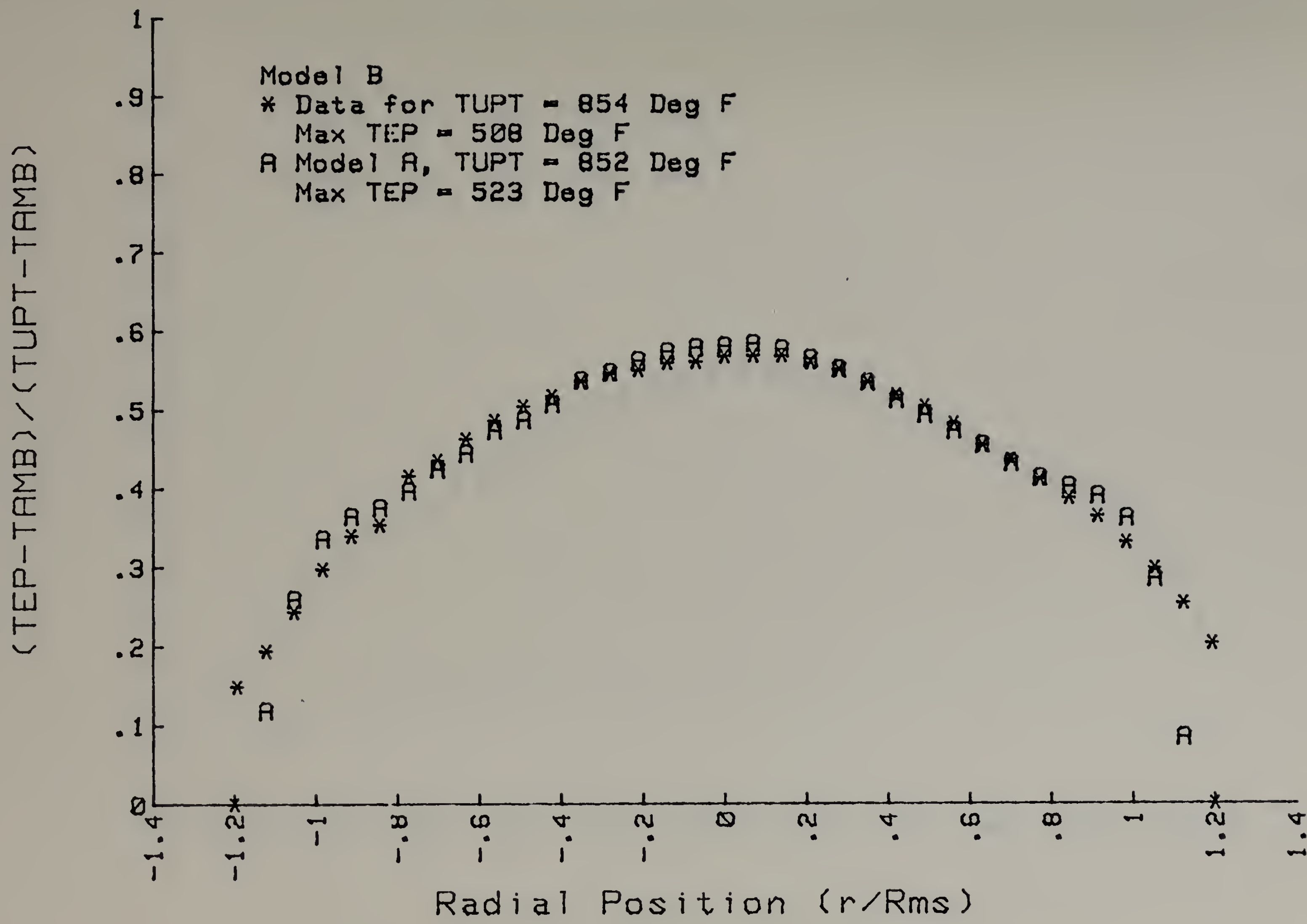

Figure 92. Exit Plane Coefficients, Model B (854^{o} F)

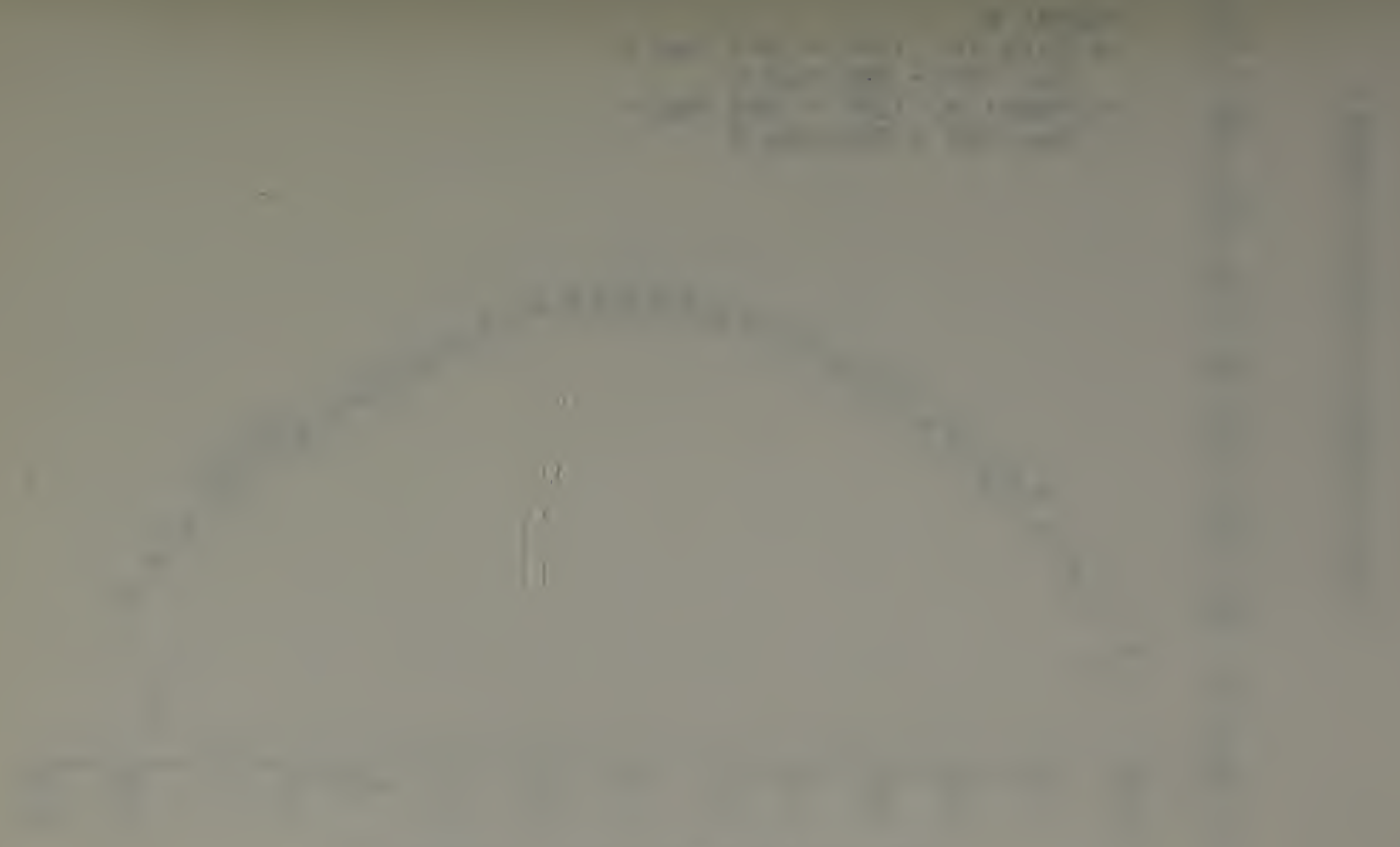

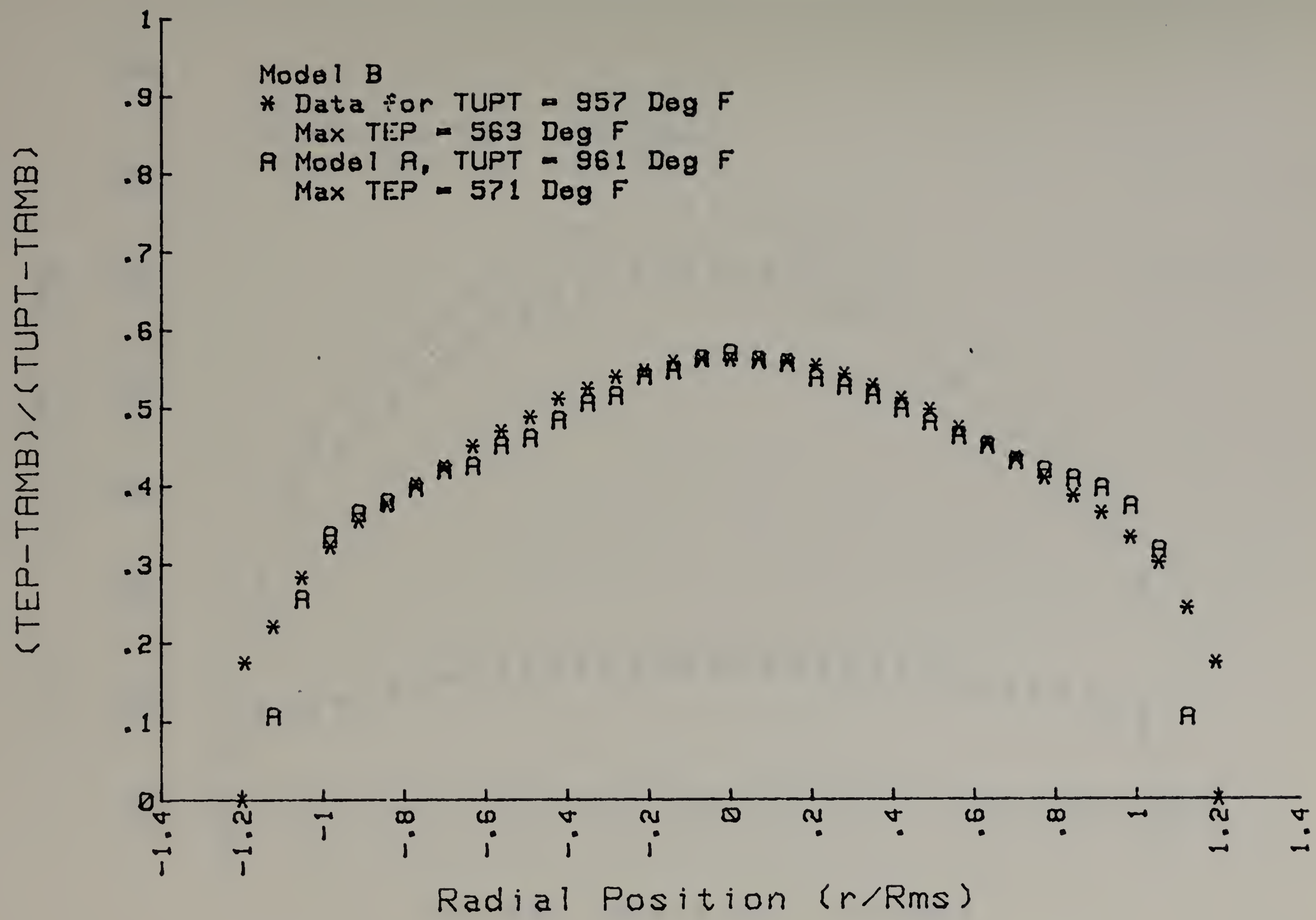

Figure 93. Exit Plane Coefficients, Model B (957° F)

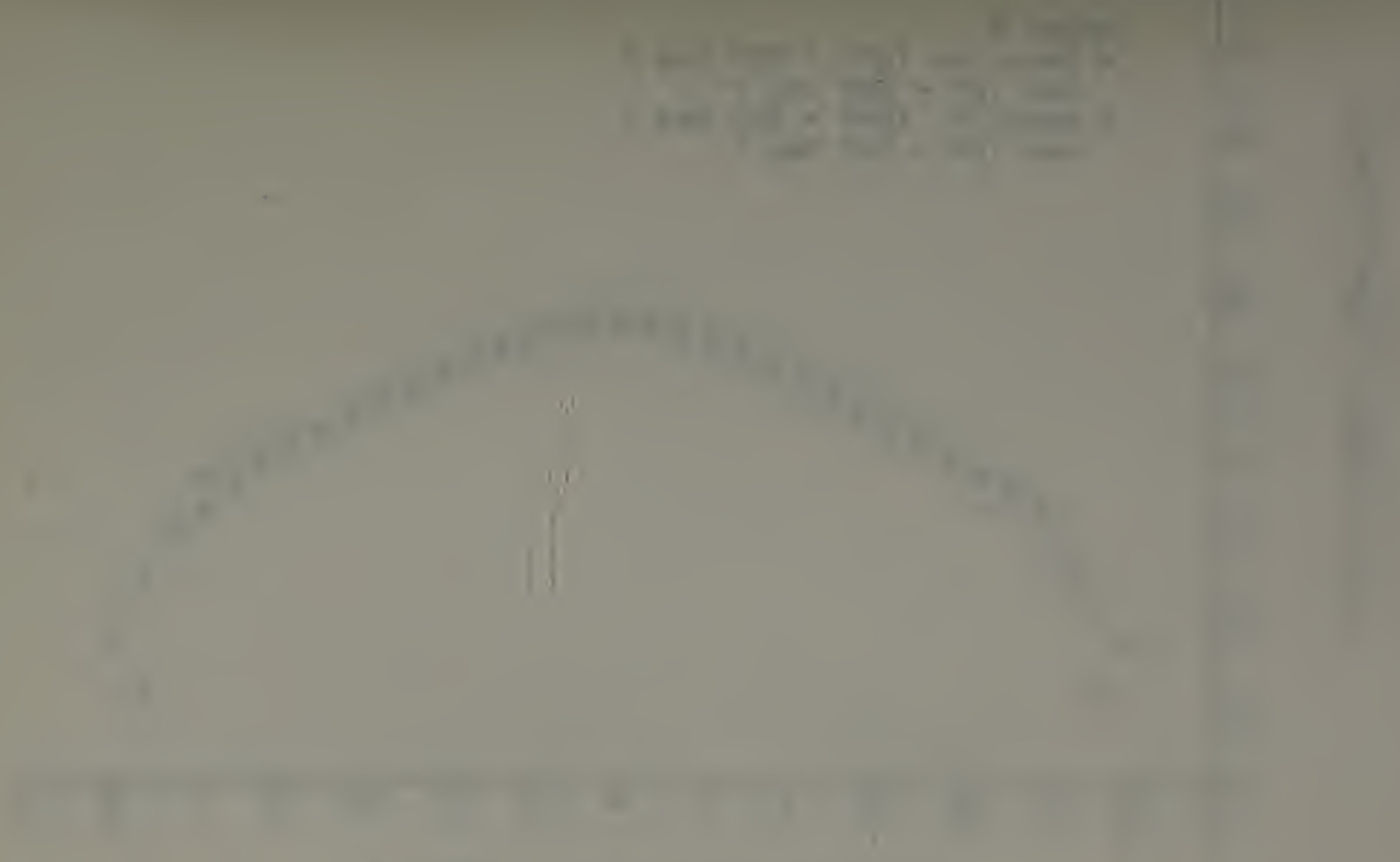

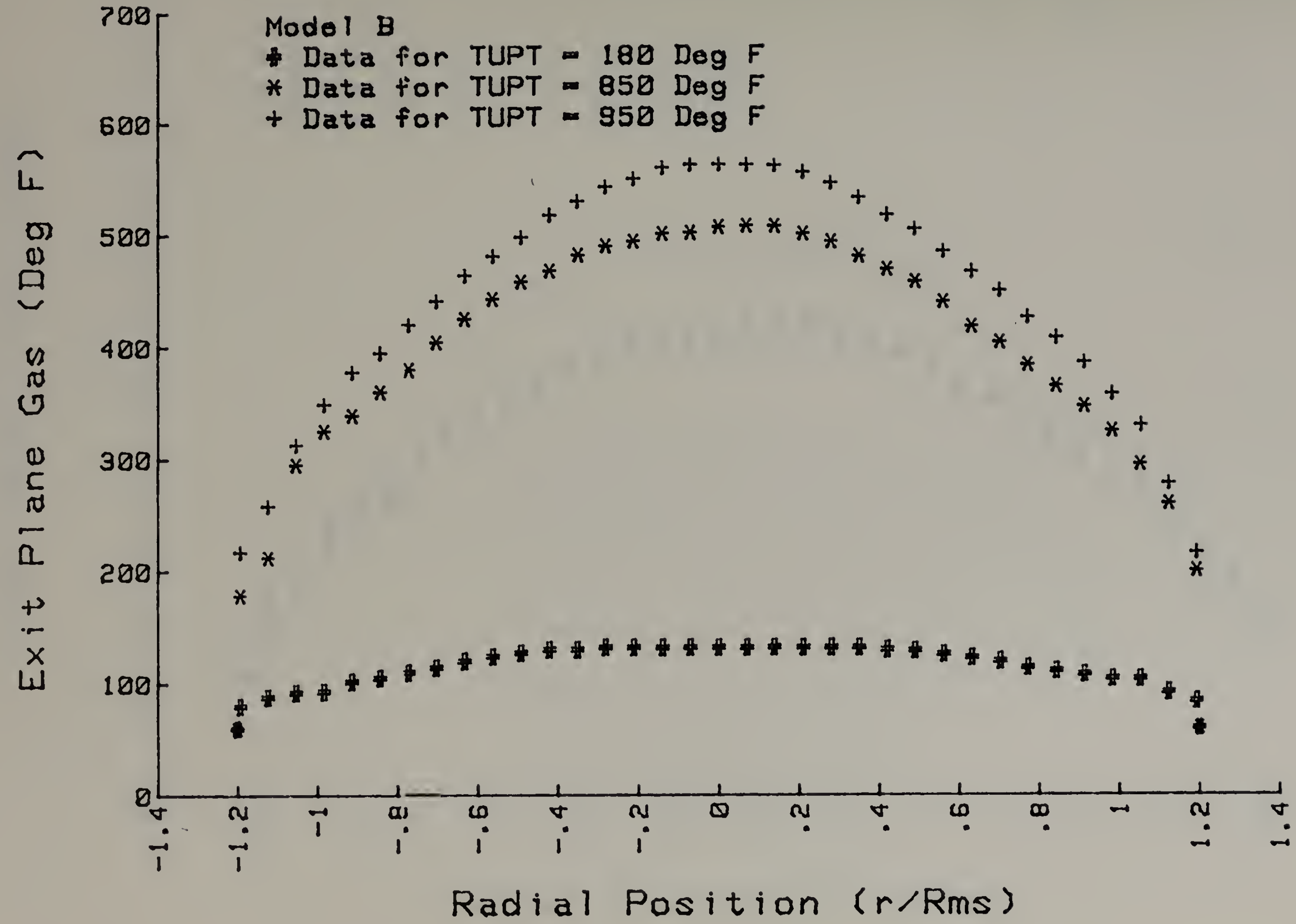

Figure 94. Exit Plane Temperature Comparison, Model B

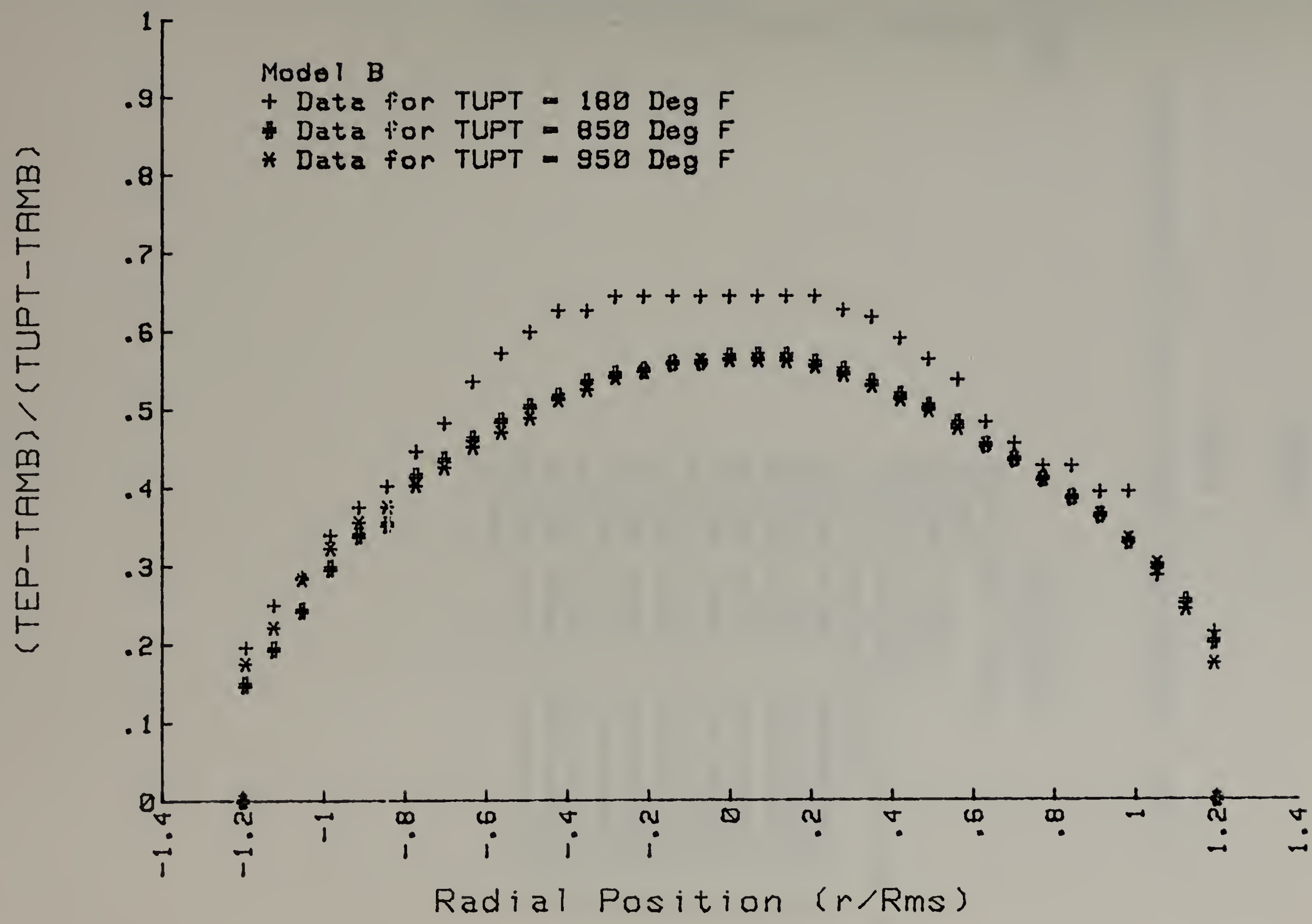

Figure 95. Exit Plane Coefficient Comparison, Model B

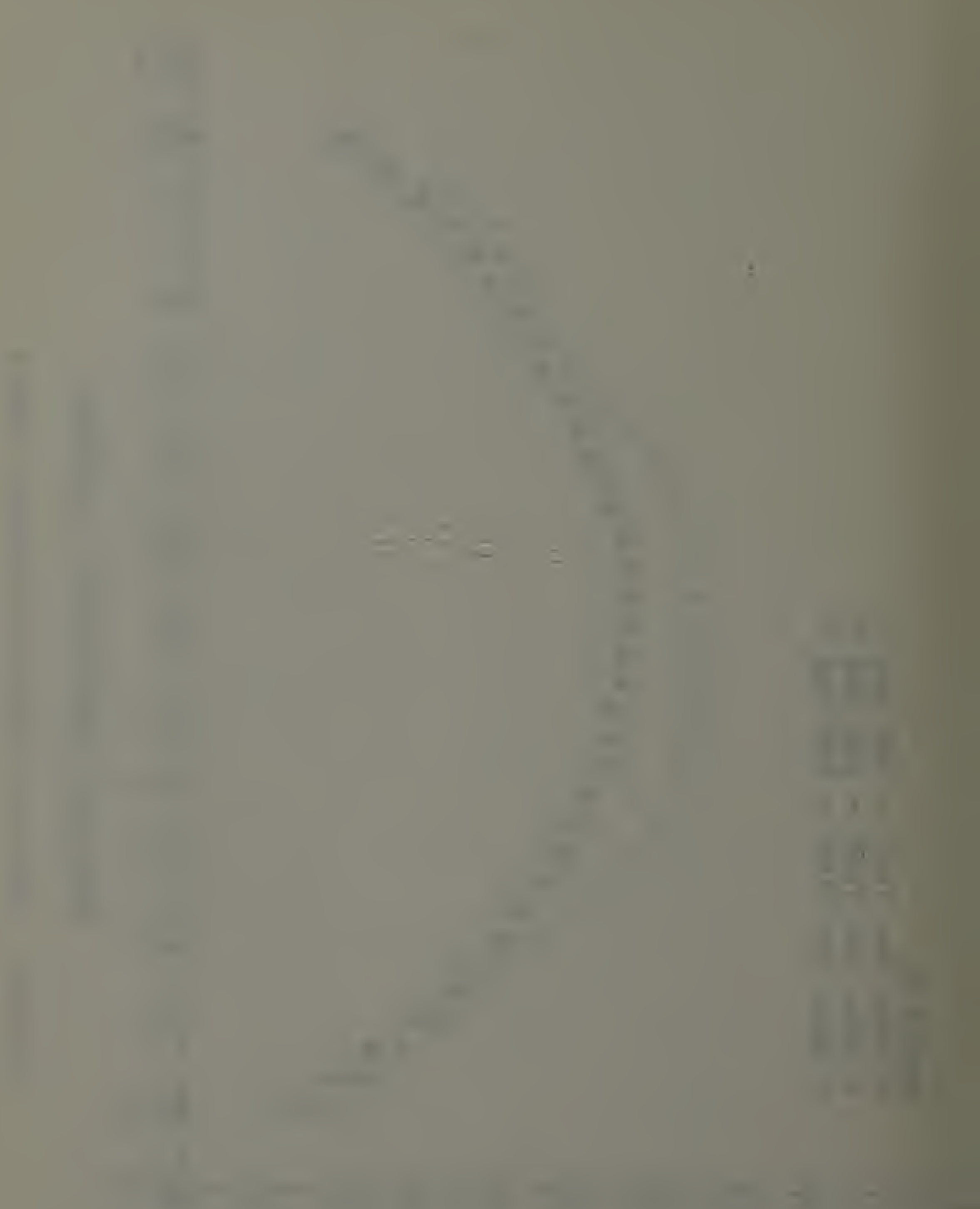

TABLES

TABLE I

THERMOCOUPLE DISPLAY CHANNEL ASSIGNMENT, TYPE K

Channel	Assignment
1	Exit plume (TEP)
2	Unused
3	Uptake (TUPT)
4	Burner (TBURN)
5	Nozzle Box set the position of the removed burner
6	Mixing stack, thermocouple 5
7	Mixing stack, thermocouple 10
8	Mixing stack, thermocouple 11
9	Mixing stack, thermocouple 8
10	Mixing stack, thermocouple 12
11	Mixing stack, thermocouple 7
12	Mixing stack, thermocouple 4
13	Mixing stack, thermocouple 6
14	Mixing stack, thermocouple 2
15	Mixing stack, thermocouple 3
16	Mixing stack, thermocouple 9
17	Mixing stack, thermocouple 1
18	Unused

TABLE II

THERMOCOUPLE DISPLAY CHANNEL ASSIGNMENT, TYPE T

Channel	Assignment
1	Fueld Supply
2	Ambient Air (TAUB)
3	Inlet Air Supply (TNH)
4	Unused
5	Model B shroud X/D = 0.20
6	Model B shroud X/D = 0.40
7	Model B shroud X/D = 0.60
8	Model B shroud X/D = 0.80
9	Model B First Diffuser Ring X/D = 0.90
10	Model B First Diffuser Ring X/D = 1.00
11	Model B Second Diffuser Ring X/D = 1.05
12	Model B Second Diffuser Ring X/D = 1.15
13	Model B Third Diffuser Ring X/D = 1.25
14	Model B Third Diffuser Ring X/D = 1.35
15	Model B Third Diffuser Ring X/D = 1.50
16-18	Unused

TABLE III

MODEL CHARACTERISTICS

	MODEL A	MODEL B
Uptake Diameter	7.51	7.51
Mixing Stack Assembly, (L/D) Overall	1.5	1.5
Mixing Stack Inside Diameter (D)	7.122"	7.122"
L/D	1.0	1.0
Rows of Film Cooling Slots	4	4
Shroud Start Position (S/D)	0.25	0.14
Shroud Length (X/D)	1.04	1.096
Number of Rings	2	3
First Ring Length (l/D)	.25	.50
Second Ring Length (l/D)	.25	.375
Third Diffuser Ring (l/D)	---	.25
Half Angle	7.3°	10.943°
Film Cooling Clearance Mixing Stack Shroud	0.076"	0.139"
Shroud-First Ring	0.076"	0.096"
First Ring-Second Ring	0.076"	0.096"
Second Ring-Third Ring	---	0.096"
Stand-Off Distance (S/D)	0.5	0.5
Primary Nozzles		
Number	4	4
Type	Tilted-Angled (15/20)	Tilted-Angled (15/20)
Am/Ap	2.5	2.5

1

*** HOT RIG PERFORMANCE *** TUPT: 180
2 RING DIFFUSER

DATE: 16 OCT08 82

NUMBER OF PRIMARY NOZZLES: 4
PRIMARY NOZZLE DIAMETER: 2.25 INCHES
UPTAKE DIAMETER: 7.510 INCHES
AREA RATIO, AM/AP: 2.50
GAMMA: 1.3991

DATA TAKEN BY A KAVALIS

MIXING STACK LENGTH: 7.20 INCHES
MIXING STACK DIAMETER: 7.122 INCHES
MIXING STACK L/D: 1.50
STANDOFF RATIO: 0.50
AMBIENT PRESSURE: 30.08 INCHES HG

NR	PNH IN HG	DELPN IN H2O	TNH DEG F	ROTA	TBURN DEG F	TUPT DEG F	TAMB DEG F	PUPT IN H2O	PPLN IN H2O	SEC AREA SQ IN
1	3.60	14.70	182.9	0.0	169.0	174.0	64.0	5.60	4.20	0.000
2	3.60	14.65	182.7	0.0	170.0	175.0	63.4	6.05	3.73	1.767
3	3.60	14.65	183.2	0.0	171.0	175.0	64.2	6.45	3.31	3.534
4	3.65	14.65	183.5	0.0	172.0	176.0	64.4	6.80	2.95	5.301
5	3.70	14.60	184.2	0.0	172.0	176.0	64.7	7.25	2.43	8.443
6	3.70	14.55	184.2	0.0	172.0	177.0	64.7	7.60	2.03	11.585
7	3.70	14.50	184.6	0.0	172.0	177.0	65.1	7.95	1.70	14.726
8	3.75	14.50	184.4	0.0	172.0	176.0	63.5	8.70	0.86	27.293
9	3.60	14.50	184.8	0.0	172.0	177.0	64.1	9.00	0.51	39.859
10	3.80	14.50	184.8	0.0	172.0	187.0	64.7	9.20	0.32	52.425
11	3.80	14.50	184.9	0.0	172.0	187.0	64.5	9.30	0.23	64.992
12	3.80	14.50	185.2	0.0	173.0	188.0	65.6	9.50	0.00	******

NR	WPA LBM/S	WF LBM/S	WP LBM/S	WS LBM/S	W*	P*	T*	P*/T*	W*T**.44	UP FT/S	UM FT/S	UU FT/S	UMACH
1	1.572	0.000	1.572	0.000	0.000	0.355	0.826	0.430	0.000	229.3	91.5	80.4	0.0652
2	1.570	0.000	1.570	0.116	0.074	0.316	0.824	0.383	0.068	229.0	97.0	80.3	0.0650
3	1.569	0.000	1.569	0.219	0.140	0.281	0.825	0.340	0.128	228.7	101.8	80.2	0.0650
4	1.570	0.000	1.570	0.310	0.198	0.250	0.824	0.303	0.182	229.0	106.3	80.3	0.0650
5	1.568	0.000	1.568	0.449	0.286	0.207	0.825	0.251	0.263	228.3	112.7	80.1	0.0648
6	1.565	0.000	1.565	0.563	0.359	0.173	0.824	0.210	0.330	228.1	118.0	80.0	0.0647
7	1.562	0.000	1.562	0.654	0.419	0.146	0.824	0.177	0.385	227.5	122.2	79.8	0.0645
8	1.563	0.000	1.563	0.864	0.553	0.074	0.823	0.090	0.507	226.8	131.7	79.6	0.0644
9	1.564	0.000	1.564	0.971	0.621	0.044	0.823	0.053	0.570	227.1	137.0	79.7	0.0644
10	1.564	0.000	1.564	1.011	0.646	0.027	0.811	0.033	0.589	230.5	140.3	80.9	0.0649
11	1.564	0.000	1.564	1.063	0.680	0.019	0.811	0.024	0.620	230.5	142.7	80.9	0.0649
12	1.564	0.000	1.564	0.000	0.000	0.000	0.811	0.000	0.000	230.6	92.1	80.9	0.0649

TABLE IV PUMPING COEFFICIENT DATA, MODEL A (180^{o}F)

1

*** HOT RIG PERFORMANCE *** TUPT: 850
2 RING DIFFUSER

DATE: 16 OCTOB 82

NUMBER OF PRIMARY NOZZLES: 4
PRIMARY NOZZLE DIAMETER: 2.25 INCHES
UPTAKE DIAMETER: 7.510 INCHES
AREA RATIO, AM/AP: 2.50
GAMMA: 1.3614

DATA TAKEN BY A KAVALIS

MIXING STACK LENGTH: 7.20 INCHES
MIXING STACK DIAMETER: 7.122 INCHES
MIXING STACK L/D: 1.50
STANDOFF RATIO: 0.50
AMBIENT PRESSURE: 30.08 INCHES HG

NR	PNH IN HG	DELPN IN H2C	TNH DEG F	ROTA	TBURN DEG F	TUPT DEG F	TAMB DEG F	PUPT IN H2O	PPLN IN H2O	SEC AREA SQ IN
1	4.60	6.80	189.6	33.0	1272.0	845.0	68.8	7.00	4.60	0.000
2	4.60	6.85	189.9	33.0	1272.0	844.0	68.5	7.50	4.10	1.767
3	4.60	6.85	189.3	33.0	1272.0	845.0	68.0	7.90	3.67	3.534
4	4.65	6.80	189.3	33.0	1270.0	847.0	68.0	8.30	3.27	5.301
5	4.65	6.85	189.2	33.0	1273.0	848.0	67.3	8.80	2.67	8.443
6	4.70	6.85	189.7	33.0	1274.0	848.0	70.8	9.20	2.20	11.585
7	4.70	6.85	190.2	33.0	1276.0	849.0	71.1	9.50	1.83	14.726
8	4.70	6.85	190.0	33.0	1274.0	850.0	70.5	10.30	0.93	27.293
9	4.70	6.85	189.6	33.0	1274.0	850.0	68.5	10.70	0.55	39.859
10	4.75	6.85	189.2	33.0	1273.0	852.0	69.3	10.80	0.35	52.425
11	4.75	6.85	189.0	33.0	1274.0	852.0	68.8	10.95	0.24	64.992
12	4.75	6.80	189.4	33.0	1277.0	852.0	70.3	11.10	0.00	******

NR	WPA LBM/S	WF LBM/S	WP LBM/S	WS LBM/S	W*	P*	T*	P*/T*	W*T**.44	UP FT/S	UM FT/S	UU FT/S	UMACH
1	1.092	0.010	1.102	0.000	0.000	0.188	0.405	0.465	0.000	331.2	132.2	115.6	0.0662
2	1.095	0.010	1.106	0.122	0.110	0.167	0.405	0.413	0.074	331.7	138.3	115.8	0.0663
3	1.096	0.010	1.106	0.230	0.208	0.149	0.404	0.369	0.140	331.7	143.6	115.8	0.0663
4	1.093	0.010	1.103	0.326	0.295	0.134	0.404	0.331	0.198	331.0	147.9	115.5	0.0661
5	1.097	0.010	1.107	0.469	0.424	0.108	0.403	0.268	0.284	331.9	155.1	115.9	0.0663
6	1.097	0.010	1.107	0.582	0.526	0.090	0.406	0.221	0.354	331.6	160.6	115.8	0.0663
7	1.097	0.010	1.107	0.675	0.610	0.075	0.406	0.184	0.410	331.5	165.0	115.8	0.0662
8	1.097	0.010	1.107	0.892	0.806	0.038	0.405	0.094	0.541	331.0	175.3	115.7	0.0661
9	1.097	0.010	1.108	1.004	0.907	0.022	0.403	0.055	0.608	330.8	180.4	115.6	0.0661
10	1.098	0.010	1.109	1.053	0.950	0.014	0.403	0.035	0.637	331.5	183.0	115.8	0.0662
11	1.098	0.010	1.109	1.081	0.975	0.010	0.403	0.024	0.654	331.4	184.3	115.8	0.0662
12	1.094	0.010	1.105	0.000	0.000	0.000	0.404	0.000	0.000	330.0	131.7	115.3	0.0659

TABLE V PUMPING COEFFICIENT DATA, MODEL A (850^{o} F)

1

*** HOT RIG PERFORMANCE *** TUPT: 950
2 RING DIFFUSER

DATE: 16 OCTOB 82 DATA TAKEN BY A KAVALIS

NUMBER OF PRIMARY NOZZLES: 4
PRIMARY NOZZLE DIAMETER: 2.25 INCHES
UPTAKE DIAMETER: 7.510 INCHES
AREA RATIO, AM/AP: 2.50
GAMMA: 1.3556

MIXING STACK LENGTH: 7.20 INCHES
MIXING STACK DIAMETER: 7.122 INCHES
MIXING STACK L/D: 1.50
STANDOFF RATIO: 0.50
AMBIENT PRESSURE: 30.08 INCHES HG

NR	PNH IN HG	DELPN IN H2O	TNH DEG F	ROTA	TBURN DEG F	TUPT DEG F	TAMB DEG F	PUPT IN H2O	PPLN IN H2O	SEC AREA SQ IN
1	6.10	6.10	190.0	36.0	1145.0	950.0	68.6	9.50	4.85	0.000
2	6.10	6.20	190.0	36.0	1149.0	950.0	70.7	9.90	4.35	1.767
3	6.10	6.20	190.5	36.0	1150.0	952.0	69.1	10.40	3.89	3.534
4	6.15	6.20	189.5	36.0	1150.0	952.0	70.1	10.80	3.45	5.301
5	6.20	6.20	189.9	36.0	1152.0	954.0	70.1	11.30	2.83	8.443
6	6.20	6.20	190.3	36.0	1155.0	955.0	70.1	11.70	2.35	11.585
7	6.20	6.20	190.7	36.0	1157.0	957.0	71.5	12.10	1.97	14.726
8	6.20	6.20	190.0	36.0	1156.0	957.0	70.1	12.90	1.01	27.293
9	6.25	6.15	190.0	36.0	1156.0	956.0	68.3	13.30	0.60	39.859
10	6.25	6.15	190.0	36.0	1158.0	959.0	69.4	13.60	0.38	52.425
11	6.25	6.15	190.2	36.0	1158.0	959.0	69.4	13.65	0.26	64.992
12	6.25	6.15	190.2	36.0	1160.0	961.0	71.2	13.80	0.00	******

NR	WPA LBM/S	WF LBM/S	WP LBM/S	WS LBM/S	W*	P*	T*	P*/T*	W*T**.44	UP FT/S	UM FT/S	UU FT/S	UMACH
1	1.057	0.011	1.069	0.000	0.000	0.181	0.375	0.482	0.000	347.3	138.6	120.4	0.0665
2	1.066	0.011	1.077	0.125	0.116	0.160	0.376	0.427	0.075	349.5	145.6	121.2	0.0669
3	1.065	0.011	1.077	0.237	0.220	0.143	0.375	0.382	0.143	349.5	151.0	121.2	0.0669
4	1.067	0.011	1.078	0.334	0.310	0.127	0.375	0.338	0.201	349.6	155.8	121.3	0.0669
5	1.067	0.011	1.079	0.482	0.447	0.104	0.375	0.277	0.290	349.7	163.0	121.3	0.0669
6	1.067	0.011	1.078	0.602	0.559	0.086	0.374	0.230	0.363	349.4	168.7	121.3	0.0668
7	1.066	0.011	1.078	0.700	0.649	0.072	0.375	0.193	0.422	349.5	173.5	121.3	0.0668
8	1.067	0.011	1.078	0.930	0.863	0.037	0.374	0.099	0.560	348.8	184.2	121.1	0.0667
9	1.064	0.011	1.075	1.049	0.976	0.022	0.373	0.059	0.632	347.1	189.0	120.5	0.0664
10	1.064	0.011	1.075	1.057	1.020	0.014	0.373	0.038	0.661	347.7	191.6	120.7	0.0664
11	1.063	0.011	1.075	1.125	1.046	0.010	0.373	0.026	0.678	347.5	192.9	120.7	0.0664
12	1.063	0.011	1.075	0.000	0.000	0.000	0.374	0.000	0.000	347.8	138.8	120.8	0.0664

TABLE VI PUMPING COEFFICIENT DATA, MODEL A (950° F)

TABLE VII

MIXING STACK PRESSURE DATA, MODEL A

	Axial Position	Mixing Stack Pressure (in H_2O referenced to B)		
Uptake Temperature		180	850	950
Position A	0.0	-1.96	-2.16	-2.25
	0.25	-1.15	-1.18	-1.23
	0.5	-0.23	-0.27	-0.17
	0.75	-1.26	-1.33	-1.25
Position B	0.0	-1.84	-2.09	-2.17
	0.25	-1.13	-1.22	-1.23
	0.5	-1.21	-1.35	-1.31
	0.75	-1.14	-1.27	-1.28
			PMS*	
Position A	0.0	-0.031	-0.017	-0.016
	0.25	-0.018	-0.009	-0.009
	0.5	-0.004	-0.002	-0.001
	0.75	-0.020	-0.010	-0.009
Position B	0.0	-0.029	-0.016	-0.015
	0.25	-0.018	-0.010	-0.009
	0.5	-0.019	-0.011	-0.009
	0.75	-0.018	-0.010	-0.009
Ambient Temperature (o F)		63.8	68.1	71.0
Primary Nozzle Velocity (ft/sec)		230.6	330.0	347.8

TABLE VIII

MIXING STACK TEMPERATURE DATA, MODEL A

Thermocouple Number	Axial Position	Mixing Stack Temperature (^oF)		
Uptake Temperature		180	850	950
6	0.0	62.0	xxxxx	xxxxx
7	0.0	57.0	xxxxx	xxxxx
8	0.41	63.0	134.0	161.0
9	0.41	65.0	155.0	207.0
10	0.36	67.0	171.0	203.0
11	0.46	66.0	130.0	139.0
12	0.61	71.0	188.0	210.0
13	0.76	83.0	247.0	262.0
14	0.89	72.0	218.0	268.0
15	0.89	92.0	292.0	309.0
16	0.84	62.0	xxxxx	xxxxx
17	0.94	82.0	233.0	254.0
Ambient		64.4	68.1	71.0

TABLE IX

SHROUD AND DIFFUSER TEMPERATURE DATA, MODEL A

	Axial Position	Temperature (o F)		
Uptake Temperature		180	850	950
Shroud	0.25	65.5	80.0	88.4
	0.5	65.9	90.3	96.7
	0.75	70.4	124.3	131.8
	1.0	78.7	185.2	204.6
	1.15	76.1	162.3	185.0
First Diffuser Ring	1.15	68.0	88.5	91.0
	1.25	68.9	92.0	95.5
Second Diffuser Ring	1.25	69.9	91.2	94.0
	1.5	79.1	156.6	170.0
Ambient		63.9	67.4	69.8

TABLE X

EXIT PLANE TEMPERATURE DATA, MODEL A

	Axial Position	r/Rms	Temperature (° F)		
Uptake Temperature			180	850	950
	0.0	1.123	81	160	165
	0.25	1.053	94	271	296
	0.5	0.983	103	330	367
	0.75	0.913	106	353	392
	1.0	0.843	108	361	404
	1.25	0.772	114	378	420
	1.5	0.702	115	400	440
	1.75	0.632	121	415	445
	2.0	0.562	126	438	468
	2.25	0.491	130	448	476
	2.5	0.421	132	464	496
	2.75	0.351	137	487	516
	3.0	0.281	138	495	524
	3.25	0.211	140	507	546
	3.5	0.140	140	515	552
	3.75	0.140	140	519	565
	4.0	0.0	140	521	571
	4.0	0.0	140	521	571
	3.75	0.070	140	523	563
	3.50	0.140	140	518	558
	3.25	0.211	140	508	545
	3.0	0.281	139	498	534
	2.75	0.351	136	485	524
	2.5	0.421	133	468	509
	2.25	0.491	125	453	494
	2.0	0.562	125	437	478
	1.75	0.632	120	423	467
	1.5	0.702	115	405	450
	1.25	0.772	112	390	439
	1.0	0.843	109	382	430
	0.75	0.913	106	372	419
	0.5	0.983	104	350	399
	0.25	1.053	94	290	350
	0.0	1.123	77	134	163
Ambient			63.8	68.7	71

*** HOT RIG PERFORMANCE ***
3 RING DIFFUSER

TUPT: 180

DATE: 4 FEB 83

DATA TAKEN BY A KAVALIS

NUMBER OF PRIMARY NOZZLES: 4
PRIMARY NOZZLE DIAMETER: 2.25 INCHES
UPTAKE DIAMETER: 7.510 INCHES
AREA RATIO, AM/AP: 2.50
GAMMA: 1.3991

MIXING STACK LENGTH: 7.20 INCHES
MIXING STACK DIAMETER: 7.122 INCHES
MIXING STACK L/D: 1.50
STANDOFF RATIO: 0.50
AMBIENT PRESSURE: 29.63 INCHES HG

NR	PNH IN HG	DELPN IN H2O	TNH DEG F	ROTA	TBURN DEG F	TUPT DEG F	TAMB DEG F	PUPT IN H2O	PPLN IN H2O	SEC AREA SQ IN
1	3.55	14.50	178.2	0.0	166.0	170.0	59.0	5.40	4.28	0.000
2	3.55	14.50	178.3	0.0	166.0	170.0	59.7	5.80	3.85	1.767
3	3.55	14.50	178.6	0.0	167.0	170.0	59.1	6.20	3.38	3.534
4	3.55	14.50	179.0	0.0	167.0	170.0	59.3	6.60	2.98	5.301
5	3.55	14.50	179.0	0.0	167.0	171.0	59.2	7.20	2.45	8.443
6	3.60	14.50	179.1	0.0	167.0	171.0	59.6	7.60	2.05	11.585
7	3.65	14.50	179.1	0.0	167.0	171.0	59.6	7.90	1.68	14.726
8	3.65	14.50	179.5	0.0	167.0	171.0	59.6	8.60	0.83	27.293
9	3.70	14.40	179.5	0.0	167.0	172.0	59.6	8.90	0.47	39.859
10	3.70	14.40	179.7	0.0	168.0	172.0	59.6	9.10	0.31	52.425
11	3.70	14.40	179.6	0.0	168.0	172.0	59.9	9.20	0.20	64.992
12	3.75	14.50	179.8	0.0	168.0	172.0	59.9	9.40	0.00	******

NR	WPA LBM/S	WF LBM/S	WP LBM/S	WS LBM/S	W*	P*	T*	P*/T*	W*T**.44	UP FT/S	UM FT/S	UU FT/S	UMACH
1	1.556	0.000	1.556	0.000	0.000	0.365	0.824	0.443	0.000	229.0	91.4	80.3	0.0653
2	1.556	0.000	1.556	0.118	0.076	0.329	0.825	0.399	0.070	228.7	97.0	80.2	0.0652
3	1.556	0.000	1.556	0.221	0.142	0.289	0.824	0.351	0.130	228.4	101.9	80.1	0.0651
4	1.555	0.000	1.555	0.311	0.200	0.256	0.824	0.310	0.184	228.1	106.1	80.0	0.0650
5	1.555	0.000	1.555	0.449	0.289	0.210	0.823	0.255	0.265	228.2	112.7	80.0	0.0650
6	1.556	0.000	1.556	0.564	0.362	0.176	0.823	0.213	0.333	228.1	118.2	80.0	0.0650
7	1.557	0.000	1.557	0.649	0.417	0.144	0.823	0.175	0.383	228.0	122.3	80.0	0.0650
8	1.557	0.000	1.557	0.845	0.543	0.071	0.823	0.087	0.499	227.5	131.4	79.8	0.0648
9	1.553	0.000	1.553	0.929	0.598	0.040	0.822	0.049	0.549	227.0	135.2	79.7	0.0647
10	1.552	0.000	1.552	0.992	0.639	0.027	0.822	0.032	0.586	226.9	138.2	79.6	0.0646
11	1.553	0.000	1.553	0.988	0.636	0.017	0.823	0.021	0.584	226.9	138.0	79.6	0.0646
12	1.559	0.000	1.559	0.000	0.000	0.000	0.823	0.000	0.000	227.6	90.9	79.9	0.0649

TABLE XI PUMPING COEFFICIENT DATA, MODEL B (180^{o} F)

*** HOT RIG PERFORMANCE *** TUPT: 850
3 RING DIFFUSER

DATE: 4 FEB 83

DATA TAKEN BY A KAVALIS

NUMBER OF PRIMARY NOZZLES: 4
PRIMARY NOZZLE DIAMETER: 2.25 INCHES
UPTAKE DIAMETER: 7.510 INCHES
AREA RATIO, AM/AP: 2.50
GAMMA: 1.3614

MIXING STACK LENGTH: 7.20 INCHES
MIXING STACK DIAMETER: 7.122 INCHES
MIXING STACK L/D: 1.50
STANDOFF RATIO: 0.50
AMBIENT PRESSURE: 29.63 INCHES HG

NR	PNH IN HG	DELPN IN H2O	TNH DEG F	ROTA	TBURN DEG F	TUPT DEG F	TAMB DEG F	PUPT IN H2O	PPLN IN H2O	SEC AREA SQ IN
1	4.30	6.50	179.2	34.0	1200.0	848.0	60.1	6.80	4.60	0.000
2	4.40	6.40	179.2	34.0	1200.0	847.0	60.1	7.20	4.17	1.767
3	4.40	6.40	179.1	34.0	1200.0	848.0	60.1	7.60	3.65	3.534
4	4.45	6.40	179.1	34.0	1200.0	851.0	59.9	7.95	3.25	5.301
5	4.45	6.40	178.9	34.0	1200.0	848.0	60.1	8.60	2.64	8.443
6	4.45	6.40	178.8	34.0	1200.0	850.0	60.2	8.90	2.17	11.585
7	4.50	6.40	178.7	34.0	1201.0	851.0	60.1	9.30	1.80	14.726
8	4.50	6.40	178.8	34.0	1202.0	850.0	60.1	10.10	0.90	27.293
9	4.60	6.40	178.7	34.0	1202.0	851.0	60.2	10.40	0.51	39.859
10	4.60	6.40	178.8	34.0	1201.0	851.0	60.1	10.60	0.33	52.425
11	4.60	6.40	178.6	34.0	1201.0	852.0	60.0	10.70	0.22	64.992
12	4.60	6.45	178.5	34.0	1202.0	854.0	60.2	10.90	0.00	******

NR	WPA LBM/S	WF LBM/S	WP LBM/S	WS LBM/S	W*	P*	T*	P*/T*	W*T**.44	UP FT/S	UM FT/S	UU FT/S	UMACH
1	1.065	0.011	1.076	0.000	0.000	0.191	0.397	0.479	0.000	329.1	131.4	114.9	0.0657
2	1.059	0.011	1.070	0.123	0.115	0.175	0.398	0.441	0.076	326.6	136.3	114.0	0.0652
3	1.059	0.011	1.070	0.229	0.214	0.153	0.397	0.386	0.143	326.4	141.4	114.0	0.0652
4	1.060	0.011	1.071	0.325	0.303	0.136	0.396	0.343	0.202	327.1	146.3	114.2	0.0653
5	1.060	0.011	1.071	0.466	0.435	0.111	0.397	0.279	0.290	325.9	152.6	113.8	0.0651
6	1.060	0.011	1.071	0.580	0.542	0.091	0.397	0.229	0.361	326.0	158.1	113.9	0.0651
7	1.061	0.011	1.072	0.671	0.627	0.075	0.397	0.190	0.417	326.2	162.6	114.0	0.0651
8	1.061	0.011	1.072	0.880	0.821	0.038	0.397	0.095	0.547	325.2	172.1	113.6	0.0650
9	1.062	0.011	1.073	0.967	0.901	0.021	0.397	0.054	0.600	325.6	176.5	113.8	0.0650
10	1.062	0.011	1.073	1.023	0.954	0.014	0.397	0.035	0.635	325.5	179.1	113.8	0.0650
11	1.062	0.011	1.073	1.036	0.965	0.009	0.396	0.023	0.642	325.7	179.7	113.8	0.0650
12	1.067	0.011	1.077	0.000	0.000	0.000	0.396	0.000	0.000	327.2	130.6	114.4	0.0653

TABLE XII PUMPING COEFFICIENT DATA, MODEL B (850° F)

*** HOT RIG PERFORMANCE ***
3 RING DIFFUSER

TUPT: 950

DATE: 4 FEB 83

DATA TAKEN BY A KAVALIS

NUMBER OF PRIMARY NOZZLES: 4
PRIMARY NOZZLE DIAMETER: 2.25 INCHES
UPTAKE DIAMETER: 7.510 INCHES
AREA RATIO, AM/AP: 2.50
GAMMA: 1.3556

MIXING STACK LENGTH: 7.20 INCHES
MIXING STACK DIAMETER: 7.122 INCHES
MIXING STACK L/D: 1.50
STANDOFF RATIO: 0.50
AMBIENT PRESSURE: 29.63 INCHES HG

NR	PNH IN HG	DELPN IN H2O	TNH DEG F	ROTA	TBURN DEG F	TUPT DEG F	TAMB DEG F	PUPT IN H2O	PPLN IN H2O	SEC AREA SQ IN
1	5.00	6.10	177.9	37.0	1241.0	950.0	58.1	7.90	4.60	0.000
2	5.00	6.10	177.9	37.0	1243.0	952.0	58.1	8.40	4.10	1.767
3	5.05	6.10	177.9	37.0	1240.0	952.0	58.1	8.80	3.62	3.534
4	5.10	6.10	177.9	37.0	1240.0	952.0	58.2	9.30	3.20	5.301
5	5.10	6.10	177.9	37.0	1240.0	952.0	58.1	9.70	2.62	8.443
6	5.10	6.10	177.9	37.0	1240.0	952.0	58.2	10.20	2.15	11.585
7	5.15	6.10	177.7	37.0	1241.0	953.0	58.3	10.50	1.78	14.726
8	5.15	6.10	177.3	37.0	1243.0	953.0	58.1	11.20	0.92	27.293
9	5.15	6.10	177.5	37.0	1242.0	955.0	58.2	11.60	0.52	39.859
10	5.15	6.10	177.5	37.0	1241.0	956.0	58.1	11.70	0.32	52.425
11	5.20	6.10	177.5	37.0	1244.0	955.0	58.0	11.90	0.23	64.992
12	5.20	6.10	177.5	37.0	1244.0	957.0	57.9	12.05	0.00	******

NR	WPA LBM/S	WF LBM/S	WP LBM/S	WS LBM/S	W*	P*	T*	P*/T*	W*T**.44	UP FT/S	UM FT/S	UL FT/S	UMACH
1	1.045	0.012	1.057	0.000	0.000	0.169	0.367	0.461	0.000	348.3	135.1	121.3	0.0670
2	1.045	0.012	1.057	0.122	0.115	0.151	0.367	0.411	0.074	348.4	145.0	121.3	0.0669
3	1.045	0.012	1.057	0.229	0.217	0.133	0.367	0.363	0.139	348.2	150.1	121.2	0.0669
4	1.046	0.012	1.058	0.323	0.305	0.118	0.367	0.321	0.196	348.1	154.5	121.2	0.0669
5	1.046	0.012	1.058	0.465	0.440	0.096	0.367	0.263	0.283	347.6	161.2	121.1	0.0668
6	1.046	0.012	1.058	0.578	0.547	0.079	0.367	0.216	0.352	347.2	166.4	120.9	0.0667
7	1.047	0.012	1.059	0.669	0.632	0.065	0.367	0.179	0.406	347.4	170.8	121.0	0.0668
8	1.047	0.012	1.059	0.891	0.842	0.034	0.367	0.092	0.541	346.8	181.1	120.8	0.0667
9	1.047	0.012	1.059	0.979	0.924	0.019	0.366	0.052	0.594	346.8	185.3	120.9	0.0666
10	1.047	0.012	1.059	1.010	0.953	0.012	0.366	0.032	0.613	346.9	186.8	120.9	0.0666
11	1.048	0.012	1.060	1.061	1.002	0.008	0.366	0.023	0.644	346.8	189.2	120.9	0.0666
12	1.048	0.012	1.060	0.000	0.000	0.000	0.365	0.000	0.000	347.1	138.6	121.0	0.0667

TABLE XIII PUMPING COEFFICIENT DATA, MODEL B (950^{O} F)

TABLE XIV

MIXING STACK PRESSURE DATA, MODEL B

	Axial Position	Mixing Stack Pressure (in H_2O referenced to B)		
Uptake Temperature		172	850	950
Position A	0.00	-1.70	-2.02	-2.18
	0.25	-1.00	-1.15	-1.20
	0.50	-0.23	-0.35	-0.20
	0.75	-1.16	-1.30	-1.26
Position B	0.00	-1.78	-2.00	-2.12
	0.25	-0.98	-1.07	-1.15
	0.50	-1.15	-1.27	-1.23
	0.75	-1.00	-1.10	-1.25
		PMS*		
Position A	0.00	-0.028	-0.016	-0.016
	0.25	-0.016	-0.009	-0.009
	0.50	-0.004	-0.003	-0.001
	0.75	-0.019	-0.009	-0.009
Position B	0.00	-0.029	-0.016	-0.016
	0.25	-0.016	-0.009	-0.008
	0.50	-0.019	-0.010	-0.009
	0.75	-0.016	-0.009	-0.010
Ambient Temperature (° F)		60.0	60.0	59.0
Primary Nozzle Velocity (ft/sec)		227.6	327.2	347.1

TABLE XV

MIXING STACK TEMPERATURE DATA, MODEL B

Thermocouple Number	Axial Position	Mixing Stack Temperature (°F)		
Uptake Temperature		172	850	950
6	0.00	56	91	110
7	0.00	55	80	98
8	0.36	66	170	202
9	0.41	61	138	158
10	0.41	65	179	215
11	0.46	63	132	146
12	0.61	74	204	228
13	0.76	82	250	276
14	0.84	82	238	260
15	0.89	69	189	215
16	0.89	83	262	290
17	0.94	56	79	92
Ambient		54	54	53.5

TABLE XVI

SHROUD AND DIFFUSER TEMPERATURE DATA, MODEL B

	Axial Position	Temperature (o F)		
Uptake Temperature		172	850	950
Shroud	0.20	61.1	62.5	63.8
	0.40	60.1	65.1	67.6
	0.60	62.4	76.2	79.8
	0.80	64.0	86.1	91.4
First Diffuser Ring	0.90	61.4	61.2	61.5
	1.00	61.8	62.8	63.3
Second Diffuser Ring	1.05	62.2	62.7	63.0
	1.15	63.7	70.4	71.3
Third Diffuser Ring	1.25	63.2	71.6	73.4
	1.35	66.1	80.7	81.7
	1.50	73.7	118.2	122.4
Ambient		60.0	60.0	58.0

TABLE XVII

MIXING STACK, SHROUD, AND DIFFUSER EXTERNAL SURFACE TEMPERATURE DATA, MODEL B

	Axial Position (L/D)	Temperature (° F)		
Uptake Temperature		172	850	950
Mixing Stack	0	61.5	76.9	79.6
	0.07	62.2	74.5	89.4
	0.14	61.2	67.7	68.4
Shroud	0.21	60.5	57.0	59.0
	0.28	60.5	58.2	60.1
	0.35	60.5	58.3	60.5
	0.42	60.6	59.4	61.1
	0.49	60.6	60.3	62.6
	0.56	60.6	62.2	65.2
	0.63	60.7	66.0	67.2
	0.70	60.8	68.4	71.0
	0.77	61.0	72.0	72.0
First Diffuser Ring	0.84	60.8	58.2	59.5
	0.91	61.0	60.5	58.4
	0.98	61.1	59.3	61.0
Second Diffuser Ring	1.05	61.4	59.6	61.4
	1.12	61.9	62.0	63.5
	1.19	62.2	63.0	66.3
Third Diffuser Ring	1.26	63.0	70.0	62.5
	1.33	64.5	77.5	79.6
	1.40	66.0	93.0	97.0
	1.47	69.3	107.0	108.0
Ambient		58.9	53.5	57.0

TABLE XVIII

EXIT PLANE TEMPERATURE DATA, MODEL B

	Axial Position	r/Rms	Temperature (° F)		
Uptake Temperature			172	850	950
	0.0	1.193	60	60	60
	0.25	1.123	80	178	217
	0.50	1.053	88	212	258
	0.75	0.983	92	295	313
	1.00	0.913	93	325	349
	1.25	0.843	102	339	378
	1.50	0.772	105	360	396
	1.75	0.702	110	380	420
	2.00	0.632	114	404	441
	2.25	0.562	120	425	464
	2.50	0.491	124	443	481
	2.75	0.421	127	458	498
	3.00	0.351	130	468	518
	3.25	0.281	130	482	530
	3.50	0.211	132	490	543
	3.75	0.140	132	494	550
	4.00	0.070	132	501	560
	4.25	0.00	132	502	563
	4.25	0.00	132	508	563
	4.00	0.070	132	508	562
	3.75	0.140	132	501	556
	3.50	0.211	132	494	546
	3.25	0.281	132	481	533
	3.00	0.351	130	469	518
	2.75	0.421	129	458	505
	2.50	0.491	126	440	485
	2.25	0.562	123	418	467
	2.00	0.632	120	404	450
	1.75	0.702	114	384	426
	1.50	0.772	115	365	408
	1.25	0.843	108	347	386
	1.00	0.913	104	325	358
	0.75	0.983	104	295	330
	0.50	1.053	92	260	278
	0.25	1.123	84	200	216
	0.00	1.193	60	60	60
Ambient			60	60	58

APPENDIX A

GAS GENERATOR OPERATION

I. PRIMARY AIR COMPRESSOR OPERATION.

The primary air flow for the gas generator is supplied by a Carrier Model 18P352 three stage centrifugal air compressor located in Building 230. The compressor is driven through a Western Gear Model 95HSA speed increasing gearbox by a 300 horsepower General Electric induction motor. The compressor serves various other experiments both in Building 230 and 249. Figure 8 is a schematic of the compressor system layout. The cooling water system serves both the Carrier compressor and the Sullivan compressor for the supersonic wind tunnel in Building 230.

Lube oil for the compressor and speed increaser bearings is supplied from an external sump by either an attached pump or an electrically driven auxiliary pump. The lube oil is cooled in a closed loop oil to fresh water heater exchanger. Cooling water circulates within its own loop and is cooled in an evaporative cooling tower which stands between Buildings 230 and 249. Makeup is automatically provided to the fresh water loop by a float operated valve in the cooling tower.

It is recommended that the lube oil system for the compressor be started approximately one hour prior to compressor lightoff. This ensures adequate pre-lubrication

and warms the oil to some degree, decreasing starting loads. This is critical, as the compressor operates at near the capacity of the breaker in the supplying substation. Should this breaker trip out during the starting sequence it will be necessary to call the trouble desk and have base electricians reset it.

During periods when operations are being conducted daily or when it is desired to operate early in the morning, it is permissable to leave the auxiliary oil pump running overnight with the cooling water system secured. This will maintain the lube oil at a temperature suitable for lightoff and eliminate this delay.

When fully warmed up the compressor supplies air to the gas generator at 170-190° F. It normally takes the compressor about one hour to reach stable operation at this temperature. Although it is possible to obtain a gas generator lightoff with a lower air supply temperature, stable operation enhances data taking and reduces the number of control adjustments required during data runs. It is, therefore, desirable to allow the system to fully stabilize prior to lighting off the gas generator or collecting data. The following lightoff sequence is recommended:

A. Check the oil level in the compressor's external sump. Oil should be within four inches of the top of the sight glass.

B. Start the auxiliary oil pump by positioning the "hand-off-automatic" switch (Figure 33) in the "hand" position. The electric pump will start and oil pressure should registered approximately 30 PSIG. Inspect the system for leaks and note the level in the external sump.

C. Wait 45 minutes to one hour. During this period the compressor bearing temperatures should rise to approximately 70° F.

D. Line up the combustion gas generator for operation.

1. Open the two manometer isolation valves at the pressure taps on either side of the inlet reducing section (Figure 20). Reconnect manometer tubing at the manometers if it has previously been disconnected.
2. Ensure the main air supply butterfly valve is fully closed (Figure 3).
3. Open the air supply bypass globe valve two and one quarter turns (Figure 3).
4. Open the manually operated 4 inch butterfly isolation valve (Figure 4).
5. Ensure that the main panel is not connected to the isolation transformer, which limits the power available to a lower level than the actual

required for the apparatus. The electric circuit of the system is shown in Figure 29.

6. Energize the main power panel (Figure 34) and open the electrically operated burner air supply and cooling air bypass valves fully.
7. Ensure the gas generator exhaust area is clear.

E. Start the air compressor fresh water cooling system:

1. Check the water level in the cooling tower; it should be at the level of the inlet line.
2. Vent the cooling water pump casing. Open the petcock on the suction side of the pump casing until all air in the suction line is expelled.
3. Ensure valve "A" to the Sullivan compressor is closed.
4. Open valve "B" to the Carrier compressor.
5. Start the cooling water pump and cooling tower fan (Figure 35). The fan is interlocked with the pump and will not start unless the pump is running.
6. Inspect the cooling tower drip lattice to ensure water is circulating.

F. Open the drain on the air compressor air cooling bank (Figure 36).

G. Ensure the compressor air suction valve is fully closed (indicator vertical) (Figure 37).

WARNING: When in operation the compressor produces hazardous noise. Ensure all personnel in the vicinity are wearing adequate hearing protection prior to starting the compressor.

H. Start the air compressor motor (Figure 7), the controller uses an automatic two stage start circuit.

I. When the compressor is fully up to speed, switch the auxiliary lube oil pump to the "automatic" position. Lube oil pressure should remain about 24-30 PSIG. Oil is now being supplied by the attached pump driven by the speed increasing gearbox. If the oil pressure should fall to 12 PSIG, the auxiliary pump will start automatically.

J. When compressor operation has stabilized, slowly open the suction valve until the indicator is in the full open (horizontal) position. Air is now being supplied to the gas generator. Bypass air from the supply to other experiments will also be discharged outside the rear of building 230. Normally it is not necessary to secure this bypass flow, but in unusual circumstances it may be stopped by closing the isolation valve on the cooling bank (Figure 36).

K. Operation of the air compressor should be monitored periodically.

1. Normal oil pressure from the attached pump is 24 PISG. Specified bearing pressures are 20-25 PSIG.

2. Normal oil pressure from the auxiliary electric pump is 30 PSIG.

3. Normal oil temperature at the outlet of the lube oil cooler is 100-105° F (135° F maximum).

4. Normal Bearing temperatures for the compressor are 140-160° F. Speed increaser oil temperature is normally 120-130° F.

5. Do not allow any bearing temperature to exceed 200° F. In the event bearing temperatures rise above 180° F during normal operation, the oil cooler should be inspected for proper water temperature and flow rate.

II. GAS GENERATOR LIGHT OFF

Allow the air compressor to operate for approximately one hour in order for air inlet temperature to the gas generator to stabilize.

A. Approximately 15 minutes prior to gas generator light off, line up the fuel system and place it in operation.

   1. Open the fuel tank suction valve (Figure 10) and bulkhead isolation valve (Figure 11).

2. Ensure the solenoid operated emergency fuel cutoff valve is closed and close the HP pump manual discharge valve.
3. Open the nozzle box drain valve.
4. If this is the first time the system is being placed in operation, open both the fuel control valve (Figure 14) and the needle trimmer valve (Figure 13) fully. If the trimmer valve is known to be properly set, it need not be adjusted as described in this and following steps.
5. Start the fuel supply pump. Fuel supply pressure will be 14-16 PSIG.
6. Start the HP pump. With both trimmer and fuel control valves fully open the discharge pressure will be 25-30 PSIG. With the trimmer valve properly set and the fuel control valve fully open, the HP pump discharge pressure will be 80 PSIG.
7. If the trimmer valve is to be adjusted, close the fuel control valve with the trimmer valve fully open. Observing the HP pump discharge pressure, slowly close the trimmer valve until the HP pump pressure reaches 350 PSIG. The trimmer valve is now set and the fuel control valve should provide smooth control over a range of 80-350 PSIG HP pump discharge pressure. All subsequent fuel

control adjustments will be made using the fuel control valve.

8. Using the fuel control valve, set the hp pump discharge pressure at 200 PSIG and allow the system to recirculate for 10-15 minutes to warm the fuel. This facilitates combustion and ensures a clean lightoff.

B. When the inlet air temperature reaches 170-180^{o} F, the gas generator may be lighted off.

1. Adjust inlet air bypass valve to obtain a pressure of approximately 4.0 in Hg at the upstream side of the inlet reducing section (PNH).

2. Ensure the burner air valve is fully open. Adjust the bypass cooling air valve to obtain a pressure drop across the U-tube of 1.60 inches H_2O. In some cases it may be necessary to leave the cooling air bypass valve fully open and reduce the inlet air pressure (PNH) slightly to obtain this setting. The pressure drop across the inlet reducing section (DELPN) will be about 15 inches H O. This provides the recommended lightoff air fuel ratio of 20.

3. Open the HP pump manual discharge valve fully.

4. Set the high temperature (Type K) readout to monitor burner temperature (TBURN). Set the low

temperature (Type T) readout to monitor air inlet temperature (TNH).

5. Ensure the gas generator exhaust area is clear.
6. Adjust the HP pump discharge pressure to 150 PSIG.
7. Turn the ignitor switch located behind the manual isolation valve, Figure 7, to the "ME IGN" position.
8. Depress and hold down the spring loaded ignitor switch for 10 seconds.
9. While continuing to hold the ignitor switch depressed, open the solenoid operated emergency fuel cutoff valve. Ignition should be observed in 6-12 seconds. If the gas generator fails to light, close the emergency fuel cutoff valve and release the ignitor switch. Allow the system to purge for 5 minutes or until no raw fuel is being expelled from the primary nozzle. If the gas generator fails to light, raw fuel will be expelled from the primary nozzles and will collect in the base of the secondary plenum. This should be wiped up prior to continuing.
10. When ignition is observed, release the ignitor switch.

11. Observe the burner temperature. When the burner temperature reaches 1000o F begin reducing fuel pressure toward minimum (70-75 PSIG at the burner nozzle, (PNOZ)) to stabilize burner temperature between 1000 and 1300o F.

WARNING: Do not allow burner temperature to exceed 1500o F.

It will be necessary to close the cooling air bypass valve to about 50 percent open to achieve stable operation at the desired burner temperature.

CAUTION: Do not allow burner temperature to fall below 1000o F. The gas generator will begin to emit white smoke when the burner temperature falls to about 950o F and combustion will cease at a burner temperature of about 800o F. If combustion ceases there will be a noticable change in sound intensity accompanied by quantities of white smoke and rapidly falling burner temperature; immediately close the emergency fuel cutoff valve. Readjust fuel and air controls to lightoff settings and reinitiate the lightoff sequence.

The prescribed lightoff sequence usually leads to stable operation with an uptake temperature or 400-500o F and an uptake Mach number of about 0.07.

<u>WARNING</u>: Do not allow uptake temperature to exceed 1200o F at any time.

---

12. When stable operation has been established, close the nozzle box drain valve prior to attempting to adjust the uptake Mach number.

III. <u>TEMPERATURE/MACH NUMBER CONTROL</u>

The control process consists of an iterative sequence of adjustments in the uptake temperature (TUPT), inlet air pressure (PNH), and bypass cooling air mass flow. Some practice is necessary to achieve reasonable accuracy in the adjustment process. It must be kept in mind that effect of the bypass cooling air valve varies depending on the valve's initial position. When the bypass valve is more than 50 percent open, opening the valve reduces air flow through the burner, increasing burner temperature (TBURN), however,the increase in the proportion of cool bypass air mixing with the combustion gas results in a lower uptake temperature. When a majority of the air flow is already passing through the

combustion chamber, that is, when the bypass valve is less than 50 percent open, and particularly when it is less than 25 percent open, the increase in burner temperature resulting from opening the bypass valve more than offsets the increased proportion of cooling air and the uptake temperature will raise when the bypass valve is opened. With these cautions in mind, the following adjustment procedure is recommended:

A. Adjust the fuel control valve to obtain the desired uptake temperature. Do not allow burner temperature to fall below 1000o F or to exceed 1300o F during this process.

B. As burner temperature approaches one of the limits, change air flow through the burner either by adjusting the bypass valve or the inlet globe valve. Choice of control device depends on the prior operating state. If the system has been stabilized at the desired Mach number it is usually best to control burner temperature during transitions by using the inlet globe valve. The key operating parameters are uptake temperature (TUPT) and uptake pressure (PUPT). Burner temperature is monitored to ensure safe combustion is maintained. For operation with uptake an Mach number of approximately 0.065, the values in Table XIX are recommended:

TABLE XIX

RECOMMENDED INITIAL CONTROL SETTINGS

TUPT (^{o}F)	PUPT (inches H_2O)
950	13.3
850	11.1
750	10.5
650	9.6
550	9.0
175	8.8

C. Compute the uptake Mach number (UMACH) using the formula:

$$UMACH = 1.037 \times 10^{-1} (TUPTR/\gamma)^{.05} \times ((((PNH + B) \times DELPN / TNHR)^{0.5} + (2.318 \times 10^{-4} \times ROTA) + 2.085 \times 10^{-1}) / (B + (PUPT / 13.5717)))$$

(eqn. A.1)

where: UMACH = Uptake Mach number

TUPTR = Absolute uptake temperature (^{o}R)

γ = Ratio of specific heats for air

TABLE XX

VALUES OF THE RATIO OF SPECIFIC HEATS FOR AIR

TUPT ($^{\circ}$F)	γ
175	1.3991
550	1.3805
650	1.3741
750	1.3677
850	1.3614
950	1.3556

PNH = Air pressure before the inlet reducing section (inches Hg)

B = Corrected atmospheric pressure (inches Hg)

DELPN = Pressure drop across the inlet reducing section (inches H_2O)

TNHR = Absolute air temperature before the inlet reducing section ($^{\circ}$R)

ROTA = Fuel mass flow rotameter reading

PUPT = Gas pressure in the uptake section (inches H_2O)

D. Adjust the uptake temperature and pressure as necessary using a combination of inlet globe valve, cooling air bypass valve, and fuel control valve changes until the desired test Mach number is obtained.

E. If inlet air temperature has been allowed to stabilize prior to gas generator operation, it will be found that, once the desired uptake temperature

and Mach number have been set, no adjustments to the system will be required during data runs. Uptake temperature will be maintained within plus or minus four degrees and uptake Mach number will vary less than 0.001 under most circumstances. The largest variations in uptake Mach number observed have been during pumping coefficient runs when changes in secondary flow induce large changes in uptake pressure. If the gas generator is at the operating point prior to closing the plenum, it will be unnecessary to make adjustments for the slight increase (0.0005 to 0.0010) in Mach number which occurs when secondary flow is shut off.

IV. SECURING THE SYSTEM

A. When data runs are complete, shut down the gas generator by reducing the fuel pressure to minimum and immediately closing the solenoid operated emergency fuel cutoff valve.

1. Shut off the high pressure fuel pump
2. Shut off the fuel supply pump.
3. Open the cooling air bypass valve fully.
4. Open the inlet bypass globe valve until an inlet pressure (PNH) of 4.0-5.0 inches Hg is obtained.

5. Allow the gas generator to run in this manner until the uptake temperature drops to approximately the inlet air temperature.

6. Close the fuel system bulkhead and tank isolation valves. It is good practice to refill the fuel service tank at the end of each operating period. Keeping the tank full of fuel reduces moisture buildup from condensation. Any water or sediment which might enter the tank during filling will have time to settle out and can be removed through the stripping connection prior to the next lightoff.

B. When the gas generator has cooled sufficiently, the air compressor may be shut down.

1. Close the compressor suction butterfly valve.

2. Stop the electric motor.

3. When the compressor oil pressure falls below 20 PSIG, switch the auxiliary oil pump control from the "automatic" to the "hand" position.

4. Allow the lube oil system to run for one hour or until the compressor bearing temperatures are less than 80° F.

5. Stop the auxiliary lube oil pump.

6. Stop the cooling tower fan and cooling water pump.

C. Close the 4 inch butterfly manual isolation valve.

D. Close the inlet bypass globe valve.

E. Open the nozzle box drain valve.

F. Close the manometer isolation valves. It is also good practice to disconnect the inlet air pressure (PNH) and reducing section pressure drop (DELPN) manometers at the manometer. Other users of the compressor operate at pressures sufficient to over-pressurize these instruments. Over-pressurization of the mercury manometer which measures the inlet pressure could result in a hazardous mercury spill.

G. De-energize the main power panel and shut off the thermocouple readouts. It is recommended for maintenance reasons, to disconnect the temperature readouts and store them in a dry environment (in the storeroom 208 at building 234) whenever runs are not taking place for a long period of time.

APPENDIX B

UNCERTAINTY ANALYSIS

The determination of he uncertainties in the experimentally determined pressure coefficients and pumping coefficients was made using the methods described by Kline and McClintock [Ref. Kline]. The basic uncertainty analysis for the cold flow eductor model test facility was conducted by Ellin [Ref. Ellin]. Hill [Ref. Hill] follows this development in analysis of the hot flow facility. Hill's analysis has been corrected by Eick [Ref. Eick] for changes in the measured uncertainties resulting from the installation of new fuel flow measuring equipment. The uncertainties obtained using the second order equation suggested by Kline and McClintock [Ref. 11] were applicable to the experimental work conducted during the present research and are listed here.

UNCERTAINTY IN MEASURED VALUES

Parameter	Value	Uncertainty
TAMB	537 R	1
TUPT	1415 R	1
B	29.83 in Hg	0.005
DELPN	6.20 in H_2O	0.05
PUPT	13.6 in $H2^O$	0.05
ROTA	28.0	0.2
PHN	5.9 in Hg	0.05
TNH	649 R	0.2
PPLN	5.18 in $H2^O$	0.01

UNCERTAINTY IN CALCULATED VALUES

P*/T*	1.7%
W*T*o	1.4%

```
C     J A HILL                     23 MAY 79,   REVISED 6 AUG 79
C     I J EICK                     REVISED 26  JUN 82
C     THIS PROGRAM READS RAW DATA FROM THE HOTRIG EXPERIMENT, PERFORMS THE
C     DATA REDUCTION AND YIELDS TABULAR OUTPUT FOR PUMPING COEFFICIENT
C     DETERMINATION.
C
C
C     **************************
C     VARIABLE NAMES
C
C     AM     AREA OF MIXING STACK, SQ FT
C     AMAP   AM/AP
C     AP     AREA OF PRIMARY NOZZLES, SQ FT
C     AUP    AREA OF UPTAKE, SQ FT
C     B      BAROMETER READING, IN HG
C     C1     CONVERSION OF P/RT TO DENSITY
C     C2     CONVERSION OF INCH WATER TO INCH HG
C     C3     CONVERSION OF DEG F TO DEG R
C     C4     CONVERSION OF IN H2O TO LBF/SQ FT
C     DATE   DATE OF RUN
C     DELPN  PRESSURE DROP ACROSS ENTRANCE NOZZLE, IN H2O
C     DM     DIAMETER OF MIXING STACK, IN
C     DP     DIAMETER OF PRIMARY NOZZLES, IN
C     DU     DIAMETER OF UPTAKE, IN
C     GAMMA  RATIO OF AIR SPECIFIC HEATS
C     LD     LENGTH TO DIAMETER RATIO OF MIXING STACK
C     LMS    LENGTH OF MIXING STACK, IN
C     MUPT   NOMINAL UPTAKE TEMPERATURE FOR THE RUN
C     MR     NUMBER OF DIFFUSER RINGS
C     NNOZ   NUMBER OF PRIMARY NOZZLES
C     NR     NUMBER OF RUNS
C     PPLN   PRESSURE DROP ACROSS SECONDARY NOZZLES, IN H2O
C     PNH    PRESSURE UPSTREAM OF ENTRANCE NOZZLE, IN HG
C     PRTR   P*/T*
C     PSTR   NON DIMENSIONAL PRESSURE, P*
C     PUPT   UPTAKE PRESSURE, IN H2O
C     RHOA   DENSITY OF AMBIENT AIR, LBM/CU FT
C     RHOM   DENSITY IN MIXING STACK, LBM/CU FT
C     RHOP   DENSITY AT PRIMARY NOZZLE, LBM/CU FT
C     RHOS   DENSITY OF SECONDARY AIR, LBM/CU FT
C     RHOUP  DENSITY IN UPTAKE, LBM/CU FT
C     ROTA   FUEL MASS FLOW ROTAMETER READING
C     SD     STANDOFF RATIO
C     TAMB   AMBIENT TEMPERATURE, DEG F
C     TAMBR  AMBIENT TEMPERATURE, DEG R
C     TBURN  BURNER TEMPERATURE, DEG F
C     TNH   ENTRANCE NOZZLE TEMPERATURE, DEG F
C     TNHR  ENTRANCE NOZZLE TEMPERATURE, DEG R
```

```
C   TSTR   NON DIMENSIONAL TEMPERATURE, T*
C   TUPT   UPTAKE TEMPERATURE, DEG F
C   TUPTR  UPTAKE TEMPERATURE, DEG R
C   UM     VELOCITY IN MIXING STACK, FT/SEC
C   UMACH  UPTAKE MACH NUMBER
C   UP     VELOCITY IN PRIMARY NOZZLES, FT/SEC
C   UU     VELOCITY IN UPTAKE, FT/SEC
C   WF     MASS FLOW OF FUEL, LBM/SEC
C   WPA    MASS FLOW OF PRIMARY AIR, LBM/SEC
C   WP     MASS FLOW THROUGH PRIMARY NOZZLES, LBM/SEC
C   WS     MASS FLOW OF SECONDARY AIR, LBM/SEC
C   WSTR   NON DIMENSIONAL MASS FLOW RATE, W*
C   WSTR44 EMPIRICAL PUMPING COEFFICIENT
C
C
C
C   **********************************
C     INPUT AND INITIAL DATA
C
      IMPLICIT REAL*8(A-H,O-W)
      REAL*4 LD,LMS
C
      DIMENSION DATE(2)
      DIMENSION PNH(13),DELPN(13),TNH(13),ROTA(13), TBURN(13),TUPT(13),
     *PUPT(13),PPLN(13),TAMB(13),SECAIR(13)
      DIMENSION WPA(13),WF(13),WP(13),WS(13),WSTR(13),PSTR(13),TSTR(13),
     *PRTR(13),WSTR44(13),UP(13),UM(13),UU(13),UMACH(13)
C
      DATA NNOZ/4/,DP/2.25D0/,DU/7.51D0/,AMAP/2.50D0/,AP/.1104466D0/
     *,DM/7.122D0/,SD/.5D0/,AM/.2766504D0/,
     *AUP/.3076148D0/
      DATA C1/1.321566D0/,C2/13.5717D0/,C3/459.67D0/,C4/5.19408D0/
      DATA SECAIR/0.0D0,1.767146D0,3.534292D0,5.301438D0,8.44303D0,
     *11.584623D0,14.726216D0,27.292583D0,39.858957D0,52.425327D0,
     *64.991698D0,2*1004.0D13/
      READ (5,80) NR,LMS,LD
80    FORMAT(I2,F6.3,F4.2)
      DO 555 JJK=1,NR
      READ (5,100) DATE,B,GAMMA,MR,MTUPT
100   FORMAT(2A8,F5.2,F6.4,I1,I3)
C
C
      DO 90 I=1,12
      READ (5,110) PNH(I),TNH(I),DELPN(I),ROTA(I),TBURN(I),TUPT(I),
     *PUPT(I),PPLN(I),TAMB(I)
110   FORMAT (10 F8.3)
C
C
```

```
C
C   ************************
C     DATA REDUCTION
C
      TUPTR=TUPT(I)+C3
      TAMBR=TAMB(I)+C3
      TNHR=TNH(I)+C3
      WPA(I)=1.74619050126D0*DSQRT((PNH(I)+B)*DELPN(I)/TNHR) +
     *0.0394759658lD0
      WF(I)=ROTA(I)
      IF (ROTA(I) .NE. 0.0D0) WF(I)=(0.40475919622D0*ROTA(I)-
     *3.0715942736D0)*1.0D-3
      WP(I)=WPA(I)+WF(I)
      RHOUP=C1*(B+(PUPT(I)/C2))/TUPTR
      RHOS=C1*(B-(PPLN(I)/C2))/TAMBR
      RHOP=RHOS*TAMBR/TUPTR
      RHOA=C1*B/TAMBR
      WS(I)=.123808D0*SECAIR(I)*DSQRT(RHOA*PPLN(I))
      WSTR(I)=WS(I)/WP(I)
      UP(I)=WP(I)/RHOP/AP
      PSTR(I)=(PPLN(I)*C4/RHOS)/(UP(I)*UP(I)/64.348D0)
      UU(I)=WP(I)/RHOUP/AUP
      RHOM=(WP(I)+WS(I))/((WS(I)/RHOS)+(WP(I)/RHOP))
      UM(I)=(WP(I)+WS(I))/RHOM/AM
      TSTR(I)=TAMBR/TUPTR
      WSTR(I)=WS(I)/WP(I)
      PRTR(I)=PSTR(I)/TSTR(I)
      WSTR44(I)=WSTR(I)*TSTR(I)**.44D0
      UMACH(I)=UU(I)/41.42658D0/DSQRT(GAMMA*TUPTR)
90    CONTINUE
C
C
C
C
C
C   ************************
C     TABULAR OUTPUT
C
      WRITE (04,500) MTUPT,MR
500   FORMAT('1',/T49,'***   HOT RIG PERFORMANCE   ***',
     *20X,'TUPT:  ',I3/T57,I1,' RING DIFFUSER'//)
      WRITE (04,510) DATE
510   FORMAT (/T4,'DATE:  ',2A8,T65,'DATA TAKEN BY I J EICK')
      WRITE (04,520)NNOZ,LMS
520   FORMAT(/T4,'NUMBER OF PRIMARY NOZZLES:  ',I2,T65,'MIXING STACK',
     *' LENGTH:  ',F5.2,'  INCHES')
      WRITE (04,530) DP,DM
530   FORMAT (T4,'PRIMARY NOZZLE DIAMETER:  ',F5.2,'  INCHES',T65,
```

```
     *'MIXING STACK DIAMETER:  ',F6.3,'  INCHES')
      WRITE (04,540) DU,LD
540   FORMAT(T4,'UPTAKE DIAMETER:  ',F5.3,'  INCHES',T65,
     *'MIXING STACK L/D:  ',F4.2)
      WRITE (04,550) AMAP,SD
550   FORMAT (T4,'AREA RATIO, AM/AP:  ', F4.2,T65,
     *'STANDOFF RATIO:  ',F4.2)
      WRITE (04,560) GAMMA,B
560   FORMAT(T4,'GAMMA:  ',F6.4,T65,'AMBIENT PRESSURE:  ',F5.2,
     *'  INCHES HG')
      WRITE (04,570)
570   FORMAT (///1X,'NR',T7,'PNH',T16,'DELPN',T25,'TNH',T34,'ROTA',
     *T41,'TBURN',T50,'TUPT',T59,'TAMB',T68,'PUPT',T77,'PPLN',
     *T86,'SEC AREA')
      WRITE (04,580)
580   FORMAT(1X,T6,'IN HG',T16,'IN H2O',T25,'DEG F',T41,'DEG F'
     *,T50,'DEG F',T59,'DEG F',T68,'IN H2O',T77,'IN H2O',T88,'SQ IN')
      WRITE (04,590) (I,PNH(I),DELPN(I),TNH(I),ROTA(I),TBURN(I),
     *TUPT(I),TAMB(I),PUPT(I),PPLN(I),SECAIR(I),I=1,12)
590   FORMAT(/1X,I2,T7,F5.2,T16,F5.2,T25,F5.1,T33,F5.1,T41,F6.1,T50,
     *F5.1,T59,F4.1,T68,F5.2,T78,F4.2,T87,F6.3)
      WRITE (04,600)
600   FORMAT (///1X,'NR',T7,'WPA',T16,'WF',T25,'WP',T34,'WS',T43,'W*',
     *T52,'P*',T61,'T*',T69,'P*/T*',T77,'W*T**.44',T88,'UP',T97,
     *'UM',T106,'UU',T113,'UMACH')
      WRITE (04,610)
610   FORMAT(1X,T6,4('LBM/S',4X),T87,3('FT/S',5X))
      WRITE (04,620) (I,WPA(I),WF(I),WP(I),WS(I),WSTR(I),PSTR(I),
     *TSTR(I),PRTR(I),WSTR44(I),UP(I),UM(I),UU(I),UMACH(I),I=1,12)
620   FORMAT(/1X,I2,T6,F5.3,T15,F5.3,T24,F5.3,T33,F5.3,T42,F5.3,T51,
     *F5.3,T60,F5.3,T69,F5.3,T78,F5.3,T87,F5.1,T96,F5.1,T105,F5.1,
     *T113,F6.4)
C
C
C
C    ************************
C
555   CONTINUE
      STOP
      END
```

LIST OF REFERENCES

1. Ellin, C. R., Model Test of Multiple Nozzle Exhaust Gas Eductor Systems for Gas Turbine Powered Ships, Engineer's Thesis, Naval Postgraduate School, June 1977.

2. Lemke, R. J. and Staehli, C. R., Performance of Multiple Nozzle Eductor Systems with Several Geometric Configurations, Master's Thesis, Naval Postgraduate School, September 1977.

3. Ross, P. D., Combustion Gas Generator for Gas Turbine Exhaust Systems Modelling, Master's Thesis, Naval Postgraduate School, December 1977.

4. Welch, D. R., Hot Flow Testing of Multiple Nozzle Exhaust Eductor Systems, Engineer's Thesis, Naval Postgraduate School, September 1978.

5. Moss, C. M., Effects of Several Geometric Parameters on the Performance of a Multiple Nozzle Eductor System, Master's Thesis, Naval Postgraduate School, September 1977.

6. Hill, J. A., Hot Flow Testing of Multiple Nozzle Exhaust Eductor Systems, Master's Thesis, Naval Postgraduate School, September 1979.

7. Eick, I.J., Testing of a Shrouded, Short Mixing Stack Gas Eductor Model Using High Temperature Primary Flow, Master's Thesis, Naval Postgraduate School, October, 1982.

8. Davis, C. C., Performance of Multiple, Angled Nozzles with Short Mixing Stack Eductor Systems, Master's Thesis, Naval Postgraduate School, September 1981.

9. Drucker, J. C., Characteristics of a Four-Nozzle, Slotted Short Mixing Stack with Shroud, Gas Eductor System, Master's Thesis, Naval Postgraduate School, March 1982.

10. Pucci, P. F., Simple Eductor Design Parameters, Ph.D. Thesis, Stanford University, September 1954.

11. Kline, S. J. and McClintock, F. A., "Describing Uncertainties in Single-Sample Experiments," Mechanical Engineering, p. 3-8, January 1953.

INITIAL DISTRIBUTION LIST

		No. Copies
1.	Defense Technical Information Center Cameron Station Alexandria, Virginia 22314	2
2.	Hellenic Navy General Staff Education Office Stratopedon Papayou Holargos, Athens, Greece	2
3.	Library, Code 0142 Naval Postgraduate School Monterey, California 93940	2
4.	Department Chairman, Code 69 Department Mechanical Engineering Naval Postgraduate School Monterey, California 93940	2
5.	Professor Paul F. Pucci, Code 69Pc Department of Mechanical Engineering Naval Postgraduate School Monterey, California 93940	3
6.	Dean of Research, Code 012 Naval Postgraduate School Monterey, California 93940	1
7.	Commander ATTN: NAVSEA, Code 0331 Naval Ship Systems Command Washington, D.C. 20362	1
8.	Mr. Olin M. Pearcy NSRDC, Code 2833 Naval Ship Research and Development Center Annapolis, Maryland 21402	1
9.	Mr. Mark Goldberg NSRDC, Code 2033 Naval Ship Research and Development Center Annapolis, Maryland 21402	1

10. Mr. Eugene P. Wienert 1
Head, Combined Power and Gas Turbine Branch
Naval Ship Engineering Center
Philadelphia, Pennsylvania 19112

11. Mr. Donald N. McCallum 1
NAVSEC Code 6136
Naval Ship Engineering Center
Washington, D.C. 21362

12. LT Anastasios Kavalis 1
Georgiou Mplessa 76
Papagos, Athens, Greece

13. LCDR Ira J. Eick, USN 1
P.O. Box 248
Lebanon, New Jersey 08833

14. LT Carl J. Drucker, USN 1
1032 Marlborough Street
Philadelphia, Pennsylvania 19125

15. LCDR C. M. Moss, USN 1
625 Midway Road
Powder Springs, Georgia 30073

16. LCDR J. P. Harrell, Jr., USNR 1
1600 Stanley
Ardmore, Oklahoma 73401

17. LCDR J. A Hill, USN 1
RFD 2, Box 116B
Elizabeth Lane
York, Maine 03909

18. LCDR R. J. Lemke, USN 1
2902 No. Cheyenne
Tacoma, Washington 98407

19. LCDR C. P. Staehli, USN 1
2808 39th St., N.W.
Gig Harbor, Washington 98335

20. LT R. S. Shaw, USN 1
147 Wampee Curve
Summerville, South Carolina 29483

21. LCDR D. L. Ryan, USN 1
6393 Caminito Luisito
San Diego, California 92111

22. LCDR C. C. Davis, USN 1
1608 Linden Drive
Florence, South Carolina 29501

23. LCDR D. Welch, USN 1
1036 Brestwick Commons
Virginia Beach, Virginia 23464

24. CDR P. D. Ross, Jr., USN 1
6050 Henderson Drive No. 8
La Mesa, California 92041

25. Anastasios Sklavidis 1
351 Delavina #15
Monterey, California 93940

201682

Thesis
K14923 Kavalis
c.1
Effect of shroud geometry on the effectiveness of a short mixing stack gas eductor model.